Linear Polyethyleneimine and Derivatives as Potential Biomaterials and Excipients for Drug Delivery

By

Sitthiphong Soradech

A Thesis Submitted in Partial Fulfillment of the Requirements for the Degree

Doctor of Philosophy

Program of Pharmacy

Reading School of Pharmacy

University of Reading

2023

Linear Polyethyleneimine and Derivatives as Potential Biomaterials and Excipients for Drug Delivery

By

Sitthiphong Soradech

A Thesis Submitted in Partial Fulfillment of the Requirements for the Degree

Doctor of Philosophy

Program of Pharmacy

Reading School of Pharmacy

University of Reading

2023

Acknowledgements

Firstly, I am very grateful to my supervisors, Professor Vitaliy Khutoryanskiy and Professor Adrian Williams for their guidance and constant motivation throughout these years of intensive research. You have inculcated me with the spirit of perseverance and accomplishment, in addition to developing my research and analytical skills.

The Chemical Analysis Facility (CAF), University of Reading is acknowledged for providing access to FT-IR and ^{1}H NMR spectroscopies, DSC analysis, TGA analysis, Scanning electron microscope (SEM) and X-ray diffractometry.

I am grateful to Thailand Institute of Scientific and Technological Research, Ministry of Higher Education, Science, Research and Innovation for funding my PhD.

My heartfelt thanks go to the pleasant people that helped with various analyses, Dr. Pedroz Rivas-Ruiz, Dr. Daulet Kaldybekov, Dr. Raymond Lau, Mr. Nicholas Spencer, Miss Amanpreet Kaur and other wonderful people that I cannot afford to express all their names.

To my research group: Claudia Aguguo, Dr. Jamila Al Mahrooqi, Dr. Sam Aspinall, Fhataheya Buang, Manfei Fu, Myrale Habel, Dr. Sayyed Ibrahim Shah, Dr. Xioning Shan, Dr. Roman Moiseev, Shiva Vanukur, Yuehual Xiong. I appreciate all your advice, laughter, and friendship.

To my beloved wife, and parents, thanks for the overwhelming sacrifice. To all my siblings and their family as well as my wife, I will forever be indebted to you because you never gave up supporting me to make this dream become a reality.

Sitthiphong Soradech

April 2023

Declaration of Original Authorship

The work described in this thesis was performed in the Reading School of Pharmacy, University of Reading, United Kingdom, between September 2019 and April 2023. I confirm that this is my own work and the use of all materials from other sources has been properly and fully acknowledged.

Sitthiphong Soradech

April 2023

Abstract

My PhD project was aimed to synthesize and evaluate linear polyethyleneimine and its derivatives as potential biomaterials and excipients for drug delivery. L-PEI was synthesized successfully by acidic hydrolysis of poly(2-ethyl-2-oxazoline) or PEOZ to remove all amide groups from the side groups. The complete conversion to L-PEI was confirmed by ^{1}H-NMR and FTIR spectroscopies. Then, L-PEI was used to prepare physically crosslinked cryogels. Dissolution of L-PEI in deionized water was achieved at 80 ^{o}C and resulted in a transparent solution, leading to an opaque gel forming upon freezing and subsequent thawing. The cryogels exhibited reversibility and after heating at 80 ^{o}C formed a clear solution due to the melting of the crystalline domains of L-PEI. Different cooling temperatures and the use of various solvent compositions on L-PEI gelation have an effect on the enthalpy of melting, degree of crystallinity, viscosity and mechanical strength of L-PEI cryogels. This study demonstrates that the physical properties of L-PEI cryogels can be manipulated by controlling the cooling rate and solvent composition used to form the cryogels and its applications for drug delivery systems or antimicrobial wound dressings.

Chemical modification of L-PEI is one approach to develop water solubility and properties of polymers. Therefore, we attempted to synthesize poly(2-hydroxyethyl ethyleneimine), P2HEEI and poly(3-hydroxypropyl ethyleneimine), P3HPEI as novel water-soluble polymers for pharmaceutical applications. P2HEEI and P3HPEI were synthesized via nucleophilic substitution reaction between L-PEI and 2-bromoethanol and 3-bromo-1-propanol, respectively. Both polymers had a good water solubility, low toxicity, and a low glass transition temperature. Due to the lower glass transition below 0 ^{o}C, these novel polymers were blended with chitosan to improve mechanical properties and the resulting polymeric films were evaluated for their applicability in transmucosal drug delivery.

Chitosan and P3HPEI in the blends were fully miscible in solid stage. Blending of chitosan with P3HPEI also significantly enhanced elasticity and strength of the resulting films. A 35:65 (%*w/w*) blend of chitosan-P3HPEI provided the optimum T_g for transmucosal drug delivery and so was selected for further investigation with haloperidol, which was chosen as a model hydrophobic drug. Microscopic and X-ray diffractogram (XRD) data indicated that the solubility of the drug in the films was ~1.5%. The inclusion of the hydrophilic polymer P3HPEI allowed rapid drug release within ~30 min, after which films disintegrated, demonstrating that

the formulations are suitable for application to mucosal surfaces, such as in buccal drug delivery.

Mucoadhesive films are one of commercially relevant formulations for buccal drug delivery due to their adaptability and ease of use. Additionally, the use of these films can prolong the time spent on the mucosa, directly delivering a precise dose of the drug to the tissue. Hence, this study aimed to synthesize poly(2-hydroxyethyl ethyleneimine) or P2HEEI and its mucoadhesive film formulations based on blends with chitosan for buccal delivery of haloperidol. Initially, P2HEEI was synthesized via nucleophilic substitution of linear polyethyleneimine (L-PEI) with 2-bromoethanol. P2HEEI exhibited good solubility in water, low toxicity in human dermal skin fibroblast cells, and low glass transition temperature (-31.6 ^{o}C). This polymer was then blended with chitosan to improve mechanical properties and these materials were used for the buccal delivery of haloperidol. Chitosan and P2HEEI formed completely miscible blends. Blending chitosan with P2HEEI improved the mechanical properties of the films, resulting in more elastic materials. Blend films were also prepared loaded with haloperidol as a model poorly water-soluble drug. The cumulative release of haloperidol from the films increased when the blends were prepared with greater P2HEEI content. Mucoadhesive properties of these films with respect to freshly excised sheep buccal mucosa were evaluated using a tensile method. It was found that all films are mucoadhesive; however, an increase in P2HEEI content in the blend resulted in a gradual reduction of their ability to adhere to the buccal mucosa. These films could potentially find applications in buccal drug delivery.

Hence, L-PEI and its derivatives have potential as biomaterials and excipients for drug delivery, enabling the development of novel formulations such as cryogels, drug-loaded films for poorly water-soluble drug administration, and mucoadhesive drug delivery system.

List of Publications

1. Sitthiphong Soradech, Adrian C. Williams and Vitaliy V. Khutoryanskiy, Physically Crosslinked Cryogels of Linear Polyethyleneimine: Influence of Cooling Temperature and Solvent Composition, Macromolecules 2022, 532105-117. **Published. (Chapter 2)**
2. Sitthiphong Soradech, Pattarawadee Kengkwasingh, Adrian C. Williams and Vitaliy V. Khutoryanskiy, Synthesis and Evaluation of Poly(3-hydroxypropyl Ethyleneimine) and Its Blends with Chitosan Forming Novel Elastic Films for Delivery of Haloperidol, Pharmaceutics 2022, 14, 2671. **Published. (Chapter 3)**
3. Sitthiphong Soradech, Adrian C. Williams and Vitaliy V. Khutoryanskiy, Polyethyleneimine and Its Derivatives for Pharmaceutical and Biomedical Applications (a review). **In preparation for submission. (Chapter 1)**
4. Sitthiphong Soradech, Pattarawadee Kengkwasingh, Adrian C. Williams and Vitaliy V. Khutoryanskiy, Synthesis of Poly(2-hydroxyethyl ethyleneimine) and Its Mucoadhesive Film Formulations Based on Blends with Chitosan for Buccal Delivery of Haloperidol. **In preparation for submission. (Chapter 4)**

List of Conferences

1. Pharmacy PhD Showcase 2020, University of Reading, 4th July 2020 – Talk (3 minutes).
2. Pharmacy PhD Showcase 2021, University of Reading, 16th April 2021 – Talk (5-minutes).
3. Pharmacy PhD Showcase 2022, University of Reading, 31st March 2022 -Talk (15 minutes).
4. International conference on Academy of Pharmaceutical Sciences at Belfast, Northern Ireland, UK, 7 – 9th September 2022 – Poster.
5. The 6th London Polymer Group meeting, University College, London, UK, 27th April 2023 – Poster.

Table Content

List of Figures

List of Tables

Abbreviations

^{1}H-NMR	^{1}H-Nuclear Magnetic Resonance Spectroscopy
MTT assay	3-(4, 5-Dimethyl-2-thiazolyl)-2, 5-diphenyl-2H-tetrazolium bromide (MTT) assay
ANOVA	Analysis of variance
B-PEI	Branched polyethyleneimine
CHI	Chitosan
η*	Complex viscosity
DS	Degree of substitution
CD_3OD	deuterated methanol
D_2O	Deuterium oxide
DSC	Differential Scanning Calorimetry
DMEM	Dulbecco's modified eagle medium
FITC	Fluorescein isothiocyanate labeled chitosan
FTIR	Fourier Transformed Infrared Spectroscopy
T_g	Glass transition temperature
IC_{50}	Half maximal inhibitory concentration
HP	Haloperidol
hPa	Hectopascal
Hz	Hertz
HCl	Hydrochloric acid
HELPEI	Hydroxyethyl-substituted linear polyethyleneimine
HPMC	hydroxypropyl methylcellulose
kDa	Kilodalton
L-PEI	Linear polyethyleneimine
G″	Loss or viscous modulus
MHz	Megahertz
T_m	Melting temperature
MWCO	Molecular weight cut off
PEtOx-PEI	Poly (2-ethyl-2-oxazoline)-co-polyethyleneimine
PEtOx, PEOZ	Poly(2-ethyl-2-oxazoline)
P2HEEI	Poly(2-hydroxyethyl ethyleneimine)

P3HPEI	Poly(3-hydroxypropyl ethyleneimine)
PAOx	Poly(oxazoline)s
PAC	Polyacrylic acid
PEI	Polyethyleneimine
PVA	Polyvinyl alcohol
QACs	Quaternary ammonium compounds
QP2HEEI	Quaternary ammonium of poly(2-hydroxyethyl ethyleneimine)
QP3HPEI	Quaternary ammonium of poly(3-hydroxypropyl ethyleneimine)
Tan δ	Relative phase angle
RT	Room temperature
SEM	Scanning Electron Microscopy
NaCl	Sodium chloride
NaOH	Sodium hydroxide
SD	Standard deviation
G'	Storage or elastic modulus
TGA	Thermogravimetric analysis
XRD	X-ray diffraction analysis

Chapter 1

Polyethyleneimine and Its Derivatives for Pharmaceutical and Biomedical Applications

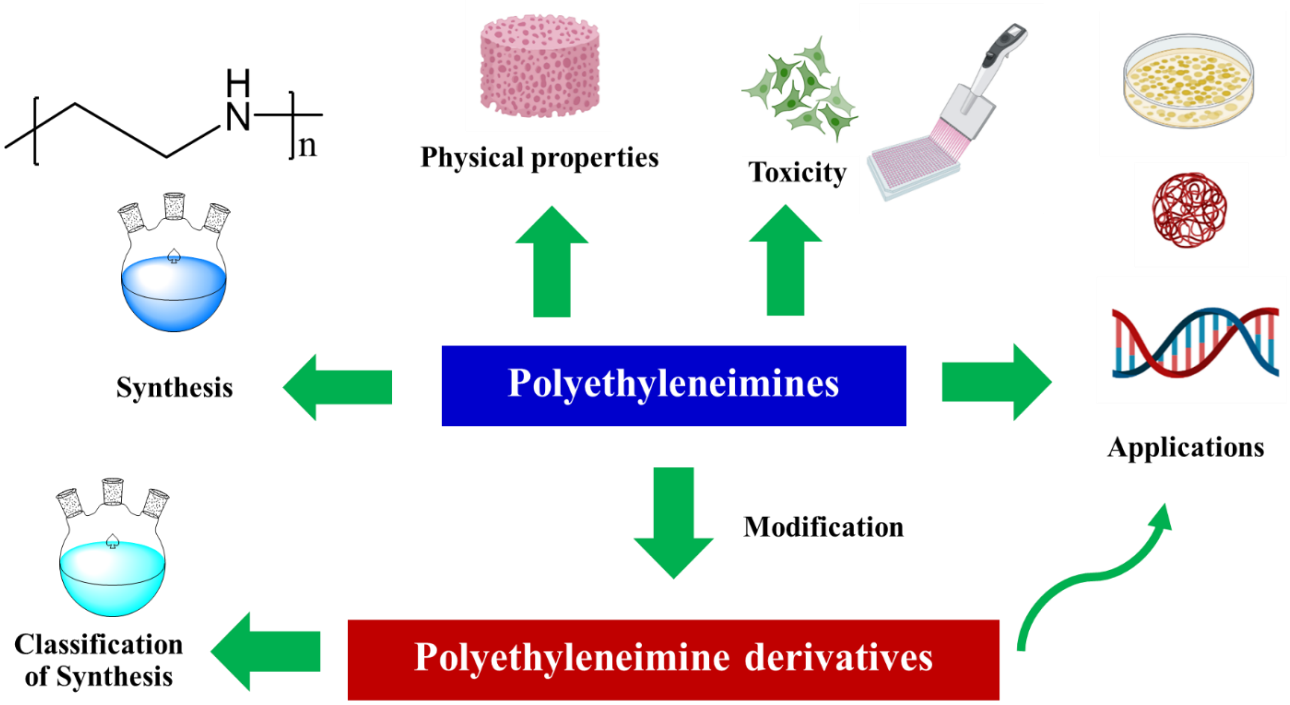

This chapter was prepared for submission as: Sitthiphong Soradech, Adrian C. Williams, and Vitaliy V. Khutoryanskiy, Polyethyleneimine and Its Derivatives for Pharmaceutical and Biomedical Applications (a review).

Chapter 1

Polyethyleneimine and its derivatives for pharmaceutical and biomedical applications

Sitthiphong Soradech, Adrian C. Williams, and Vitaliy V. Khutoryanskiy*

Reading School of Pharmacy, University of Reading, Whiteknights, Reading, RG6 6AD, UK

***Corresponding author:**
Postal address: Reading School of Pharmacy, University of Reading, Whiteknights, PO Box 224, RG6 6AD, Reading, United Kingdom
E-mail address: v.khutoryanskiy@reading.ac.uk
Telephone: +44(0) 118 378 6119
Fax: +44(0) 118 378 4703

Abstract

Polyethyleneimine (PEI) and its derivatives have been used for numerous pharmaceutical and biomedical applications since their properties can be tailored for particular uses. In this review, we consider both linear and branched PEI as well as their derivatives and review their physical properties, including solid-state properties and behavior in aqueous and non-aqueous solutions. Complexation of PEI with anionic polymers and metal ions is described and biocompatibility, solubility and toxicity of the parent and derivative polymers is discussed. Further, we review uses of these materials spanning gene delivery, antimicrobial formulations, mucoadhesion, polymer blending, hydrogels and wound dressing.

Keywords: Polyethyleneimine (PEI), pharmaceutical, biomedical, and toxicology

1. Introduction

In the pharmaceutical and biomedical industries, polymers are widely used [1]. Among many applications for the cationic polymer PEI, gene delivery, drug delivery and polymer therapeutics are widely reported [2-5]. It can use as an antifouling coating and has antibacterial properties [2-5]. As a cationic polymer, PEI is water soluble, it forms flexible films and has been reported to be non-immunogenic, biocompatible [2-5] and nondegradable polymer [6].

PEI repeating units are two carbons aliphatic CH_2CH_2 spacers and an amine group **(Fig. 1)**. As a chemical class, PEIs, are among the most extensively developed polycations [6] and are investigated due to both their highly positive charge and diverse structures. PEI can be synthesized and used as either linear (usually denoted L-PEI) or branched (B-PEI), which significantly affects their properties [7].

L-PEI is semi-crystalline and only dissolves in water at high temperatures [8, 9] with a melting point between 60 and 69 ^{o}C [10]. L-PEI is also soluble in water at low pH, and in methanol, ethanol, and chloroform, but not in cold water or non-polar solvents (ethyl ether, acetone, and benzene) [7]. The temperature-dependent solubility in water is attributed to polymer crystallinity; crystalline domains are found at < 60 ^{o}C whereas above this chain mobility increases with crystallite melting allowing dissolution in water [11, 12]. L-PEI solubility is also pH dependent and the amine groups result in a broad pKa range, with no simple or obvious definition for pKa [13, 14]. Using NaOH to titrate the polymer solution results in opacity changes from transparent to cloudy as the polymer forms semi crystalline and crystalline domains around pH 9.4 [15].

In contrast, branched PEI is a viscous colourless liquids containing mixtures of various primary, secondary, and tertiary amines. B-PEI is an amorphous polymer that is readily soluble in water [13].

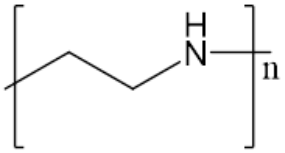

(a)

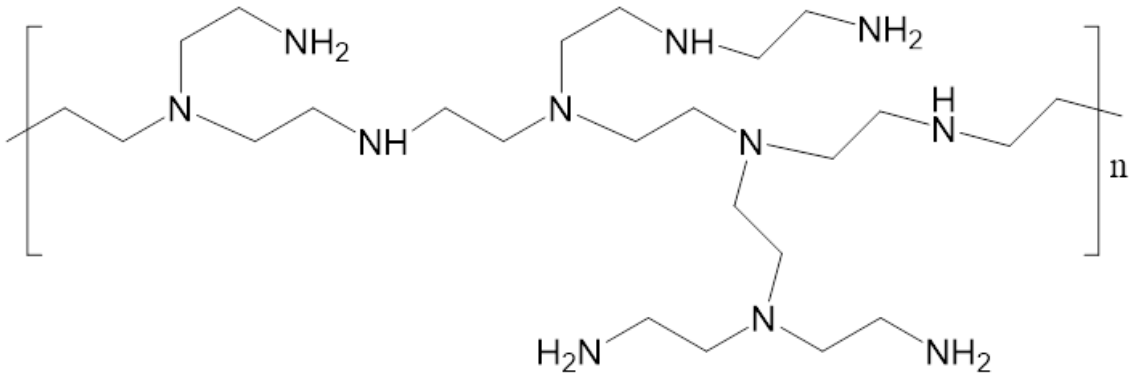

(b)

Fig.1. Chemical structure of linear (a) and branched PEI (b).

Here, we focus on the synthesis and physical properties of linear and branched PEI and complexation of PEI with anionic polymers and metal ions. PEI derivatives have been studied in terms of biocompatibility, solubility, and toxicology. Finally, applications of PEI and its derivatives in pharmaceutics and biomedicine are discussed.

2. Synthesis of polyethyleneimines

Both L-PEI and B-PEI can be prepared by ring-opening polymerization of azirdines [16]. Additionally, L-PEI can be synthesized by hydrolysis of poly-(2-ethyl-2-oxazoline), PEOZ [17].

2.1. Ring opening polymerization of azirdines

L-PEI can be synthesized by cationic ring-opening polymerization of poly (2-ethyl-2-oxazoline) or azirdines, which is then hydrolyzed under acidic conditions to yield L-PEI; B-PEI can be likewise be synthesized by ring-opening polymerization of aziridine **(Fig. 2)**.

Using cationic ring-opening polymerization of 2-oxazoline, Saegusa et al. [18] first characterized L-PEI. Alternatively, L-PEI can also be generated by polymerizing aziridines with cationic ring-opening and hydrolysis of the side chain. Substitution of aziridines with polymerized benzyl, alkyl, perfluoro, or acyl sulfonyl groups initiate this reaction before hydrolysis of the side chain and deprotonation of polyaziridines yields L-PEI with only

secondary amines in the polymer backbone [16]. Alternatively, Rivas et al. [17] used a cationic ring-opening method to synthesize acylated PEI by polymerizing 2-oxazoline before hydrolysis under acidic or alkaline conditions to produce L-PEI. Jäger et al. [16] reported the 6-step synthesis of B-PEI from ring-opening of aziridine. Firstly, ring opening is initiated by electrophilic attack of a Lewis acid (or protons) on an aziridine monomer. Then, the active aziridinium ion is attacked by a nucleophilic species to obtain the ring opening product. The aziridine monomer serves as a nucleophile in this process which results in a product with a secondary amino group and a new aziridium species at the terminus. Linear propagation of the chain results from multiple consecutive attack of aziridine. However, the secondary and tertiary amine groups during the polymerization process can also react to form branched PEI. Deprotonation, which can protonate an aziridine monomer to create a new chain, follows. Finally, by targeting the polymerization process of B-PEI using nucleophile substances such as water or methanol, polymerization can be terminated. According to Kunath et al. [19] , the ratio of primary, secondary, and tertiary amines in the backbone of B-PEI is 1:2:1.

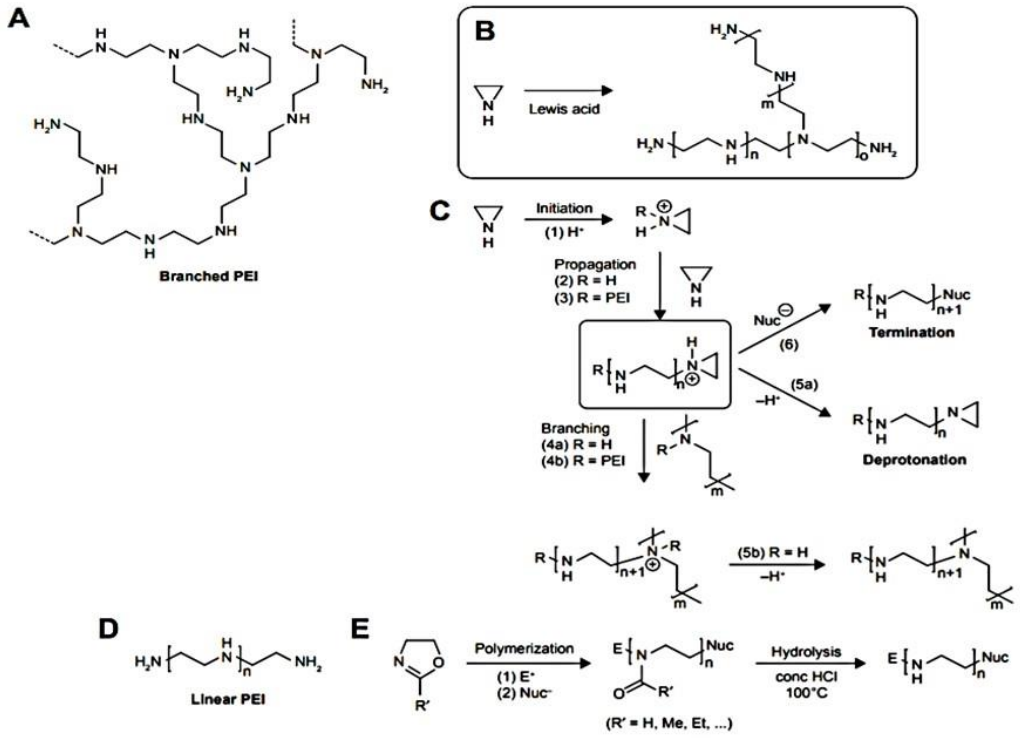

Fig. 2. Synthesis of B-PEI and L-PEI by ring-opening polymerization method [16].

2.2. Hydrolysis of poly(2-ethyl-2-oxazoline)

To eliminate all the amide groups on the side chains of L-PEI, complete hydrolysis of poly(2-ethyl-2oxazoline), PEOZ, has been conducted under acidic or basic conditions. Additionally, partial hydrolysis has been used to form the co-polymer poly(2-ethyl-2-oxazoline-co-ethyleneimine) (PEOZ-EI copolymer [20]. **Fig. 3** illustrates the general scheme for these reactions.

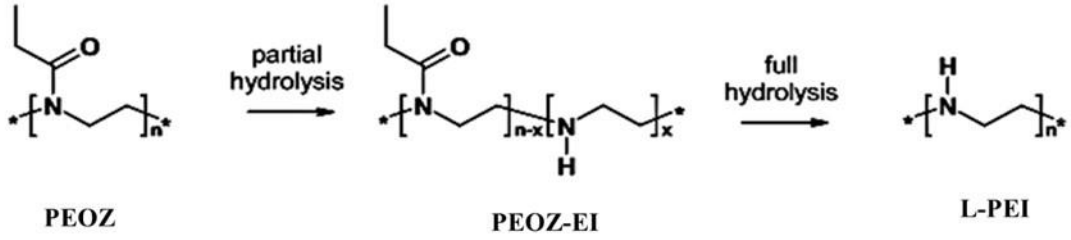

Fig. 3. Schematic diagram of partial and full hydrolysis of PEOZ [20].

2.2.1. Acidic hydrolysis

Acid hydrolysis is generally preferred since it confers greater control over the reaction than basic hydrolysis. **Fig. 4** illustrates the mechanism of acidic hydrolysis; initially water molecules attack the protonated from of amide groups in PEOZ which provides the rate-determining step. The resultant tetrahedral intermediate is transformed into an amine whilst liberating a propionic acid. Under acidic conditions, PEI is protonated [15]. However, repulsion effects were also evident from PEOZ hydrolysis so the reaction is pushed to completion, resulting in protonation of all PEOZ amine groups. Adding HCl to generate strongly acidic conditions can thus produce L-PEI from PEOZ. Further, temperature also affects the hydrolysis of PEOZ to L-PEI; increasing the temperature above 180 ^{o}C caused the polymer backbone to degrade under acidic hydrolysis conditions, resulting in the conversion of amines to a protonated form [21, 22].

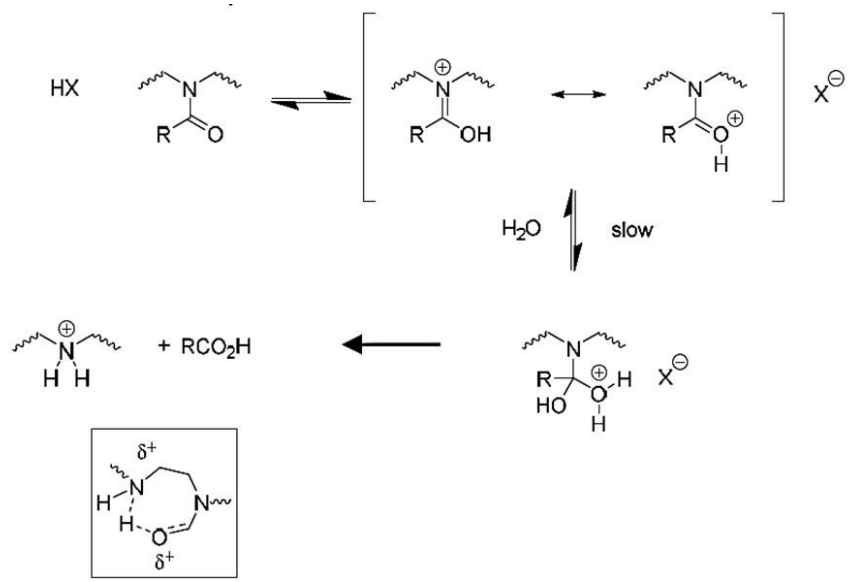

Fig. 4. Schematic diagram of acidic hydrolysis of PEOZ to form linear PEI [15].

2.2.2. Basic hydrolysis

Alkaline conditions can be used to hydrolyze PEOZ [15]. Initially, the -OH can attack carbonyl groups of PEOZ, and a tetrahedral intermediate is also deprotonated. Subsequently, the carboxylate at the side chain is released, resulting in the formation of L-PEI, as shown in **Fig. 5**. Saegusa et al.[23] used cationic polymerization of 2-oxazoline or 2-methyl-oxazoline in dimethyl formamide and subsequently hydrolyzed the product under alkaline conditions [21]. Different molecular weights of the semicrystalline PEI melted at 58.5 ^{o}C but the resultant polymers did not exceed 10^4 Da.

Lambermont-Thijs et al. [12] reported that the value of basic hydrolysis of PEOZ in generating L-PEI is limited due to partial backbone degradation. As a result of significant contact with the column material, it was not possible to quantify the molecular weight of L-PEI using size exclusion chromatography (SEC). Due to the low molar mass the authors found that hexafluoroisopropanol was a preferable solvent for reducing interaction in the column [24].

Fig. 5. Schematic diagram of basic hydrolysis of PEOZ to form linear PEI [15].

2.2.3. Partial hydrolysis

By varying reaction time, partial hydrolysis of PEOZ can allow production of PEOZ-PEI copolymers containing different degrees of PEI units and the remaining PEOZ units [22]. Kem [25] first demonstrated partial hydrolysis of PEOZ and hypothesized that new polymers could be prepared for copolymer synthesis. More recently, PEOZ-PEI copolymers have been demonstrated to be biocompatible for up to 25% hydrolysis. Kuringen et al.[20] reported partial hydrolysis of poly (2-ethyl-2-oxazoline) for biomedical applications. Initially, PEOZ-200K was hydrolyzed in simulated gastric fluid (pH 1.2) generating a degree of hydrolysis < 0.2% at 37 ^{o}C for 6 hrs. Using 5.8 M hydrochloric acid at 57, 73, 90, or 100 ^{o}C, PEtOx-200k was shown to be completely hydrolyzed in 5.8 M HCl at 100 ^{o}C within 120 mins, while the hydrolysis tended to decline to 54% (90 ^{o}C) 14% (73 ^{o}C) and 4% (57 ^{o}C), respectively. Partial hydrolysis can be achieved not only via chemical reaction but also through enzymatic hydrolysis as reported by Wang et al. [26].

3. Physical properties of PEI

3.1. Crystallinity and amorphous states of PEI

In polymers, crystallization is the partial alignment of their molecular chains during cooling processes from solvent evaporation, melting, or mechanical stretching. As a result of polymer crystallization, mechanical, thermal, optical and chemical properties change. Solid-state polymers can be either crystalline or amorphous and can contain both crystalline and amorphous domains; in this semi-crystalline phase, the crystallinity of L-PEI can vary from 10 to 80 % [27].

Further, L-PEI, contains varied crystalline phases that changes depending on the humidity and can be anhydrate, hemihydrate, sesquihydrate, and dehydrate, determined from their water/ethylene imine (EI) ratio **(Fig. 6)** [28, 29]. Hashida, Tashiroa, and Inaki [30] reported the changing crystallinity of L-PEI with water content. PEI exhibits four different crystalline hydrates: anhydrate (EI/water 1/0), hemihydrate (1/0.5), sesquihydrate (1/1.5), and dihydrate (1/2). The chain conformation changes from a double helix in the anhydrate to a planar zigzag form in the three hydrates.

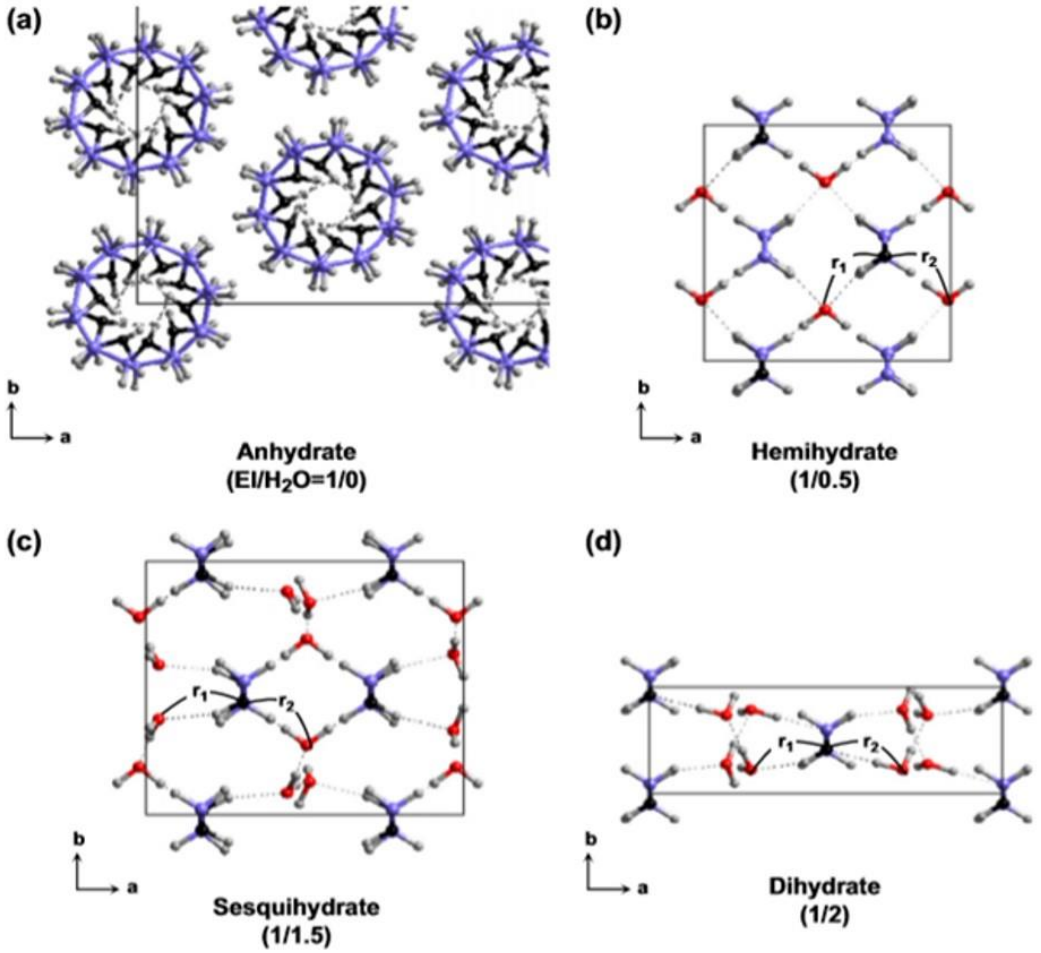

Fig. 6. Crystal structures of poly(ethylene imine) [30].

Hashida and Tashiro [31] explored changes to the L-PEI chain conformation, from a double helix to a single chain, using DSC and X-ray diffraction, as illustrated in **Fig. 7**. **Fig. 7a** shows the melting temperature of the PEI dried sample (anhydrate), which is lower than the melting temperature of the hydrated PEI. FTIR spectroscopy showed that the N-H stretching mode shifted with increasing temperature indicating weakening of intermolecular hydrogen bonds between molecules. At ~55 ^{o}C, the anhydrate double helix split into single chains which then melted at 66 °C. The melting of hydrate PEI was investigated using a mixture of anhydrate and hemihydrate PEI using thermal analysis and X-ray diffractometry. The anhydrate crystalline peak was lost at >60 °C, but was retained for the hemihydrate, up to 80 °C **(Fig 7 b)**. The melting of hydrated PEI revealed the formation of a partial hemihydrate due to the presence of a trace amount of water. As illustrated in **Fig. 7c**, the melting behavior of PEI-hydrated samples with a high proportion of water exhibits a pronounced amorphous phase

transition. The PEI sample consisted of a mixture of hemihydrate and sesquihydrate, which was stored at 33 °C. After heating, the hemihydrate content decreased, and the material melted at 93 ^{o}C. In contrast, the sesquihydrate PEI was observed between 60 and 80 °C, which then melted at 93 °C, the same temperature as the hemihydrate form. The transition from hemihydrate to sesquihydrate was responsible for the exothermic peak observed at 75 ^{o}C **(Fig. 7c)**. The interactions between water and L-PEI are clearly complex and indeed are dynamic during thermal analysis.

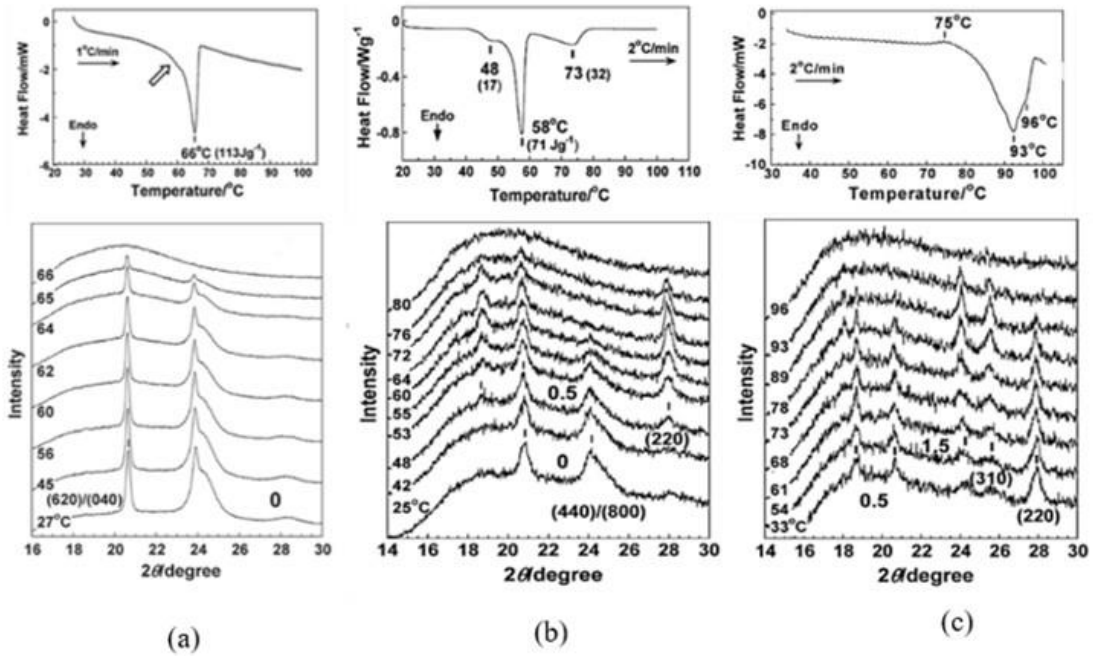

Fig. 7. DSC thermograms and X-ray diffraction patterns of PEI dried sample (a), PEI hydrated sample (b), and PEI hydrated with a large amount of water (c) [31].

Interactions of L-PEI with water have also been explored in studies of hydrogels. Yuan and Jin [32] formed thermoreversible physical hydrogels from L-PEI. The anhydrated and hydrated forms of linear PEI have a significant tendency to crystallise. The solid PEIs prior to hydrogelation were crystallised in an aqueous solution including ammonia via deprotonation of PEI/HCl salt. to the authors concluded that the development of hydrogels was associated with the crystallisation of PEIs during cooling of a heated PEI-containing aqueous solution.

Solid-state L-PEI used to prepare hydrogels exhibited XRD diffraction peaks at 2θ = 12.0, 18.8, 20.6, and 27.9° from to the hemihydrated crystalline structure of PEI. In comparison, for the dihydrate, a hydrogel containing 5% L-PEI produced XRD diffraction

peaks at 2θ = 13.5, 20.3, 27.2, and 27.9° whilst lyophilization increased the amorphous phase of L-PEI [32].

Soradech et al. [29] developed physical cryogels from linear polyethyleneimine (L-PEI). The L-PEI starting material showed diffraction peaks at 2θ = 18, 20 and 28°, in agreement with the above literature reports for the hemihydrate crystalline structure. The cryogels provided diffraction peaks at 2θ = 20, 27 and 28° **(Fig. 8-9)**, typical for the dihydrate crystalline state. Further, when the cryogels were re-heated at 80 ºC, again forming a clear solution, the diffractogram showed no evidence of crystalline domains. The formation of physical cryogels based on L-PEI is attributed to the change in polymer chain conformation from a double helix in the anhydrate to a planar-zigzag as water molecules are absorbed into the L-PEI lattice, and to the formation of NH-O and OH-N bonds between the zigzag PEI chains and water molecules[29].

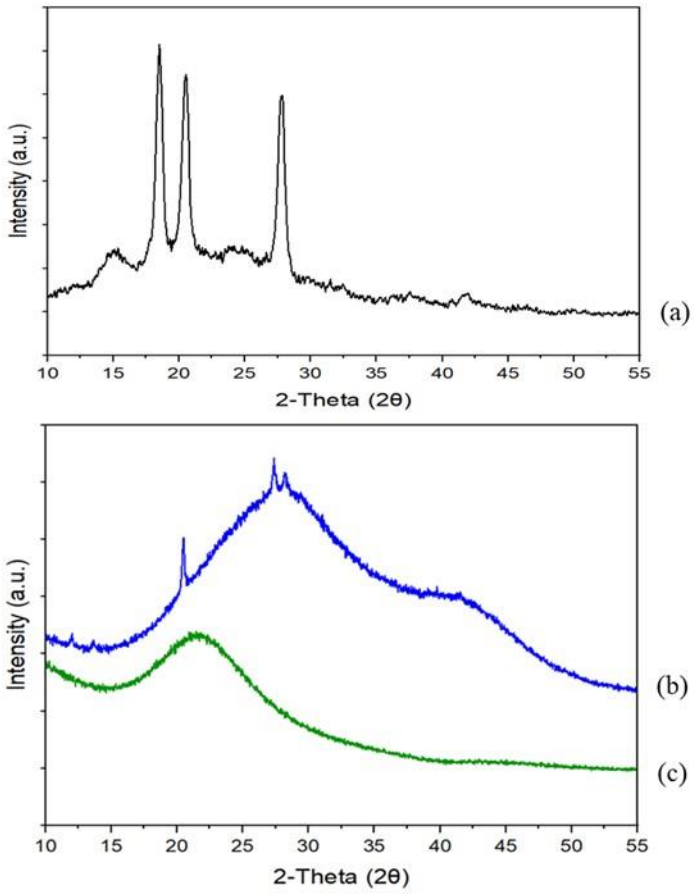

Fig. 8. X-ray diffraction patterns for L-PEI (a) and cryogel prepared from 5 % L-PEI solution (b) and this sample after heating at 80 ºC (c)[29].

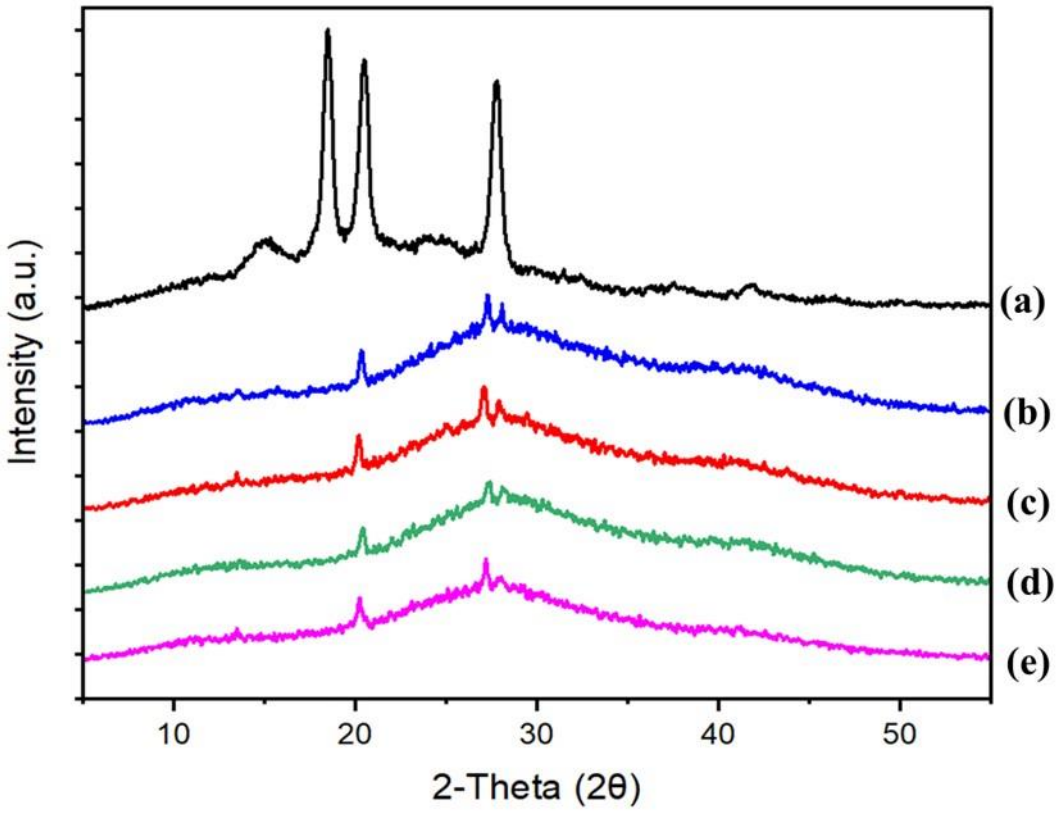

Fig. 9. X-ray diffraction spectra of dry L-PEI (a) and wet L-PEI cryogels prepared at various freezing temperatures: -196 ^{o}C (b), -80 ^{o}C (c), -30 ^{o}C (d) and 0 ^{o}C (e) [29].

3.2. Thermal properties of L-PEI and PEOZ-EI copolymers

Thermal behavior is important for pharmaceutical processes such as film coatings or granulation. Differential scanning calorimetry (DSC) is commonly used to determine the glass transition temperature (T_g) and melting temperature (T_m) of polymers [32].

Tanaka et al. [21] reported two distinct endothermic peaks of L-PEI following the first and second DSC scans up to 140 ^{o}C. Furthermore, due to water vapor escaping from the sample pan, the DSC curve of L-PEI in the first scan showed two endothermic peaks at 55-60 ^{o}C and 70-80 ^{o}C, before the sample was slowly cooled. Only the 55-60 ^{o}C endotherm was evident after the second scan with the larger 70-80 ^{o}C thermal event lost. These results were attributed to melting of sesqui or dihydrate crystals of L-PEI, [11]. Saegusa et al. [23] also reported a T_m peak at 55-60 ^{o}C for L-PEI.

Yuan and Jin [32] developed a thermoreversible hydrogel by heating L-PEI at 80 ^{o}C and cooling at room temperature From DSC, the starting L-PEI powder provided a melting point of ~56 °C, consistent with the above. The first heating (at 10 °C/min) resulted in an endothermic peak at 64.7 °C. After a hold period of 10 mins at 90 °C, the sample was cooled at 10 °C/min generating an exothermic event at 29.6 °C. A second heating scan the revealed an endothermic peak at 62.7 °C, corresponding to the first scan feature **(Fig.10)**. The results demonstrated a thermoreversible hydrogel with the melting event attributed to the dihydrate PEI crystalline structure. In comparison, a solid state sample of L-PEI containing 16% water was held at 150 ^{o}C to remove "crystalline water" before cooling to 0 °C (at 10 °C/min). Anhydrate PEI formed as a result of the removal of water molecules and generated a lower melting peak (T_m) of L-PEI (55.9 ^{o}C) on the second scan.

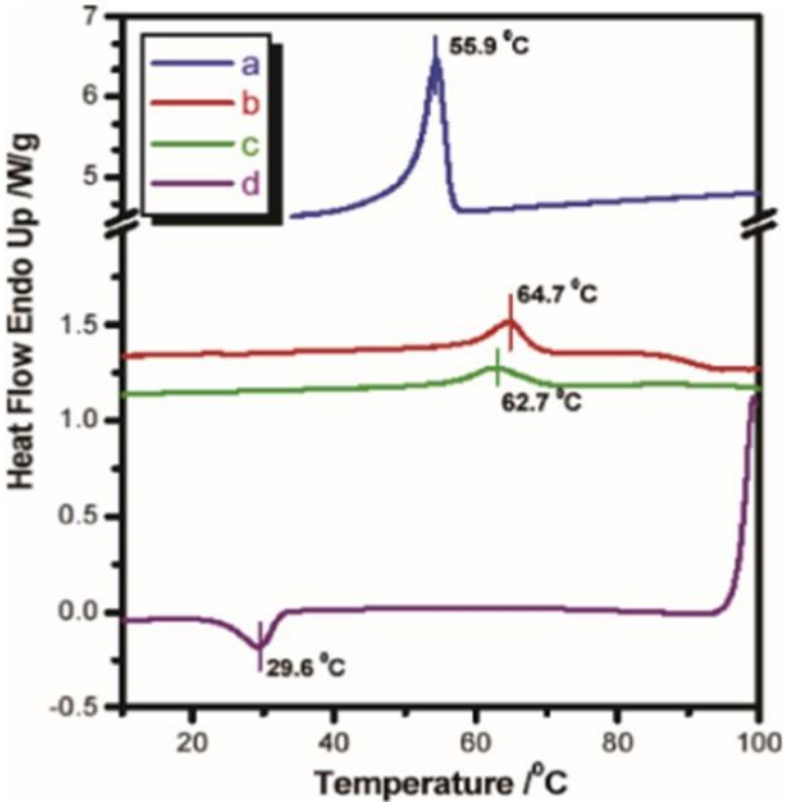

Fig. 10. DSC thermograms of the L-PEI (a) and physical hydrogels from L-PEI (b-d). The lines of b, d, and c were from the first heating run, the cooling run, and the second heating run, respectively [32].

Partial hydrolysis of poly (2-ethyl-2-oxyazoline) was reported by Kuringen et al. [20] and the series of PEOZ-EI copolymers were examined using DSC and thermogravimetric analysis (TGA.) All copolymers decomposed in a single step and were stable up to at least 306 ^{o}C (5% weight loss). TGA demonstrated that partially hydrolyzed copolymers are more hygroscopic than the parent polymer and contain some water, i.e., 3% for PEOZ-EI-6, even after complete drying of the solid polymer samples. The increased hygroscopicity of PEOZ after partial hydrolysis can be attributed to the strong hydrogen bond donating ability of L-PEI combined with the strong hydrogen bond accepting ability of PEOZ, resulting in the capture of water. PEOZ is an amorphous polymer with a glass transition temperature (T_g) of 61.8 ^{o}C and a melting temperature (T_m) of 60 ^{o}C, whereas L-PEI is semicrystalline as described above (with a T_g of -29.5 ^{o}C and a T_m of ~60 ^{o}C depending on hydrate state). All of the partly hydrolyzed copolymers were shown to be amorphous with intermediate T_g values ranging from 5.1 to 62.3 ^{o}C (**Table 1**).

Table 1. Thermal properties of PEOZ-EI co-polymers as determined by DSC and TGA.

Polymer	**Glass transition temperature (^{o}C)**	**Meting temperature (^{o}C)**	**TGA 5% weight loss (^{o}C)**	**Water loss (%)**
PEOZ	61.8	-	402	0
PEOZ-EI-6	62.3	-	357	3
PEOZ-EI-9	n.d.	-	351	3
PEOZ-EI-25	58.9	-	332	4
PEOZ-EI-43	47.6	-	312	6
PEOZ-EI-71	5.1	-	306	16
L-PEI	-29.5	60	376	6

Source : Kuringen et al. [20].

3.3. Behavior in aqueous and non-aqueous solutions

Soradech and co-worker [29] reported that L-PEI can be dissolved at 80 ^{o}C in water in order to break crystalline domains before freezing at -80 ^{o}C, followed by subsequent thawing at room temperature (25 ^{o}C), forming stable cryogels **(Fig. 11)**. The cryogels formed a dihydrated structure due to the high absorption of water molecules into L-PEI lattices. In addition, thermal cycling promoted physical crosslinking via the formation of structured crystalline domains of the polymer chains through phase separation. Several phases form

during the thermal cycling process. Initially, as the gel cools to low temperatures, the water phase freezes. This creates regions of high polymer concentration which can thus form crystallites and regions of low polymer concentration resulting in pore formation. The frozen gel was then thawed at room temperature to obtain interconnected macro-porous gels [33]. Reversibility of the L-PEI cryogels, shown by reheating the gel at 80 ^{o}C to form a transparent solution, confirmed their physical rather than chemical crosslinking (**Fig. 11**).

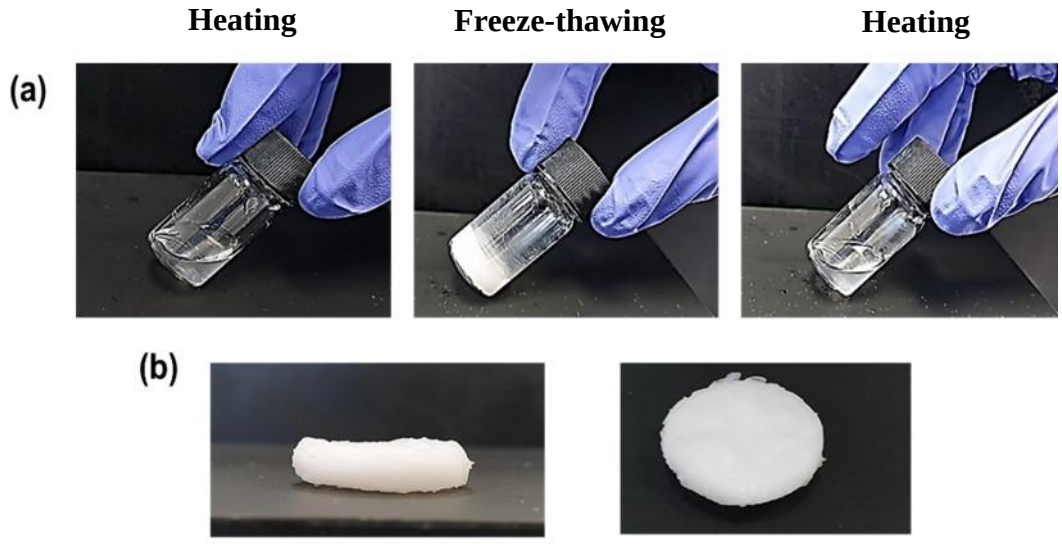

Fig. 11. Solution – gel – solution transition of L-PEI cryogels. The solution is initially heated to 80 °C forming a transparent solution. After freezing at - 80 ^{o}C for 3 h and then thawing at room temperature, an opaque gel is produced which, on subsequent heating to 80 °C, returns to a transparent solution (a). Appearance of L-PEI cryogels (b) [29].

The influence of solvent composition on the formation and physicochemical properties of L-PEI cryogels was also reported [29]. L-PEI was dissolved in ethanol-water mixtures before freezing at -80 ^{o}C for 3 h, and subsequent thawing at 25 ^{o}C. Dissolving L-PEI in ethanol alone did not result in the formation of cryogels; samples were cooled to -80 ^{o}C whereas the freezing point of ethanol is -115 ^{o}C**.** However, L-PEI in mixtures of water with ethanol did form gels. With increasing ethanol content, the gels became softer, probably due to reduced intermolecular hydrogen bonding between L-PEI macromolecules due to competition with solvent molecules (**Fig. 12)**. The transition from hard to soft gels was associated with a decrease in gel viscosity as the concentration of ethanol in the solvent mixtures increased. These results also correspond with literature reports that increasing concentrations of alcohol in aqueous mixtures decreased both rigidity and fusion temperature of PVA cryogels [34].

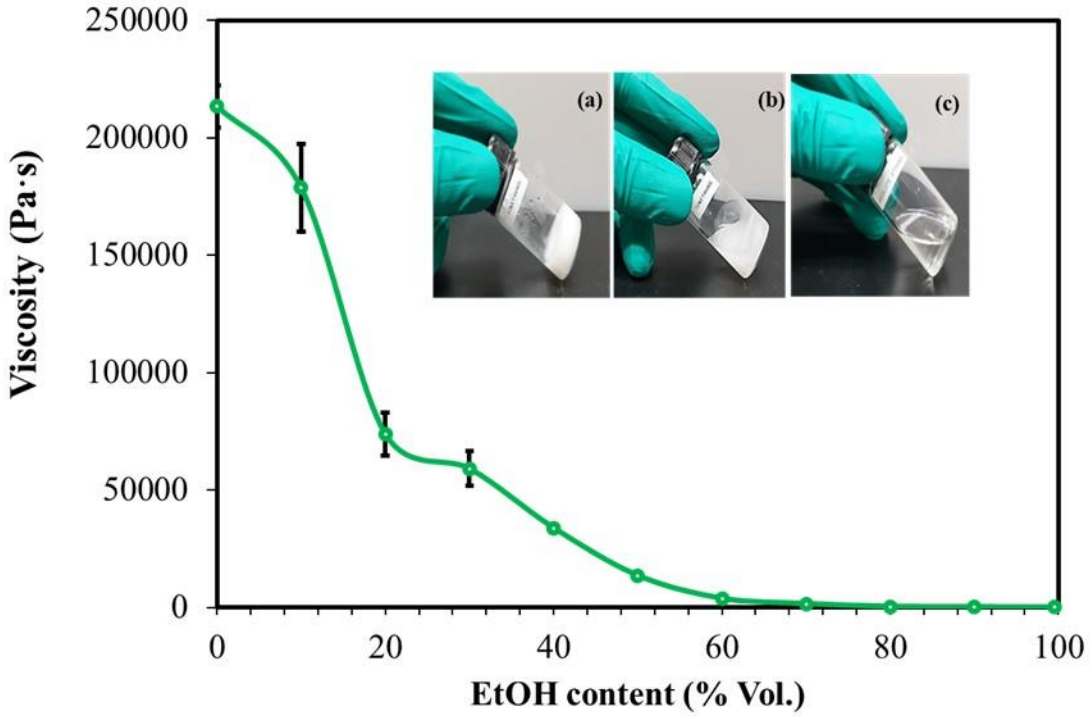

Fig. 12. Viscosities of L-PEI samples following their freezing and thawing in different ethanol/water mixtures and images of samples prepared at 20 % (a), 50 % (b) and 100 % (c) EtOH [29].

3.4. Complexes of polyethyleneimines

Polyelectrolyte complexes can be formed by strong electrostatic interactions between polycationic and polyanionic polymers with opposing charges [35]. When polyelectrolytes with opposite charges are mixed in aqueous solutions, new compounds can form immediately via salt bonding [36, 37]. Under acidic conditions, polyethyleneimine (PEI), a cationic polymer, has a positive charge ($CH_2CH_2NH_2^+$) [9]. Many studies have shown that complexes between PEI and anionic polymers can be formulated into a variety of dosage forms such as films [36], hydrogels [38], nanoparticles [39], beads [40], and liposomes [41].

Kopylova et al. [38] developed hydrogels from polyacrylic acid (PAC) and branched polyethyleneimine (B-PEI). PAC as a polycarboxylic acids with the polymeric amine formed polyelectrolyte complex hydrogels, with inter-chain salt bonds converting to covalent bonds.

Furthermore, Mülle et al. [39] created polyelectrolyte complex nanoparticles by combining B-PEI and poly (acrylic acid) (PAC) solutions, which they used in a drug delivery

system. The mixing ratio, mixing order, polyelectrolyte concentration, molecular weight and pH all influenced the size and internal structure of a complex formed by B-PEI and PAC.

Zezin et al. [36] presented a schematic diagram for polyelectrolyte complexes formed by PEI and PAC, which is shown in **Fig. 13**. They illustrate that the opposing positive charge of NH_2^+ in PEI and the negative charge of COO^- in PAC caused the PEI and PAC polyelectrolyte complex to form a film. The film was transparent and brittle when dry, and could swell when wet. The modulus of this film was approximately 2 to 10 MPa, and the elongation at break was approximately 500%. The PEI/PAC polyelectrolyte complex films exhibited high water permeability.

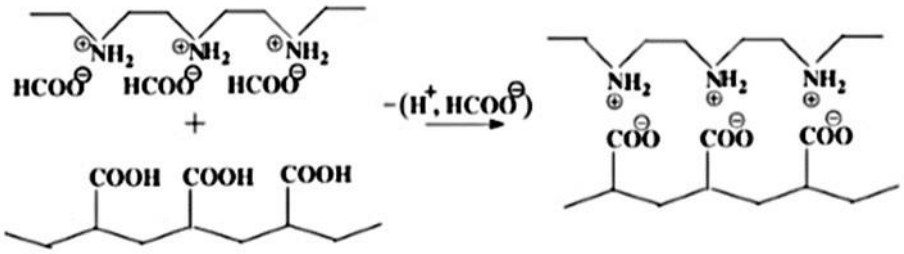

Fig. 13. Schematic diagram of polyelectrolyte complex between PEI and PAC [36].

Liu et al. [42] developed a lipo-polyethylene glycol-polyethyleneimine (PEI) complex (LPPC), a cationic lipocomplex designed to bind an active protein at a surface. LPPC can readily form LPPC/protein complexes and could capture antibodies, protein immunogens and beta-glucuronidase (G), through noncovalent binding it. Lin et al. [41] also created a cationic liposomal polyethyleneimine and polyethylene glycol complex (LPPC) for protein delivery.

Ray et al. [40] used a polyelectrolyte complex of sodium carboxymethyl xanthan gum and PEI to create a multiunit sustained release dosage form of diltiazem hydrochloride. The PEI-treated diltiazem resin was complexed with xanthan gum, and the beads formed between the two polymers with different charges. Drug release at pH 1.2 and pH 6.8 was 40% and 80%, respectively, depending on the formulation. Reduced swelling of the beads resulted in slower release of the drug due to the PEI treatment.

In addition to polyelectrolyte complex formed between PEI and anionic polymers, PEI can form complexes with various metal ions, including copper (II) [37, 43 - 45], nickel (II)

[46] and cobalt (II) [45, 46]. Takagishi et al. [47] explored complexation between branched PEI and divalent metal ions such as Co^{2+}, Zn^{2+}, Cu^{2+}, Ni^{2+} and azo dyes with hydroxyl groups (-OH) in their structures. The results showed that the addition of metal ions into PEI-dye binding systems resulted in a significant increase in binding. Also, it has been found that hydrolysis of nitrophenyl caproate by modified PEIs containing imidazole moieties is markedly enhanced in the presence of divalent metal ions and the order of effectiveness is $Cu^{2+} > Co^{2+} > Zn^{2+} > Ni^{2+} > Mn^{2+}$. During the course of these investigations, it was discovered that metal ions, specifically cupric ion, have a remarkable affinity for associating with PEI and its derivatives. In addition, it is well-known that amines form stable complexes with metal ions.

Lázaro-Martnez et al. [43] reported the formation of copper complexes with linear poly(ethylenimine hydrochloride) of different molecular weights (22, 87 and 217 kDa), discovering that the coordination of copper ions can produce a significant reduction in the chain mobility of its polymer, yielding homogeneous and ordered materials when Cu^{2+} was desorbed.

Pergushov et al. [37] studied the sorption of metal ions by polyelectrolyte complexes and reported that the monomer units of PAA and PEI polyelectrolyte complex were crosslinked with chelating ligands. As shown in **Fig. 14**, the interaction of metal ions with IPECs results in the sandwiching of these ions between PAA and PEI, which is coordinated by their functional groups, leading to the creation of triple (tricomponent) macromolecular co-assemblies containing metal ions.

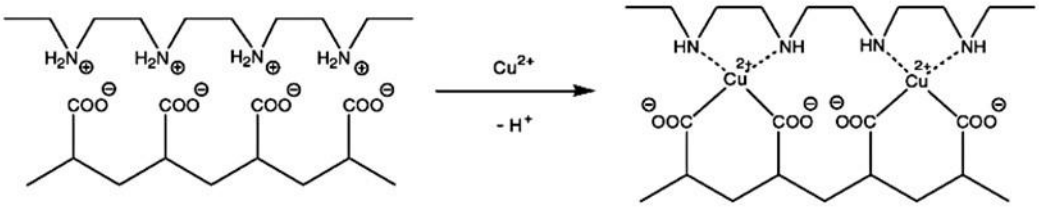

Fig. 14. Schematic diagram of macromolecular co-assemblies consisting of metal ions [37].

4. Toxicology of polyethyleneimines and derivatives

As a cationic polymer, PEI contains abundant amino groups and as a result has a certain degree of cytotoxicity. Cationic PEI enters cells by adhering to negatively charged transmembrane heparanproteoglycans, which can cause cell damage through membrane destabilization [49]. Additionally, the internalized PEI causes apoptotic cell death by forming pores in the mitochondrial membrane [50]. Whilst the cationic properties of PEI are advantageous for complexation, the relatively high charge density raises concerns for toxicity when in contact with biological tissues and cells. The toxicity of the polymers has thus been explored in various systems and models.

4.1. Cell based assays

Cytotoxicity assays have been extensively used to assess the safety of polymers and other materials. The 3-(4, 5-dimethyl-2-thiazolyl)-2, 5-diphenyl-2H-tetrazolium bromide (MTT) assay uses a colorimetric reaction to determine cellular metabolic activity since the MTT reagent can be reduced to a colored formazan product by viable cells. Other cytotoxicity tests include the sulforhodamine B (SRB) assay, the WST assay, and the clonogenic assay [48].

Using the MTT assay, Soradech et al. [49] showed that linear PEI is highly toxic to human dermal fibroblasts with an IC_{50} of 0.04 mg/mL, which correlates with previous literature reports [20]. L-PEI toxicity can be attributed to disruption of cell membranes, resulting in necrotic cell death, and disruption of mitochondrial membranes, resulting in cell apoptosis [50]. Furthermore, as a cationic polymer L-PEI accumulated on the outer cell membrane, causing necrosis [51]. Fischer et al. [52] reported that, due to its positive surface charge, L-PEI can bind to the negative charge of cell membrane phospholipids, cell membrane proteins, and blood proteins, resulting in cellular damage. The cytotoxicity of PEI is thus a major issue when using this polymer in pharmaceutical and biomedical applications [54] with numerous studies exploring cytotoxicity of linear and branched PEI and its analogues such as PEtOx-EI [20, 53-55].

Gibney et al. [53] reported that both concentration and molecular weight of PEI affects the viability of human papillomavirus type 18 DNA cells (HEp-2 cells, a liver cancer cell line) after 1 h, as shown in **Fig. 15** and **Table 2**. The highest toxicity in HEp-2 cells was reported for 10,000 kDa branched PEI, with an 80 % reduction in cell viability when cells were dosed at 10 µg/mL for 1 h. At the same concentration, only a marginal reduction in cell viability was

seen for branched polymers with lower molecular weights (600 and 1800 kDa). As expected, increasing exposure time also adversely affected cell viability.

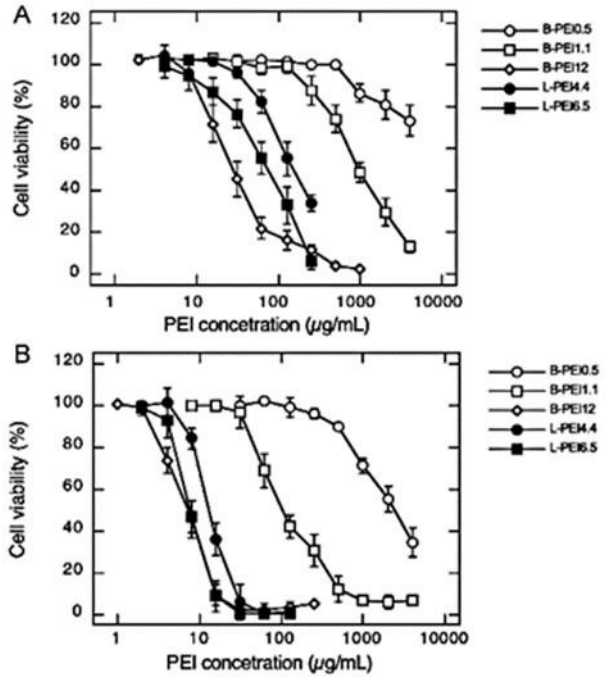

Fig. 15. Human epithelial (HEp2) cell viability after 1 h (a) and 24 h (b) exposure time to PEIs [53].

Table 2. Cytotoxicity of PEIs to human epithelial HEp2 cells [53]. (EC_{50} = Half maximal effective concentration whereas IC_{50} = Half maximal inhibitory concentration).

Type of PEI	**Mw (kDa)**	**EC_{50} (μg/mL)**	**IC_{50} (μg/mL)**	
			1 h	24 h
B-$PEI_{0.5}$	600	>4000	>4000	2305 ± 225
B-$PEI_{1.1}$	1800	>4000	1026 ± 90	116 ± 16
B-PEI_{12}	10000	>4000	27 ± 3	7 ± 0.4
L-$PEI_{4.4}$	2500	>250	155 ± 15	13 ± 0.9
L-$PEI_{6.5}$	25000	>250	69 ± 0.1	8 ± 0.4

Others have reported similar findings that an increase in either molecular weight or concentration of L-PEI decreased cell viability. Wang et al. [56], reported that the higher the molecular weight of PEI, the greater the toxicity in Chinese Hamster Ovary (CHO) and C2C12 myoblasts cells. No cytotoxicity was observed for L-PEI (0.8 and 1.2 kDa) at 20 μg/mL, whereas PEI 25kDa at the same concentration reduced cell viability by ~15%. Beyond the

concentration and molecular weight of PEI, Okon et al. [55] reported that linear PEI was less toxic than branched PEI in both HeLa and Vero cells, results which correlated with those from Gibney et al. [53].

Kafil and Omidi [54] reported cytogenomic testing of L-PEI and B-PEI in A431 cells (an epidermal cell line) to investigate the mechanism of apoptosis induction. They showed that internalization of B-PEI is higher than that of L-PEI, inducing greater toxicity in cell cultures. To assess the degree of possible DNA fragmentation within treated cells with polymers alone or as complexed with DNA, the widely used single cell electrophoresis or comet assay was exploited. **Fig. 16** shows the typical results obtained by means of the comet assay for A431 cells treated with PEI polymers and their polyplexes as well as with hydrogen peroxide, H_2O_2 (as a positive control known to induce DNA damage). There is no diffusion of fragmented DNA in untreated A431 cells (16a) or cells treated with L-PEI (16c). Diffusion of DNA fragments is seen when cells are treated with B-PEI (16b) and hydrogen peroxide (19d). Therefore, it was deduced that L-PEI is safer than B-PEI, though its transfection efficiency is lower than B-PEI.

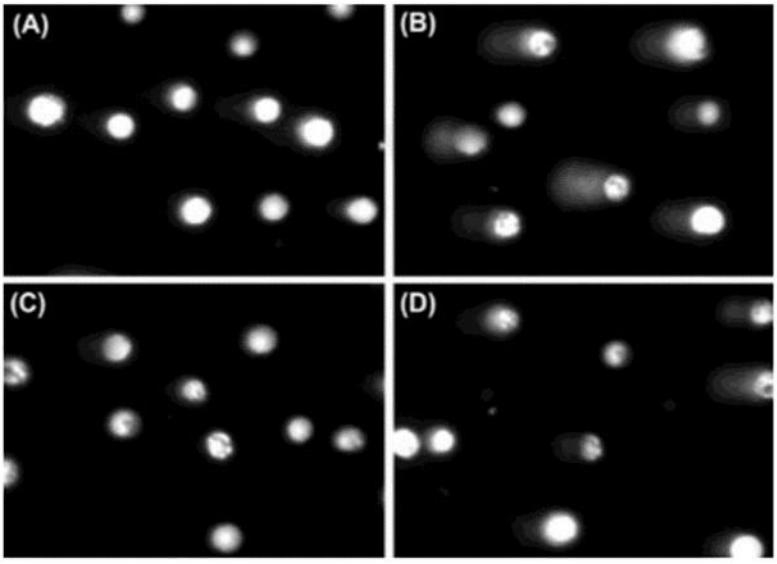

Fig. 16. DNA damaged detection in A431 cells using comet assay of untreated cells (a) Treated cells with hydrogen peroxide (b), treated cells with L-PEI (c), and B-PEI (d)[54].

4.2. Non-cell based assays of PEI toxicity

Beyond cell-based assays, the slug mucosal irritation (SMI) test has been employed to assess the toxicity of PEI [20], proving that this material is nontoxic, non-allergic and non-irritating [57]. The slug mucosal irritation (SMI) *in vivo* study, developed by Adriaens and co-workers [58]. The SMI assay has been used to predict irritation caused by materials and for rapid screening studies as opposed to using higher order animals in preliminary toxicological studies[59, 60]. The mucosal layer of the slug is located on the body's surface and is hence easily observable by the investigator. In this test, colorless mucus, secreted by slugs after contact with a test substance, is a good initial indicator of biocompatibility. The total amount of mucus produced serves as the main criterion to test the biocompatibility of formulations since these increases on exposure to stronger irritants [61]. These assessments provide quantifiable data for test materials to be classified as nonirritating, mild, moderate, or severely irritating[60].

This approach was used to test the toxicity of L-PEI and various polyoxazolines and their co-polymers. Mucus secretion by slugs in response to stimuli can predict sensitization in humans. After exposing slugs to polymer solutions (or films) the production and color of mucus are determined and compared to negative (phosphate buffered saline) and positive (1% benzalkonium chloride) controls. Slugs were exposed to solutions at 10 mg/mL for 1 h after which their mucus remained colourless, and there was no slug mortality, indicating severe tissue damage had not occured **(Fig. 17)**. Polyethyloxazoline (PEtOx) and PEtOx-PEI containing up to 25% L-PEI produced minimal mucus, and not statistically different to the negative control, showing that they are nonirritating. However, polymers with higher L-PEI contents and pure L-PEI resulted in mucus production, which may indicate that prolonged exposure may cause irritation and tissue damage[20].

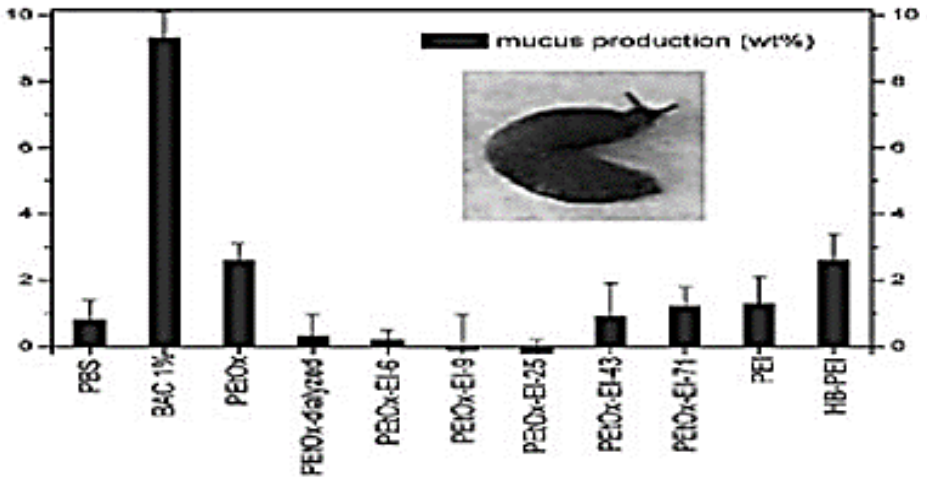

Fig. 17. Production of mucus by slugs on exposure to various polyoxazolines and co-polymers with PEI (slug mucosal irritation assay) [20].

5. Derivatives of polyethyleneimines

In order to improve biocompatibility of the polymer, or to alter its physical properties, numerous studies have reported modifications to PEI and are discussed below.

5.1. Thiolated PEI

Aravindan et al. [62] compared redox-sensitive crosslinked compounds to branched polyethyleneimine (25 kDa) as transfection agents. Using N-succinimidyl 3-(2-pyridyldithio) propionate as a hetero-bifunctional reagent, thiol derivatives of polyethyleneimine were synthesized **(Fig. 18)**. The PEI chain has thiol groups due to the reduction of pyridyl disulfide derivatives from 1, 4-dithiothreitol (DTT). Thiolated polymers had 390 to 2300 mmol SH groups/mol, whilst polymeric backbones were also crosslinked by disulfide bonds giving polymers with lower thiol concentrations. Thiolated and cross-linked derivatives of PEI caused less hemolysis than the parent PEI. **Fig. 19** shows the transfection efficiencies of original PEI, thiolated PEI and crosslinked derivatives in HEK293 cells. Unmodified PEI and PEI treated with 3% H_2O_2 at 1:10 DNA:polymer w/w had similar transfection efficiencies, however thiolated and crosslinked PEI gave better transfection efficiencies than unmodified PEI. Also, increasing the polymer derivatives' thiol concentration boosted transfection efficiency, albeit not as much as crosslinked derivatives. Compared to other crosslinked derivatives, PEI-SS5

(disulfide linked PEI prepared by oxidation of thiolated PEI SH5) had a lower transfection efficiency [62].

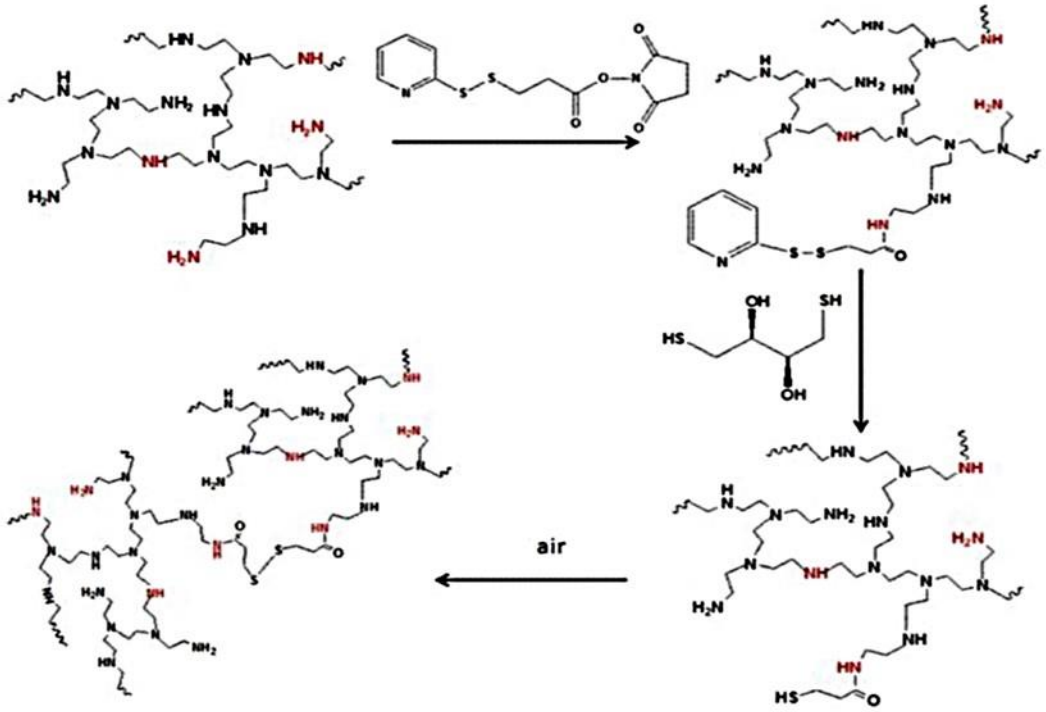

Fig. 18. Synthesis of thiolated polyethyleneimines using N-succinimidyl 3-(2-pyridyldithio) propionate and 1, 4-dithiothreitol and subsequent crosslinking to form disulfide bonds [62].

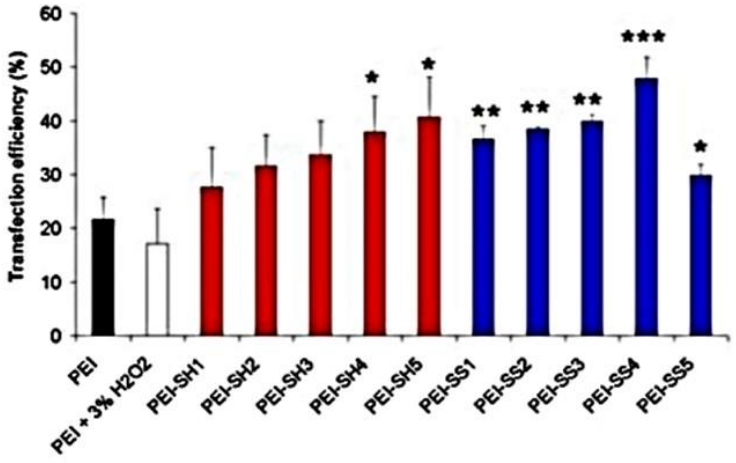

Fig. 19. Transfection efficiency between thiolated and crosslinked derivatives of PEI, in comparison to unmodified PEI and unmodified PEI containing 3% H_2O_2 [62]. SH indicates thiolated PEI; b) SS indicates disulfide linked PEI. These samples were prepared by oxidation of PEI-SH samples (e.g., PEI-SS1 was prepared by oxidation of PEI-SH1).

5.2. Acetylated PEI

Commercially available branched 25 kDa PEI was acylated using acetic anhydride or propionic anhydride to modify the primary and secondary amines on the polymeric backbone to secondary and tertiary amides, substituted with acetyl (ACAN) or propionyl group (PRAN), as shown in **Fig. 20**. ^{1}H-NMR spectroscopy showed that the PEI had 31% primary, 41% secondary, and 28% tertiary amines, with a branching degree of 1.46. Due to the higher steric barrier of the longer acyl groups, the percentage of modification decreased from ACAN to PRAN and the polymer's buffering capacity and DNA binding ability changed when comparted to the parent polymer, due to a reduction in primary amines. However, the acylated branched 25 kDa PEI were more hemocompatible and less cytotoxic than B-PEI, with higher transfection efficiencies due to effective plasmid release in the cytoplasm. Polymers with buffering capabilities > 50% but <80% of PEI demonstrated increased transfection efficiency [63]. When compared to acetic anhydride modified polymers, propionic anhydride modified polymers demonstrated greater membrane contact and optimal binding strength with plasmid DNA, making them superior transfection agents; a vector of 0.3 mol propionic anhydride at a 1:2 w/w DNA:polymer composition was the most effective in terms of transfection efficiency and cytotoxicity [63].

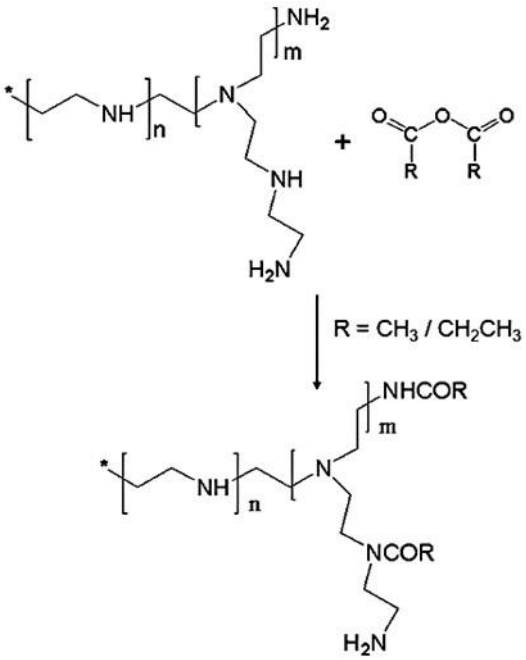

Fig. 20. Scheme of synthesis of acylated polyethyleneimine with acetic and propionic anhydride [63].

5.3. Synthesis of poly (2-oxazolines) by functionalized L-PEI

Using functionalized L-PEI, it is possible to produce poly(2-oxazolines) that contain a series of carboxylic acids in the side chain of the amino groups of L-PEI, the amount of which varies depending on the coupling reagent used [15] **(Fig. 21)**.

Fig. 21. Synthesis of poly(2-oxazolines) from functionalized L-PEI [15].

Sedlacek et al. [5] described a novel method for producing superhydrophilic poly(2-alkyl-2-oxazoline)s (PAOx) from poly(2-ethyl-2-oxazoline) (PEtOx). Hydrolysis of PEtOx yielded L-PEI, which was then acylated with amine groups of L-PEI by a series of carboxylic acids. L-PEI amidation was accomplished using a standard peptide coupling protocol that included (benzotriazol-1-yloxy)-tripyrrolidinophosphonium hexafluorophosphate (PyBOP) as a coupling agent, DIPEA as a base, and dry DMF as a solvent, as shown in **Fig. 22**. The physicochemical and biological properties of hydrophilic poly(2-alkyl-2-oxazoline)s or PAOx's were evaluated for biomedical applications. The results showed that the modification of L-PEI with carboxylic acid increased the relative hydrophilicity of the polymers, with poly(2-methoxymethyl-2-oxazoline) or PMeOMeOx having the highest hydrophilicity whereas poly(2-[methoxy-ethoxy-ethoxymethyl]-2-oxazoline) or PDEGOx had the lowest glass transition temperature (Tg). All modified L-PEI's were found to be non-cytotoxic at 0.1 mg/mL, suggesting potential use in pharmaceutical and biomedical products.

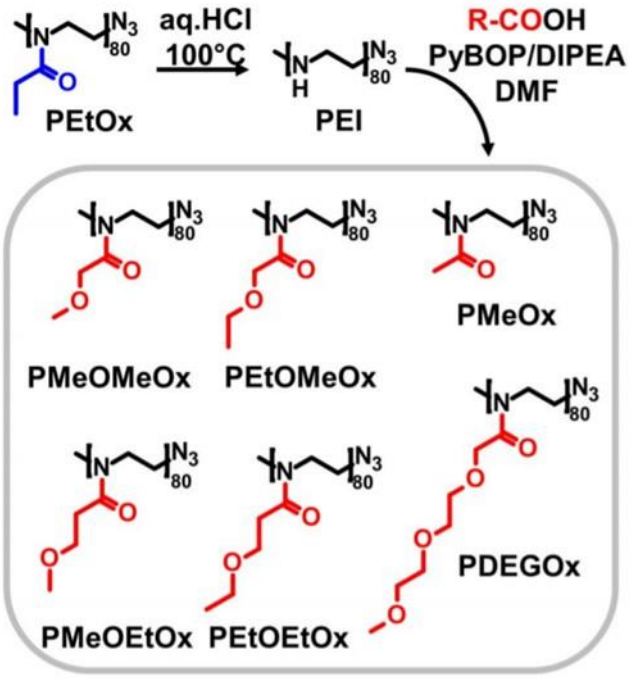

Fig. 22. Synthesis of poly (2-oxazolines) series by functionalisation of L-PEI including poly(2-methoxymethyl-2-oxazoline)(PMeOMeOx), poly(2-ethoxymethyl-2-oxazoline) (PEtOMeOx), poly(2-methyl-2-oxazoline)(PMeOx),poly(2-methoxyethyl-2-oxazoline)(PMeOEtOx), poly(2-ethoxyethyl-2-oxazoline) (PEtOEtOx) and poly(2-[methoxy-ethoxy-ethoxymethyl]-2-oxazoline) (PDEGOx) [5].

Shan et al. [64] synthesized a series of poly(oxazolines) from commercially available 50 kDa PEOZ, including poly(2-methyl-2-oxazoline) (PMOZ), poly(2-propyl-2-oxazoline) (PnPOZ), and poly(2-isopropyl-2-oxazoline) (PiPOZ) via PEI **(Fig. 23)**. The synthesis hydrolysed PEOZ to obtain poly(ethylene imine), which was then functionalized with acetic, butyric, or isobutyric anhydrides. The poly(2-oxazolines) series was used to make solid dispersions of haloperidol, a model poorly-water soluble drug. The results revealed that increasing the number of hydrophobic groups (-CH_2- and -CH_3) in the polymer contributed to greater inhibition of haloperidol crystallinity in the order: PnPOZ = PEOZ > PMOZ. Because of the lower critical solution temperature and the insolubility of this polymer in the dissolution medium, solid dispersions of drug with poly(n-propyl-2-oxazoline released the drug very slowly.

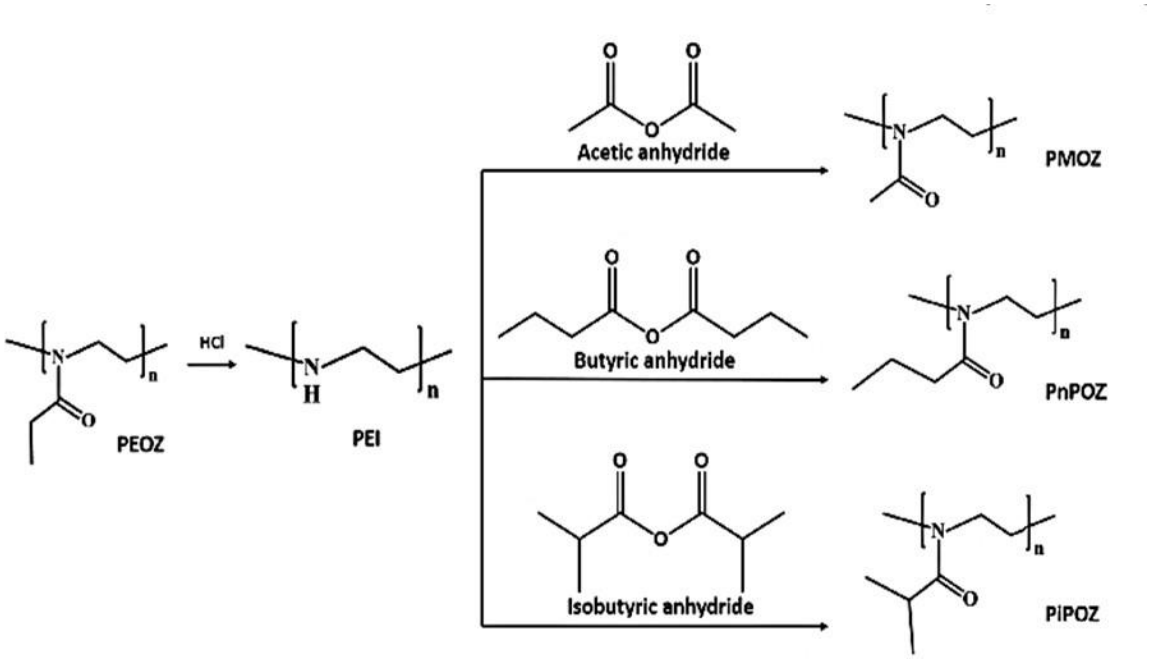

Fig. 23. Synthesis of high molar weight poly(2-methyl-2-oxazoline) or PMOZ, poly(2-propyl-2-oxazoline) or PnPOZ and poly(2-isopropyl-2-oxazoline) or PiPOZ by hydrolysis of PEOZ [64].

Shan et al.[60] also synthesized methacrylated poly(2-ethyl-2-oxazoline) (MAPEOZ) by partial hydrolysis of 500 kDa PEOZ, which was then reacted with methacrylic anhydride to obtain poly[(2-ethyl-2-oxazoline)-co-ethylenimine] P(EOZ-co-EI) **(Fig. 24)**. The secondary amines in P(EOZ-co-EI) provide reactive sites for additional methacrylation via reaction with methacrylic anhydride in the presence of TEA as a basic catalyst. P(EOZ-co-EI) copolymers were chosen for further methacrylation after 0.5, 1, 2, and 3 hours of partial hydrolysis. The temperature-responsive properties of MAPEOZ were dependent on the degree of methacrylation. On that basis, three soluble MAPEOZ derivatives with varying degrees of methacrylation were chosen and tested for cytotoxicity against the HEK293 cell line, revealing no significant cytotoxicity and PEOZ and MAPEOZ did not cause mucosal irritation in a slug mucosal irritation assay. The presence of methacryloyl groups and residual amines had a remarkable synergistic effect on mucoadhesive properties of these polymers.

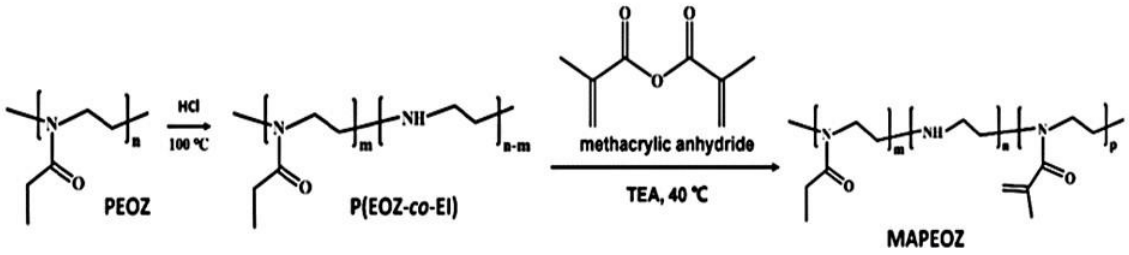

Fig. 24. Synthesis of methacrylated poly(2-ethyl-2-oxazoline) (MAPEOZ) [60].

5.4. Nucleophilic substitution or alkylation of PEI

L-PEI contains a secondary amine with a free electron pair, allowing it to be used in nucleophilic substitutions with, for example, an alkyl halide. Alkylation with an alkyl halide is a common method for substituting L-PEI, which is then reacted with an alkaline reagent, such as potassium bicarbonate or potassium carbonate [15].

L-PEI can be substituted with 4(5)-bromomethylimidazole [15]. Sanders et al. [65] synthesized and characterised linear poly(methyl ethylene imine) (LPMEI) conductivities using alkylated linear PEI. Lambermont-Thijs et al. [66] synthesized linear poly(benzyl ethylene imine) (PBnEI) by nucleophilic substitution of PEI (nucleophile) with benzyl bromide (electrophile). The synthesis of PBnEI used bromide as a leaving group and potassium carbonate as a weak base, which deprotonated via post-nucleophilic substitution (SN_2). The competitive alkylation of benzyl bromide and potassium carbonate results in the formation of a secondary amine, which can then be alkylated to give the tertiary amine. A viscous and sticky PBnEI wax with a glass transition temperature (T_g) of -18 ^oC was obtained and was insoluble in water and a mixture of water and ethanol due to the increased hydrophobicity.

Soradech et al. [49] synthesized poly(3-hydroxypropyl ethyleneimine) (P3HPEI) using nucleophilic substitution of L-PEI with 3-bromo-1-propanol in absolute ethanol, with potassium carbonate as a base, as shown in **Fig. 25**. NMR and FTIR spectroscopies confirmed successful conversion of L-PEI to P3HPEI. P3HPEI had good water solubility, was significantly less toxic than the parent L-PEI and had a low glass transition temperature (T_g = -38.6 ^oC).

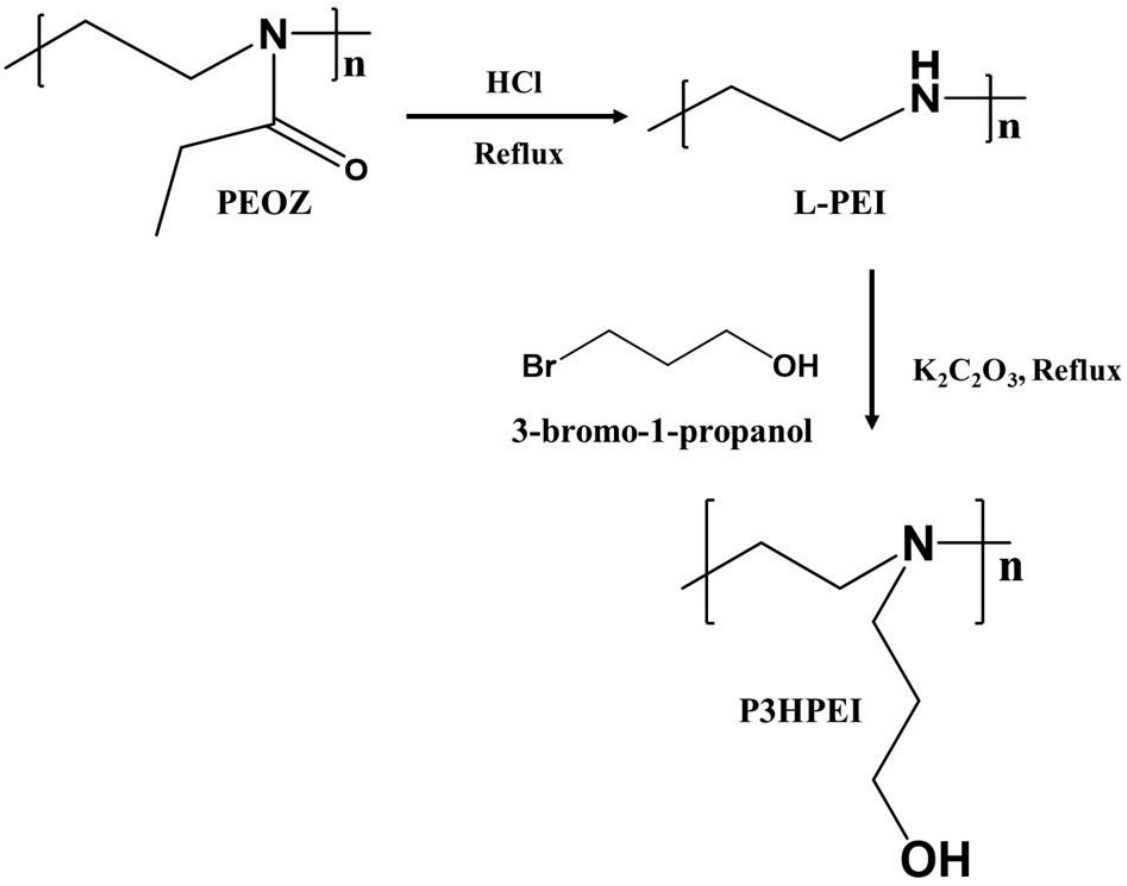

Fig. 25. Synthesis of poly(3-hydroxypropyl ethyleneimine) or P3HPEI from poly(ethyloxazoline) via linear PEI. [49].

Patil et al. [67] synthesized hydroxyethyl substituted L-PEI, using nucleophilic substitution between L-PEI and 2-bromoethanol, as a carrier for siRNA delivery. The L-PEI was modified to produce hydroxyethyl-substituted L-PEI with a degree of substitution ranging from 15% to 45%. The effect of modification on the physicochemical properties of the polymer, including buffering capacity, solubility, biocompatibility and stability was investigated. Surprisingly, despite the absence of ionizable amines, substitution enhanced solubility and even overcame the pH-dependent solubility of L-PEI.

Soradech et al. [68] modified L-PEI using nucleophilic substitution between L-PEI and amides with different side-chain lengths including 2-bromoacetamide, 3-chloropropionamide and 2-bromopropionamide to obtain poly(2-acetamide ethyleneimine), poly(2-propionamide ethyleneimine) and poly(3-propionamide ethyleneimine), respectively; an example is in **Fig 26**. Poly(2-acetamide ethyleneimine) and poly(2-propionamide ethyleneimine) were water-soluble and presented low toxicity (< 5 mg/mL) in human dermal fibroblast cells, whilst poly(3-

propionamide ethyleneimine) was also water-soluble but was more toxic than the above two polymers (< 1 mg/mL). **Table 3** summarizes some of the modified PEI materials synthesized in our laboratories and their key features and uses.

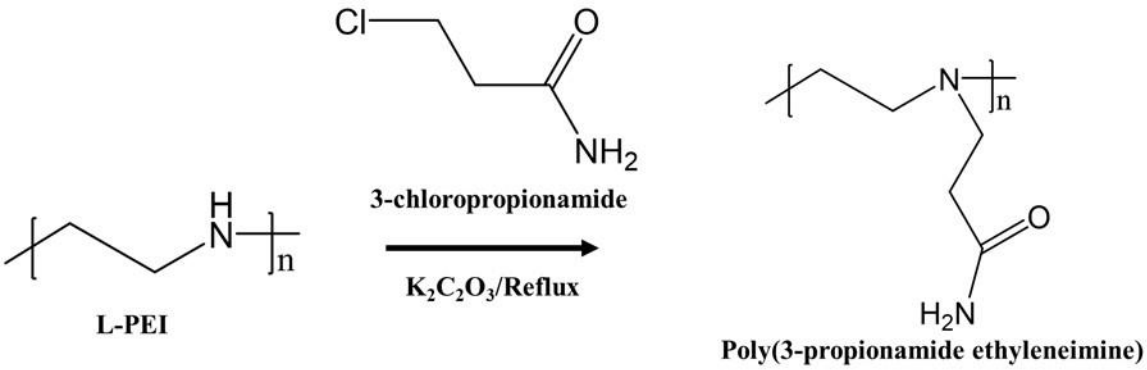

Fig. 26. Synthesis of poly(3-propionamide ethyleneimine) from linear PEI.

Table 3. Summary of some modified PEI materials using nucleophilic substitution with different alkyl halides and their resultant properties.

Modified L-PEI	Alkyl halide	Chemical structure of final product	Properties and applications
Poly(2-hydroxyethylethyleneimine) [67].	2-bromoethanol	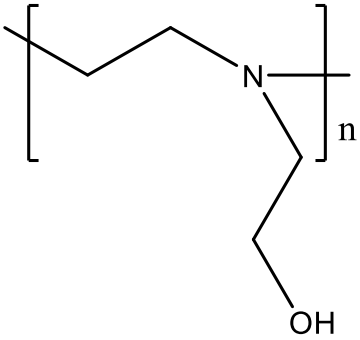	▪ Soluble in water ▪ Low glass transition temperature (below 0 ^{o}C) ▪ Low toxicity above 5 mg/mL ▪ Sticky ▪ Liquid at room temperature

Poly(3-hydroxypropyl ethyleneimine) [49]	3-bromo-1-propanol	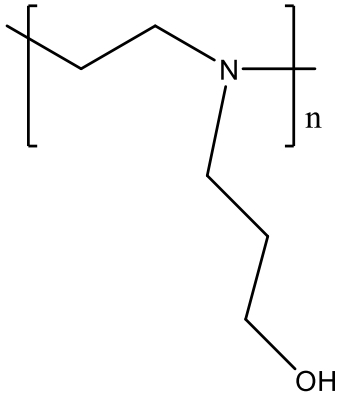	▪ Soluble in water ▪ Low glass transition temperature (below 0 °C) ▪ Low toxicity in human dermal fibroblast cells above 5 mg/mL ▪ Sticky ▪ Liquid at room temperature
Poly(benzyl ethylene imine) [66]	Benzyl bromide	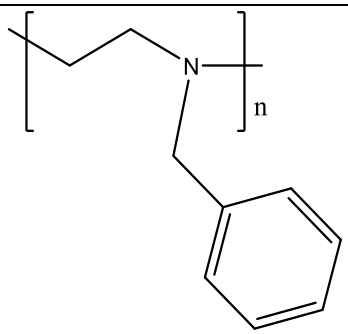	▪ Insoluble in water ▪ Low glass transition temperature (below 0 °C) ▪ Sticky
Poly (methyl ethylene imine) [65]	Methyl iodide	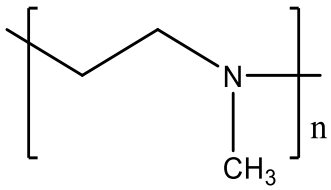	▪ Soluble in chloroform, THF, acetone, ethanol, methanol, N,N-dimethylformamide, HFIP and water at room temperature and in n-hexane above 45 °C ▪ Yellow powder
Poly (2-acetamide ethyleneimine) [68]	2-bromoacetamide	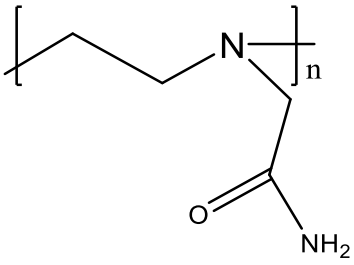	▪ Soluble in water ▪ Glass transition temperature ~ 80 °C ▪ Low toxicity in human dermal fibroblast cells below 5 mg/mL

Poly (3-propionamide ethyleneimine) [68]	3-chloro propionamide	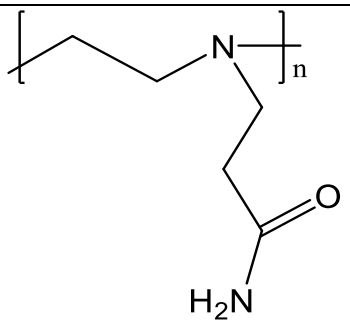	▪ White powder ▪ Soluble in water ▪ Glass transition temperature ~ 25^{o}C ▪ Low toxicity in human dermal fibroblast cells below 1 mg/mL
Poly (2-propionamide ethyleneimine) [68]	2-bromo propionamide	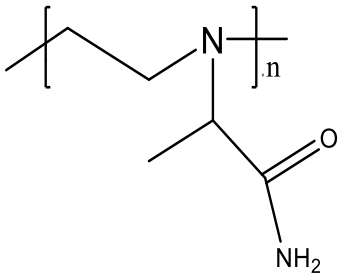	▪ Yellowish powder ▪ Soluble in water ▪ Glass transition temperature ~ 80 ^{o}C ▪ Low toxicity in human dermal fibroblast cells below 5 mg/mL

5.5. Reductive methylation of PEI

By reducing alkylation, Lambermont-Thijs et al. [66] produced linear poly(ethyl ethylene imine) (PEEI) and linear poly-(methyl ethylene imine) (PMEI). Because poly(2-methyl-2-oxazoline) or PMeOX is insoluble in any solvent for a reduction process, the synthesis of PEEI was initiated with L-PEI; L-PEI was dissolved in acetic acid and then sodium borohydride ($NaBH_4$) was slowly added drop-wise. As ~half of the secondary amines were converted to ethylated monomer units, some acetamido-groups were also obtained. The reduction was then be completed by dissolving the polymer in dry tetrahydrofuran (THF) and adding borane/dimethylsulfide (BH_3/DMS) as a reducing agent to form PEEI. Proton NMR spectroscopy validated the synthesis. Reductive methylation was also used to synthesise PMEI by dissolving L-PEI in water and adding formaldehyde and formic acid. The polymer was then purified using CH_2Cl_2.

5.6. Chitosan conjugation on PEI

Jiang et al. [69] improved chitosan transfection efficiency by grafting with L-PEI (CHIg-PEI). As shown in **Fig. 27**, the synthesis was via an imine reaction between periodate-oxidized chitosan and polyethyleneimine (PEI). Multi-angle laser scattering and proton NMR was used to characterise the CHI-g-PEI copolymer, which varied with molecular weight and composition. Complexation between the copolymers and plasmid DNA (pDNA) at various charge ratios was also studied. The results showed that CHI-g-PEI had a high efficiency of DNA binding, implying that it would protect DNA from nuclease attack within cells. Furthermore, a reduction in particle size of the CHI-g-PEI/DNA complexes was seen with increasing charge ratios. The conjugated chitosan had lower cytotoxicity than 25 kDa L-PEIand CHI-g-PEI/DNA complexes at high nitrogen:phosphate (N/P) ratios resulted in higher transfection efficiencies in HeLa, 293T, and HepG2 cell lines.

Triphati et al. [70] also created linear polyethyleneimine-graft-chitosan copolymers (L-PEI-g-CS). In comparison to L-PEI and chitosan, L-PEI-g-CS again demonstrated significantly improved transfection, endosomal escape and DNA release kinetics.

Wong et al. [71] reported that low MW L-PEI grafted with chitosan resulted in higher transfection efficiency of L-PEI-g-CS, with improved biocompatibility, cellular uptake, and buffering ability compared to PEI alone (25 kDa). According to Park et al. [72], increasing the level of the targeting ligand tended to increase the transfection efficiency of PEI-g-CS polymers.

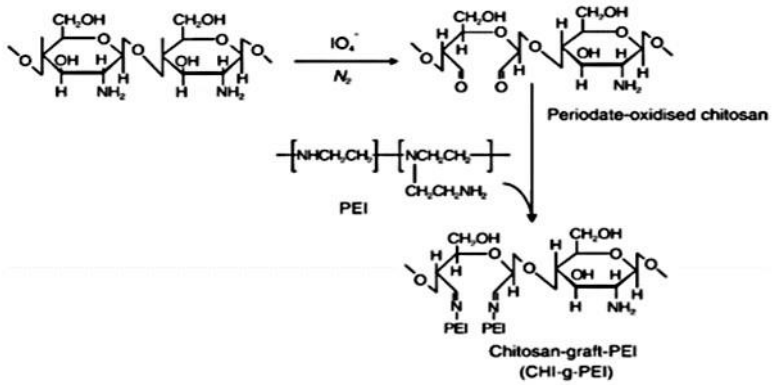

Fig. 27. Synthesis of chitosan grafted with PEI (CHI-g-PEI) [69].

5.7. PEGylation of branched polyethyleneimine

As described above, a notable limitation to the widespread biomedical use of L-PEIs is the high cytotoxicity in cells caused by their positive charge[73]. To mitigate this, surface modification by PEGylation of PEIs has been explored [74, 75].

Wen et al. [76] modified PEI surfaces by covalent modification of the amines, including neutralizing negatively charged PEI with acetic anhydride (PEI–Ac), succinic anhydride (PEI–SAH), or by hydroxylating PEI with glycidol (PEI–Gly) or poly(ethylene glycol) (PEI–poly(ethylene glycol)) **(Fig. 28)**. There were no cytotoxic effects of the PEI derivatives in mouse fibroblast (L929) cells at concentrations up to 200 μg/mL whereas 10 μg/mL PEI was toxic to these cells. The PEI surface charge could be tailored to be positive, negative or neutral, with partial neutralization of the surface amines of PEI derivatives potentially useful for gene delivery. In addition, it improves efficiency for drug delivery, for example, PEGylation of B-PEI provided an efficient strategy to target tumor microenvironment, in turn afforded superior therapeutic outcome in anti-tumor activity [75].

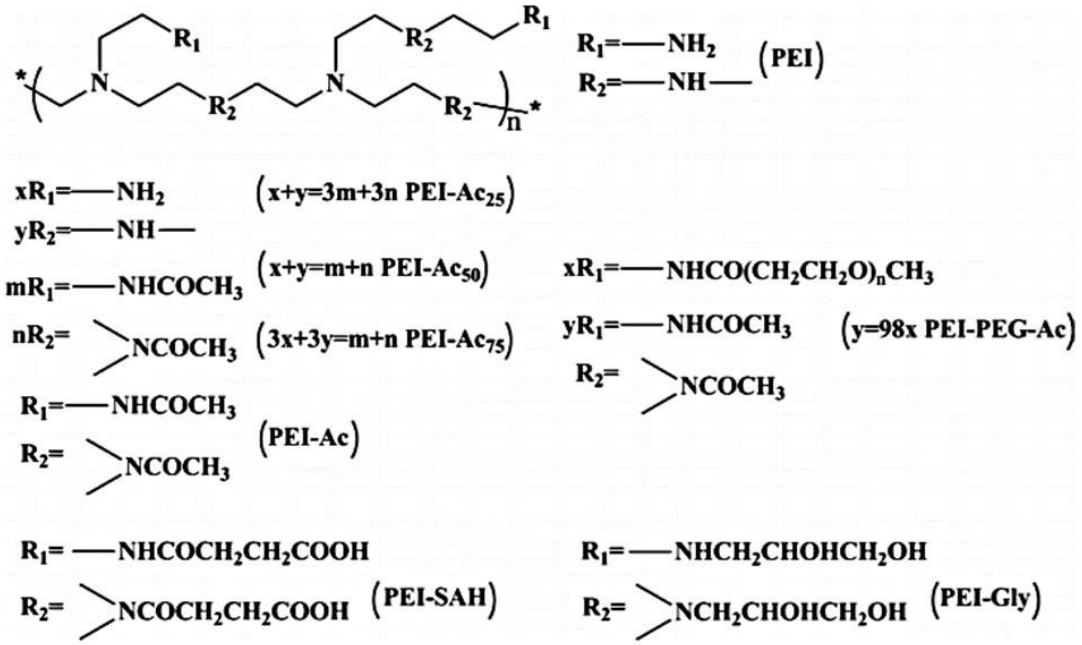

Fig. 28. Surface modification of B-PEI by PEGylation [76].

6. Pharmaceutical and biomedical applications

6.1. Gene delivery

Gene delivery (usually DNA) is only effective if the material is protected throughout its transport through a cell to reach the endogenous genome within the cell nucleus. Vectors used for gene delivery can be broadly classified as those that use a virus as a carrier (usually a recombinant virus) or synthetic vectors. Critical issues include the ability to deliver the gene to the correct (target cell), cellular toxicity from the vector and efficiency or gene transfer and subsequent expression [77].

These is extensive literature regarding development of non-viral gene delivery systems such as liposomes or nanoparticles. The ability to protect DNA from degradation in the extracellular medium, to cross the cell membrane, and to release the gene(s) with low toxicity and high efficiency to the cells is a key criterion for a capable vector [78]. Among polymers, cationic PEI is commonly used for gene delivery since PEI can complex with DNA molecules core [79 - 81], resulting in small homogeneous particles (less than 100 nm) [82]. The small and uniform particle size results in more efficient transfection, with a significant increase in DNA protection against degradation by nucleases when compared to other polycation vectors, attributed to the higher charge density and greater complex efficiency with DNA (and oligonucleotides) [82]. Guillem et al. [83] created an immune-polyplex from streptavidin-polyethyleneimine (St–PEI), as a targeted non-viral vector for gene delivery in human lymphoma cell lines. The St–PEI was created by covalently coupling N-succinimidyl 3-(2-pyridildithio)-propionate or SPDP linker molecules with both streptavidin and PEI resulting in an immune-polyplex system. Due to its specificity and selectivity in nucleic acid transfer, the immune-polyplex was an efficient and effective non-viral vector. As shown in **Table 4**, many modified PEI have been developed to improve gene delivery properties.

Table 4. Examples of modified PEIs that have been evaluated for gene delivery.

Modified PEI	Positive and negative effect	References
1. Grafting targeting ligands on PEI		
HIV-1 Tat peptides (RGD) grafted with SPDP	Increase in gene expression	Kunath et al. [84]
2. Polyplexes (PEI/DNA) coated with PEGylated PEI		
Grafting RGD on PEI/DNA complexes and coated by PEGylated PEIs	Improving cellular uptake and transfection efficiency in neuronal cells	Kursa et al. [85] and Suk et al.[86]
3.PEI gaffing with poly (amino acids)		
Poly (γ-benzyl l-glutamate) (PBLG-) grafted PEI	Effect on down-regulated luciferase for gene expression in cells.	Chen et al.[87]
Poly(phenylalanine) grafted PEI	Inducted tumor apoptosis and inhibited tumor growth.	Xia et al. [88]
4. Linear aliphatic acids and steroids grafted with PEI		
Oleic and stearic acid grafted PEI	Generation of water- soluble lipopolymers, Enhancement of membrane interaction and trafficking into cells.	Alshamsan et al.[89]
5.Chitosan conjugation on PEI		
L-PEI grafted chitosan (PEI-g-CS)	Increase in transfection efficiency, endosomal escape, and kinetic release of DNA.	Tripathi et al.[90]
Galactosylated poly(ethylene glycol)-chitosan-graft-PEI	Enhanced DNA delivery to liver cells.	Jiang et al[91]
6. Disulfide cross-linked PEI		
6.1 Disulfide cross-linked PEI/DNA complexes using the homo-functional cross-linker *N*-succinimidyl 3-[2-pyridyldithio]- propionate	Increasing transfection efficiency and increasing the half-life of the pDNA in blood.	Neu et al.[92]
6.2 Disulfide cross-linked linked PEI using cross-linkers dithiobis (succinimidyl propionate) and dimethyl-3,3'-dithiobispropionimidate	Enhanced transfection efficiency in CHO cells.	Gosselin et al.[93]
7. Liposome polyethylenimine complexes	Enhanced DNA and siRNA delivery.	Schäfer et al. [94]
8. PEGylation of PEI	Reduced cytotoxicity and hemolytic activity. Increased *In vitro* transfection efficiency compared to PEI25.	Mao et al. [95]
9. Polyester conjugation on PEI	-Beneficial effect of PEG-co-PCL grafting onto PEI25 in buffering capacity, stability, and surface charge of polyplexes [96] -Reduced toxicity with significant siRNA-mediated gene silencing compared to parent polymer (PEI25)[97]. -Reduced the inherent toxicity of cationic polymers by virtue of surface charge neutralization [98].	Zheng et al. [96] Liu et al. [97] Merdan et al. [98]
10. PEI-based organic–inorganic composites nanoparticles	- Increased efficient gene delivery to targeted glioblastoma cells and the further inhibition of protein expression.	Kong et al. [99]
11. PEI-derived copolymers or conjugation of a hydrophilic polymer layer onto the surface of preformed complexes	Promote gene delivery in the case of vectors with ahigh intrinsic endosomolytic capacity	Petersen et al. [100 - 101]

6.2. Antimicrobial formulations

Cationic polymer based on PEI have been widely used as antimicrobial agents due to the positive charge from cationic PEI which can electrostatically interact with negatively charged bacterial cell surfaces.

Khalil et al. [102] reported that addition of PEI to both hydrophilic and hydrophobic antibiotics increased their efficacy. Azevedo et al. [103] discovered that PEI can penetrate into and disrupt bacterial cell membranes, so inhibiting bacterial growth. Traditionally, cationic poly(ethylene imine) polymers (PEIs) have been utilised as drug carriers in biomedical application because of their ability to enter cells or permeabilize cell membranes [103 - 105]. Gibney et al. [53] studied the effects of molecular architecture and size of a series of relatively low molecular weight B-PEIs and L-PEIs on antibacterial activity. The activity against *E. coli and S. aureus* was dependent on both the PEI structure and molecular weight and it was notable that the PEIs exhibited greater activity against the Gram positive organism *S. aureus* than against the Gram negative *E. coli* yet. Membrane permeabilization assays suggested that PEIs exerted their antibacterial activity by mechanisms other than membrane disruption.

Silver (Ag^{+}) has long been used for its antimicrobial properties in wound dressing, creams and as a coating on medical devices. Xu et al. [106] used PEI 25kDa to synthesize PEI-capped silver nanoclusters (AgNCs), and the antibacterial activity of PEI-AgNCs determined. Although PEI demonstrates strong antimicrobial activity, the incorporation of silver nanoclusters resulted in higher surface-to-volume ratios than with more traditional nanomaterials. PEI-AgNCs were synthesized by varying the molecular weights of PEI (0.6 to 25 kDa) before the antibacterial activities were determined using agar plate and broth dilution techniques. PEI-AgNCs had higher antibacterial activity when used with a lower molecular weight PEI. **(Fig. 29)**.

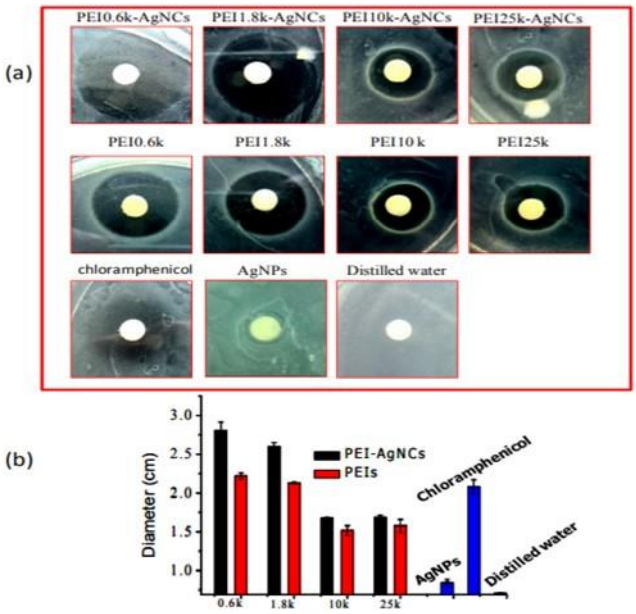

Fig. 29. Antibacterial activity against *E. coli.* of PEI-capped silver nanoclusters (AgNCs) or PEI-AgNCs, PEIs, and silver nanoclusters (AgNPs) [106].

Quaternary ammonium polyethyleneimine (QPEI) possesses excellent antibacterial activity because of the combined effects of the antibacterial groups on the macromolecular chains [107, 108]. The QPEI disrupts cell membranes and releases the intracellular contents [109]; Generally, cationic polymers exhibit excellent antibacterial activity resulting from the strong electrostatic interactions with the negatively charged bacterial cell surface [110].

Gao et al. [109] reported that propylene oxide was used as an alkylating agent to alkylate the primary and secondary amine groups on the macromolecule chains of PEI. TPEI was created as a result of the ring-opening and addition reactions of propylene oxide and PEI. Tertiary amine groups of TPEI were quaternized using benzyl chloride, yielding quaternized PEI, or QPEI. QPEI exhibited strong antibacterial activity due to its higher density of quaternary ammonium groups on the backbone, resulting in electrostatic interactions and strong adsorption between QPEI and *E. coli*. The quaternary ammonium structure on PEI caused disruption of the cell membranes, intracellular content release and hence cell death.

Lana et al. [111] synthesised four quaternized ammonium branched PEI derivatives with different alkyl halides i.e., bromoethane (C2), 1-bromobutane (C4), 1-bromohexanel (C6) and 1-bromoheptane (C8) (**Fig. 30**), which exhibited broad-spectrum antimicrobial activity against both Gram-negative (*E. coli* and *P. aeruginosa*) and Gram-positive (*B.*

amyloliquefaciens and *S. aureus*) bacteria. Branched PEI substituted with 1-bromohexanel (QPEI-C6) exhibited the highest antimicrobial activity again demonstrating that activity is related to molecular weight; QPEI-C6 was also shown to be biocompatible at the minimal inhibitory concentrations.

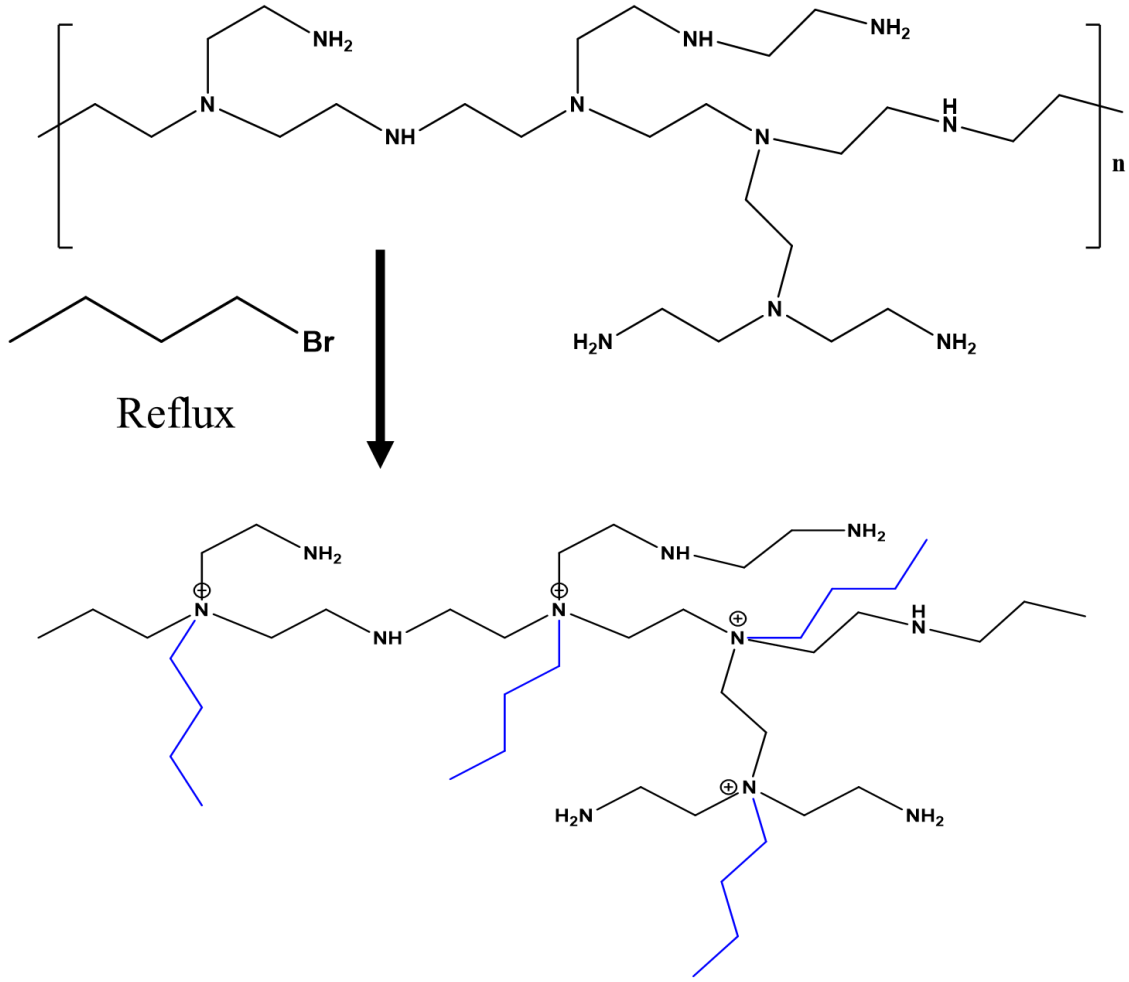

Fig. 30. Schematic synthesis of the quaternary ammonium polyethyleneimine derivative with 1-bromobutane (C4).

Kwolek et al. [112] also synthesized quaternary ammonium derivatives of polyethylenimine (QPEI) for antibacterial application **(Fig. 31)**, but using branched PEI. B-PEI methylation (BPEI-met) was achieved using iodomethane in N-methyl-2-pyrrolidone (NMP) and generated 87% quaternization with a large excess of iodomethane. BPEI-met strongly interacted with negatively charged lipid membranes, acting as a model for bacterial cell membranes. BPEI-met had strong bacteriostatic effects on Gram-positive bacteria but was less effective against Gram-negative bacteria.

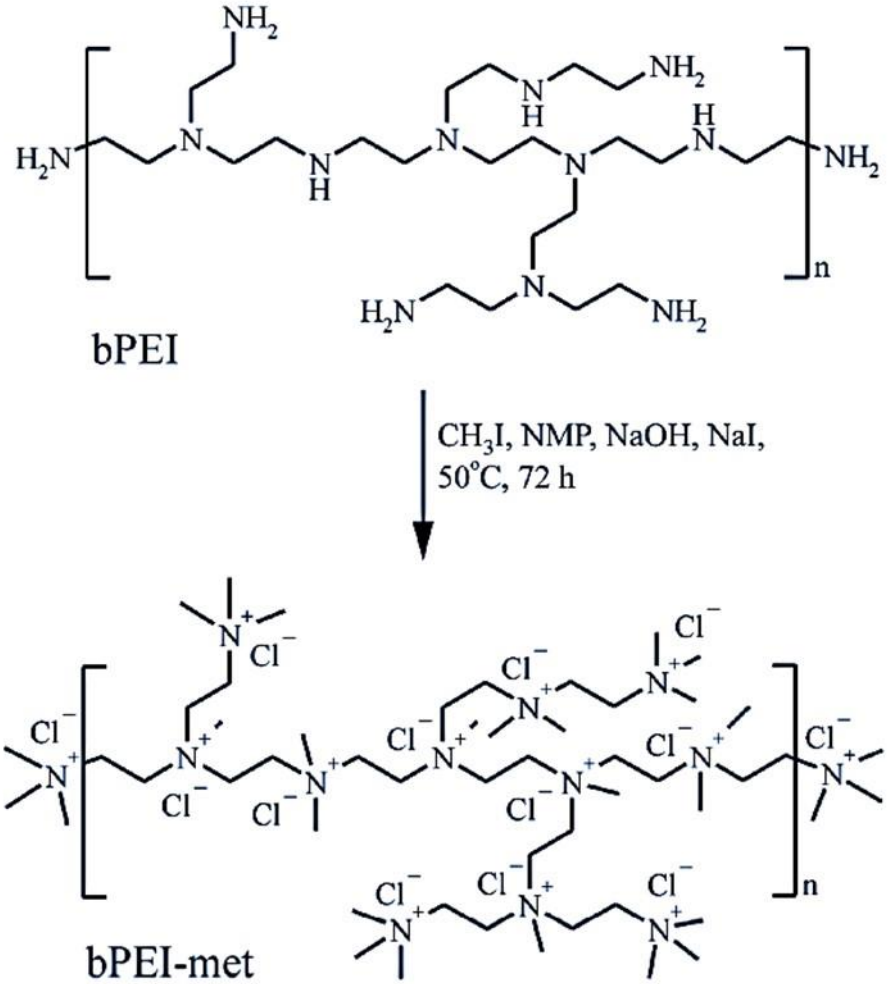

Fig. 31. The synthesis and the chemical structure of quaternary ammonium derivatives of BPEI (BPEI-met) [112].

6.3. Mucoadhesive applications

Mucoadhesion is the ability of materials to adhere to mucosal membranes (usually in the human body), providing temporary retention. Mucoadhesive dosage forms are valuable for targeted drug delivery via the buccal, oral, nasal, ocular, and vaginal routes [113, 114]. Consequently, researchers have sought to develop polymeric mucoadhesive materials to act as drug carriers or for coatings on, for example, tablets [115, 116] or wafers [117]. Hydrophilic polymers possessing charged groups and/or non-ionic functional groups capable of forming hydrogen bonds with mucosal surfaces tend to be strongly mucoadhesive. [113].

Polyethyleneimine (PEI) is cationic polymer which has a high density of cationic charge and it is able to interact electrostatically with negatively charged surfaces to adhere to mucosal surfaces [119]. PEI has been investigated for use in drug delivery systems [118] and due to its charge density, PEI acts as a proton sponge in response to changes in pH. Dextran (DS) is an anionic polysaccharide formed from the condensation of glucose, containing 2.3 mol of sulphate groups per glucosyl unit, and has been widely used in pharmaceutical formulations due to its biodegradability and biocompatibility [120]. The opposite charges of PEI and DS contribute to an ionic interaction that results in the formation of PEI–DS nanoparticles (PDNPs), which have been as mucoadhesive materials for oral drug delivery[121].

Tiyaboonchai et al. [122] reported the mucoadhesive properties of polyethyleneimine–dextran sulphate nanoparticles (PDNPs) for oral mucosal drug delivery. The active ingredient, *Punica granatum* peel extract (PGE), was loaded into PDNPs to reduce oral malodor and prevent carries. Again, because of the opposite charges of the polymers, polyethylenimine (PEI) and dextran sulphate (DS) (with polyethylene glycol 400, PEG 400 as a stabilizer), formed particles by polyelectrolyte complexation. The PDNPs were mucoadhesive and provided sustained release of the active ingredient and efficacy against oral bacteria.

Calixto et al. [123] developed and characterised four liquid crystalline precursor systems (LCPSs) with different aqueous phases such as water alone (FW) or aqueous solutions containing chitosan (FC), polyethyleneimine (FP), or chitosan/PEI (FPC) . In this study, the oil phase was oleic acid, and the surfactant was ethoxylated and propoxylated cetyl alcohol. The LCPSs containing chitosan and PEI (FPC) demonstrated suitable buccal properties and regulated drug release towards the treatment of a variety of oral diseases [124]. Then, 30% (FW30, FC30, FP30, FPC30) or 100% (FW100, FC100, FP100, FPC100) artificial saliva was added to the FW, FC, FP, and FPC preparations. The addition of 30% saliva into the formulations significantly enhanced their mucoadhesion, and this was the case for all formulations, as shown in **Fig. 32**. Regardless of formulation, the addition of 100 % saliva further significantly increased mucoadhesion relative to formulations without saliva or those containing 30 % saliva. The formulations FC100, FP100, and FPC100 achieved comparable levels of mucoadhesion; however, only the FP100 formulation had a significant difference in mucoadhesion compared to the formulation containing the aqueous phase (FW100).

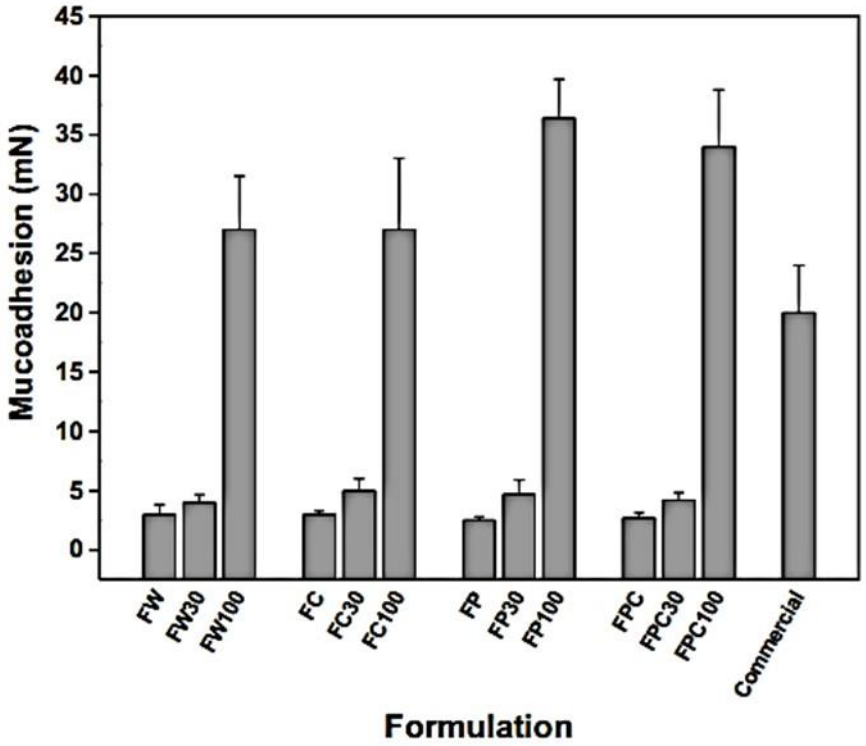

Fig. 32. Mucoadhesion of the different formulations of liquid crystalline precursor systems (LCPSs) composed of different aqueous phases; water (FW), chitosan (FC), polyethyleneimine (FP), or chitosan/PEI (FPC). Artificial saliva added at 30% (FW30, FC30, FP30, FPC30) or 100% (FW100, FC100, FP100, FPC100) [123].

Shan et al. [60] demonstrated methacrylation of poly(2-ethyl-2-oxazoline) by reacting hydrolyzed poly(2-ethyl-2-oxazoline) to obtain partially hydrolyzed PEI, which was then substituted with methacrylic anhydride. As shown in **Fig. 33**, methacrylation significantly increased mucoadhesion on nasal mucosa tissue compared to the parent poly(2-ethyl-2-oxazoline), owing to synergistic binding of methacrylate groups as well as residual secondary amines being available to interact with the mucosal surface. Methacrylated PEOZ has the potential to be used in dosage forms as a mucoadhesive material for transmucosal drug delivery.

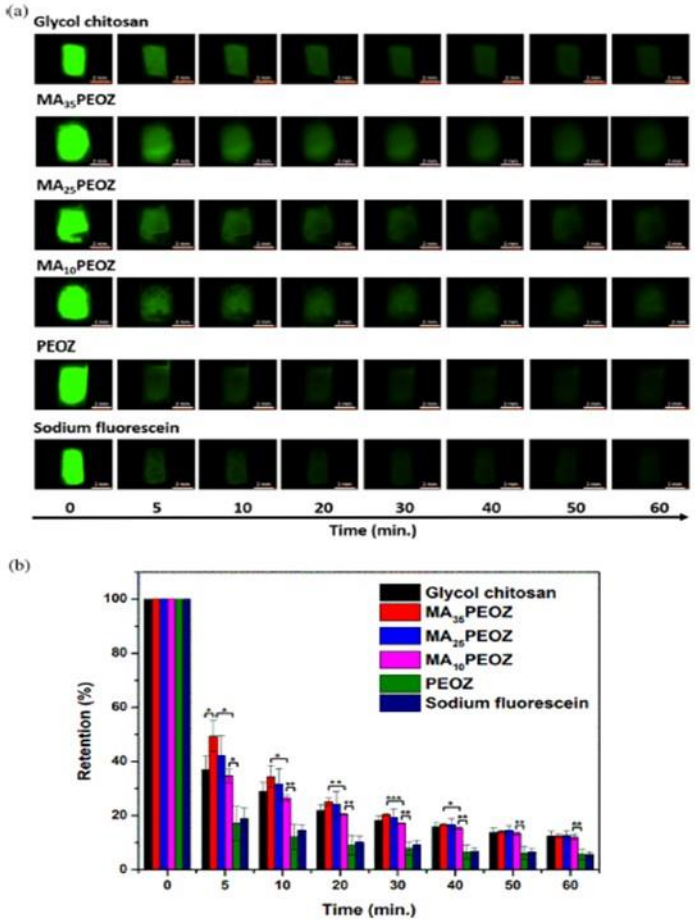

Fig. 33. Fluorescence images showing retention of 1 mg/mL glycol chitosan, PEOZ, P(EOZ-co-EI$_{15}$), MA$_{10}$PEOZ, P(EOZ-co-EI$_{28}$), MA$_{25}$PEOZ, P(EOZ-co-EI$_{53}$ and MA$_{35}$PEOZ solutions using 0.05 mg/mL sodium fluorescein as the solvent and pure 0.05 mg/mL sodium fluorescein solution on sheep nasal mucosa and washed with artificial nasal fluid (ANF). Scale bars are 2 mm. (b) Retention of 1 mg/mL glycol chitosan, PEOZ, MA10PEOZ, MA25PEOZ, and MA35PEOZ solutions using 0.05 mg/ mL sodium fluorescein as the solvent and pure 0.05 mg/mL sodium fluorescein solution on sheep nasal mucosa as washed with different volumes of ANF [61].

6.4. Polymer blends

Polymer blends are commonly used to tailor physicochemical and mechanical properties for defined uses [125, 126]. Combinations span two natural polymers (e.g. proteins and polysaccharides, proteins and lipids, polysaccharides and lipids) two synthetic polymers or combinations of natural and synthetic materials [127]. The mechanical and barrier properties of blended polymeric films is dependent on the constituting polymer characteristics and their

compatibility[128]. For example, the brittle nature of some hydrophobic or rigid polymers, such as chitosan, can be improved by blending with a hydrophilic polymer or polymer acting as a plasticizer [129, 130]. The addition of a hydrophilic polymer (or plasticizer) is commonly used to enhance the mechanical and physical properties of hydrophobic films [131] or of polymeric films with high glass transition temperatures [132].

L-PEI is semi-crystalline [8] with a glass transition temperature ~29.5 ^{o}C [20] and, therefore, appears to be a suitable candidate to blend with chitosan in order to improve film mechanical properties and drug release profiles. However, L-PEI only dissolves in water at high temperatures [8], forms a gel at room temperature [32] and has been shown to cause cytotoxicity [49]. Chemical modifications of L-PEI to increase water solubility and decrease its toxicity have been reported [133].

Soradech et al. [68] developed novel flexible and mucoadhesive films based on chitosan and poly(2-hydroxyethyl ethyleneimine) or P2HEEI. P2HEEI was synthesized via nucleophilic substitution of linear polyethyleneimine (L-PEI) with 2-bromoethanol. P2HEEI exhibited good solubility in water, low toxicity in human dermal skin fibroblast cells, and a low glass transition temperature (-31.6 °C). This polymer was blended with chitosan to improve mechanical properties for buccal delivery of haloperidol. Differential scanning calorimetry and scanning electron microscopy confirmed that chitosan and P2HEEI formed miscible blends and the mechanical properties of films cast from the blend resulting in more elastic drug delivery systems than chitosan alone. Haloperidol release from the films increased with increasing P2HEEI content. The mucoadhesive properties of these films were evaluated on freshly excised sheep buccal mucosa and showed that, as P2HEEI content in the blend increased, mucoadhesion declined.

Soradech et al. [49] also developed novel elastic films based on poly(3-hydroxypropyl ethyleneimine) and chitosan for rapid delivery of haloperidol. Poly(3-hydroxypropyl ethyleneimine) or P3HPEI was synthesized using nucleophilic substitution of linear polyethyleneimine (L-PEI) with 3-bromo-1-propanol, and demonstrated good solubility in water, low toxicity, and a low glass transition temperature. P3HPEI was subsequently blended with chitosan to generate novel flexible films by casting from aqueous solutions and evaporating the solvent. The polymers were miscible in the solid state and again blending chitosan with P3HPEI significantly affected the elasticity and strength of films (increased elongation at the break but reduced puncture strength). A 35: 65 (% w/ w) blend of

chitosan/ P3HPEI provided the optimum glass transition temperature for the delivery of haloperidol through mucosal membranes. Microscopic and XRD analyses indicated that the solubility of haloperidol in the films was ~1.5%. The inclusion of the hydrophilic polymer P3HPEI allowed rapid drug release followed by disintegration due to rapid water diffusion into the films, swelling, and erosion, supported by the relaxation of the polymer chains. The drug release profiles were consistent with the physicochemical properties of P3HPEI, a hydrophilic polymer with a low T_g. Hence, blending P3HPEI with chitosan allows the selection of desirable physicochemical and mechanical properties of the films for the loading and rapid delivery of haloperidol, a model poorly water-soluble drug for transmucosal drug delivery, such as buccal or ocular administration [49].

6.5. Hydrogels and cryogels

Hydrogels are swelling polymeric materials with a three-dimensional network structure that can be synthesized physically or chemically using hydrophilic polymers or a combination of the two polymers [134]. Due to their valuable properties including biocompatibility, flexibility, high water content, and softness, hydrogels have been widely used in pharmaceutical and biological applications [135, 136].

Hydrogels are typically classified as either physical (reversible) or chemical (permanent) [135, 137]. Physically crosslinked hydrogels form through various interactions, including hydrophobic forces, ionic bonds and hydrogen bonds, and can redissolve in response to changes in environmental parameters such as temperature, ionic strength, and pH. Chemical hydrogels, on the other hand, are formed by a network of covalent linkages incorporating diverse macromolecular chains, for example by crosslinking polymers [138, 139]. Hydrogels can be charged or uncharged, depending on the type of the functional groups included within their molecular structure [138] and typically swell in response to variations in pH, with shape changes [140]. In general, two approaches are used to create chemically crosslinked hydrogels. The first approach, referred to as three-dimensional polymerization, utilizes a hydrophilic monomer to polymerize with the aid of a functional cross-linking agent. Alternatively, water-soluble polymers can be crosslinked directly. Polymerization is typically facilitated by free-radical producing chemicals, such as ammonium peroxodisulphate, benzoyl peroxide, and 2, 2-azo-isobutyronitrile, or by the application of electron beam, ultraviolet, or gamma radiation.

PEI has been used to create physical and chemical hydrogels [32, 141, 142]. According to Yuan et al. [32], linear PEI backbone gelation in water was generated by cooling heated aqueous solutions to ambient temperature and then forming a physical (thermoreversible) gel. The L-PEI physical hydrogel was created by mixing L-PEI with distilled water and heating to 80 °C until PEI fully dissolved before cooling to room temperature; this resultant opaque gel converted back to a transparent solution by re-heating at 80 °C.

According to Paciello and Santonicola [141], partially methacrylated polyethyleneimine (PEI-MA) was used to form a methacrylated branched polyethyleneimine (PEI-MA) hydrogel. To synthesize this polymer, different molar ratios of methacrylic anhydride were used at room temperature for 18 h in dichloromethane (DCM) with triethanolamine as an alkaline catalyst **(Fig. 34)**. Nucleophilic attack of the primary and secondary amine groups of B-PEI on the carbonyl group of methacrylic anhydride resulted in the formation of amide bonds.

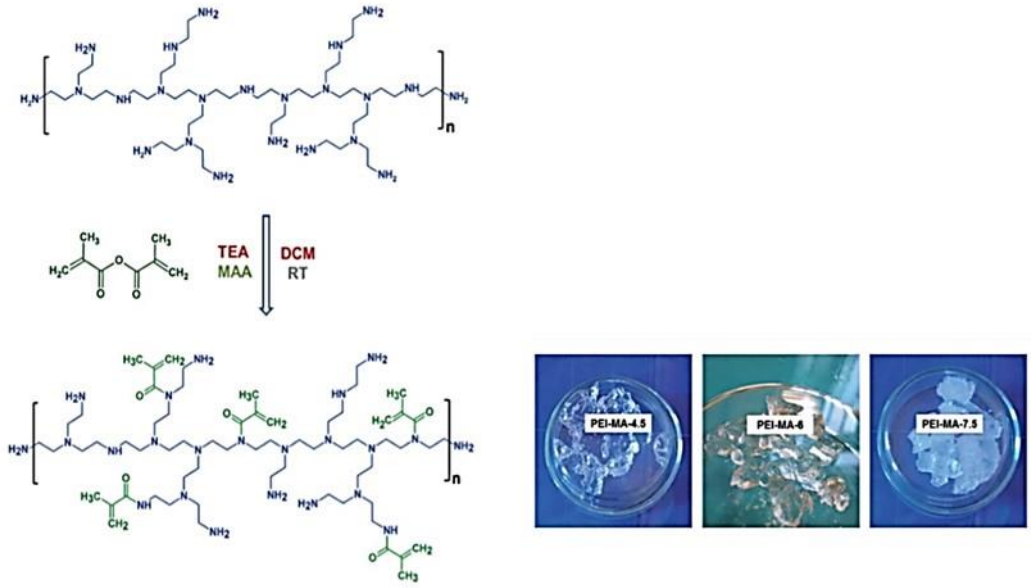

Fig. 34. Synthesis of partially methacrylated branched polyethyleneimine (PEI-MA) hydrogel [141].

Wahid et al. [142] reported that, whilst bacterial cellulose (BC) has useful properties for various applications, however, it lacks antibacterial activity. To address this, crosslinked BC and PEI-based antibacterial hydrogels were formulated containing an epichlorohydrin (ECH) as a coupling agent **(Fig. 35)**. As described above, PEI is a cationic polymer that has good antibacterial activity. The addition of ECH to the BC solution was stepped and

homogenised before crosslinking with different concentrations of PEI. The antibacterial properties of the BC/PEI hydrogels were tested against *S. aureus* and *E. coli* using the agar diffusion method. PEI content affected the antibacterial activity of all hydrogels with highest antibacterial activity against both strains at 12.88 mg/mL of PEI. The hydrogels were developed as putative wound dressing materials.

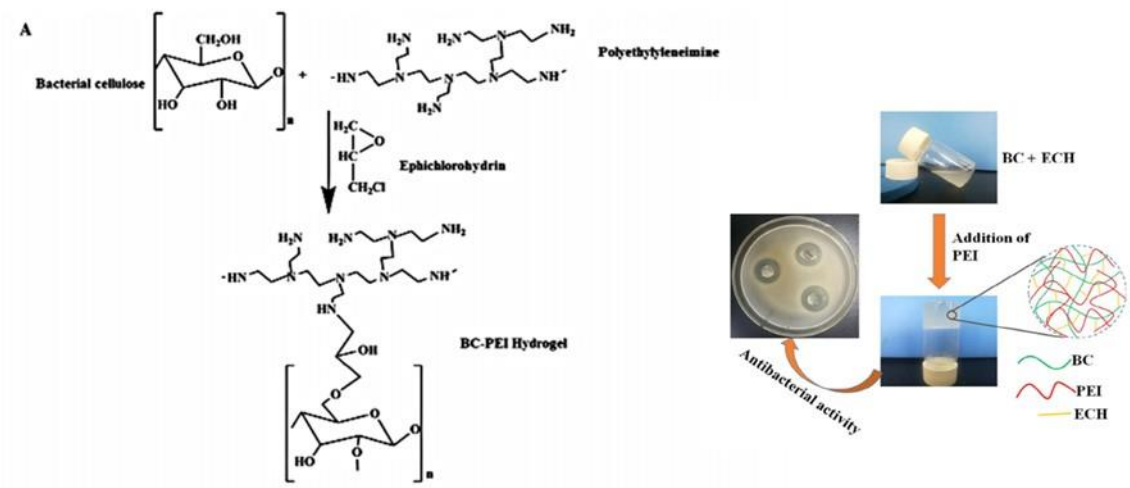

Fig. 35. Crosslinking process of bacterial cellulose (BC) and polyethyleneimine (PEI) with epichlorohydrin[142].

Cryogels can be generated from appropriate monomers or polymeric precursors using a cryogelation technique and form supermacroporous gel. Cryogels also typically offer osmotic stability and tensile strength and so have been promoted for use as a biomedical scaffold material [143]. According to Kumar et al. [144], cryogels are gel matrices formed by polymerization at temperatures below zero. Whilst the polymerization process takes place in the unfrozen domains, ice crystals also form and act as pore forming agents. At the end of polymerization, once the cryogels are thawed, supermacropores are thus formed within the cryogel structure. One of the most often utilised processes for generating physically cross-linked hydrogels is cytotropic gelation. In this process, the polymer solution passes through one or more freeze-thaw cycles, resulting in the creation of an interior structure of interconnected pores [33, 145 – 147]. After reaching the solvent crystallisation temperature, the system is essentially a heterogeneous block containing solvent crystals and the unfrozen liquid micro-phase (UFLMP), where the reagents rapidly concentrate (a phenomenon known as cryoconcentration), resulting in gelation [34, 148]. The solvent acts as a pore-forming agent in this case: when the solvent crystals melt, they leave a macro and micro-porous network

inside the gel (cryogel). The size of the system's macro-pores, as well as its mechanical properties such as the elastic modulus, are directly proportional to the concentration of the gel-forming chemicals used, as well as the number and conditions of the freeze-thawing cycles [149, 150].

In comparison to conventional hydrogels, cryogels tend to be more flexible, are highly porous, and respond rapidly to stimuli [151]. Sahiner et al. [152] used a cryopolymerization process with glycerol diglycidyl ether (GDE) to produce branched PEI-based cryogels, as illustrated in **Fig. 36**. The study demonstrated the formation of superporous PEI cryogels, which responded rapidly to external influences (pH, solvent, and temperature), were highly elastic and offered a high mechanical strength.

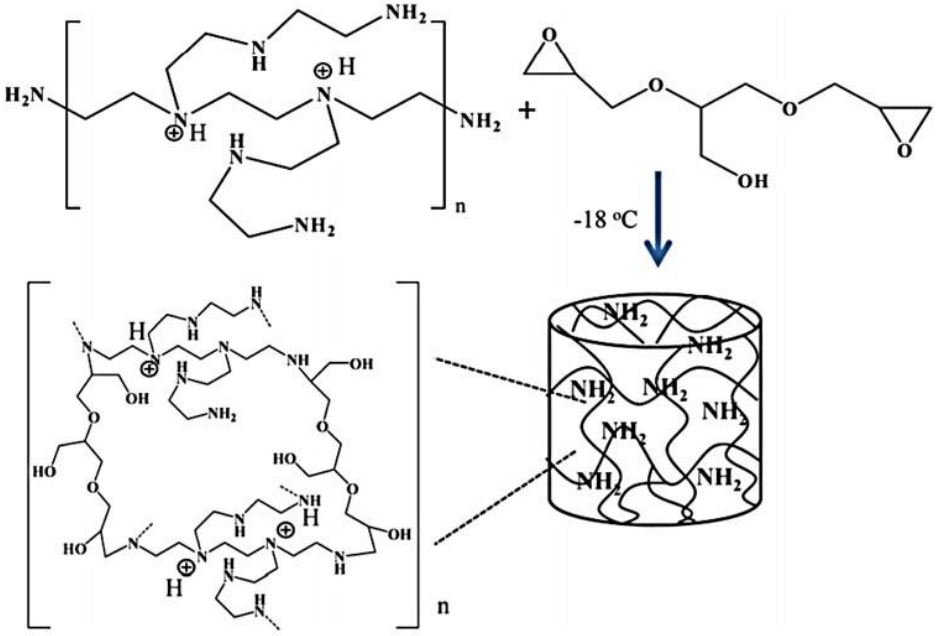

Fig. 36. Glycerol diglycidyl ether (GDE) crosslinked branched PEI cryogels [152].

As described earlier (Section 3.3), Soradech et al. [29] developed physically crosslinked cryogels based on linear polyethyleneimine (L-PEI) using a freeze-thawing technique. Dissolution of L-PEI in deionized water was achieved at 80 °C and resulted in a transparent solution, which then formed an opaque gel forming upon freezing and subsequent thawing. The cryogels exhibited reversibility; heating at 80 °C regenerated a clear solution**.** L-PEI cryogels were evaluated after freezing aqueous solutions to various temperatures (-196, -80, -30 and 0 °C) for 3 h and subsequent thawing at 25°C for 24 h. Gel rigidity correlated with the freezing

temperature and gels were strongest when cooled to -196 ^{o}C, consistent with determinations of the degree of crystallinity in the gels, the enthalpy of fusion and rheological behaviour. The effect of solvent mixtures on the crystallinity and rheological properties of L-PEI cryogels was also investigated. Water/ethanol mixtures containing a higher proportion of ethanol significantly reduced the strength, viscosity and degree of crystallinity of the L-PEI cryogels. Thus, by controlling the freezing temperature or modifying the solvent, L-PEI cryogels were designed with desired mechanical properties.

6.6. Other biomedical applications

PEI and its derivatives have been used to prepare various organic/organic or organic/inorganic hybrid materials for different biomedical applications as illustrated in **Table 5**.

Table 5. Summary of modified PEI for applications in biomedical fields.

Modified PEI	Application	Benefits	References
Polyethyleneimine-modified scaffolds with polyethylene oxide, chitin and chitosan.	Regeneration of cartilaginous tissue	Increase in adhesion efficiency of bovine knee chondrocytes Proliferation of bovine knee chondrocytes (BKCs), secretion of glycosaminoglycans, and production of collagen	Kuo et al.[153]
Polyethyleneimine grafted chitosan films (Ch-g-PEI)	Enzyme technology	Increase in the immobilizations of enzyme laccase	Metin [154]
Polyethyleneimine-modified silica nanoparticles	Regenerative medicine	Sustained delivery growth factors and promoted stem cell differentiation.	Wang et al. [155]
Polyethyleneimine-grafted collagen fiber	Immobilization of biological cells	Carrier for cell immobilization	Zhu et al. [156]
Gelatin-polyethylenimine blend nanofibers (GEL/PEI)	Tissue engineering	Promotion of cell adhesion and an increase in cell viability	Lakra et al.[157]
Polydextran aldehyde/PEI nanofibers	Antibacterial coatings	Maintain cytocompatibility to fibroblasts, high effective and long-acting for antibacterial activity	Meng et al. [158]
Nanofiber composed of poly(ε-caprolactone) and polyethylenimine	Scaffolds for tissue engineering	Promoting the attachment and proliferation of human umbilical vein endothelial cells	Jing et al. [159]

Polyethylenimine and sodium cholate-modified ethosomes complex	Transdermal delivery	Increase skin penetration and effective means for treating melanoma	Ma et al. [160]
Hydroxypropyl β-cyclodextrin-grafted polyethyleneimine	Transdermal delivery	Penetration enhancer for transdermal drug delivery	Wang et al.[161]
Hyaluronic acid/poly(ethylenimine) polyelectrolyte multilayer coatings	Layer-by-layer thin films and coatings	prevention of restenosis on molecular level	Koenig et al. [162]
Polyethyleneimine and graft-copolyimide with polymethacrylic acid side chains	Polyelectrolyte nanocapsules	Controlled release of drug	Ibragimova et al.[163]
PVA/B-PEI Nanofiber Mats	Wound healing	Increase in cell migration and wound healing by B-PEI nanofibers (97% wound coverage in 17 h) when compared to B-PEI (15% wound coverage in 17 h).	Mary et al. [164]
Polyethylenimine-Based Nanogels	Biomedical applications (gene therapy, drug delivery and bioimaging)	Increased a targeted diagnosis and therapy of cancer	Zou et al. [165]
PEI amine groups onto the surface PEI-stabilized iron oxide nanoparticles (NPs)	Biomedicine	Targeted cancer imaging	Li et al. [166]
Ligand-modified PEI possessing pH-responsiveness	Biomedicine	A carrier system to encapsulate anticancer drug for targeted delivery to cancer cells	Zhou et al. [167]
Gold nanoparticle (AuNP)-PEI conjugates	Biologically applicable materials	Gene-carriers for genome editing or nanoscale positive control for nanotoxicology	Cho et al. [168]
PEI as a colloidal stabilizer coating on magnetic Fe_3O_4 particles in bio-imaging	Bioimaging probes	Magnetic bioimaging probes as applied for magnetic resonance imaging and therapy	Cai et al. [169]
Redox ferrocene (Fc) modified PEI multilayers with tunable stiffness by using a LBL self-assembly method	Cell culture matrices	Controlling the interaction between cells and the substrate	Sun et al. [170]

7. Conclusions

Polyethyleneimine is widely used in multiple sectors as a detergent, adhesive and water treatment agent, amongst others. It is extensively researched for use in biomedical sciences and for use in drug delivery. Here, the various synthetic approaches to linear PEI and branched PEI have been considered before the physical properties of both forms of PEI, such as solid-state and behavior in aqueous and non-aqueous solutions, were discussed. As a major limitation to the widespread adoption of PEI in medicine, the toxicity of PEI has been assessed using a variety of techniques, including cytotoxicity, slug mucosal irritation (SMI) and cytogenomic testing. To mitigate these adverse effects of the polymer, researchers have developed multiple chemical and structural modifications to PEI through varied chemistries. In general terms, the PEI derivatives tend to have improved biocompatibility, transfection efficiency, solubility and reduced toxicity, predominantly by effectively removing (substituting) amine groups from the PEI structure. PEI and its modified polymers have been explored for multiple pharmaceutical and biomedical applications ranging from gene delivery vectors to mucoadhesive formulation excipients to transdermal drug delivery adjuvants, as antibacterial agents, for hydrogels as well as a scaffold for tissue stem cell engineering and wound healing. Given the breadth and depth of studies, it is clear that PEI and in particular its modifications will have an expanding role in pharmaceutical and biomedical sciences.

CRediT authorship contribution statement

Sitthiphong Soradech: Conceptualization, Review, Writing original draft.
Adrian C. Williams: Writing - review & editing, Supervision.
Vitaliy V. Khutoryanskiy: Conceptualization, Writing –review & editing, Supervision.

Declaration of Competing Interest

The authors declare that they have no known competing financial interests or personal relationships that could appear to have influenced the work described in this paper.

Acknowledgements

The authors are grateful to Thailand Institute of Scientific and Technological Research, Ministry of Higher Education, Science, Research and Innovation for funding the PhD studentship of Sitthiphong Soradech.

References

[1] O. Sedlacek, D. Bera, R. Hoogenboom, Poly(2-amino-2-oxazoline)s: A new class of thermoresponsive polymers, Polym. Chem. 10 (2019) 4683–4689. https://doi.org/10.1039/c9py00943d.

[2] R. Langer, D. Phd, Langer, R. & Tirrell, D. A. Designing materials for biology and medicine. Nature 428, 487-492, Nature. 428 (2004) 487–492. https://doi.org/10.1038/nature02388.

[3] D. Putnam, Putnam, D. Polymers for gene delivery across length scales. Nat Mater 5: 439-451, Nat. Mater. 5 (2006) 439–451. https://doi.org/10.1038/nmat1645.

[4] A. Lendlein, A.T. Neffe, C. Jérôme, Advanced Functional Polymers for Medicine, Adv. Healthc. Mater. 3 (2014) 1939–1940. https://doi.org/10.1002/adhm.201400718.

[5] O. Sedlacek, O. Janouskova, B. Verbraeken, H. Richard, Straightforward Route to Superhydrophilic Poly(2-oxazoline)s via Acylation of Well-Defined Polyethylenimine, Biomacromolecules. 20 (2018). https://doi.org/10.1021/acs.biomac.8b01366.

[6] Z. Chen, Z. Lv, Y. Sun, Z. Chi, G. Qing, Recent advancements in polyethyleneimine-based materials and their biomedical, biotechnology, and biomaterial applications, J. Mater. Chem. B. 8 (2020) 2951–2973. https://doi.org/10.1039/c9tb02271f.

[7] C. Shen, J. Li, Y. Zhang, Y. Li, G. Shen, J. Zhu, J. Tao, Polyethylenimine-based micro/nanoparticles as vaccine adjuvants, Int. J. Nanomedicine. 12 (2017) 5443–5460. https://doi.org/10.2147/IJN.S137980.

[8] C.N. Lungu, M. V. Diudea, M. V. Putz, I.P. Grudziński, Linear and branched PEIs (Polyethylenimines) and their property space, Int. J. Mol. Sci. 17 (2016). https://doi.org/10.3390/ijms17040555.

[9] W.T. Godbey, K.K. Wu, A.G. Mikos, Poly(ethylenimine) and its role in gene delivery,

J. Control. Release. 60 (1999) 149–160. https://doi.org/10.1016/S0168-3659(99)00090-5.

[10] O. Yemul, T. Imae, Synthesis and characterization of poly(ethyleneimine) dendrimers, Colloid Polym. Sci. 286 (2008) 747–752. https://doi.org/10.1007/s00396-007-1830-6.

[11] Y. Chatani, H. Tadokoro, T. Saegusa, H. Ikeda, Structural Studies of Poly (ethylenimine). 1. Structures of Two Hydrates of Poly (ethylenimine): Sesquihydrate and Dihydrate, Macromolecules. 14 (1981) 315–321. https://doi.org/10.1021/ma50003a017.

[12] H.M.L. Lambermont-Thijs, F.S. van der Woerdt, A. Baumgaertel, L. Bonami, F.E. Du Prez, U.S. Schubert, R. Hoogenboom, Linear Poly(ethylene imine)s by Acidic Hydrolysis of Poly(2-oxazoline)s: Kinetic Screening, Thermal Properties, and Temperature-Induced Solubility Transitions, Macromolecules. 43 (2010) 927–933. https://doi.org/10.1021/ma9020455.

[13] G.J.M. Koper, M. Borkovec, Exact affinity distributions for linear polyampholytes and polyelectrolytes, J. Chem. Phys. 104 (1996) 4204–4213. https://doi.org/10.1063/1.471232.

[14] J.D. Ziebarth, Y. Wang, Understanding the protonation behavior of linear polyethylenimine in solutions through Monte Carlo simulations, Biomacromolecules. 11 (2010) 29–38. https://doi.org/10.1021/bm900842d.

[15] M.A. Mees, R. Hoogenboom, Full and partial hydrolysis of poly(2-oxazoline)s and the subsequent post-polymerization modification of the resulting polyethylenimine (co)polymers, Polym. Chem. 9 (2018) 4968–4978. https://doi.org/10.1039/c8py00978c.

[16] M. Jäger, S. Schubert, S. Ochrimenko, D. Fischer, U.S. Schubert, Branched and linear poly(ethylene imine)-based conjugates: Synthetic modification, characterization, and application, Chem. Soc. Rev. 41 (2012) 4755–4767. https://doi.org/10.1039/c2cs35146c.

[17] B.L. Rivas, S.I. Ananías, Ring opening polymerization of 2-ethyl-2-oxazoline, Polym. Bull. 18 (1987) 189–194. https://doi.org/10.1007/BF00255109.

[18] T. Saegusa, H. Ikeda, H. Fujii, Crystalline Polyethylenimine, Macromolecules. 5

(1972) 108. https://doi.org/10.1021/ma60025a029.

[19] K. Kunath, A. Von Harpe, D. Fischer, H. Petersen, U. Bickel, K. Voigt, T. Kissel, Low-molecular-weight polyethylenimine as a non-viral vector for DNA delivery: Comparison of physicochemical properties, transfection efficiency and in vivo distribution with high-molecular-weight polyethylenimine, J. Control. Release. 89 (2003) 113–125. https://doi.org/10.1016/S0168-3659(03)00076-2.

[20] H.P.C. Van Kuringen, J. Lenoir, E. Adriaens, J. Bender, B.G. De Geest, R. Hoogenboom, Partial Hydrolysis of Poly(2-ethyl-2-oxazoline) and Potential Implications for Biomedical Applications?, Macromol. Biosci. 12 (2012) 1114–1123. https://doi.org/10.1002/mabi.201200080.

[21] R. Tanaka, I. Ueoka, Y. Takaki, K. Kataoka, S. Saito, High molecular weight linear polyethylenimine and poly(N-methylethylenimine), Macromolecules. 16 (1983) 849–853. https://doi.org/10.1021/ma00240a003.

[22] H.M.L. Lambermont-Thijs, J.P.A. Heuts, S. Hoeppener, R. Hoogenboom, U.S. Schubert, Selective partial hydrolysis of amphiphilic copoly(2-oxazoline)s as basis for temperature and pH responsive micelles, Polym. Chem. 2 (2011) 313–322. https://doi.org/10.1039/c0py00052c.

[23] T. Saegusa, H. Ikeda, H. Fujii, Isomerization polymerization of 2-oxazoline: I. Preparation of unsubstituted 2-oxazoline polymer, Polym. J. 34 (2002) 62–66. https://doi.org/10.1295/polymj.3.35.

[24] V.R. De La Rosa, E. Bauwens, B.D. Monnery, B.G. De Geest, R. Hoogenboom, Fast and accurate partial hydrolysis of poly(2-ethyl-2-oxazoline) into tailored linear polyethylenimine copolymers, Polym. Chem. 5 (2014) 4957–4964. https://doi.org/10.1039/c4py00355a.

[25] K.M. Kem, Kinetics of the Hydrolysis of Linear Poly[(acylimino) - ethylenes], 17 (1990) 1977–1990.

[26] C.H. Wang, K.R. Fan, G.H. Hsiue, Enzymatic degradation of PLLA-PEOz-PLLA triblock copolymers, Biomaterials. 26 (2005) 2803–2811. https://doi.org/10.1016/j.biomaterials.2004.07.064.

[27] S.R. Byrn, G. Zografi, X.S. Chen, Solid-State Properties and Pharmaceutical

Development, Solid State Prop. Pharm. Mater. (2017) 1–21. https://doi.org/10.1002/9781119264408.ch1.

[28] T. Hashida, K. Tashiro, S. Aoshima, Y. Inaki, Structural investigation on water-induced phase transitions of poly(ethylene imine). 1. Time-resolved infrared spectral measurements in the hydration process, Macromolecules. 35 (2002) 4330–4336. https://doi.org/10.1021/ma012204l.

[29] S. Soradech, A.C. Williams, V. V. Khutoryanskiy, Physically Cross-Linked Cryogels of Linear Polyethyleneimine: Influence of Cooling Temperature and Solvent Composition, Macromolecules. 55 (2022) 9537–9546. https://doi.org/10.1021/acs.macromol.2c01308.

[30] T. Hashida, K. Tashiro, Y. Inaki, Structural Investigation of Water-Induced Phase Transitions of Poly(ethylene imine). III. The Thermal Behavior of Hydrates and the Construction of a Phase Diagram, J. Polym. Sci. Part B Polym. Phys. 41 (2003) 2937–2948. https://doi.org/10.1002/polb.10611.

[31] T. Hashida, K. Tashiro, Structural study on water-induced phase transitions of poly(ethylene imine) as viewed from the simultaneous measurements of wide-angle X-ray diffractions and DSC thermograms, Macromol. Symp. 242 (2006) 262–267. https://doi.org/10.1002/masy.200651036.

[32] J.J. Yuan, R.H. Jin, Fibrous crystalline hydrogels formed from polymers possessing a linear poly(ethyleneimine) backbone, Langmuir. 21 (2005) 3136–3145. https://doi.org/10.1021/la047182l.

[33] F.M. Plleva, I.Y. Galaev, B. Mattiasson, Macroporous gels prepared at subzero temperatures as novel materials for chromatography of particulate-containing fluids and cell culture applications, J. Sep. Sci. 30 (2007) 1657–1671. https://doi.org/10.1002/jssc.200700127.

[34] V.I. Lozinsky, L.G. Damshkaln, I.N. Kurochkin, I.I. Kurochkin, Cryostructuring of polymeric systems. 36. Poly(vinyl alcohol) cryogels prepared from solutions of the polymer in water/low-molecular alcohol mixtures, Eur. Polym. J. 53 (2014) 189–205. https://doi.org/10.1016/j.eurpolymj.2014.01.020.

[35] C. Schatz, A. Domard, C. Viton, C. Pichot, T. Delair, Versatile and efficient formation

of colloids of biopolymer-based polyelectrolyte complexes, Biomacromolecules. 5 (2004) 1882–1892. https://doi.org/10.1021/bm049786+.

[36] A.B. Zezin, V.B. Rogacheva, V.I. Feldman, P. Afanasiev, A.A. Zezin, From triple interpolyelectrolyte-metal complexes to polymer-metal nanocomposites, Adv. Colloid Interface Sci. 158 (2010) 84–93. https://doi.org/10.1016/j.cis.2009.09.002.

[37] D. V Pergushov, A.A. Zezin, A.B. Zezin, A.H.E. Müller, Advanced Functional Structures Based on Interpolyelectrolyte Complexes BT - Polyelectrolyte Complexes in the Dispersed and Solid State I: Principles and Theory, in: M. Müller (Ed.), Springer Berlin Heidelberg, Berlin, Heidelberg, 2014: pp. 173–225. https://doi.org/10.1007/12_2012_182.

[38] Y.M. Kopylova, S.P. Valuyeva, B.S. El'tsefon, V.B. Rogacheva, A.B. Zezin, Structure and properties of crosslinked hydrogels based on the polyelectrolyte complex polyacrylic acid-polyethyleneimine, Polym. Sci. U.S.S.R. 29 (1987) 577–586. https://doi.org/10.1016/0032-3950(87)90265-6.

[39] M. Müller, B. Keßler, J. Fröhlich, S. Poeschla, B. Torger, Polyelectrolyte complex nanoparticles of poly(ethyleneimine) and poly(acrylic acid): Preparation and applications, Polymers (Basel). 3 (2011) 762–778. https://doi.org/10.3390/polym3020762.

[40] S. Ray, S. Maiti, B. Sa, Polyethyleneimine-Treated xanthan beads for prolonged release of diltiazem: In vitro and in vivo evaluation, Arch. Pharm. Res. 33 (2010) 575–583. https://doi.org/10.1007/s12272-010-0412-1.

[41] Y.L. Lin, C.H. Chen, Y.K. Liu, T.H. Huang, N.M. Tsai, S.C. Tzou, K.W. Liao, Lipo-PEG-PEI complex as an intracellular transporter for protein therapeutics, Int. J. Nanomedicine. 14 (2019) 1119–1130. https://doi.org/10.2147/IJN.S188970.

[42] Y.K. Liu, Y.L. Lin, C.H. Chen, C.M. Lin, K.L. Ma, F.H. Chou, J.S. Tsai, H.Y. Lin, F.R. Chen, T.L. Cheng, C.C. Chang, K.W. Liao, A unique and potent protein binding nature of liposome containing polyethylenimine and polyethylene Glycol: A nondisplaceable property, Biotechnol. Bioeng. 108 (2011) 1318–1327. https://doi.org/10.1002/bit.23048.

[43] J.M. Lázaro-Martínez, E. Rodríguez-Castellón, D. Vega, G.A. Monti, A.K. Chattah,

Solid-state studies of the crystalline/amorphous character in linear poly (ethylenimine hydrochloride) (PEI·HCl) polymers and their copper Complexes, Macromolecules. 48 (2015) 1115–1125. https://doi.org/10.1021/ma5023082.

[44] D.R. Ustyakina, A.S. Chevtaev, A.I. Tabunshchikov, A.S. Ozerin, F.S. Radchenko, I.A. Novakov, Complexes of Polyethyleneimine with Cu2+ Ions in Aqueous Solutions as Precursors for Obtaining Copper Nanoparticles, Polym. Sci. Ser. B. 61 (2019) 261–265. https://doi.org/10.1134/S1560090419030151.

[45] A.S. Ozerin, T.S. Kurkin, F.S. Radchenko, Y. V Shulevich, I.A. Novakov, Complexes of Polyethylenimine with Copper and Cobalt Ions as Precursors for Preparing Metal Nanoparticles, Russ. J. Appl. Chem. 94 (2021) 210–216.

[46] V.N. Kislenko, L.P. Oliynyk, Complex formation of polyethyleneimine with copper(II), nickel(II), and cobalt(II) ions, J. Polym. Sci. Part A Polym. Chem. 40 (2002) 914–922. https://doi.org/10.1002/pola.10157.

[47] T. Takagishi, S. Okuda, N. Kuroki, H. Kozuka, Binding of Metal Ions By Polyethylenimine and Its Derivatives., J. Polym. Sci. A1. 23 (1985) 2109–2116. https://doi.org/10.1002/pol.1985.170230804.

[48] F. Fan, K. V. Wood, Bioluminescent assays for high-throughput screening, Assay Drug Dev. Technol. 5 (2007) 127–136. https://doi.org/10.1089/adt.2006.053.

[49] S. Soradech, P. Kengkwasingh, A.C. Williams, V. V Khutoryanskiy, Synthesis and Evaluation of Poly (3-hydroxypropyl Ethylene-imine) and Its Blends with Chitosan Forming Novel Elastic Films for Delivery of Haloperidol, Pharmaceutics. 14 (2022) 1–22. https://doi.org/https://doi.org/10.3390/pharmaceutics14122671.

[50] S.M. Moghimi, P. Symonds, J.C. Murray, A.C. Hunter, G. Debska, A. Szewczyk, A two-stage poly(ethylenimine)-mediated cytotoxicity: Implications for gene transfer/therapy, Mol. Ther. 11 (2005) 990–995. https://doi.org/10.1016/j.ymthe.2005.02.010.

[51] L. Gholami, H.R. Sadeghnia, M. Darroudi, R. Kazemi Oskuee, Evaluation of genotoxicity and cytotoxicity induced by different molecular weights of polyethylenimine/DNA nanoparticles, Turkish J. Biol. 38 (2014) 380–387. https://doi.org/10.3906/biy-1309-51.

[52] D. Fischer, Y. Li, B. Ahlemeyer, J. Krieglstein, T. Kissel, In vitro cytotoxicity testing of polycations: Influence of polymer structure on cell viability and hemolysis, Biomaterials. 24 (2003) 1121–1131. https://doi.org/10.1016/S0142-9612(02)00445-3.

[53] K.A. Gibney, I. Sovadinova, A.I. Lopez, M. Urban, Z. Ridgway, G.A. Caputo, K. Kuroda, Poly(ethylene imine)s as antimicrobial agents with selective activity, Macromol. Biosci. 12 (2012) 1279–1289. https://doi.org/10.1002/mabi.201200052.

[54] Y. Omidi, V. Kafil, Cytotoxic Impacts of Linear and Branched Polyethylenimine Nanostructures in A431 Cells, BioImpacts. 1 (2011) 23–30.

[55] E.U. Okon, G. Hammed, P. Abu, E. Wafa, O. Abraham, N. Case, E. Henry, In-vitro cytotoxicity of Polyethyleneimine on HeLa and Vero Cells, 5 (2014) 192–199.

[56] M. Wang, P. Lu, B. Wu, J.D. Tucker, C. Cloer, Q. Lu, High efficiency and low toxicity of polyethyleneimine modified Pluronics (PEI-Pluronic) as gene delivery carriers in cell culture and dystrophic mdx mice, J. Mater. Chem. 22 (2012) 6038–6046. https://doi.org/10.1039/c2jm15625c.

[57] N.T. Chevala, J.A. Dsouza, H. Saini, L. Kumar, Design and development of tranexamic acid loaded film-forming gel to alleviate melasma, J. Cosmet. Dermatol. (2022) 6863–6874. https://doi.org/10.1111/jocd.15426.

[58] E. Adriaens, J.P. Remon, Gastropods as an Evaluation Tool for Screening the Irritating Potency of Absorption Enhancers and Drugs, Pharm. Res. 16 (1999) 1240–1244. https://doi.org/10.1023/A:1014801714590.

[59] C. Callens, E. Adriaens, K. Dierckens, J.P. Remon, Toxicological evaluation of a bioadhesive nasal powder containing a starch and Carbopol 974 P on rabbit nasal mucosa and slug mucosa., J. Control. Release Off. J. Control. Release Soc. 76 (2001) 81–91. https://doi.org/10.1016/s0168-3659(01)00419-9.

[60] X. Shan, S. Aspinall, D.B. Kaldybekov, F. Buang, A.C. Williams, V. V. Khutoryanskiy, Synthesis and Evaluation of Methacrylated Poly(2-ethyl-2-oxazoline) as a Mucoadhesive Polymer for Nasal Drug Delivery, ACS Appl. Polym. Mater. (2021). https://doi.org/10.1021/acsapm.1c01097.

[61] E. Adriaens, J.P. Remon, Evaluation of an Alternative Mucosal Irritation Test Using Slugs, Toxicol. Appl. Pharmacol. 182 (2002) 169–175.

https://doi.org/https://doi.org/10.1006/taap.2002.9444.

[62] L. Aravindan, K.A. Bicknell, G. Brooks, V. V. Khutoryanskiy, A.C. Williams, A comparison of thiolated and disulfide-crosslinked polyethylenimine for nonviral gene delivery, Macromol. Biosci. 13 (2013) 1163–1173. https://doi.org/10.1002/mabi.201300103.

[63] L. Aravindan, K.A. Bicknell, G. Brooks, V. V. Khutoryanskiy, A.C. Williams, Effect of acyl chain length on transfection efficiency and toxicity of polyethylenimine, Int. J. Pharm. 378 (2009) 201–210. https://doi.org/10.1016/j.ijpharm.2009.05.052.

[64] X. Shan, A.C. Williams, V. V. Khutoryanskiy, Polymer structure and property effects on solid dispersions with haloperidol: Poly(N-vinyl pyrrolidone) and poly(2-oxazolines) studies, Int. J. Pharm. 590 (2020) 119884. https://doi.org/10.1016/j.ijpharm.2020.119884.

[65] R.A. Sanders, A.G. Snow, R. Frech, D.T. Glatzhofer, A spectroscopic and conductivity comparison study of linear poly(N-methylethylenimine) with lithium triflate and sodium triflate, Electrochim. Acta. 48 (2003) 2247–2253. https://doi.org/10.1016/S0013-4686(03)00211-1.

[66] H.M.L. Lambermont-Thijs, L. Bonami, F.E. Du Prez, R. Hoogenboom, Linear poly(alkyl ethylene imine) with varying side chain length: Synthesis and physical properties, Polym. Chem. 1 (2010) 747–754. https://doi.org/10.1039/b9py00344d.

[67] S. Patil, R. Lalani, P. Bhatt, I. Vhora, V. Patel, H. Patel, A. Misra, Hydroxyethyl substituted linear polyethylenimine for safe and efficient delivery of siRNA therapeutics, RSC Adv. 8 (2018) 35461–35473. https://doi.org/10.1039/C8RA06298F.

[68] S. Soradech, Development of Novel Formulations Based on Linear Polyethyleneimine and Its Derivatives for Pharmaceutical and Biomedical applications, University of Reading, 2023.

[69] H.L. Jiang, Y.K. Kim, R. Arote, J.W. Nah, M.H. Cho, Y.J. Choi, T. Akaike, C.S. Cho, Chitosan-graft-polyethylenimine as a gene carrier, J. Control. Release. 117 (2007) 273–280. https://doi.org/10.1016/j.jconrel.2006.10.025.

[70] S.K. Tripathi, R. Goyal, P. Kumar, K.C. Gupta, Linear polyethylenimine-graft-chitosan copolymers as efficient DNA/siRNA delivery vectors in vitro and in vivo,

Nanomedicine Nanotechnology, Biol. Med. 8 (2012) 337–345. https://doi.org/10.1016/j.nano.2011.06.022.

[71] K. Wong, G. Sun, X. Zhang, H. Dai, Y. Liu, C. He, K.W. Leong, PEI-g-chitosan, a novel gene delivery system with transfection efficiency comparable to polyethylenimine in vitro and after liver administration in vivo, Bioconjug. Chem. 17 (2006) 152–158. https://doi.org/10.1021/bc0501597.

[72] S.C. Park, J.P. Nam, Y.M. Kim, J.H. Kim, J.W. Nah, M.K. Jang, Branched polyethylenimine-grafted-carboxymethyl chitosan copolymer enhances the delivery of pDNA or siRNA in vitro and in vivo, Int. J. Nanomedicine. 8 (2013) 3663–3677. https://doi.org/10.2147/IJN.S50911.

[73] A.C. Hunter, Molecular hurdles in polyfectin design and mechanistic background to polycation induced cytotoxicity, Adv. Drug Deliv. Rev. 58 (2006) 1523–1531. https://doi.org/10.1016/j.addr.2006.09.008.

[74] S. Nimesh, A. Aggarwal, P. Kumar, Y. Singh, K.C. Gupta, R. Chandra, Influence of acyl chain length on transfection mediated by acylated PEI nanoparticles, Int. J. Pharm. 337 (2007) 265–274. https://doi.org/10.1016/j.ijpharm.2006.12.032.

[75] A. Zintchenko, A. Philipp, A. Dehshahri, E. Wagner, Simple modifications of branched PEI lead to highly efficient siRNA carriers with low toxicity, Bioconjug. Chem. 19 (2008) 1448–1455. https://doi.org/10.1021/bc800065f.

[76] S. Wen, F. Zheng, M. Shen, X. Shi, Surface modification and PEGylation of branched polyethyleneimine for improved biocompatibility, J. Appl. Polym. Sci. 128 (2013) 3807–3813. https://doi.org/10.1002/app.38444.

[77] L.P. Brewster, E.M. Brey, H.P. Greisler, Cardiovascular gene delivery: The good road is awaiting, Adv. Drug Deliv. Rev. 58 (2006) 604–629. https://doi.org/10.1016/j.addr.2006.03.002.

[78] S. Mansouri, P. Lavigne, K. Corsi, M. Benderdour, E. Beaumont, J.C. Fernandes, Chitosan-DNA nanoparticles as non-viral vectors in gene therapy: Strategies to improve transfection efficacy, Eur. J. Pharm. Biopharm. 57 (2004) 1–8. https://doi.org/10.1016/S0939-6411(03)00155-3.

[79] S. Choosakoonkriang, B. Lobo, G. Koe, J. Koe, C. Middaugh, Biophysical

characterization of PEI/DNA complexes, J. Pharm. Sci. 92 (2003) 1710–1722. https://doi.org/10.1002/jps.10437.

[80] Y. He, Y. Nie, L. Xie, H. Song, Z. Gu, P53 mediated apoptosis by reduction sensitive shielding ternary complexes based on disulfide linked PEI ternary complexes, Biomaterials. 35 (2014) 1657–1666. https://doi.org/10.1016/j.biomaterials.2013.10.073.

[81] I.J. Hildebrandt, M. Iyer, E. Wagner, S.S. Gambhir, Optical imaging of transferrin targeted PEI/DNA complexes in living subjects, Gene Ther. 10 (2003) 758–764. https://doi.org/10.1038/sj.gt.3301939.

[82] D. Rahmat, D. Sakloetsakun, G. Shahnaz, G. Perera, R. Kaindl, A. Bernkop-Schnürch, Design and synthesis of a novel cationic thiolated polymer, Int. J. Pharm. 411 (2011) 10–17. https://doi.org/10.1016/j.ijpharm.2011.02.063.

[83] V.M. Guillem, M. Tormo, F. Revert, I. Benet, J. García-Conde, A. Crespo, S.F. Aliño, Polyethyleneimine-based immunopolyplex for targeted gene transfer in human lymphoma cell lines, J. Gene Med. 4 (2002) 170–182. https://doi.org/10.1002/jgm.228.

[84] K. Kunath, T. Merdan, O. Hegener, H. Häberlein, T. Kissel, Integrin targeting using RGD-PEI conjugates for in vitro gene transfer, J. Gene Med. 5 (2003) 588–599. https://doi.org/10.1002/jgm.382.

[85] M. Kursa, G. Walker, V. Roessler, M. Ogris, W. Rödl, K. Ralf, E. Wagner, Novel Shielded Transferrin−Polyethylene Glycol−Polyethylenimine/DNA Complexes for Systemic Tumor-Targeted Gene Transfer, Bioconjug. Chem. 14 (2003) 222–231. https://doi.org/10.1021/bc0256087.

[86] J.S. Suk, J. Suh, K. Choy, S.K. Lai, J. Fu, J. Hanes, Gene delivery to differentiated neurotypic cells with RGD and HIV Tat peptide functionalized polymeric nanoparticles, Biomaterials. 27 (2006) 5143–5150. https://doi.org/10.1016/j.biomaterials.2006.05.013.

[87] J. Chen, H. Tian, Z. Guo, J. Xia, A. Kano, A. Maruyama, X. Jing, X. Chen, A highly efficient siRNA carrier of PBLG modified hyperbranched PEI, Macromol. Biosci. 9 (2009) 1247–1253. https://doi.org/10.1002/mabi.200900249.

[88] J. Xia, L. Chen, J. Chen, H. Tian, F. Li, X. Zhu, G. Li, X. Chen, Hydrophobic

Polyphenylalanine-Grafted Hyperbranched Polyethylenimine and its in vitro Gene Transfection, Macromol. Biosci. 11 (2011) 211–218. https://doi.org/10.1002/mabi.201000302.

[89] A. Alshamsan, A. Haddadi, V. Incani, J. Samuel, A. Lavasanifar, H. Uludag, Formulation and Delivery of siRNA by Oleic Acid and Stearic Acid Modified Polyethylenimine, Mol. Pharm. 6 (2009) 121–133. https://doi.org/10.1021/mp8000815.

[90] S. Tripathi, R. Goyal, P. Kumar, K. Gupta, Linear polyethylenimine-graft-chitosan copolymers as efficient DNA/siRNA delivery vectors in vitro and in vivo, Nanomedicine. 8 (2011) 337–345. https://doi.org/10.1016/j.nano.2011.06.022.

[91] H.-L. Jiang, J.-T. Kwon, Y.-K. Kim, E.-M. Kim, R. Arote, H.-J. Jeong, J.-W. Nah, Y.-J. Choi, T. Akaike, M.-H. Cho, C.-S. Cho, Galactosylated chitosan-graft-polyethylenimine as a gene carrier for hepatocyte targeting, Gene Ther. 14 (2007) 1389–1398. https://doi.org/10.1038/sj.gt.3302997.

[92] M. Neu, D. Fischer, T. Kissel, Recent advances in rational gene transfer vector design based on poly(ethylene imine) and its derivatives, J. Gene Med. 7 (2005) 992–1009. https://doi.org/10.1002/jgm.773.

[93] M. Gosselin, W. Guo, R. Lee, Efficient Gene Transfer Using Reversibly Cross-Linked Low Molecular Weight Polyethylenimine, Bioconjug. Chem. 12 (2001) 989–994. https://doi.org/10.1021/bc0100455.

[94] J. Schäfer, S. Höbel, U. Bakowsky, A. Aigner, Liposome-polyethylenimine complexes for enhanced DNA and siRNA delivery, Biomaterials. 31 (2010) 6892–6900. https://doi.org/10.1016/j.biomaterials.2010.05.043.

[95] S. Mao, M. Neu, O. Germershaus, O. Merkel, J. Sitterberg, U. Bakowsky, T. Kissel, Influence of polyethylene glycol chain length on the physicochemical and biological properties of poly(ethylene imine)-graft-poly(ethylene glycol) block copolymer/SiRNA polyplexes, Bioconjug. Chem. 17 (2006) 1209–1218. https://doi.org/10.1021/bc060129j.

[96] M. Zheng, D. Librizzi, A. Kiliç, Y. Liu, H. Renz, O.M. Merkel, T. Kissel, Enhancing in vivo circulation and siRNA delivery with biodegradable polyethylenimine-graft-

polycaprolactone-block-poly(ethylene glycol) copolymers, Biomaterials. 33 (2012) 6551–6558. https://doi.org/10.1016/j.biomaterials.2012.05.055.

[97] Y. Liu, O. Samsonova, B. Sproat, O. Merkel, T. Kissel, Biophysical characterization of hyper-branched polyethylenimine-graft- polycaprolactone-block-mono-methoxyl-poly(ethylene glycol) copolymers (hy-PEI-PCL-mPEG) for siRNA delivery, J. Control. Release. 153 (2011) 262–268. https://doi.org/10.1016/j.jconrel.2011.04.017.

[98] T. Merdan, K. Kunath, H. Petersen, U. Bakowsky, K.H. Voigt, J. Kopecek, T. Kissel, PEGylation of poly(ethylene imine) affects stability of complexes with plasmid DNA under in vivo conditions in a dose-dependent manner after intravenous injection into mice, Bioconjug. Chem. 16 (2005) 785–792. https://doi.org/10.1021/bc049743q.

[99] L. Kong, J. Qiu, W. Sun, J. Yang, M. Shen, L. Wang, X. Shi, Multifunctional PEI-entrapped gold nanoparticles enable efficient delivery of therapeutic siRNA into glioblastoma cells, Biomater. Sci. 5 (2017) 258–266. https://doi.org/10.1039/C6BM00708B.

[100] H. Petersen, P.M. Fechner, A.L. Martin, K. Kunath, S. Stolnik, C.J. Roberts, D. Fischer, M.C. Davies, T. Kissel, Polyethylenimine-graft-Poly(ethylene glycol) Copolymers: Influence of Copolymer Block Structure on DNA Complexation and Biological Activities as Gene Delivery System, Bioconjug. Chem. 13 (2002) 845–854. https://doi.org/10.1021/bc025529v.

[101] H. Petersen, P.M. Fechner, D. Fischer, T. Kissel, Synthesis, Characterization, and Biocompatibility of Polyethylenimine-graft-poly(ethylene glycol) Block Copolymers, Macromolecules. 35 (2002) 6867–6874. https://doi.org/10.1021/ma012060a.

[102] H. Khalil, T. Chen, R. Riffon, R. Wang, Z. Wang, Synergy between polyethylenimine and different families of antibiotics against a resistant clinical isolate of Pseudomonas aeruginosa, Antimicrob. Agents Chemother. 52 (2008) 1635–1641. https://doi.org/10.1128/AAC.01071-07.

[103] M.M. Azevedo, P. Ramalho, A.P. Silva, R. Teixeira-Santos, C. Pina-Vaz, A.G. Rodrigues, Polyethyleneimine and polyethyleneimine-based nanoparticles: Novel bacterial and yeast biofilm inhibitors, J. Med. Microbiol. 63 (2014) 1167–1173. https://doi.org/10.1099/jmm.0.069609-0.

[104] M.E. Davis, Non-viral gene delivery systems, Curr. Opin. Biotechnol. 13 (2002) 128–131. https://doi.org/https://doi.org/10.1016/S0958-1669(02)00294-X.

[105] J.-H. Jang, T.L. Houchin, L.D. Shea, Gene delivery from polymer scaffolds for tissue engineering, Expert Rev. Med. Devices. 1 (2004) 127–138. https://doi.org/10.1586/17434440.1.1.127.

[106] D. Xu, Q. Wang, T. Yang, J. Cao, Q. Lin, Z. Yuan, L. Li, Polyethyleneimine capped silver nanoclusters as efficient antibacterial agents, Int. J. Environ. Res. Public Health. 13 (2016). https://doi.org/10.3390/ijerph13030334.

[107] N. Beyth, I. Yudovin-Farber, M. Perez-Davidi, A.J. Domb, E.I. Weiss, Polyethyleneimine nanoparticles incorporated into resin composite cause cell death and trigger biofilm stress in vivo, Proc. Natl. Acad. Sci. U. S. A. 107 (2010) 22038–22043. https://doi.org/10.1073/pnas.1010341107.

[108] A.N. Vereshchagin, N.A. Frolov, K.S. Egorova, M.M. Seitkalieva, V.P. Ananikov, Quaternary Ammonium Compounds (QACs) and Ionic Liquids (ILs) as Biocides: From Simple Antiseptics to Tunable Antimicrobials., Int. J. Mol. Sci. 22 (2021). https://doi.org/10.3390/ijms22136793.

[109] B. Gao, X. Zhang, Y. Zhu, Studies on the preparation and antibacterial properties of quaternized polyethyleneimine, J. Biomater. Sci. Polym. Ed. 18 (2007) 531–544. https://doi.org/10.1163/156856207780852523.

[110] F. Nederberg, Y. Zhang, J.P.K. Tan, K. Xu, H. Wang, C. Yang, S. Gao, X.D. Guo, K. Fukushima, L. Li, J.L. Hedrick, Y.-Y. Yang, Biodegradable nanostructures with selective lysis of microbial membranes, Nat. Chem. 3 (2011) 409–414. https://doi.org/10.1038/nchem.1012.

[111] T. Lan, Q. Guo, X. Shen, Polyethyleneimine and quaternized ammonium polyethyleneimine: the versatile materials for combating bacteria and biofilms, J. Biomater. Sci. Polym. Ed. 30 (2019) 1243–1259. https://doi.org/10.1080/09205063.2019.1627650.

[112] U. Kwolek, K. Wójcik, M. Janiczek, M. Nowakowska, M. Kepczynski, Synthesis and antibacterial properties of quaternary ammonium derivative of polyethylenimine, Polimery/Polymers. 62 (2017) 311–315. https://doi.org/10.14314/polimery.2017.311.

[113] V. V. Khutoryanskiy, Advances in Mucoadhesion and Mucoadhesive Polymers, Macromol. Biosci. 11 (2011) 748–764. https://doi.org/10.1002/mabi.201000388.

[114] O.M. Kolawole, W.M. Lau, V. V Khutoryanskiy, Methacrylated chitosan as a polymer with enhanced mucoadhesive properties for transmucosal drug delivery, Int. J. Pharm. 550 (2018) 123–129. https://doi.org/https://doi.org/10.1016/j.ijpharm.2018.08.034.

[115] S. Koirala, P. Nepal, G. Ghimire, R. Basnet, I. Rawat, A. Dahal, J. Pandey, K. Parajuli-Baral, Formulation and evaluation of mucoadhesive buccal tablets of aceclofenac., Heliyon. 7 (2021) e06439. https://doi.org/10.1016/j.heliyon.2021.e06439.

[116] I.A. Sogias, A.C. Williams, V. V Khutoryanskiy, Chitosan-based mucoadhesive tablets for oral delivery of ibuprofen, Int. J. Pharm. 436 (2012) 602–610. https://doi.org/https://doi.org/10.1016/j.ijpharm.2012.07.007.

[117] F. Buang, A. Chatzifragkou, M.C.I.M. Amin, V. V. Khutoryanskiy, Synthesis of Methacryloylated Hydroxyethylcellulose and Development of Mucoadhesive Wafers for Buccal Drug Delivery, Polymers (Basel). 15 (2023). https://doi.org/10.3390/polym15010093.

[118] G. Lemkine, B. Demeneix, Polyethylenimines for in vivo gene delivery, Curr. Opin. Mol. Ther. 3 (2001) 178–182.

[119] B.K. Suh, J.; Paik, H-J.; Hwang, Ionization of PEI and PAA at Various pH's, Bioorg. Chem. 22 (1994) 318–327.

[120] W. Tiyaboonchai, J. Woiszwillo, C.R. Middaugh, Formulation and characterization of DNA – polyethylenimine – dextran sulfate nanoparticles, 19 (2003) 191–202.

[121] W. Tiyaboonchai, J. Woiszwillo, C. Middaugh, Formulation and characterization of Amphotericin-B–polyethylenimine–dextran sulfate nanoparticles, J. Pharm. Sci. 90 (2001) 902–914. https://doi.org/10.1002/jps.1042.

[122] W. Tiyaboonchai, I. Rodleang, A. Ounaroon, Mucoadhesive polyethylenimine-dextran sulfate nanoparticles containing Punica granatum peel extract as a novel sustained-release antimicrobial, Pharm. Dev. Technol. 20 (2015) 426–432. https://doi.org/10.3109/10837450.2013.879884.

[123] G.M.F. Calixto, F.D. Victorelli, L.N. Dovigo, M. Chorilli, Polyethyleneimine and Chitosan Polymer-Based Mucoadhesive Liquid Crystalline Systems Intended for

Buccal Drug Delivery, AAPS PharmSciTech. 19 (2018) 820–836. https://doi.org/10.1208/s12249-017-0890-2.

[124] D.B. Kaldybekov, P. Tonglairoum, P. Opanasopit, V. V Khutoryanskiy, Mucoadhesive maleimide-functionalised liposomes for drug delivery to urinary bladder, Eur. J. Pharm. Sci. 111 (2018) 83–90. https://doi.org/https://doi.org/10.1016/j.ejps.2017.09.039.

[125] S. Soradech, J. Nunthanid, S. Limmatvapirat, M. Luangtana-Anan, An approach for the enhancement of the mechanical properties and film coating efficiency of shellac by the formation of composite films based on shellac and gelatin, J. Food Eng. 108 (2012) 94–102. https://doi.org/10.1016/j.jfoodeng.2011.07.019.

[126] M. Luangtana-anan, S. Soradech, S. Saengsod, J. Nunthanid, S. Limmatvapirat, Enhancement of Moisture Protective Properties and Stability of Pectin through Formation of a Composite Film: Effects of Shellac and Plasticizer, J. Food Sci. 82 (2017) 2915–2925. https://doi.org/10.1111/1750-3841.13956.

[127] S. Soradech, S. Limatvapirat, M. Luangtana-anan, Stability enhancement of shellac by formation of composite film: Effect of gelatin and plasticizers, J. Food Eng. 116 (2013) 572–580. https://doi.org/10.1016/j.jfoodeng.2012.12.035.

[128] M.A. García, A. Pinotti, M.N. Martino, N.E. Zaritzky, Characterization of composite hydrocolloid films, Carbohydr. Polym. 56 (2004) 339–345. https://doi.org/10.1016/j.carbpol.2004.03.003.

[129] K. Luo, J. Yin, O. V. Khutoryanskaya, V. V. Khutoryanskiy, Mucoadhesive and elastic films based on blends of chitosan and hydroxyethylcellulose, Macromol. Biosci. 8 (2008) 184–192. https://doi.org/10.1002/mabi.200700185.

[130] G.K. Abilova, D.B. Kaldybekov, E.K. Ozhmukhametova, A.Z. Saimova, D.S. Kazybayeva, G.S. Irmukhametova, V. V. Khutoryanskiy, Chitosan/poly(2-ethyl-2-oxazoline) films for ocular drug delivery: Formulation, miscibility, in vitro and in vivo studies, Eur. Polym. J. 116 (2019) 311–320. https://doi.org/10.1016/j.eurpolymj.2019.04.016.

[131] B. Qussi, W.G. Suess, The influence of different plasticizers and polymers on the mechanical and thermal properties, porosity and drug permeability of free shellac

films, Drug Dev. Ind. Pharm. 32 (2006) 403–412. https://doi.org/10.1080/03639040600559099.

[132] J. Yin, K. Luo, X. Chen, V. V. Khutoryanskiy, Miscibility studies of the blends of chitosan with some cellulose ethers, Carbohydr. Polym. 63 (2006) 238–244. https://doi.org/10.1016/j.carbpol.2005.08.041.

[133] S. Taranejoo, J. Liu, P. Verma, K. Hourigan, A review of the developments of characteristics of PEI derivatives for gene delivery applications, J. Appl. Polym. Sci. 132 (2015). https://doi.org/10.1002/app.42096.

[134] Q. Chai, Y. Jiao, X. Yu, Hydrogels for Biomedical Applications: Their Characteristics and the Mechanisms behind Them, Gels. 3 (2017) 6. https://doi.org/10.3390/gels3010006.

[135] G.S. Irmukhametova, G.A. Mun, V. V Khutoryanskiy, Hydrogel Dressings, Ther. Dressings Wound Heal. Appl. (2020) 185–207. https://doi.org/doi:10.1002/9781119433316.ch9.

[136] E. V Hackl, V. V Khutoryanskiy, I. Ermolina, Hydrogels based on copolymers of 2-hydroxyethylmethacrylate and 2-hydroxyethylacrylate as a delivery system for proteins: Interactions with lysozyme, J. Appl. Polym. Sci. 134 (2017). https://doi.org/https://doi.org/10.1002/app.44768.

[137] E. Caló, J.M.S.D. Barros, M. Fernández-Gutiérrez, J. San Román, L. Ballamy, V. V. Khutoryanskiy, Antimicrobial hydrogels based on autoclaved poly(vinyl alcohol) and poly(methyl vinyl ether-: Alt -maleic anhydride) mixtures for wound care applications, RSC Adv. 6 (2016) 55211–55219. https://doi.org/10.1039/c6ra08234c.

[138] E. Caló, V. V. Khutoryanskiy, Biomedical applications of hydrogels: A review of patents and commercial products, Eur. Polym. J. 65 (2015) 252–267. https://doi.org/10.1016/j.eurpolymj.2014.11.024.

[139] E. Caló, J. Barros, L. Ballamy, V. V. Khutoryanskiy, Poly(vinyl alcohol)-Gantrez® AN cryogels for wound care applications, RSC Adv. 6 (2016) 105487–105494. https://doi.org/10.1039/c6ra24573k.

[140] A.M. Mathur, S.K. Moorjani, A.B. Scranton, Methods for Synthesis of Hydrogel Networks: A Review, J. Macromol. Sci. Part C. 36 (1996) 405–430.

https://doi.org/10.1080/15321799608015226.

[141] A. Paciello, M.G. Santonicola, Supramolecular polycationic hydrogels with high swelling capacity prepared by partial methacrylation of polyethyleneimine, RSC Adv. 5 (2015) 88866–88875. https://doi.org/10.1039/c5ra16576h.

[142] F. Wahid, H. Bai, F.P. Wang, Y.Y. Xie, Y.W. Zhang, L.Q. Chu, S.R. Jia, C. Zhong, Facile synthesis of bacterial cellulose and polyethyleneimine based hybrid hydrogels for antibacterial applications, Cellulose. 27 (2020) 369–383. https://doi.org/10.1007/s10570-019-02806-1.

[143] V. Lozinsky, Cryostructuring of Polymeric Systems. 50.† Cryogels and Cryotropic Gel-Formation: Terms and Definitions, Gels. 4 (2018) 77. https://doi.org/10.3390/gels4030077.

[144] M. Bakhshpour, N. Idil, I. Perçin, A. Denizli, Biomedical applications of polymeric cryogels, Appl. Sci. 9 (2019) 1–22. https://doi.org/10.3390/app9030553.

[145] Y. Shi, D.S. Xiong, Y. Peng, N. Wang, Effects of polymerization degree on recovery behavior of PVA/PVP hydrogels as potential articular cartilage prosthesis after fatigue test, Express Polym. Lett. 10 (2016) 125–138. https://doi.org/10.3144/expresspolymlett.2016.13.

[146] S.K. H. Gulrez, S. Al-Assaf, G. O, Hydrogels: Methods of Preparation, Characterisation and Applications, Prog. Mol. Environ. Bioeng. - From Anal. Model. to Technol. Appl. (2011). https://doi.org/10.5772/24553.

[147] V. Pazos, R. Mongrain, J.C. Tardif, Polyvinyl alcohol cryogel: Optimizing the parameters of cryogenic treatment using hyperelastic models, J. Mech. Behav. Biomed. Mater. 2 (2009) 542–549. https://doi.org/10.1016/j.jmbbm.2009.01.003.

[148] A. Kumar, R. Mishra, Y. Reinwald, S. Bhat, Cryogels: Freezing unveiled by thawing, Mater. Today. 13 (2010) 42–44. https://doi.org/https://doi.org/10.1016/S1369-7021(10)70202-9.

[149] N.A. Peppas, S.R. Stauffer, Reinforced uncrosslinked poly (vinyl alcohol) gels produced by cyclic freezing-thawing processes: a short review, J. Control. Release. 16 (1991) 305–310. https://doi.org/https://doi.org/10.1016/0168-3659(91)90007-Z.

[150] A.S. Hickey, N.A. Peppas, Mesh size and diffusive characteristics of semicrystalline

poly(vinyl alcohol) membranes prepared by freezing/thawing techniques, J. Memb. Sci. 107 (1995) 229–237. https://doi.org/https://doi.org/10.1016/0376-7388(95)00119-0.

[151] P. Karacan, O. Okay, Ethidium bromide binding to DNA cryogels, React. Funct. Polym. 73 (2013) 442–450. https://doi.org/10.1016/j.reactfunctpolym.2012.11.014.

[152] N. Sahiner, S. Demirci, Poly ionic liquid cryogel of polyethyleneimine: Synthesis, characterization, and testing in absorption studies, J. Appl. Polym. Sci. 133 (2016) 1–13. https://doi.org/10.1002/app.43478.

[153] Y.C. Kuo, I.N. Ku, Application of polyethyleneimine-modified scaffolds to the regeneration of cartilaginous tissue, Biotechnol. Prog. 25 (2009) 1459–1467. https://doi.org/10.1002/btpr.232.

[154] A.Ü. Metin, Immobilization of laccase onto polyethyleneimine grafted chitosan films: Effect of system parameters, Macromol. Res. 21 (2013) 1145–1152. https://doi.org/10.1007/s13233-013-1146-y.

[155] M. Wang, X. Yang, P. Zhang, L. Cai, X. Yang, Y. Chen, Y. Jing, J. Kong, X. Yang, F.L. Sun, Sustained Delivery Growth Factors with Polyethyleneimine-Modified Nanoparticles Promote Embryonic Stem Cells Differentiation and Liver Regeneration, Adv. Sci. 3 (2016) 1–13. https://doi.org/10.1002/advs.201500393.

[156] D. Zhu, X. Li, X. Liao, B. Shi, Polyethyleneimine-grafted collagen fiber as a carrier for cell immobilization, J. Ind. Microbiol. Biotechnol. 42 (2014) 189–196. https://doi.org/10.1007/s10295-014-1566-5.

[157] R. Lakra, M. Kiran, K. Purna Sai, Electrospun gelatin–polyethylenimine blend nanofibrous scaffold for biomedical applications, J. Mater. Sci. Mater. Med. 30 (2019). https://doi.org/10.1007/s10856-019-6336-5.

[158] Q. Meng, Y. Li, C. Shen, Antibacterial Coatings of Biomedical Surfaces by Polydextran Aldehyde/Polyethylenimine Nanofibers, ACS Appl. Bio Mater. 2 (2018). https://doi.org/10.1021/acsabm.8b00708.

[159] X. Jing, H.-Y. Mi, M.R. Salick, T. Cordie, J. McNulty, X.-F. Peng, L.-S. Turng, In vitro evaluations of electrospun nanofiber scaffolds composed of poly(ε-caprolactone) and polyethylenimine, J. Mater. Res. 30 (2015) 1808–1819. https://doi.org/DOI:

10.1557/jmr.2015.117.

[160] L. Ma, X. Wang, J. Wu, D. Zhang, L. Zhang, X. Song, H. Hong, C. He, X. Mo, S. Wu, G. Kai, H. Wang, Polyethylenimine and sodium cholate-modified ethosomes complex as multidrug carriers for the treatment of melanoma through transdermal delivery, Nanomedicine. 14 (2019) 2395–2408. https://doi.org/10.2217/nnm-2018-0398.

[161] K. Wang, Y. Yan, G. Zhao, W. Xu, K. Dong, C. You, L. Zhang, J. Xing, In vitro and in vivo application of hydroxypropyl-β-cyclodextrin- grafted polyethyleneimine used as a transdermal penetration enhancer, Polym. Chem. 5 (2014) 4658–4669. https://doi.org/10.1039/c4py00286e.

[162] O. Koenig, B. Neumann, C. Schlensak, H.P. Wendel, A. Nolte, Hyaluronic acid/poly(ethylenimine) polyelectrolyte multilayer coatings for siRNA-mediated local gene silencing, PLoS One. 14 (2019) 1–17. https://doi.org/10.1371/journal.pone.0212584.

[163] A.R. Ibragimova, A.B. Mirgorodskaya, E.A. Vasilieva, E.I. Khairutdinova, T.K. Meleshko, I. V. Ivanov, A. V. Yakimansky, I.R. Nizameev, M.K. Kadirov, L.Y. Zakharova, Polyelectrolyte nanocapsules with controlled properties fabricated by layer-by-layer deposition of polyethyleneimine and graft-copolyimide with polymethacrylic acid side chains, Colloids Surfaces A Physicochem. Eng. Asp. 526 (2017) 20–28. https://doi.org/10.1016/j.colsurfa.2016.11.065.

[164] A.S. Mary, V.S. Raghavan, S. Kagula, V. Krishnakumar, M. Kannan, S.S. Gorthi, K. Rajaram, Enhanced in Vitro Wound Healing Using PVA/B-PEI Nanofiber Mats: A Promising Wound Therapeutic Agent against ESKAPE and Opportunistic Pathogens, ACS Appl. Bio Mater. 4 (2021) 8466–8476. https://doi.org/10.1021/acsabm.1c00985.

[165] Y. Zou, D. Li, M. Shen, X. Shi, Polyethylenimine-Based Nanogels for Biomedical Applications, Macromol. Biosci. 19 (2019) 1–11. https://doi.org/10.1002/mabi.201900272.

[166] J. Li, Y. He, W. Sun, Y. Luo, H. Cai, Y. Pan, M. Shen, J. Xia, X. Shi, Hyaluronic acid-modified hydrothermally synthesized iron oxide nanoparticles for targeted tumor MR imaging., Biomaterials. 35 (2014) 3666–3677. https://doi.org/10.1016/j.biomaterials.2014.01.011.

[167] B. Zhou, L. Zhao, M. Shen, J. Zhao, X. Shi, A multifunctional polyethylenimine-based nanoplatform for targeted anticancer drug delivery to tumors in vivo., J. Mater. Chem. B. 5 (2017) 1542–1550. https://doi.org/10.1039/c6tb02620f.

[168] T.J. Cho, J.M. Gorham, J.M. Pettibone, J. Liu, J. Tan, V.A. Hackley, Parallel Multiparameter Study of PEI-Functionalized Gold Nanoparticle Synthesis for Biomedical Applications: Part 2. Elucidating the Role of Surface Chemistry and Polymer Structure in Performance, Langmuir. 36 (2020) 14058–14069. https://doi.org/10.1021/acs.langmuir.0c02630.

[169] H. Cai, X. An, J. Cui, J. Li, S. Wen, K. Li, M. Shen, L. Zheng, G. Zhang, X. Shi, Facile Hydrothermal Synthesis and Surface Functionalization of Polyethyleneimine-Coated Iron Oxide Nanoparticles for Biomedical Applications, ACS Appl. Mater. Interfaces. 5 (2013) 1722–1731. https://doi.org/10.1021/am302883m.

[170] Y. Sun, K. Ren, J. Wang, G. Chang, J. Ji, Electrochemically Controlled Stiffness of Multilayers for Manipulation of Cell Adhesion, ACS Appl. Mater. Interfaces. 5 (2013) 4597–4602. https://doi.org/10.1021/am401088w.

Chapter 2

Physically Crosslinked Cryogels of Linear Polyethyleneimine: Influence of Cooling Temperature and Solvent Composition

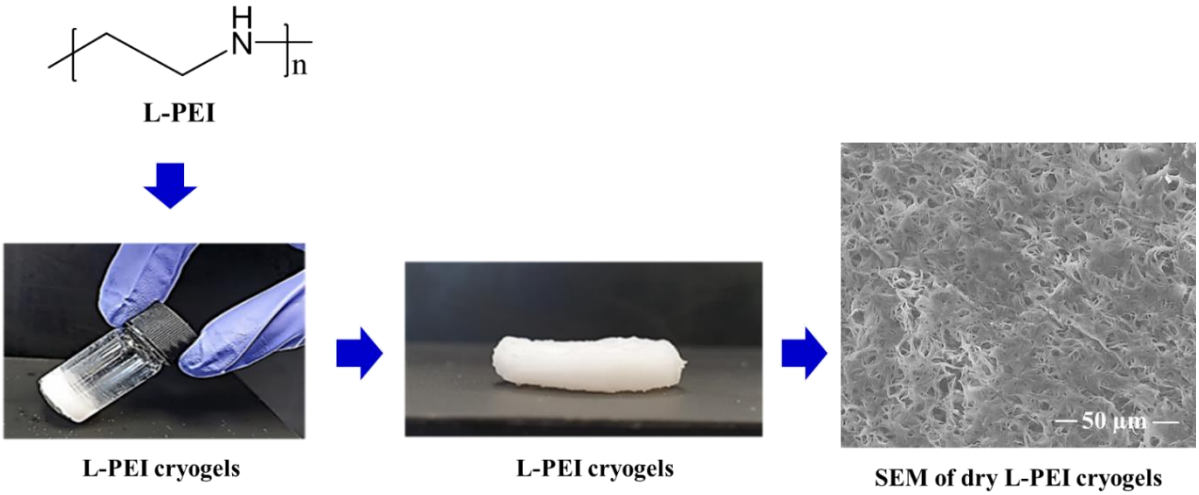

This chapter was published as: Sitthiphong Soradech, Adrian C. Williams, and Vitaliy V. Khutoryanskiy, Physically Crosslinked Cryogels of Linear Polyethyleneimine: Influence of Cooling Temperature and Solvent Composition, Macromolecules, 2022, 55, 21, 9537–9546. https://doi.org/10.1021/acs.macromol.2c01308

Chapter 2

Physically Crosslinked Cryogels of Linear Polyethyleneimine: Influence of Cooling Temperature and Solvent Composition

Sitthiphong Soradech[1, 2], Adrian C. Williams[1], and Vitaliy V. Khutoryanskiy[1]*

[1]Reading School of Pharmacy, University of Reading, Whiteknights, Reading, RG6 6AD, UK

[2]Expert Centre of Innovative Herbal Products, Thailand Institute of Scientific and Technological Research, Pathum Thani, 12120, Thailand.

***Corresponding author:**
Postal address: Reading School of Pharmacy, University of Reading, Whiteknights, PO Box 224, RG6 6AD, Reading, United Kingdom
E-mail address: v.khutoryanskiy@reading.ac.uk
Telephone: +44(0) 118 378 6119
Fax: +44(0) 118 378 4703

ABSTRACT

Physically crosslinked cryogels can be prepared using linear polyethyleneimine (L-PEI) and a freeze-thawing technique. L-PEI was synthesized by hydrolysis of poly(2-ethyl-2-oxazoline) under acidic conditions. Dissolution of L-PEI in deionized water was achieved at 80 ^{o}C and resulted in a transparent solution, leading to an opaque gel forming upon freezing and subsequent thawing. The cryogels exhibited reversibility and after heating at 80 ^{o}C formed a clear solution due to the melting of the crystalline domains of L-PEI. The effects of different cooling temperatures and the use of various solvent compositions on L-PEI gelation were also studied. L-PEI cryogels were produced by freezing aqueous solutions to various temperatures (-196, -80, -30, and 0 °C) for 3 h and subsequent thawing at 25°C for 24 h. Gel rigidity correlated with the freezing temperature and was strongest when cooled to -196 ^{o}C, consistent with determinations of the degree of crystallinity in the gels, the enthalpy of fusion and rheological behaviour. The effect of solvent mixtures on the crystallinity and rheological properties of L-PEI cryogels was also investigated. Water/ethanol mixtures containing a higher proportion of ethanol significantly reduced the strength, viscosity and degree of crystallinity of the L-PEI cryogels. Thus, by controlling the freezing temperature or modifying the solvent, L-PEI cryogels can be designed with desired mechanical properties for applications ranging from cell immobilisation and tissue culture scaffolds to drug delivery systems or antimicrobial wound dressings.

1. INTRODUCTION

Polymeric gels are extensively used for biomedical applications due to their flexibility, high water content, biocompatibility, and softness [1]. They are also widely used in drug delivery systems, chromatography, as immobilization matrices, for biomedical scaffolds and in wound healing products. Gels are defined as three-dimensional cross-linked polymer networks, which are swollen in solvents [2, 3]. Networks swollen in water provide hydrogels, whereas those swollen in organic solvents are organogels. Polymeric gels are broadly classified as physical and chemical gels. Physical gels can be prepared through physical crosslinking of polymer chains via hydrophobic effects, ionic or hydrogen bonds and through the formation of crystallites within the network. Physical gels commonly re-dissolve upon changes in environmental conditions such as temperature, ionic strength, and pH. In contrast, chemical gels form by cross-linking through covalent bonds, leading to irreversibly insoluble networks [4].

Cryotropic gelation has been used to prepare physically cross-linked gels by freezing and subsequent thawing aqueous solutions of poly(vinyl alcohol) (PVA)[5]. PVA cryogels form via hydrogen bonds between PVA chains in the unfrozen phase, leading to microcrystalline domains that act as crosslinks [6]. PVA cryogels can be prepared from water or dimethyl sulfoxide (DMSO)[7]; with DMSO as the solvent, transparent gels formed whereas opaque PVA cryogels were formed from aqueous solutions [8]. The properties of PVA cryogels depended on multiple factors including the molecular weight and concentration of PVA in the initial solution, additives, the solvent from which they were formed, the cryogenic conditions (temperature and time of freezing, rates of thawing) and on the number of freezing and thawing cycles [7, 9].

Physically crosslinked cryogels with antimicrobial properties and surface charge control would be beneficial for biomedical, wound healing, and pharmaceutical applications. Due to the nonionic nature of PVA, its physically cross-linked cryogels do not exhibit antimicrobial properties. Therefore, physical cryogels based on cationic polymers are of interest for antimicrobial applications.

Polyethyleneimine (PEI) is a cationic polymer consisting of two carbon aliphatic (-CH_2CH_2-) spacer groups and primary, secondary and tertiary amine groups in each repeating unit. PEI is either linear or branched, which differ in structure and some properties [10]. In linear PEI all amine groups are secondary whereas branched PEI has primary, secondary and tertiary

amine groups. Branched PEI is usually synthesized by ring-opening polymerization of aziridine and L-PEI can be prepared by hydrolysis of poly(2-ethyl-2-oxazoline) under acidic or basic conditions to eliminate all the amide groups in the side chains [11,12]. Branched PEI is an amorphous polymer that is readily soluble in water[13], whereas L-PEI is semi-crystalline and only dissolves in water at high temperatures[13, 14]. Chantani et al.[14] demonstrated that temperatures > 60 ^{o}C lead to increased chain mobility of L-PEI, resulting in the melting of crystallites and eventual dissolution in water [15]. PEI is used in a wide range of applications, including gene delivery[16], pharmaceutical[10], antimicrobial[17,18] and enviromental applications[19]. Branched PEI cannot be used to prepare physically crosslinked hydrogels via cryo-gelation techniques, but it may form hydrogels through covalent cross-linking with various reagents, such as epichlorohydrin, diglycidyl ethers of glycols, and glutaraldehyde[20, 21]. In contrast, L-PEI is capable of forming physically crosslinked hydrogels, as shown by Yuan et al [22]. They reported gelation of L-PEI in water by cooling its hot aqueous solutions to room temperature, forming physical or thermoreversible gels[22]. This work provided new opportunities for the development of L-PEI hydrogels as a potential candidate for biorelated applications such as scaffolds for cell culture and controlled drug delivery [22].

To the best of our knowledge, there are no reports in the literature on L-PEI cryogels formed by freezing and subsequent thawing of its aqueous solutions. Thus, the fabrication of physically crosslinked cryogels based on L-PEI via cryotropic gelation has advantages, since this method does not require the use of cross-linkers or initiators. Therefore, the purpose of this study was to develop L-PEI as physically crosslinked cryogels using a freeze-thawing technique and to study the influence of cooling temperature and solvent composition on thermal, crystallinity, and rheological properties of these systems.

2. EXPERIMENTAL SECTION

2.1.Materials

Poly(2-ethyl-2-oxazoline) (50 kDa), deuterated methanol (CD_3OD) and sodium hydroxide, hydrochloric acid and ethanol were purchased from Merck (Gillingham, UK). All other chemicals were of analytical grade and used without further purification.

2.2. Synthesis of L-PEI

L-PEI was synthesized by hydrolysis of poly(2-ethyl-2-oxazoline) as described by Shan et al [23]. Briefly, 10 g of poly(2-ethyl-2-oxazolines) (PEOZ) was dissolved in 100 mL of 18.0 % (w/w) hydrochloric acid and then refluxed at 100 ^{o}C for 14 h to remove all amide groups in the side chains**.** The PEI solution obtained in hydrochloric acid was then diluted with cold deionized water (500 mL). Cold aqueous sodium hydroxide (4M) was added dropwise to the suspension until the polymer dissolved, but with further addition of 4 M sodium hydroxide, the base form of L-PEI precipitated at pH 10 - 11 [11]. The precipitate was recovered by filtration, washed with deionized water and re-precipitated twice before drying under vacuum to obtain L-PEI as a white power (yielding 3.8 g (88.4 %)).

2.3. General Method to Prepare Cryogels from L-PEI

5 % (w/w) L-PEI cryogels were prepared by a freezing and thawing method. For each cryogel, 100 mg of L-PEI powder was dispersed in 2 mL of deionized water. All samples were then heated at 80 ^{o}C until clear solutions were formed. The L-PEI solutions were then frozen for 3 h before being placed in an incubator at 25 ^{o}C for 24 h to thaw. As a reversibility control, the cryogels were re-heated at 80 ^{o}C until they formed a clear solution. The cryogels and reversible control were characterised using X-ray diffraction. All samples were prepared in triplicate.

2.4. Effect of Thawing Temperature on the Formation of L-PEI Cryogels

5 % (w/w) L-PEI cryogels were prepared as above and were all frozen at -80 ^{o}C for 3 h. Samples were then allowed to thaw at various temperatures between 20 – 80 ^{o}C for 24 h.

2.5. Effect of Different Freezing Temperatures on Physicochemical Properties of L-PEI Cryogels

Cryogel solutions were prepared as above and then cooled to various temperatures (-196 ^{o}C, -80 ^{o}C, -30 ^{o}C and 0 ^{o}C) for 3 h followed by thawing in an incubator at 25 ^{o}C for 24 h. Cooling used liquid nitrogen (-196 ^{o}C) and controlled temperature freezers at -80 ^{o}C and -30 ^{o}C. In addition, L-PEI solution was placed in normal ice to cool to 0 ^{o}C.

2.6. Effect of Solvent on the Formation and Physicochemical Properties of L-PEI Cryogels

Firstly, 100 mg of L-PEI was added to 2 mL ethanol-water mixtures. Ethanol-water mixtures that generated suspensions were heated at 80 ^{o}C in a water bath to form clear solutions whereas samples in which L-PEI readily dissolved were prepared using a vortex mixer at room temperature. The solutions were then cooled at -80 ^{o}C for 3 h followed by thawing in an incubator at 25 ^{o}C overnight. The rheological properties of the cryogels were characterised using a Brookfield rheometer (DV II, Germany). Samples of all cryogels were dried in a vacuum oven at 40 ^{o}C until constant weight and then characterised using FTIR spectroscopy and X-ray diffractometry. All samples were investigated in triplicate.

2.7. ^{1}H-Nuclear Magnetic Resonance Spectroscopy (^{1}H-NMR)

After dissolving 20 mg of dried PEOZ and L-PEI in methanol-d_4, ^{1}H NMR data were collected using a 400 MHz ULTRASHIELD PLUSTM B-ACS 60 spectrometer (Bruker, UK). Spectral analysis used MestReNova software.

2.8. Fourier Transformed Infrared (FTIR) Spectroscopy

Solid samples of PEOZ, L-PEI and dried L-PEI cryogels were scanned from 4000 to 400 cm^{-1} at 4 cm^{-1} resolution using a Nicolet iS5-iD5 ATR FT-IR spectrometer (Thermo Scientific, UK). Data was processed based on the average of six scans per spectrum.

2.9. Rheology

The rheological properties of L-PEI cryogels were evaluated using a strain-controlled rheometer (TA Instruments) fitted with a plate−plate geometry (25 mm diameter). The storage modulus (G′), loss modulus (G′′) and complex viscosity (η*) were recorded as a function of temperature from 20 to 80 ^{o}C for gel-sol transition experiments. The η* was calculated according to equations (1) and (2). In addition, the oscillation frequency mode was used to measure G′, G′′ and complex viscosity (η*) at 25 ^{o}C for cryogels prepared at different cooling temperatures. The following conditions were used in these experiments: a strain of 0.5%, a gap of 0.5 mm, constant frequency of ω = 6.28 rad/s to establish the linear viscoelastic region and a frequency sweep in the range of 0.01–100 Hz [24].

$$\eta^* = G^*/\omega \quad (1),$$

$$G^* = \sqrt{G'^2 + G''^2} \quad (2),$$

where η* is the complex viscosity, which is a measure of the total resistance to flow as a function of angular frequency (ω) given by the quotient of the maximum stress amplitude and maximum strain rate amplitude. G* is the complex shear modulus which allows the viscous and elastic components contributing to the total material stiffness.

The viscoelastic behavior of samples was quantified through dynamic measurements in terms of relative phase angle (tan δ = G´´/ G´, where δ was the loss angle). If tan δ is <1 then this indicates predominantly elastic behavior and a tan δ >1 shows predominantly viscous behavior [25].

2.10. Differential Scanning Calorimetry (DSC)

Thermal analysis of samples was performed using DSC (TA Instruments, Germany). Dried L-PEI powder (~3 mg) was loaded into pierced Tzero aluminum pans, whereas wet cryogel samples (~3 mg) were loaded into non-pierced Tzero aluminum pans to prevent evaporation of the water. The thermal behaviour of each sample was investigated from 30 to 100 ºC at 10 ◦C/min in a nitrogen atmosphere. The values of the melting (T_m) and enthalpy of samples were determined. All samples were analysed in triplicate.

2.11. X-ray Diffraction Analysis (XRD)

Wet or dried L-PEI crygels were placed on a silica slide and analyzed in a Bruker D8 ADVANCE PXRD equipped with a LynxEye detector and monochromatic Cu $K\alpha_1$ radiation (λ = 1.5406 Å). Samples were rotated at 30 rpm and data collected over an angular range of 5 - 60 º 2θ for 1 h, with a step of 0.05º (2θ) and count time of 1.2 s. The results were analyzed using Origin software. All samples were analysed in triplicate.

From the data, the percentage of crystallinity (χ) and crystallite size (*P*) were calculated according to equations (3) and (4), as follows [26]:

$$\chi = \frac{\int Ac}{(\int Ac + \int Aa)} \quad (3),$$

where *Ac* and *Aa* are the values of area under the peaks corresponding to crystalline and amorphous phases, respectively.

$$\boldsymbol{P = \frac{K\lambda}{\beta cos\theta}} \quad (4),$$

where *P* is the mean size of the ordered (crystalline) domains, *K* is 0.9 (Scherrer's constant), λ is the X-ray wavelength (0.15406 nm), β is peak full width at half maximum (FWHM, radians), θ is the Bragg angle that is obtained from the peak position (radians).

2.12. Scanning Electron Microscopy (SEM)

SEM was used to investigate the porous structure of L-PEI cryogels. Briefly, samples of freeze-dried cryogel samples were examined using a FEI Quanta 600 FEG SEM microscope (Field Electron and Ion Company, USA) with an acceleration voltage of 20 kV. Samples were coated with gold sputter to facilitate high resolution imaging.

2.13. Swelling Analysis

Freezed-dry L-PEI cryogels were placed into petri dishes with 40 mL of deionised water at 25 ^{o}C. The petri dishes were then placed on graph paper and changes in the sizes of the dry cryogels were measured over time. The diameter of each sample was measured 5 times in different directions and mean ± standard deviation values were calculated. The swelling ratio of L-PEI cryogels was calculated according to equation (5):

Swelling ratio = diameter of swollen gels/diameter of dry gels

2.14. Statistical Analysis

Results are presented as mean ± standard deviations for no fewer than three independent experiments. Student's t-test and one-way ANOVA was used for the analysis of the data to determine the extent of any differences between cryogel preparation methods.

3. RESULTS AND DISCUSSION

3.1. Formation of Physically Crosslinked Cryogels based on L-PEI

To prepare our initial L-PEI cryogels, the polymer was first dissolved at 80 ^{o}C in water in order to break crystalline domains before freezing at -80 ^{o}C, followed by subsequent thawing at room temperature (25 ^{o}C), forming stable cryogels **(Figure 1)**. It is known that L-PEI

exhibits water-induced phase transitions between four types of crystalline hydrates, dependent on the amount of absorbed water; anhydrate (EI monomer unit:water molecules = 1:0), hemihydrate (1:0.5), sequihydrate (1:1.5) and dihydrate (1:2) [27]. The polymer chain conformation changes from a double helix in the anhydrate to a planar-zigzag form in the hemi-, sesqui- and dihydrate forms. In brief, the PEI double helix forms via intermolecular NH···N hydrogen bonds. When water molecules are absorbed into the lattice, NH···O and OH···N bonds form between zigzags of PEI chains and water molecules [28]. In this study, L-PEI cryogels in water formed a dihydrated structure due to the high absorption of water molecules into L-PEI lattices (determined by XRD, see below). In addition, thermal cycling promotes physical crosslinking via the formation of structured crystalline domains of the polymer chains through phase separation. Several phases form during the thermal cycling process. Initially, as the gel cools to low temperatures the water phase freezes. This creates regions of high polymer concentration which can thus form crystallites and regions of low polymer concentration resulting in pore formation. The frozen gel was then thawed at room temperature to obtain interconnected macro-porous gels [29]. Whilst formation of physically crosslinked cryogels from L-PEI using freezing and thawing method has not been previously reported, it is likely that the mechanisms are similar to those in PVA cryogels [30]. Lozinsky et al. [31] found that PVA cryogel rigidity increased with increasing concentrations of PVA, due to the increase in hydroxyl groups for intermolecular hydrogen bonds. Hassan and Peppas [32] reported that increasing the concentration of PVA resulted in a highly stable gel due to the high degree of crystallinity and lower secondary crystallization. Caló et al.[8] reported poly(vinyl alcohol)-Gantrez® AN cryogels formed by a freezing and thawing technique. Inter- and intra-chain hydrogen bonding formed more rapidly in the unfrozen liquid micro-phases where the reagents were more highly concentrated by the formation and expansion of solvent crystals during freezing. Subsequent thawing resulted in a network of interconnected pores within the cryogel internal structure which influenced the physical and mechanical properties of the samples.

Reversibility of our L-PEI cryogels, shown by reheating the gel at 80 ^{o}C which formed a transparent solution, confirms their physical rather than chemical crosslinking (**Figure 1**).

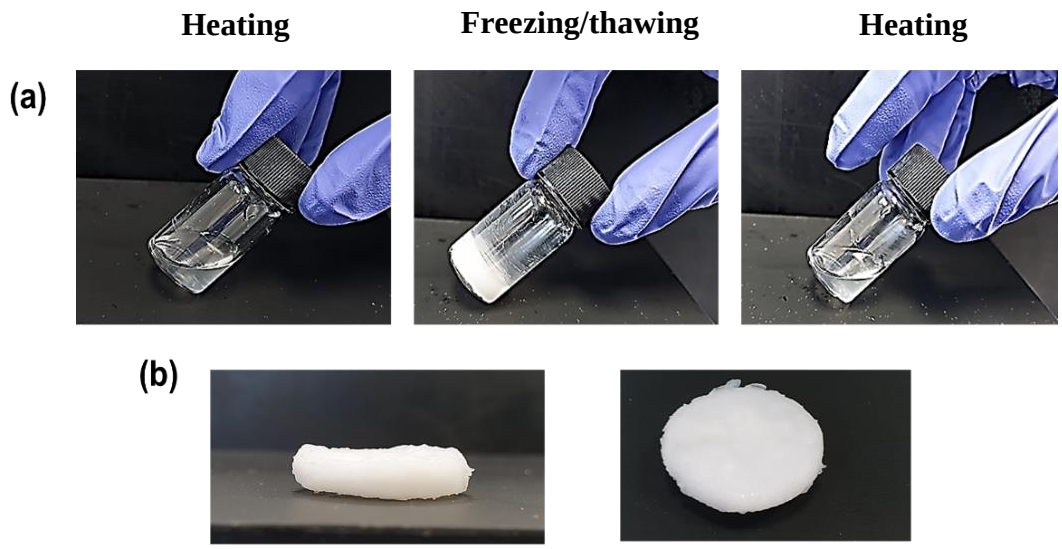

Figure 1. Solution – gel – solution transition of L-PEI cryogels. The solution is initially heated to 80 °C forming a transparent solution. After freezing at - 80 ºC for 3 h and then thawing at room temperature, an opaque gel is produced which, on subsequent heating to 80 °C, returns to a transparent solution (a). Appearance of L-PEI cryogels (b).

Evidence for crystalline domains was obtained by X-ray diffractometry. The L-PEI starting material showed diffraction peaks at 2θ = 18, 20, and 28°, in agreement with literature reports for the hemihydrated crystalline structure of PEI [22]. The cryogels provided diffraction peaks at 2θ = 20, 27, and 28° **(Figure 2),** typical for the dihydrate crystalline state [16, 19]. The formation of physical cryogels based on L-PEI is caused by the change in polymer chain conformation from a double helix in the anhydrate to a planar-zigzag as water molecules are absorbed into the L-PEI lattice, and the formation of NH···O and OH···N bonds between the zigzag PEI chains and water molecules [28]. Further, when the cryogels were re-heated at 80 ºC, again forming a clear solution, the diffractogram showed no evidence of crystalline domains due to their melting caused by the breakdown of hydrogen bonds at high temperatures. Yuan et al [22] reported gelation of L-PEI following heating of L-PEI solutions at 80 ºC and then cooling to room temperature. Again, gel formation was attributed to crystallization of L-PEI and they showed that the L-PEI used to prepare gels was semi-crystalline whereas their 5% L-PEI hydrogel gave the same diffraction pattern as our cryogels, with PEI in a dihydrate crystalline state.

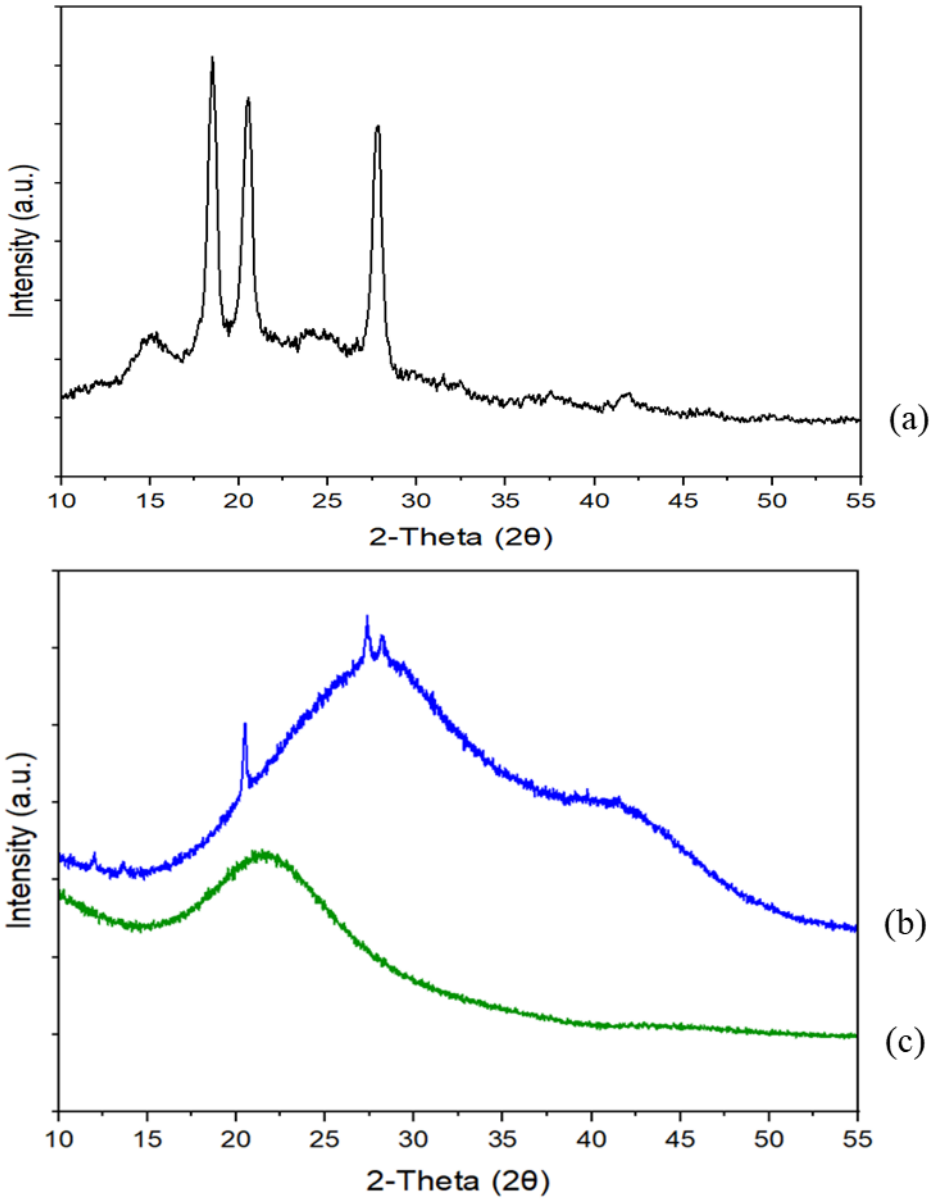

Figure 2. X-ray diffraction patterns for dry L-PEI (a) and wet cryogel prepared from L-PEI solution (b) and this sample after heating (to solution) at 80 ^{o}C (c).

3.2. Effect of Different Freezing Temperatures on Thermal, Crystallinity and Rheological Properties of Cryogels based on L-PEI

Given the role of phase separation in cryogel formation, we anticipated that the size of ice crystals formed during freezing L-PEI solutions would affect the mechanical and physical properties of the cryogels. Specifically, the rate and extent of freezing could affect both PEI crystallization and the pore size resultant from ice crystals. Ceylan and Okay [33] previously

reported the effect of freezing temperature on the properties of gels prepared by solution crosslinking of butyl rubber in frozen benzene solutions using sulfur monochloride as a crosslinking agent. Therefore, the effect of freezing conditions on the physical properties of L-PEI cryogels was evaluated in this work.

Figure 3 shows X-ray diffractograms of dry L-PEI and L-PEI cryogels produced when polymer solutions were frozen to -196 ^{o}C, -80 ^{o}C, - 30 ^{o}C and 0 ^{o}C, respectively. The XRD patterns of all cryogels were in agreement with the above results, giving peaks at 2θ = 20 ^{o}, 27 ^{o} and 28^{o} typical for the dihydrate crystalline form (EI:H_2O = 1:2).

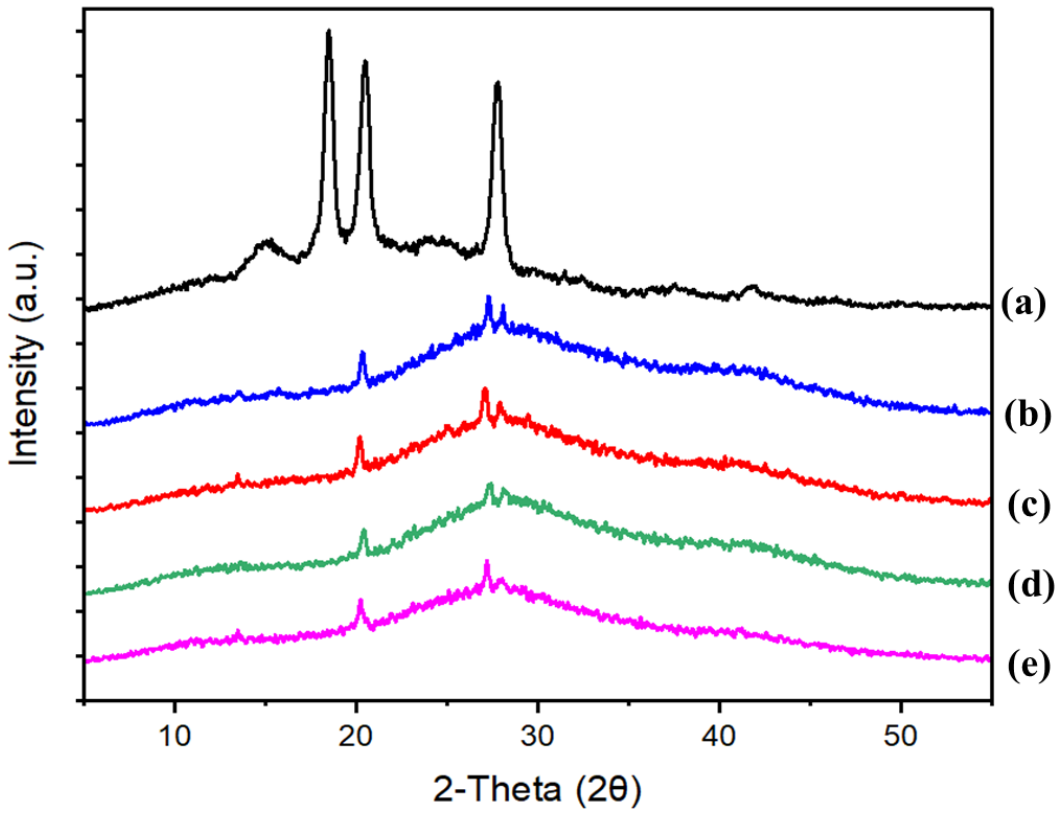

Figure 3. X-ray diffraction spectra of dry L-PEI (a) and wet L-PEI cryogels prepared at various freezing temperatures: -196 ^{o}C (b), -80 ^{o}C (c), -30 ^{o}C (d) and 0 ^{o}C (e).

The degree of crystallinity of L-PEI in cryogels can be estimated using the area under the sharp (crystalline) peaks over the total area and was clearly dependent on the freezing temperature; crystallinity within the samples increased as the freezing temperature fell, with over 1.6 % crystallinity seen when the solutions were rapidly frozen at -196 ^{o}C. **(Table 1)**. As expected, the size of the crystallites also reduced when frozen more rapidly since molecular

mobility is hindered at lower temperatures. This inhibits crystallite growth resulting in a greater number of smaller crystallites when frozen rapidly to -196 ^{o}C compared to the larger but fewer crystallites when frozen to 0 ^{o}C. These results are in good agreement with other studies[28, 29]. A lower freezing temperature contributed to smaller cryogel crystals and a smaller cross-section of macropores within the gel [34].

Table 1. Enthalpy, degree of crystallinity and mean crystal size of L-PEI cryogels prepared at different freezing temperatures.

Freezing temperature (^{o}C)	**Enthalpy (ΔH, J/g) ***	**Degree of crystallinity (%)****	**Mean crystal size (nm)****
Dry L-PEI	94.2 ± 14.9	30.8 ± 0.39	3.50 ± 0.03
-196	10.7 ± 0.2	1.65 ± 0.10	0.73 ± 0.07
- 80	9.8 ± 0.8	1.51 ± 0.18	0.76 ± 0.03
- 30	9.2 ± 0.1	1.17 ± 0.22	0.78 ± 0.02
0	7.7 ± 1.7	1.00 ± 0.14	0.83 ± 0.08

*Determined from DSC experiments.

**Determined from XRD experiments.

Figure 4A shows DSC thermograms of L-PEI and L-PEI cryogels produced when frozen to -196 ^{o}C, -80 ^{o}C, - 30 ^{o}C and 0 ^{o}C, respectively. It is known that dry L-PEI exhibits a sharp endothermic transition at 66.9 °C, which corresponds to melting of its crystalline domains and the melting temperature of L-PEI correlated to a report of Shan et al. [23] All thermograms of L-PEI cryogels also show this endothermic event around this temperature, but the peaks are broad and potentially show two overlapping events, one from melting of crystalline domains as above and a second thermal event with an earlier onset possibly due to thermal dissociation of intermacromolecular hydrogen bonds. The area under the endothermic peak was calculated to provide the enthalpy of these processes **(Table 1)**. The enthalpy of L-PEI melting was 94.2 J/g, whereas L-PEI cryogels exhibited the highest enthalpy values when frozen at -196 ^{o}C, followed by -80, -30, and 0 ^{o}C with a linear correlation (R^2=0.9035) between the enthalpy values and the XRD-determined degree of crystallinity **(Figure 4B)**.

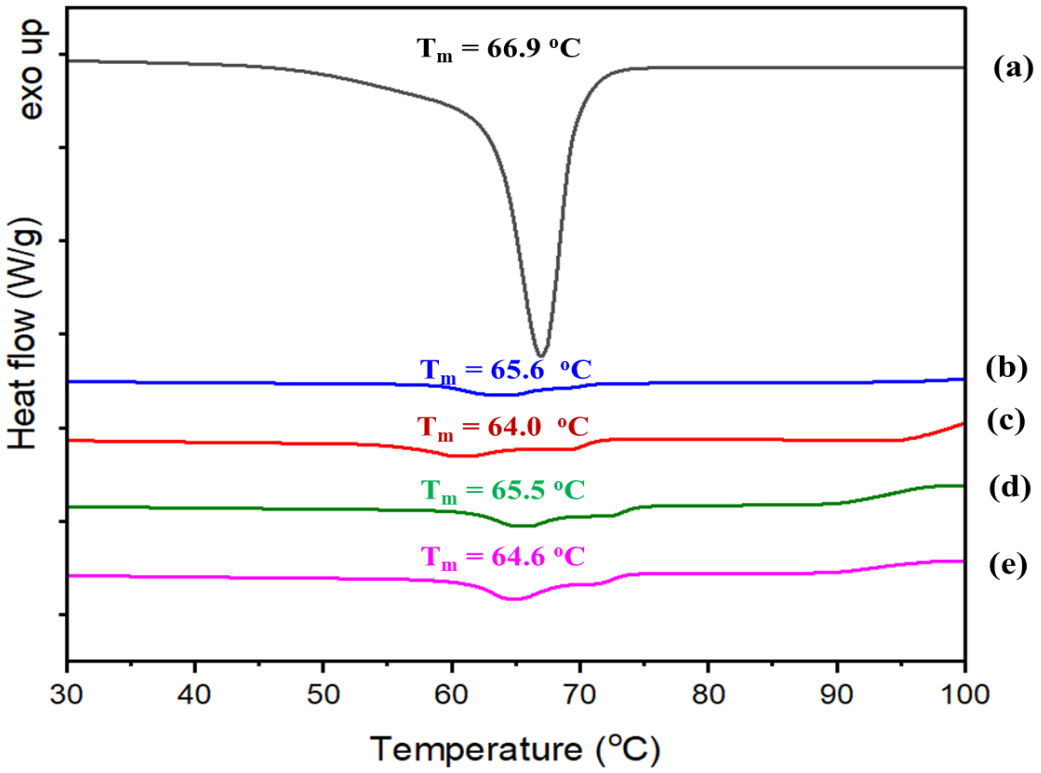

(A)

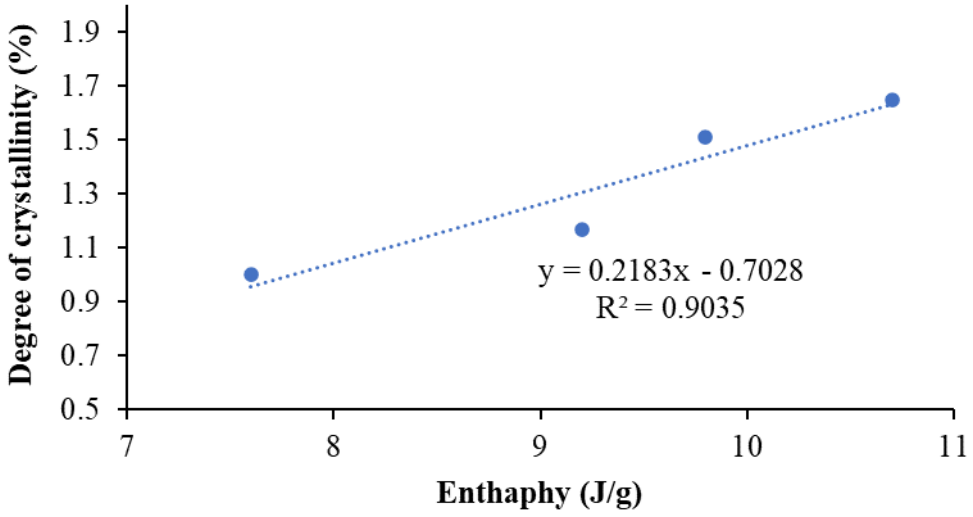

(B)

Figure 4. DSC thermograms of dry L-PEI (a) and wet L-PEI cryogels prepared at various freezing temperatures: -196 °C (b), -80 °C (c), -30 °C (d) and 0 °C (e)(A) and correlation between enthalpy (J/g) and degree of crystallinity (%) (B).

The porous structure of freeze-dried L-PEI cryogel samples generated at various freezing temperatures was investigated using scanning electron microscopy (SEM). **Figure 5** shows SEM images of selected cryogel samples. The results indicate that all L-PEI cryogels have a macroporous structure, with highly interconnected pores. Unfortunately, due to the irregular shape of the pores, average pore size could not be determined. However, these images indicate that the freezing temperatures does not radically change the porosity of the samples.

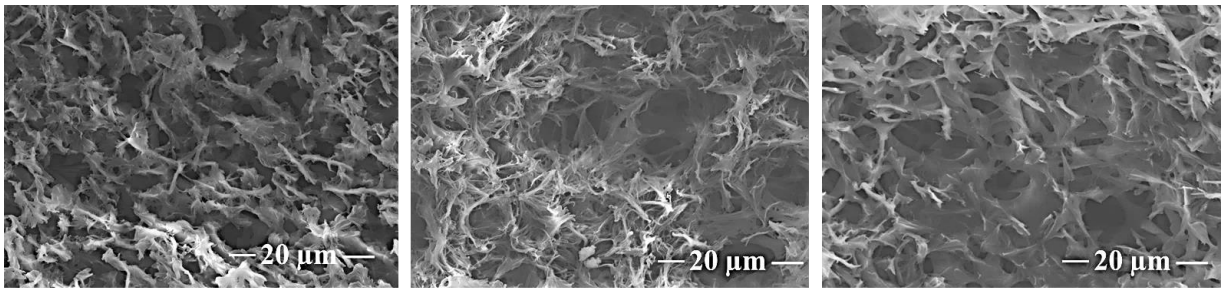

Figure 5. SEM images of freeze-dried L-PEI cryogels prepared at various freezing temperatures: -196 ^{o}C (a), -80 ^{o}C (b) and 0 ^{o}C (c).

Initially, an attempt was made to study the swelling properties of freeze-dried cryogels using a gravimetric technique. However, once immersed in deionised water, the cryogels rapidly lost their integrity and disintegrated during sample handling. The swelling and mechanical properties of these samples are very different to the cryogels based on PVA-Gantrez® AN, reported by Caló and co-workers [8]. L-PEI cryogels are more fragile and can easily disintegrate upon swelling, whereas PVA-Gantrez® AN were highly elastic and achieve high swelling ratios. Therefore, a less invasive approach was subsequently used with visual inspection of changes to L-PEI cryogel volumes. **Figure 6** presents the changes in the appearance and swelling ratio of dry L-PEI cryogels prepared at different freezing temperatures during swelling in deionised water. In general, swelling ratios were modest with no significant changes over the first 6 h for any given cryogel or between cryogels prepared at different freezing temperatures. After 24 h, the material prepared by freezing at 0 ^{o}C gave a significantly greater swelling ratio than that prepared at -196 ^{o}C ($p < 0.05$), and this sample, produced at the lowest temperature, had increased swelling at 24 h compared to its initial size. These modest changes are consistent with the SEM data: the similarity in sample porosity results in similar swelling behaviour.

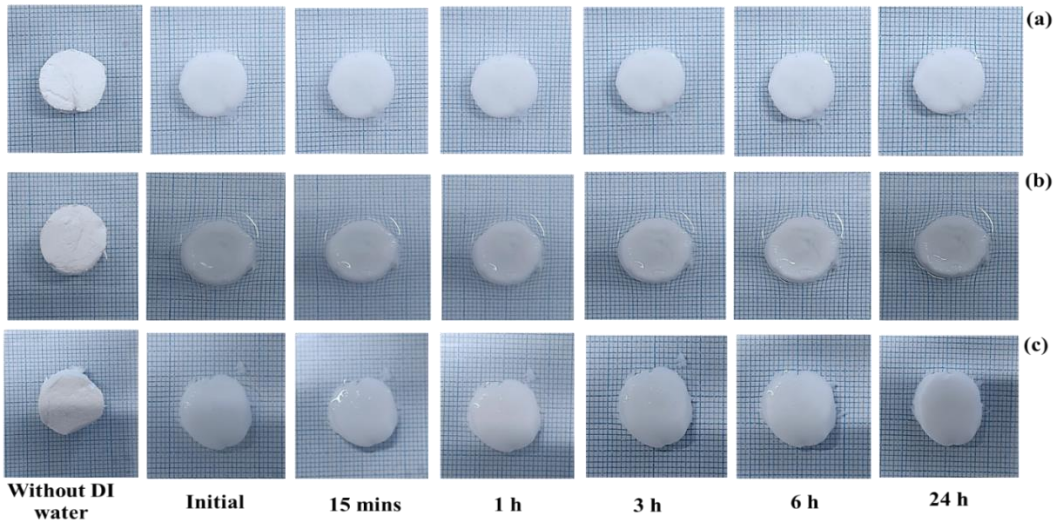

(A)

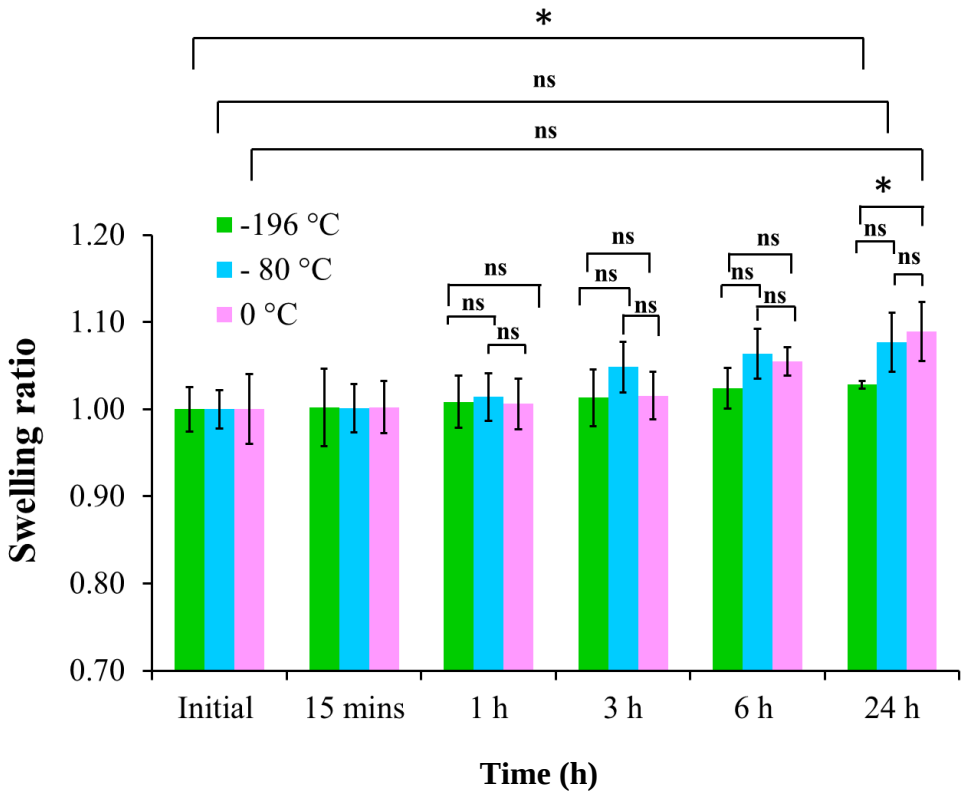

(B)

Figure 6. Swelling of freeze-dried L-PEI cryogels prepared at different freezing temperatures: -196 ºC (a), - 80 ºC (b) and 0 ºC (c) in deionised water: physical appearance (A) and swelling ratios (B). Statistically significant differences are given as: * - $p < 0.05$; ns - no significance.

The rheological behaviour of L-PEI cryogels prepared at the different freezing temperatures was studied in an oscillation frequency mode at 0.1 to 100 Hz with a fixed strain of 0.5% (**Figure 7)**. The results demonstrated that freezing temperature affected the elastic behaviour of L-PEI cryogels. The storage (or elastic) modulus values (G') of all the samples was greater than the loss (also known as the viscous) modulus (G″) over the whole frequency range, demonstrating predominantly gel-like rheological behavior. The storage modulus has been used to predict the stiffness of a material [29, 30] and so the greater G' values seen with samples produced at lower freezing temperatures indicates increased mechanical strength. Likewise, the loss modulus (G″) generally increased as the freezing temperature declined. However, between 0.1 and ~1 Hz, the loss modulus fell for all samples and then rose again with increasing oscillation frequency up to 100 Hz due to reduction in the intermolecular hydrogen bonding as the cryogels were disrupted. Consequently, the complex viscosity (η*) fell as oscillation frequency increased from 0.1 to 100 Hz, which is consistent with the reduction in the intermolecular hydrogen bonding as a result of disruption of the cryogels. Our rheological data correlates well with that from X-ray diffraction and thermal analysis. Comparison of the degrees of crystallinity values with the rheological properties of the samples indicates that mechanically stronger gels are more crystalline; the crystallites act as physical cross-linking junctions and also smaller water crystals formed at lower freezing temperature resulting in smaller pores in the cryogels. Lozinsky [35] also reported that preparing physically crosslinked polysaccharide cryogels at lower freezing temperatures resulted in increased gel strength.

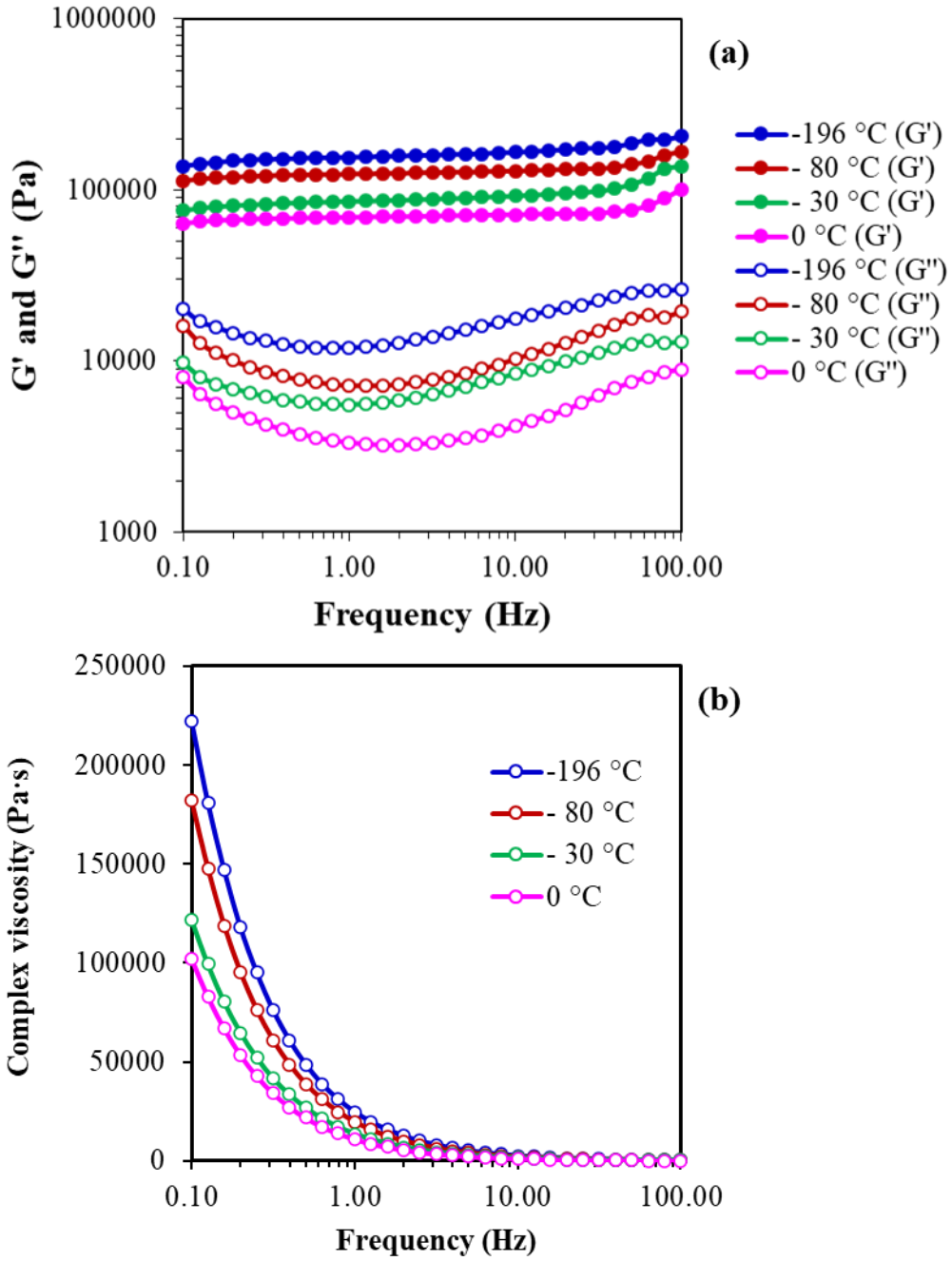

Figure 7. Storage (G') and loss (G") modulus (a), and complex viscosity (η*, b) of L-PEI cryogels prepared at different freezing temperatures.

The storage modulus (G′), the loss modulus (G″) and complex viscosity (η*) of L-PEI cryogels were investigated as a function of temperature from 20 to 80 ^{o}C. **Figure 8** shows the effect of temperature on the rheological properties of L-PEI cryogels prepared at different freezing temperatures. As expected, both the storage and loss modulus values as well as shear viscosity fall with increasing temperature. Interestingly, the G′, G″ and η* data suggest that the cryogels are essentially liquid at 60 ^{o}C. Our thermal analysis (**Figure 4**) showed L-PEI melting at ~67 ^{o}C, though the onset for the melt was earlier. Thus, it may be that the gel-sol transition seen by rheology is predominantly driven by disruption of the intermacromolecular hydrogen bonds before melting of the polymer crystalline domains. To explore this further, the relative phase angle (tan δ = G″/ G′, where δ was the loss angle) was calculated (**Figure 8 c**). When tan δ is lower than 1, then this indicates predominantly gel behavior whereas values higher than 1 reflect viscous or liquid behavior [25]. The data show a gradual increase in phase angle between 60 and 70 ^{o}C, and only exceeds a value of 1 beyond the melting temperature of L-PEI. This indicates that, whilst gel structure is initially lost by disruption of the intermolecular hydrogen bonds, the cryogels retained some structural organisation from the crystalline domains until melting where the systems were truly liquid. However, the rheological data demonstrates that it is the hydrogen bonds that are predominantly responsible for the structural integrity of the cryogels.

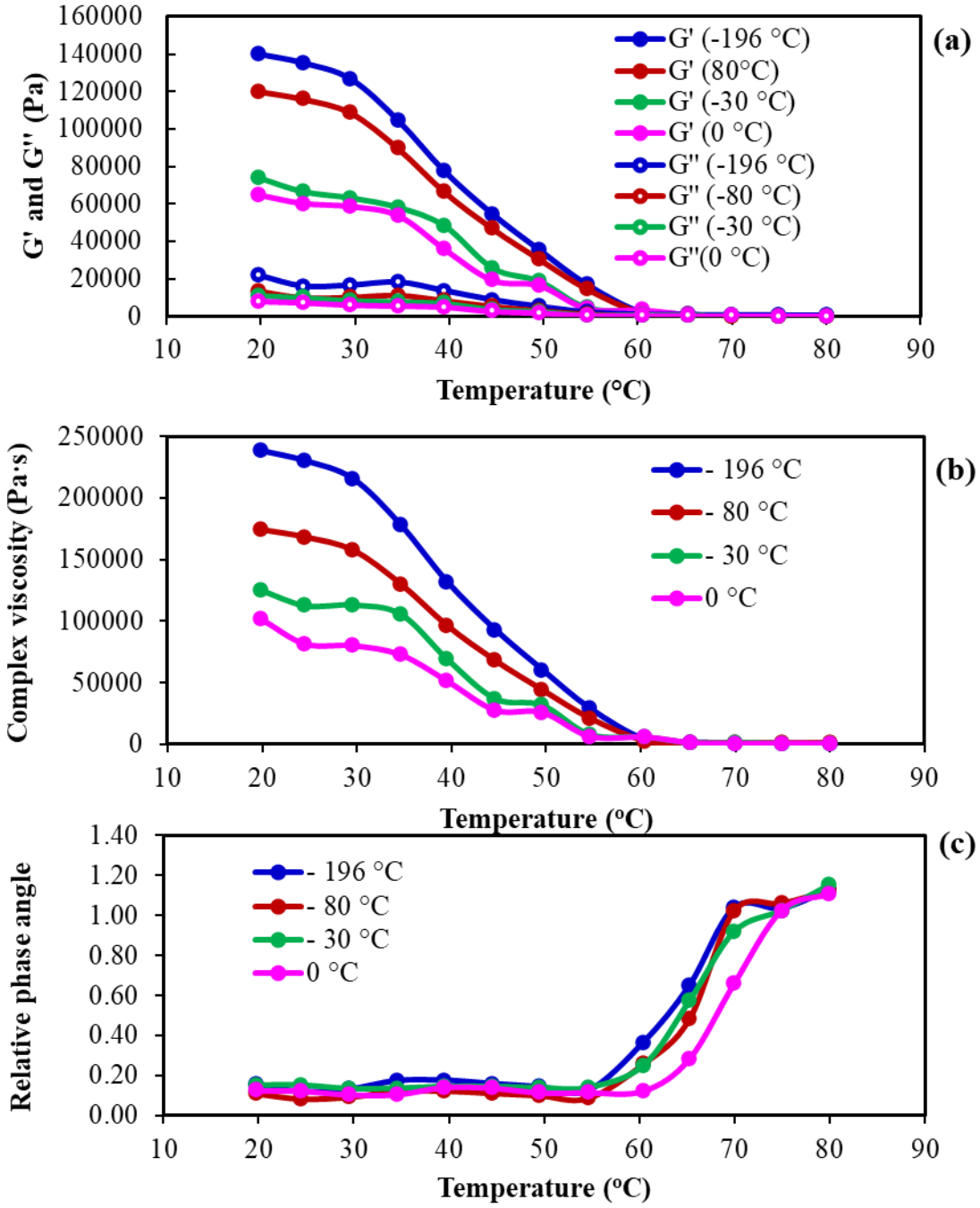

Figure 8. Storage (G') and loss (G") modulus (a), complex viscosity (η*, b) and relative phase angle (c) of L-PEI cryogels, prepared at different freezing temperatures, as a function of temperature.

3.3. Effect of Solvent Composition on Formation, Crystallinity and Rheological Properties of Cryogels based on L-PEI

The influence of solvent composition on the formation and physicochemical properties of L-PEI cryogels was explored. L-PEI was dissolved in ethanol-water mixtures before freezing at -80 ^{o}C for 3 h, and subsequent thawing at 25 ^{o}C. Dissolving L-PEI in ethanol alone did not result in the formation of cryogels; our samples were cooled to -80 ^{o}C whereas the freezing point of ethanol is -115 ^{o}C **(Table S2)**. However, L-PEI in mixtures of water with ethanol did form gels. With increasing ethanol content, the gels became softer, probably due to reduced intermolecular hydrogen bonding between L-PEI macromolecules because of competition with solvent molecules (**Figure 9)**. The transition from hard to soft gels was associated with a decrease in gel viscosity as the concentration of ethanol in the solvent mixtures increased. These results also correspond with literature reports that increasing concentrations of alcohol in aqueous mixtures decreased both rigidity and fusion temperature of PVA cryogels [9].

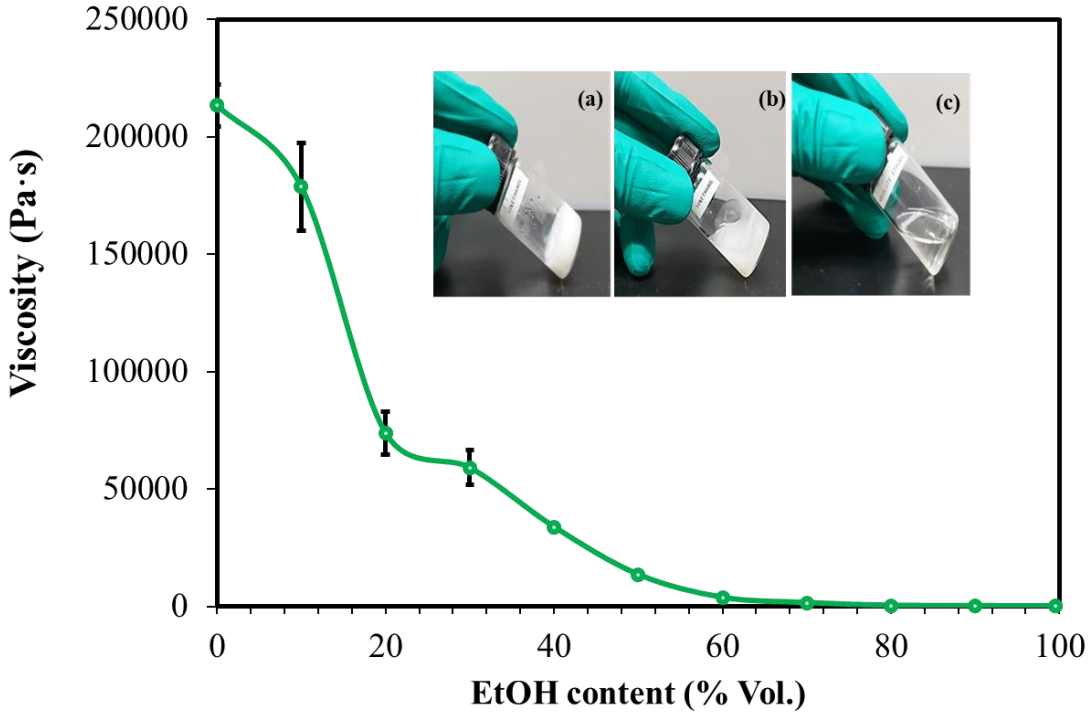

Figure 9. Viscosities of L-PEI samples following their freezing and thawing in different ethanol/water mixtures and images of samples prepared at 20 % (a), 50 % (b) and 100 % (c) EtOH.

As described above, L-PEI starting material was shown to be a hemihydrate which then reverted to a dihydrate structure when formed into a hydrogel from water. When dried to constant weight, these samples transitioned to a sesquihydrate (EI: H_2O = 1:1.5), with further diffraction peaks at 2θ = 24 and 25° (**Figure 10a**). These findings are consistent with data from Hashida and Tashiro [36] who demonstrated that PEI exhibits water-induced phase transitions between four crystalline hydrates: anhydrate (El/water=1/0), hemihydrate (1/0.5), sesquihydrate (1/1.5), and dihydrate (1/2). From the diffraction patterns, the L-PEI and dried L-PEI cryogels were estimated to have a crystallinity of 31 and 40 %, respectively **(Table S3)**, similar to studies of Lázaro-Martnez et al. [37]. The increased crystallinity of dried L-PEI cryogels when compared to L-PEI may result from intermolecular hydrogen bonding between NH···O and OH···N in L-PEI molecules.

Figure 10b shows the XRD patterns of dried (to constant weight) L-PEI cryogels prepared in various ethanol/water mixes, with significant peaks at 2θ = 20, 24, 25, 27, and 28°. The sample from 100% ethanol did not form a cryogel but was dried to constant weight giving a diffraction pattern consistent with the starting L-PEI (as a hemihydrate). The diffraction peaks in the dried hydrogels are in agreement with the typical pattern of sesquihydrates, consistent with the literature [36] and with the pattern resulting from the dried cryogel produced from water alone. The degree of crystallinity of L-PEI in the dried cryogels tended to decrease ($p < 0.05$) as the concentration of ethanol in L-PEI ethanol/water mixtures increased, and was significant ($p < 0.05$) when comparing the gel produced from water (39.9% crystalline) and when recovered from ethanol alone (31.5 %) **(Figure 10c)**. It is feasible that ethanol either competes with, or interferes with, the intermolecular hydrogen bonding between NH···O and OH···N in L-PEI.

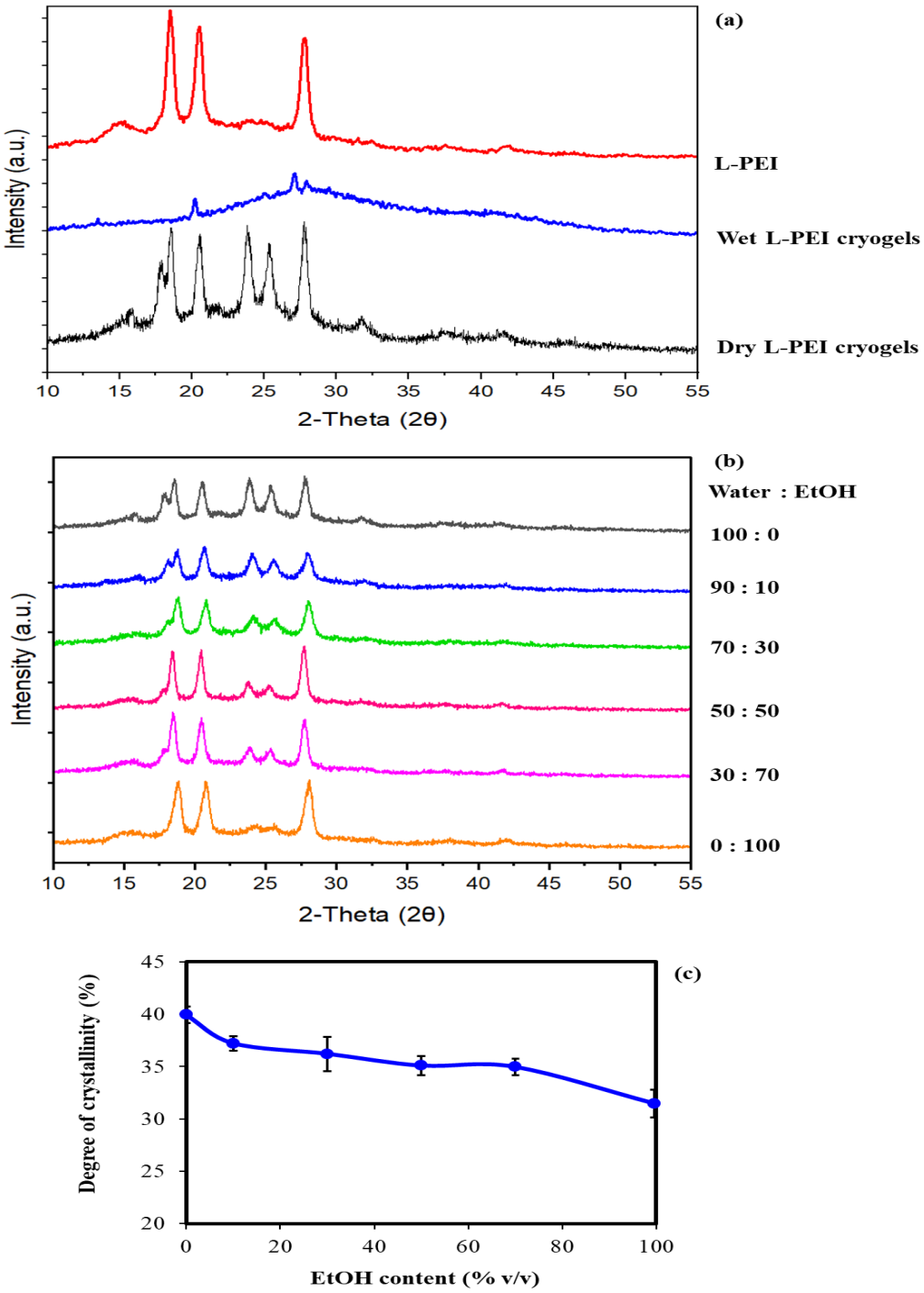

Figure 10. XRD spectra of L-PEI, wet and dried to constant weight L-PEI cryogels formed from water (a); XRD spectra (b); and degree of crystallinity (c) of dried L-PEI cryogels prepared from different ethanol/water mixtures. Sample prepared from 100% ethanol did not form a gel but was dried and resulted in the same diffraction pattern as the starting L-PEI (as in **Figure 10a**).

4. CONCLUSIONS

Cryogels based on L-PEI were formed by freeze/thaw processing of concentrated L-PEI solutions in water. The physically crosslinked cryogels were also validated by demonstrating that they formed a clear solution upon heating to 80 ^{o}C due to the melting of the L-PEI crystalline domains. L-PEI cryogels were found to have a higher enthalpy, crystallinity, and strength when cooled to temperatures below 0 ^{o}C. Additionally, increasing ethanol content in water-ethanol mixture used to prepare L-PEI cryogels resulted in a decrease in mechanical strength, crystallinity, and viscosity. This could be because the intermolecular hydrogen bonds between NH···O and OH···N in L-PEI decreased, most likely due to hydrogen bond competition from the solvent molecules. This study demonstrates that the physical properties of L-PEI cryogels can be manipulated by controlling the cooling rate and solvent composition used to form the cryogels. Hence, due to the unique chemical and physical properties of L-PEI, these novel physical cryogels have potential for biomedical and antimicrobial applications.

AUTHOR INFORMATION

Corresponding Author

Vitaliy V. Khutoryanskiy - Reading School of Pharmacy, University of Reading, Whiteknights, PO Box 224, RG6 6DX, Reading, United Kingdom E-mail address: v.khutoryanskiy@reading.ac.uk https://orcid.org/0000-0002-7221-2630

Authors

Sitthiphong Soradech - Reading School of Pharmacy, University of Reading, Whiteknights, PO Box 224, RG6 6DX, Reading, United Kingdom; Expert Centre of Innovative Herbal Products, Thailand Institute of Scientific and Technological Research, Pathum Thani, 12120, Thailand. https://orcid.org/0000-0002-9964-4177

Adrian C. Williams- Reading School of Pharmacy, University of Reading, Whiteknights, PO Box 224, RG6 6DX, Reading, United Kingdom. https://orcid.org/0000-0003-3654-7916

Author Contributions

Sitthiphong Soradech: Methodology, Investigation, Validation, Writing original draft.

Adrian C. Williams: Writing - review & editing, Supervision.

Vitaliy V. Khutoryanskiy: Conceptualization, Writing –review & editing, Supervision.

Notes

The authors declare that they have no known competing financial interests or personal relationships that could have appeared to influence the work reported in this paper.

ACKNOWLEDGEMENTS

The authors are grateful to Thailand Institute of Scientific and Technological Research, Ministry of Higher Education, Science, Research and Innovation for funding the PhD studentship of Sitthiphong Soradech. The assistance of staff at the Chemical Analysis Facility (CAF, University of Reading) with ^{1}H-NMR, FTIR, DSC SEM and XRD experiments is also acknowledged.

REFERENCES

(1) Lozinsky, V. I.; Galaev, I. Y.; Plieva, F. M.; Savina, I. N.; Jungvid, H.; Mattiasson, B. Polymeric Cryogels as Promising Materials of Biotechnological Interest. *Trends Biotechnol.* **2003**, *21* (10), 445–451. https://doi.org/10.1016/j.tibtech.2003.08.002.

(2) Okay, O. *Polymeric Cryogels Macroporous Gels with Remarkable Properties*; 2014; Vol. 263. https://doi.org/10.1007/978-3-319-05846-7.

(3) Păduraru, O. M.; Ciolacu, D.; Darie, R. N.; Vasile, C. Synthesis and Characterization of Polyvinyl Alcohol/Cellulose Cryogels and Their Testing as Carriers for a Bioactive Component. *Mater. Sci. Eng. C* **2012**, *32* (8), 2508–2515. https://doi.org/10.1016/j.msec.2012.07.033.

(4) Caló, E.; Khutoryanskiy, V. V. Biomedical Applications of Hydrogels: A Review of Patents and Commercial Products. *Eur. Polym. J.* **2015**, *65*, 252–267. https://doi.org/10.1016/j.eurpolymj.2014.11.024.

(5) Lozinsky, V. I.; Damshkaln, L. G.; Ezernitskaya, M. G.; Glotova, Y. K.; Antonov, Y. A. Cryostructuring of Polymer Systems. Wide Pore Poly(Vinyl Alcohol) Cryogels Prepared Using a Combination of Liquid-Liquid Phase Separation and Cryotropic Gel-Formation Processes. *Soft Matter* **2012**, *8* (32), 8493–8504. https://doi.org/10.1039/c2sm25818h.

(6) Lozinsky, V. I.; Plieva, F. M. Poly(Vinyl Alcohol) Cryogels Employed as Matrices for Cell Immobilization. 3. Overview of Recent Research and Developments. *Enzyme Microb. Technol.* **1998**, *23* (3–4), 227–242. https://doi.org/10.1016/S0141-0229(98)00036-2.

(7) Pazos, V.; Mongrain, R.; Tardif, J. C. Polyvinyl Alcohol Cryogel: Optimizing the Parameters of Cryogenic Treatment Using Hyperelastic Models. *J. Mech. Behav. Biomed. Mater.* **2009**, *2* (5), 542–549. https://doi.org/10.1016/j.jmbbm.2009.01.003.

(8) Caló, E.; Barros, J.; Ballamy, L.; Khutoryanskiy, V. V. Poly(Vinyl Alcohol)-Gantrez® AN Cryogels for Wound Care Applications. *RSC Adv.* **2016**, *6* (107), 105487–105494. https://doi.org/10.1039/c6ra24573k.

(9) Lozinsky, V. I.; Damshkaln, L. G.; Kurochkin, I. N.; Kurochkin, I. I. Cryostructuring of Polymeric Systems. 36. Poly(Vinyl Alcohol) Cryogels Prepared from Solutions of the Polymer in Water/Low-Molecular Alcohol Mixtures. *Eur. Polym. J.* **2014**, *53* (1), 189–205. https://doi.org/10.1016/j.eurpolymj.2014.01.020.

(10) Shen, C.; Li, J.; Zhang, Y.; Li, Y.; Shen, G.; Zhu, J.; Tao, J. Polyethylenimine-Based Micro/Nanoparticles as Vaccine Adjuvants. *Int. J. Nanomedicine* **2017**, *12*, 5443–5460. https://doi.org/10.2147/IJN.S137980.

(11) Sedlacek, O.; Janouskova, O.; Verbraeken, B.; Richard, H. Straightforward Route to Superhydrophilic Poly(2-Oxazoline)s via Acylation of Well-Defined Polyethylenimine. *Biomacromolecules* **2018**, *20*. https://doi.org/10.1021/acs.biomac.8b01366.

(12) Mees, M. A.; Hoogenboom, R. Full and Partial Hydrolysis of Poly(2-Oxazoline)s and the Subsequent Post-Polymerization Modification of the Resulting Polyethylenimine (Co)Polymers. *Polym. Chem.* **2018**, *9* (40), 4968–4978. https://doi.org/10.1039/c8py00978c.

(13) Lungu, C. N.; Diudea, M. V.; Putz, M. V.; Grudziński, I. P. Linear and Branched PEIs (Polyethylenimines) and Their Property Space. *Int. J. Mol. Sci.* **2016**, *17* (4). https://doi.org/10.3390/ijms17040555.

(14) Chatani, Y.; Tadokoro, H.; Saegusa, T.; Ikeda, H. Structural Studies of Poly (Ethylenimine). 1. Structures of Two Hydrates of Poly (Ethylenimine): Sesquihydrate and Dihydrate. *Macromolecules* **1981**, *14* (2), 315–321. https://doi.org/10.1021/ma50003a017.

(15) Lambermont-Thijs, H. M. L.; van der Woerdt, F. S.; Baumgaertel, A.; Bonami, L.; Du Prez, F. E.; Schubert, U. S.; Hoogenboom, R. Linear Poly(Ethylene Imine)s by Acidic Hydrolysis of Poly(2-Oxazoline)s: Kinetic Screening, Thermal Properties, and

Temperature-Induced Solubility Transitions. *Macromolecules* **2010**, *43* (2), 927–933. https://doi.org/10.1021/ma9020455.

(16) Choosakoonkriang, S.; Lobo, B.; Koe, G.; Koe, J.; Middaugh, C. Biophysical Characterization of PEI/DNA Complexes. *J. Pharm. Sci.* **2003**, *92*, 1710–1722. https://doi.org/10.1002/jps.10437.

(17) Xu, D.; Wang, Q.; Yang, T.; Cao, J.; Lin, Q.; Yuan, Z.; Li, L. Polyethyleneimine Capped Silver Nanoclusters as Efficient Antibacterial Agents. *Int. J. Environ. Res. Public Health* **2016**, *13* (3). https://doi.org/10.3390/ijerph13030334.

(18) Gibney, K. A.; Sovadinova, I.; Lopez, A. I.; Urban, M.; Ridgway, Z.; Caputo, G. A.; Kuroda, K. Poly(Ethylene Imine)s as Antimicrobial Agents with Selective Activity. *Macromol. Biosci.* **2012**, *12* (9), 1279–1289. https://doi.org/10.1002/mabi.201200052.

(19) Demirci, S.; Sahiner, N. PEI-Based Ionic Liquid Colloids for Versatile Use: Biomedical and Environmental Applications. *J. Mol. Liq.* **2014**, *194*, 85–92. https://doi.org/10.1016/j.molliq.2014.01.015.

(20) Sahiner, N.; Demirci, S. Poly Ionic Liquid Cryogel of Polyethyleneimine: Synthesis, Characterization, and Testing in Absorption Studies. *J. Appl. Polym. Sci.* **2016**, *133* (22), 1–13. https://doi.org/10.1002/app.43478.

(21) Malakhova, I.; Privar, Y.; Parotkina, Y.; Mironenko, A.; Eliseikina, M.; Balatskiy, D.; Golikov, A.; Bratskaya, S. Rational Design of Polyamine-Based Cryogels for Metal Ion Sorption. *Molecules* **2020**, *25* (20), 1–17. https://doi.org/10.3390/molecules25204801.

(22) Yuan, J. J.; Jin, R. H. Fibrous Crystalline Hydrogels Formed from Polymers Possessing a Linear Poly(Ethyleneimine) Backbone. *Langmuir* **2005**, *21* (7), 3136–3145. https://doi.org/10.1021/la047182l.

(23) Shan, X.; Williams, A. C.; Khutoryanskiy, V. V. Polymer Structure and Property Effects on Solid Dispersions with Haloperidol: Poly(N-Vinyl Pyrrolidone) and Poly(2-Oxazolines) Studies. *Int. J. Pharm.* **2020**, *590* (September), 119884. https://doi.org/10.1016/j.ijpharm.2020.119884.

(24) Serres-Gómez, M.; González-Gaitano, G.; Kaldybekov, D. B.; Mansfield, E. D. H.; Khutoryanskiy, V. V; Isasi, J. R.; Dreiss, C. A. Supramolecular Hybrid Structures and Gels from Host-Guest Interactions between α-Cyclodextrin and PEGylated Organosilica Nanoparticles. *Langmuir* **2018**, *34* (36), 10591–10602. https://doi.org/10.1021/acs.langmuir.8b01744.

(25) Hao, Z. Q.; Chen, Z. J.; Chang, M. C.; Meng, J. L.; Liu, J. Y.; Feng, C. P. Rheological Properties and Gel Characteristics of Polysaccharides from Fruit-Bodies of Sparassis

Crispa. *Int. J. Food Prop.* **2018**, *21* (1), 2283–2295. https://doi.org/10.1080/10942912.2018.1510838.

(26) Jain, K.; Madhu, G.; Bhunia, H.; Bajpai, P. K.; Nando, G. B.; Reddy, M. S. Physico-Mechanical Characterization and Biodegradability Behavior of Polypropylene/Poly(L-Lactide) Polymer Blends. *J. Polym. Eng.* **2015**, *35* (5), 407–415. https://doi.org/10.1515/polyeng-2014-0179.

(27) Hashida, T.; Tashiro, K.; Inaki, Y. Structural Investigation of Water-Induced Phase Transitions of Poly(Ethylene Imine). III. The Thermal Behavior of Hydrates and the Construction of a Phase Diagram. *J. Polym. Sci. Part B Polym. Phys.* **2003**, *41* (22), 2937–2948. https://doi.org/10.1002/polb.10611.

(28) Hashida, T.; Tashiro, K. Structural Investigation on Water-Induced Phase Transitions of Poly(Ethylene Imine), Part IV: Changes of Intra- and Intermolecular Hydrogen Bonds in the Hydration Processes as Revealed by Time-Resolved Raman Spectral Measurements. *Polymer (Guildf).* **2007**, *48* (26), 7614–7622. https://doi.org/10.1016/j.polymer.2007.10.031.

(29) Plleva, F. M.; Galaev, I. Y.; Mattiasson, B. Macroporous Gels Prepared at Subzero Temperatures as Novel Materials for Chromatography of Particulate-Containing Fluids and Cell Culture Applications. *J. Sep. Sci.* **2007**, *30* (11), 1657–1671. https://doi.org/10.1002/jssc.200700127.

(30) Mastrangelo, R.; Chelazzi, D.; Poggi, G.; Fratini, E.; Buemi, L. P.; Petruzzellis, M. L.; Baglioni, P. Twin-Chain Polymer Hydrogels Based on Poly(Vinyl Alcohol) as New Advanced Tool for the Cleaning of Modern and Contemporary Art. *Proc. Natl. Acad. Sci. U. S. A.* **2020**, *117* (13), 7011–7020. https://doi.org/10.1073/pnas.1911811117.

(31) Lozinsky, V. I.; Damshkaln, L. G.; Shaskol'Skii, B. L.; Babushkina, T. A.; Kurochkin, I. N.; Kurochkin, I. I. Study of Cryostructuring of Polymer Systems: 27. Physicochemical Properties of Poly(Vinyl Alcohol) Cryogels and Specific Features of Their Macroporous Morphology. *Colloid J.* **2007**, *69* (6), 747–764. https://doi.org/10.1134/S1061933X07060117.

(32) Hassan, C. M.; Stewart, J. E.; Peppas, N. A. Diffusional Characteristics of Freeze/Thawed Poly(Vinyl Alcohol) Hydrogels: Applications to Protein Controlled Release from Multilaminate Devices. *Eur. J. Pharm. Biopharm.* **2000**, *49* (2), 161–165. https://doi.org/10.1016/S0939-6411(99)00056-9.

(33) Ceylan, D.; Okay, O. Macroporous Polyisobutylene Gels: A Novel Tough Organogel with Superfast Responsivity. *Macromolecules* **2007**, *40* (24), 8742–8749.

https://doi.org/10.1021/ma071605j.

(34) Libbrecht, K. G. The Physics of Snow Crystals. *Reports Prog. Phys.* **2005**, *68* (4), 855–895. https://doi.org/10.1088/0034-4885/68/4/r03.

(35) Lozinsky, V. I. Cryogels on the Basis of Natural and Synthetic Polymers: Preparation, Properties and Application. *Usp. Khim.* **2002**, *71* (6), 579–584. https://doi.org/10.1070/rc2002v071n06abeh000720.

(36) Hashida, T.; Tashiro, K. Structural Study on Water-Induced Phase Transitions of Poly(Ethylene Imine) as Viewed from the Simultaneous Measurements of Wide-Angle X-Ray Diffractions and DSC Thermograms. *Macromol. Symp.* **2006**, *242*, 262–267. https://doi.org/10.1002/masy.200651036.

(37) Lázaro-Martínez, J. M.; Rodríguez-Castellón, E.; Vega, D.; Monti, G. A.; Chattah, A. K. Solid-State Studies of the Crystalline/Amorphous Character in Linear Poly (Ethylenimine Hydrochloride) (PEI·HCl) Polymers and Their Copper Complexes. *Macromolecules* **2015**, *48* (4), 1115–1125. https://doi.org/10.1021/ma5023082.

Supplementary information

Physically Crosslinked Cryogels of Linear Polyethyleneimine: Influence of Cooling Temperature and Solvent Composition

Sitthiphong Soradech[1, 2], Adrian C. Williams[1], and Vitaliy V. Khutoryanskiy[1]*

[1]Reading School of Pharmacy, University of Reading, Whiteknights, Reading, RG6 6DX, UK

[2] Expert Centre of Innovative Herbal Products, Thailand Institute of Scientific and Technological Research, Pathum Thani, 12120, Thailand.

*__Corresponding author:__
Postal address: School of Pharmacy, University of Reading, Whiteknights, RG6 6AX, Reading, United Kingdom
E-mail address: v.khutoryanskiy@reading.ac.uk
Telephone: +44(0) 118 378 6119
Fax: +44(0) 118 378 4703

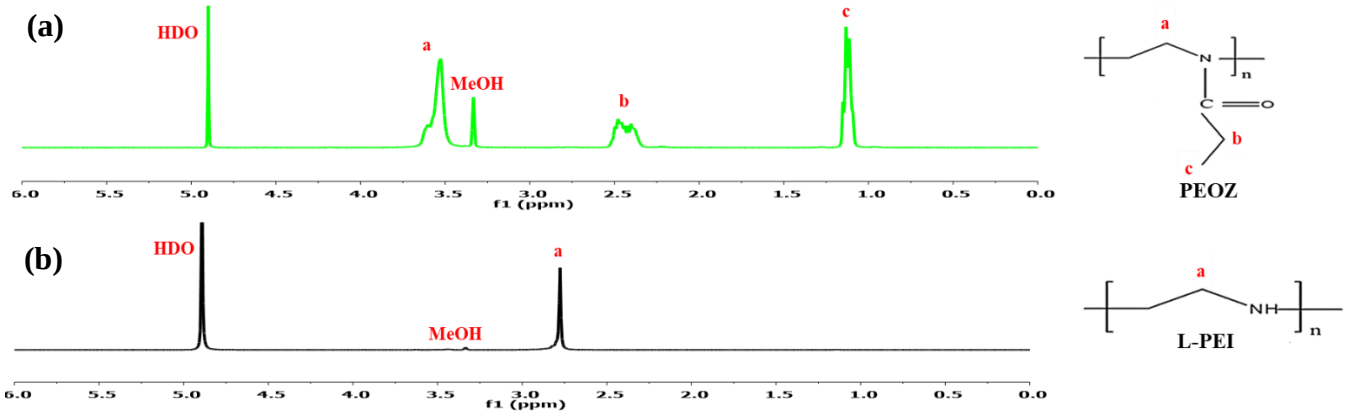

Figure S1. ^{1}H NMR spectra of PEOZ (a) and L-PEI (b) in methanol-d4.

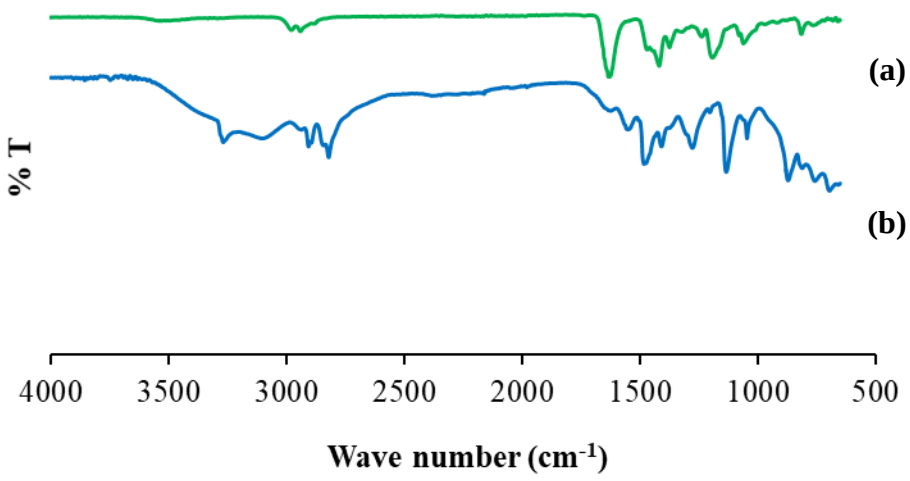

Figure S2. FTIR spectra of PEOZ (a) and L-PEI (b).

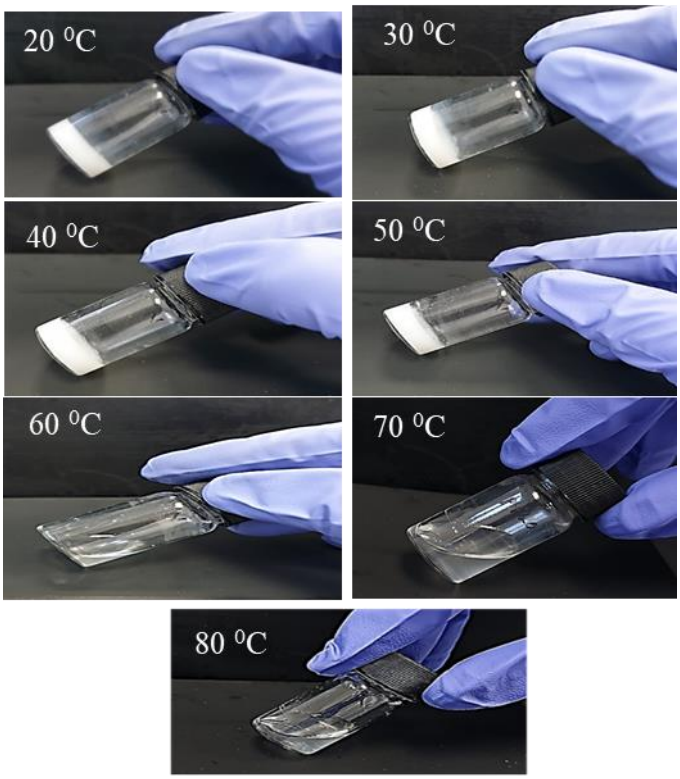

Figure S3. Effect of thawing temperatures on the formation of L-PEI cryogels.

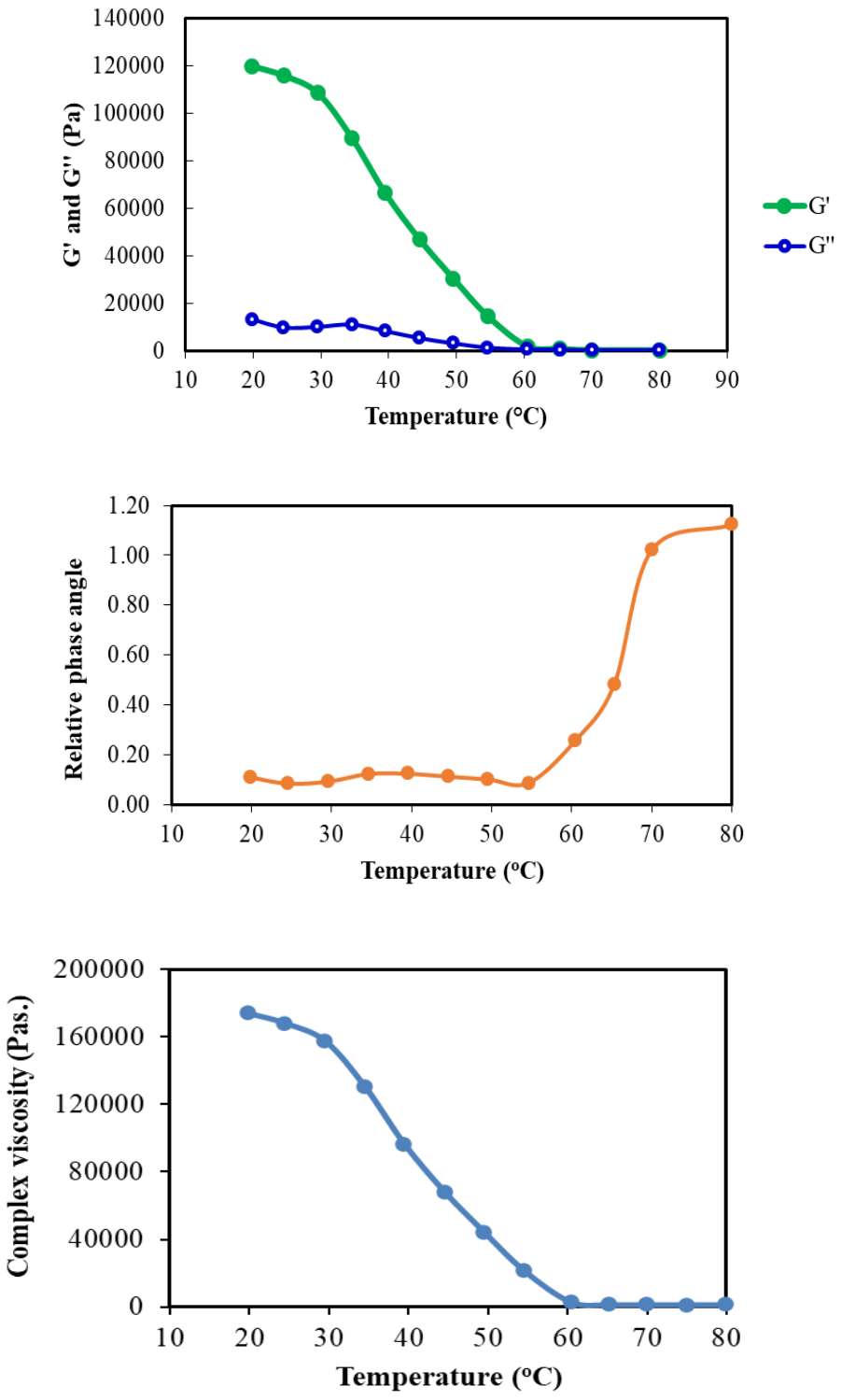

Figure S4. Effect of temperature on rheological behaviour of L-PEI cryogels.

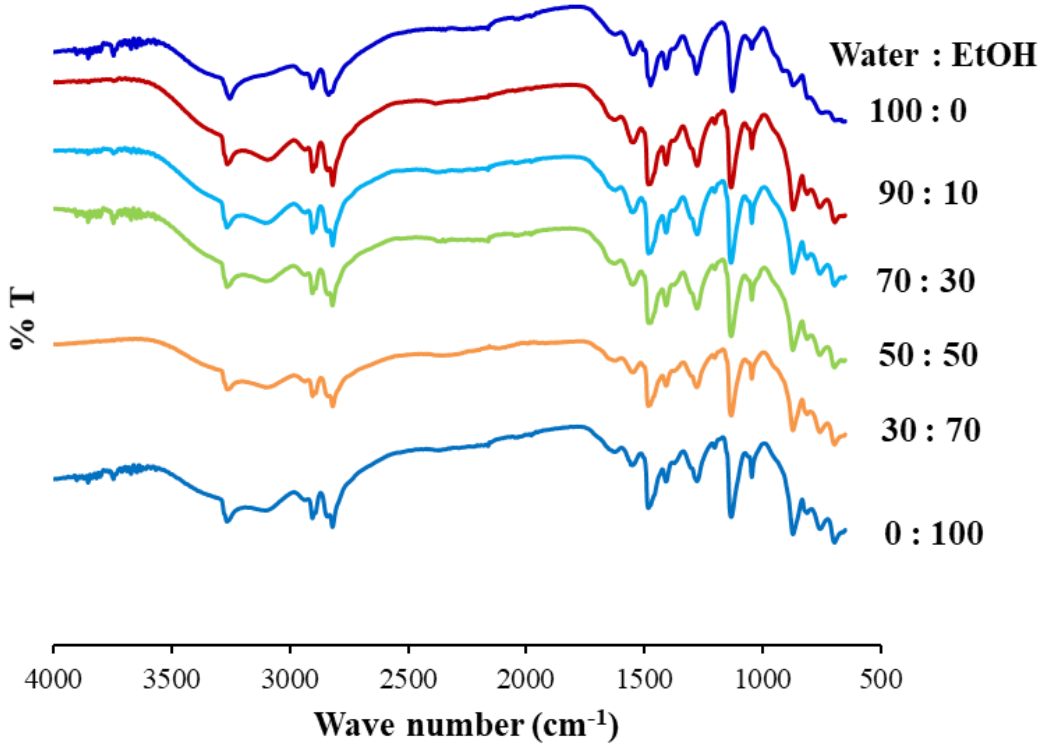

Figure S5. FTIR spectra of dried L-PEI cryogels with different alcohol/water mixtures.

Table S1. FTIR peaks of dried L-PEI cryogels with different alcohol/water mixtures.

Functional groups of L-PEI cryogels in mixture between water and alcohol ratios	**IR bands (cm^{-1})**				
	***r*(CH₂) + *r*(NH) + *r* (OH)**	***w*(CH₂) + *t*(CH₂)**	**ν_a (CH₂)**	**ν_s(CH₂)**	***ν*(NH)**
Anhydrate L-PEI	856 [1]	1281[1]	2877[2]	2807[2]	3219[2]
Hemihydrate L-PEI	876[1]	1289[1]	2909[2]	2821[2]	3267[1]
Sequihydrate L-PEI	876[1]	1289[1]	2909[2]	2837[2]	3259[2]
Dihydrate L-PEI	918[1]	1282[1]	2911[2]	2848[2]	3271[2]
L-PEI	873	1280	2905	2821	3268
100: 0	872	1279	2905	2836	3255
10: 90	871	1277	2905	2819	3265
30: 70	872	1277	2905	2820	3267
50: 50	872	1278	2905	2820	3266
70: 30	872	1278	2904	2819	3265
0: 100	872	1278	2905	2820	3266

Where r = rocking mode, ω =wagging mode, t = twisting mode, ν= stretching mode, ν_a = antisymmetric and ν_s = symmetric.

Source Hashida et al.[1] and Kakuda et al. [2]

Table S2. Freezing point of water/ethanol mixture solvent

Water : Ethanol	**Freezing point (ºC)**
100: 0	0
90 : 10	-4
80 : 20	-9
70 : 30	-15
60 : 40	-23
50 : 50	-32
40 : 60	-37
30 : 70	-48
20 : 80	-59
10 : 90	-73
0 : 100	-115

Table S3. Degree of crystallinity and average size of crystals of L-PEI and dried L-PEI cryogels.

Sample	Degree of crystallinity (%)	Average size of crystals (nm)
L-PEI	30.79 ± 0.30	3.50 ± 0.03
Dried L-PEI cryogels	39.96 ± 0.78	3.60 ± 0.05

References

[1] T. Hashida, K. Tashiro, S. Aoshima, Y. Inaki, Structural investigation on water-induced phase transitions of poly(ethylene imine). 1. Time-resolved infrared spectral measurements in the hydration process, Macromolecules. 35 (2002) 4330–4336. https://doi.org/10.1021/ma012204l.

[2] H. Kakuda, T. Okada, T. Hasegawa, Temperature-induced molecular structural changes of linear polyethylene imine in water studied by mid-infrared and near-infrared spectroscopies, J. Phys. Chem. B. 113 (2009) 13910–13916. https://doi.org/10.1021/jp9048204.

Chapter 3

Synthesis and evaluation of poly (3-hydroxypropyl ethyleneimine) and its blends with chitosan forming novel elastic films for delivery of haloperidol

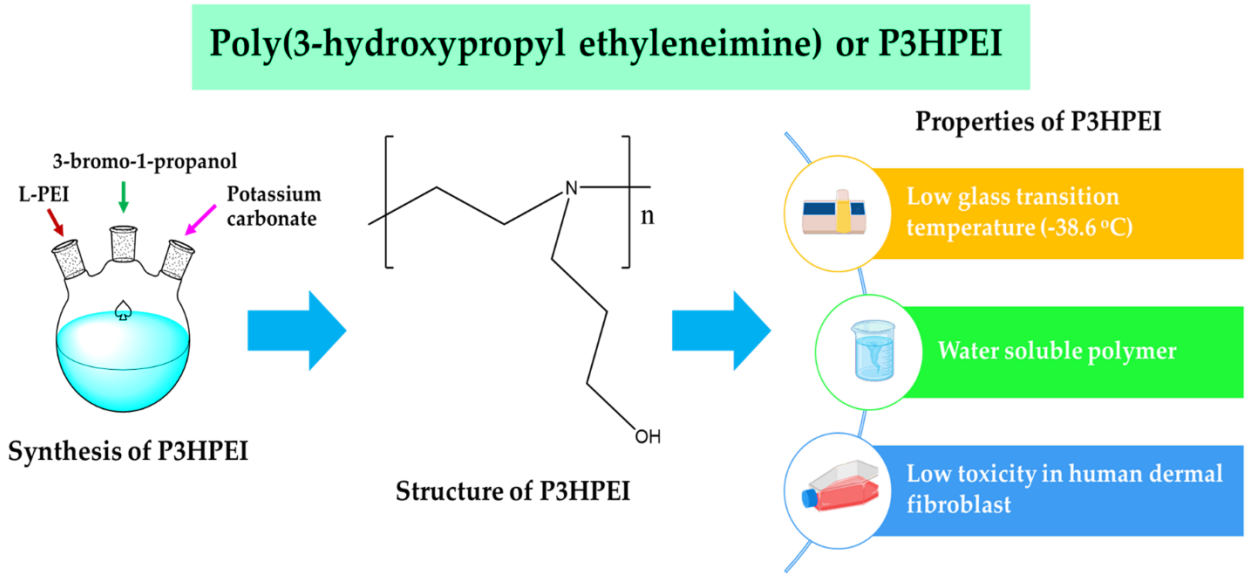

This chapter was published as: Sitthiphong Soradech, Pattarawadee Kengkwasingh, Adrian C. Williams, and Vitaliy V. Khutoryanskiy. Synthesis and Evaluation of Poly(3-hydroxypropyl Ethyleneimine) and Its Blends with Chitosan Forming Novel Elastic Films for Delivery of Haloperidol. Pharmaceutics 2022, 14, 2671.https://doi.org/10.3390/pharmaceutics14122671

Chapter 3

Synthesis and evaluation of poly (3-hydroxypropyl ethyleneimine) and its blends with chitosan forming novel elastic films for delivery of haloperidol

Sitthiphong Soradech [1, 2], Pattarawadee Kengkwasingh [2], Adrian C. Williams [1], and Vitaliy V. Khutoryanskiy [1*]

[1]Reading School of Pharmacy, University of Reading, Whiteknights, Reading, RG6 6AD, UK.

[2]Expert Centre of Innovative Herbal Products, Thailand Institute of Scientific and Technological Research, Pathum Thani, 12120, Thailand.

***Corresponding author:**

Postal address: Reading School of Pharmacy, University of Reading, Whiteknights, PO Box 224, RG6 6AD, Reading, United Kingdom

E-mail address: v.khutoryanskiy@reading.ac.uk

Telephone: +44(0) 118 378 6119

Fax: +44(0) 118 378 4703

Abstract

This study aimed to develop novel elastic films based on chitosan and poly(3-hydroxypropyl ethyleneimine) or P3HPEI for the rapid delivery of haloperidol. P3HPEI was synthesized using a nucleophilic substitution reaction of linear polyethyleneimine (L-PEI) with 3-bromo-1-propanol. ^{1}H-NMR and FTIR spectroscopies confirmed the successful conversion of L-PEI to P3HPEI, and the physicochemical properties and cytotoxicity of P3HPEI were investigated. P3HPEI had good solubility in water and was significantly less toxic than the parent L-PEI. It had a low glass transition temperature (T_g = −38.6 °C). Consequently, this new polymer was blended with chitosan to improve mechanical properties, and these materials were used for the rapid delivery of haloperidol. Films were prepared by casting from aqueous solutions and then evaporating the solvent. The miscibility of polymers, mechanical properties of blend films, and drug release profiles from these formulations were investigated. The blends of chitosan and P3HPEI were miscible in the solid state and the inclusion of P3HPEI improved the mechanical properties of the films, producing more elastic materials. A 35:65 (%*w/w*) blend of chitosan–P3HPEI provided the optimum glass transition temperature for transmucosal drug delivery and so was selected for further investigation with haloperidol, which was chosen as a model hydrophobic drug. Microscopic and X-ray diffractogram (XRD) data indicated that the solubility of the drug in the films was ~1.5%. The inclusion of the hydrophilic polymer P3HPEI allowed rapid drug release within ~30 min, after which films disintegrated, demonstrating that the formulations are suitable for application to mucosal surfaces, such as in buccal drug delivery. Higher release with increasing drug loading allows flexible dosing. Blending P3HPEI with chitosan thus allows the selection of desirable physicochemical and mechanical properties of the films for delivery of haloperidol as a poorly water-soluble drug.

Keywords: Chitosan, poly(3-hydroxypropyl ethyleneimine), polymer blend, elastic films, miscibility, and transdermal drug delivery.

1. Introduction

Buccal drug delivery is commonly used to administer drugs to and through the buccal mucosa to provide local or systemic pharmacological effects [1] and has generated interest as an alternative to oral drug delivery. The advantages of the buccal route include direct access to the systemic circulation via the jugular vein, rapid onset of action, circumventing hepatic first-pass metabolism, avoidance of gastrointestinal acid-related hydrolysis, increased patient compliance (particularly those with dysphagia), and a wide variety of drugs and excipients exist that cause little or no mucosal damage or irritation [2]. Mucoadhesive films are commercially available and these drug delivery systems can prolong the time spent on the mucosa, directly delivering active pharmaceutical ingredient to or through the tissue [2, 3].

Chitosan, a natural cationic polysaccharide [5], is widely used in numerous applications, including drug delivery systems, artificial skin, cosmetics, nutrition, and food additives, due to its biocompatibility, biodegradability, adhesivity, antimicrobial properties, and film-forming abilities [2,3,4]. Further, chitosan has been reported to improve skin penetration and wound healing by increasing the function of inflammatory and repair cells [5–7] and has been used to control drug release for transdermal [6] or transmucosal [8] delivery. However, chitosan-based films have some limitations, including low elasticity and brittleness [9]. In addition, the glass transition temperature (T_g) of film-forming polymers affects the drug release profile, since temperatures above T_g enable polymer chain movement, which facilitates drug release [10]. The physiological temperature of mucosal membranes is ~35–37 °C and external skin temperature is ~32 °C [11], whereas chitosan has a high glass transition temperature (~131 °C) [9], which can restrict drug release from films applied to these biological surfaces.

The poor mechanical properties and high glass transition temperature of chitosan can be moderated by blending with other water-soluble polymers [12]. Blending provides a simple and low-cost approach to design materials with tailored properties. For example, improved mechanical and mucoadhesive properties of chitosan-based films were achieved by combining cellulose ethers and chitosan [13]. Chitosan has also been blended with poly(N-vinyl pyrrolidone) [14], poly(ethylene oxide) [15], and poly(vinyl alcohol) [16] to improve physicochemical properties. Luo et al. [12] developed elastic films using chitosan–hydroxyethylcellulose blends (HEC), whereas Abilova et al. [9] developed films using chitosan and poly(2-ethyl-2-oxazoline) (PEOZ) blends. The T_g of films based on chitosan and PEOZ

decreased from 131 to 63 °C, although the mechanical properties of the resultant films were also compromised as the proportion of PEOZ increased [9].

Linear polyethyleneimine (L-PEI) is a cationic polymer composed of two aliphatic carbon spacer groups (-CH_2CH_2-) and secondary amine groups in each repeating unit [17]. It can be synthesized by hydrolysis of poly(2-ethyl-oxazoline) to remove all amide side chains [18,19]. Generally, L-PEI is semi-crystalline [20,21] with a glass transition temperature ~−29.5 °C [22] and, therefore, appears to be a suitable candidate to blend with chitosan in order to improve film mechanical properties and drug release profiles. However, L-PEI only dissolves in water at high temperatures [20], forms a gel at room temperature [23], and has been shown to cause cytotoxicity [22,24]. The solubility and toxicity of L-PEI is naturally a significant concern when considering its use in pharmaceutical and biomedical applications [25]. Chemical modifications of L-PEI is one approach to increasing solubility in water and decreasing its toxicity [26]. Patil et al. [26] used nucleophilic substitution to synthesize hydroxyethyl-substituted linear polyethyleneimine (HELPEI) for the delivery of siRNA therapeutics; the cytotoxicity of HELPEI on human bronchial epithelial cells decreased as the degree of substitution increased. Here, we selected poly(3-hydroxypropyl ethyleneimine) (P3HPEI) as a suitable candidate to blend with chitosan to produce films to deliver haloperidol and report, for the first time, its synthesis using nucleophilic substitution reaction of linear polyethyleneimine with 3-bromo-1-propanol.

Haloperidol (HP), an antipsychotic drug, is associated with the side effect of drug-induced extrapyramidal syndrome (EPS) in conventional monotherapy [27]. It is poorly water soluble and is commonly formulated as a solution for oral administration or injections and as tablets [18]. The average oral dose of haloperidol ranges from 0.5 to 30 mg per day [28]. Further, HP is a BCS class 2 drug, characterized by low solubility but high permeability [29] and has poor oral bioavailability (59%) [28]. Consequently, Samanta et al. [27] developed HP-loaded matrix dispersion films with Eudragit NE 30D as a controlled release transdermal dosage form. Gidla et al. [29] developed HP-loaded buccal films to provide rapid onset of drug action, with improved patient compatibility and without requiring swallowing. However, HP-loaded films using Eudragit NE 30D [27] or hydroxypropyl methylcellulose (HPMC) [29] have some limitations due to the high glass transition temperature of these polymers, which can restrict drug release from the films when applied to skin or mucosal surface. Therefore, loading HP in polymer blends where the glass transition temperature (T_g) has been optimized to below the temperature of mucosal membranes (~35–37 °C) or external skin (32 °C)[11] can improve drug release into mucosal tissue and also improve the mechanical properties of films.

Here, we aimed to develop novel elastic films based on chitosan and poly(3-hydroxypropyl ethyleneimine) or P3HPEI for the rapid buccal delivery of haloperidol. P3HPEI was synthesized as a novel water-soluble polymer for pharmaceutical and biomedical applications. The physicochemical properties and cytotoxicity of this new material were assessed before it was blended with chitosan to fabricate elastic films for the rapid delivery of haloperidol, chosen as a model poorly water-soluble drug. Miscibility between polymers and the mechanical properties of blend films are reported. An optimal composition of chitosan and P3HPEI blend was then selected for drug incorporation and release studies.

2. Materials and Methods

2.1. Materials

High molecular weight chitosan (CHI, MW∼310–375 kDa, degree of deacetylation: 75–85%), poly(2-ethyl-2-oxazoline) (PEOZ, MW∼50 kDa, PDI 3–4), 3-bromo-1-propanol, hydrochloric acid solution, fluorescein isothiocyanate (FITC), and haloperidol were purchased from Merck (Gillingham, UK), while phosphate-buffered saline (PBS) tablets and sodium hydroxide were from Fisher Chemicals (Fisher Scientific, UK). All other chemicals were of analytical grade and used without further purification.

2.2. Synthesis of Linear Poly(ethyleneimine) (L-PEI)

L-PEI was synthesized by hydrolysis of poly(2-ethyl-2-oxazoline), as described in our previous study [17]. Briefly, 10 g of poly(2-ethyl-2-oxazolines) (PEOZ) was dissolved in 100 mL of 18.0% (*w/w*) hydrochloric acid and then refluxed at 100 °C for 14 h to remove all amide groups in the side chains**.** The L-PEI solution was then diluted with cold deionized water (500 mL). Cold aqueous sodium hydroxide (4M) was added dropwise to the suspension until the polymer dissolved, with further addition of 4 M sodium hydroxide, the base form of L-PEI precipitated at pH 10–11 [30]. The precipitate was recovered by using a vacuum filtration, washed with deionized water, and re-precipitated twice before drying under vacuum oven at 25–30 °C for several days to obtain L-PEI as a white powder yielding 3.8 g (89%).

2.3. Synthesis of Poly(3-hydroxypropyl ethyleneimine) (P3HPEI)

L-PEI (0.02 moles per repeating unit, 1.0 g) was dissolved in absolute ethanol (60 mL) in a three-necked round-bottom flask before 0.06 moles of 3-bromo-1-propanol (5.3 mL) were added. As a proton abstractor, 0.06 moles of potassium carbonate (8.1 g) were then added

before the reaction mixture was refluxed at 78 °C for 24 h; the reaction scheme is shown in Figure S1. After centrifugation of the reaction mixture, the supernatant was collected and evaporated using a rotary evaporator at 40 °C and 280 rpm. The resulting mixture was diluted with deionized water and purified using dialysis with a cellulose-based membrane (MWCO = 3.5 kDa) at room temperature. P3HPEI was recovered as dry residue (77% yield) by freeze-drying (−56.5 °C and 0.25 hPa) for several days.

2.4. Preparation of Films

Chitosan (CHI) films and their blends with P3HPEI were prepared by casting and solvent evaporation, as schematically shown in Figure 1. In this study, chitosan with a high molecular weight was used to form a film due to its high viscosity, excellent film forming properties, and adequate thickness. Initially, 1.0% *w/v* aqueous solutions of CHI and P3HPEI were prepared at room temperature; CHI solution (pH~2.0) was prepared in 0.1 M hydrochloric acid by stirring magnetically for 24 h, whereas P3HPEI solutions (pH~6.8) were prepared in deionized water and allowed to stir continuously for 1 h. The polymer solutions were mixed at different volume ratios, denoted as CHI 100:0 and CHI/P3HPEI: 80:20, 60:40, 40:60 and 20:80. The pH of the combined solutions was in the range of 3.0–4.0. All CHI/P3HPEI solutions were magnetically agitated for 3 h to ensure a homogeneous mixture formed. Then, 45 mL of each solution was poured into 90 mm diameter Petri dishes and dried at ~30 ± 2 °C in a hot air oven for several days until dry films formed.

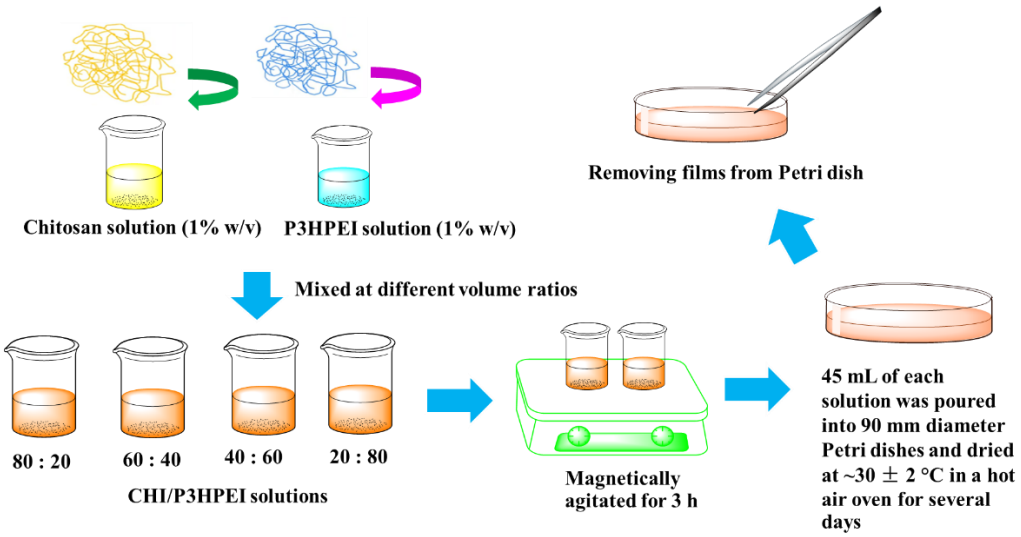

Figure 1. Scheme of CHI/P3HPEI films preparation.

2.5. Preparation of Haloperidol-Loaded Films

A stock solution of haloperidol (5 mg/mL) was prepared by initially dissolving 50 mg of the drug in 5 mL of absolute ethanol. Subsequently, the total volume of haloperidol solution was adjusted to 10 mL. Aliquots were added to 10 mL of 1.0% CHI/P3HPEI solution to obtain 1.0–5.0% drug loading, followed by stirring for 2 h before casting and drying into films, as described above, but instead using 10 mL of solution decanted into 35 mm diameter Petri dishes. The content of haloperidol in each film of 35 mm in diameter was 1.25 to 5.00 mg.

2.6. Characterization of Polymers and Films

2.6.1. ^{1}H-Nuclear Magnetic Resonance Spectroscopy (^{1}H-NMR)

Approximately 20 mg of dried PEOZ or L-PEI was dissolved in 1 mL methanol-d_4, whereas P3HPEI was dissolved in 1 mL D_2O, before the samples were added into NMR tubes and analyzed using a 400 MHz ULTRASHIELD PLUSTM B-ACS 60 spectrometer (Bruker, UK). Data processing used MestReNova software. The degree of substitution (DS) of P3HPEI was determined using peak integration, according to Equation (1):

$$\% \text{ DS} = \frac{\int \text{Peak b}/\text{n}_\text{b}}{\int \text{Peak a}/\text{n}_\text{a}} \text{x } 100 \qquad (1)$$

where peak a corresponds to CH_2CH_2 on the main backbone adjacent to nitrogen, Peak *b* corresponds to CH_2 on side group, n_a is the number of protons in CH_2CH_2 on the main backbone adjacent to nitrogen, and n_b is number of protons in CH_2 on the side group.

2.6.2. Fourier Transformed Infrared (FTIR) Spectroscopy

Polymer and film samples were scanned from 4000 to 400 cm^{-1} at a resolution of 4 cm^{-1}. Data were processed from the average of six scans per spectrum generated by the Nicolet iS5-iD5 ATR FT-IR spectrometer (Thermo Scientific, Leicestershire, UK).

2.6.3. Differential Scanning Calorimetry

Thermal analysis used a Q100 DSC (TA Instruments, Germany). Polymer and film samples (~3–5 mg) were loaded into pierced Tzero aluminum pans. The thermal behavior of each sample was investigated in a nitrogen atmosphere with a heating/cooling rate of 10 °C/min (−70 to 180 °C). The glass transition temperatures (T_g) of polymers were determined from the second heating cycle.

2.6.4. Thermogravimetric Analysis (TGA)

Thermogravimetric analysis used a Q50 TGA analyzer (TA Instruments, UK) over the range between 20 and 600 °C heating at 10 °C/min under a nitrogen atmosphere. Prior to analysis, the films dried in a vacuum oven (as above) and were placed in a desiccator over dry silica gel for 3 days. Moisture content in each film was determined from the weight loss corresponding to the first step weight loss in their TGA curves (up to ~150 °C).

2.6.5. Powder X-ray Diffractometry (PXRD)

Dry polymers or films were placed on a silica slide and analyzed with a Bruker D8 ADVANCE PXRD equipped with a LynxEye detector and monochromatic Cu $K\alpha_1$ radiation ($\lambda = 1.5406$ Å). Samples were rotated at 30 rpm and data collected over an angular range (2θ) of 5–60° for 1 h, with a step of 0.05° (2θ), and count time of 1.2 s. The data were analyzed using Origin software.

2.6.6. Film Thickness

Polymer film thicknesses were measured with a digital micrometer (Mitutoyo, Japan) with 0.001 mm resolution. Measurements were taken at several points of the film before the mean values ± SD were calculated (Table S1).

2.6.7. Scanning Electron Microscopy (SEM)

SEM experiments used an FEI Quanta 600 FEG Environmental Scanning Electron Microscope instrument (FEI UK Ltd., Cambridge, UK), with an acceleration voltage of 20 kV. Images were taken from the fracture surface of the materials, which were first frozen in liquid nitrogen and coated with gold sputter to facilitate high resolution imaging.

2.6.8. Fluorescence Microscopy

The fluorescein isothiocyanate (FITC)-labelled chitosan was synthesized, according to Cook et al. [31]. High molecular weight chitosan (CHI, MW∼310–375 kDa, degree of deacetylation: 75–85%) was used in this study. Briefly, dehydrated methanol (100 mL) and FITC (2 mg/mL in methanol, 50 mL) were added to a chitosan solution (1% *w/v* in 0.1 M hydrochloric acid, 100 mL). The reaction was carried out in the dark at room temperature for 3 h before precipitation in NaOH (0.1 M, 1 L). The resulting precipitate was filtered and dialyzed in deionized water (4 L, replaced daily) until FITC was not detected in the dialysate, before the product was freeze-dried. Then, films were prepared as described before (see Section

2.4), albeit using 10 mL of each solution poured into 30 mm diameter Petri dishes before drying. The morphology of the films was analyzed using fluorescence microscopy at 20× magnification.

2.6.9. Polarized Light Microscopy

Films were examined for the presence of haloperidol crystals using a polarized light microscope (Mettler Toledo FP90, Germany) at 20× magnification; images were analyzed using Infinity 1 camera (Lumenera Corporation, Ontario, Canada).

2.6.10. Mechanical Properties

The mechanical properties of the films—puncture strength, elongation at puncture, and modulus at puncture—were determined using a TA.XT Plus Texture Analyser (Stable Micro Systems Ltd., Godalming, UK) in compression mode, adapted from our previous studies [9,32,33]. Square of film samples (30 × 30 mm) was fixed between two plates with a cylindrical hole of 10 mm diameter (area of the sample holder hole: Ar_s, 78.57 mm^2) and compressed by the upper load 5 mm stainless steel spherical ball probe (P/5S) at 1.0 mm/s. The plate was stabilized to avoid movements using two pins. The measurements started once the probe was in contact with the sample surface and continued until each film sample broke. Test settings were: pre-test speed 2.0 mm/s; test speed 1.0 mm/s; post-test speed 10.0 mm/s; target mode distance; 5 mm; trigger force 0.049 N. The force required to puncture the films (N) was used to calculate the puncture strength by:

$$\text{Puncture strength} = \frac{F_{max}}{Ar_s} \quad (2)$$

where F_{max} is the maximum applied force, Ar_s is area of the sample holder hole, with $Ar_s = \pi r^2$, where r is the radius of the hole.

$$\text{Elongation (\%)} = \left(\frac{\sqrt{r^2+d^2}-r}{r}\right) x\ 100 \quad (3)$$

where r is the radius of the film exposed in the cylindrical hole of the film holder and d represents the displacement of the probe from the point of contact to point of puncture.

$$\text{Modulus at puncture} = \frac{\text{Puncture strength}}{\text{Elongation (\%)}} \quad (4)$$

2.7. In Vitro Drug Release Study

Haloperidol release from films was assessed using a modified Franz diffusion cell (FDC), which was adapted from Samanta et al. [27]. The receptor compartment was filled with 20 mL of 20% PEG 400 (PEG 400 is a water-soluble oligomer with hydrophilic nature so it is used as a penetration enhancer to improve drug solubility and drug release with poor water solubility) in phosphate-buffered saline (pH = 7.4) to ensure sink conditions [27] and was stirred at 600 rpm at 37 °C throughout the experiment. Films containing 5.0, 2.5, and 1.25% haloperidol were placed between the donor and receptor compartments. 1 mL aliquots were taken from the receptor compartment at predetermined time intervals and replaced with 1 mL fresh receiver medium to maintain a constant volume. Drug release was monitored for 180 min, with the drug concentration determined spectrophotometrically at its respective wavelength. A standard calibration curve of haloperidol, ranging from 5–50 µg/mL, was prepared (Figure S10). The protocol used for the preparation of stock solution of haloperidol is described in supplementary information. For each type of film, three replicates were performed.

2.8. Cytotoxicity Test

Polymer cytotoxicity was evaluated using an MTT assay. Briefly, L-PEI was dissolved in 95% ethanol and then diluted with Dulbecco's modified eagle medium (DMEM) to obtain polymer concentrations between 5–5000 µg/mL, whereas PEOZ and P3HPEI were dissolved directly in Dulbecco's modified eagle medium (DMEM) and then diluted with DMEM to prepare solutions with polymer concentrations ranging between 5–5000 µg/mL. Human dermal fibroblasts (ATCC CRL-2522) were seeded at 1 x 10^5 cells/mL in a 96 well plate and allowed to attach overnight before being incubated with the polymer samples at 5, 50, 500, 1000, 2500, and 5000 µg/mL for 24 h. As a positive control, 10% DMSO (*v/v*) in DMEM was used, and for the negative control we used 10% fetal bovine serum in DMEM. Then, 100 µL of 3-(4, 5-dimethylthiazol-2-yl)-2, 5-diphenyl tetrazolium bromide (MTT) solution was added into each well before the plate was incubated at 37 °C in a CO_2 incubator for 3 h. The amount of formazan produced was then quantified from the absorbance at 570 nm using a standard plate reader (Thermo Scientific™ Multiskan™ GO, Vantaa, Finland).

2.9. Statistical Analysis

Data are presented as mean values ± standard deviation (SD) for no fewer than three independent experiments. Student's *t*-test and one-way ANOVA were used to determine the extent of any differences between samples.

3. Results and discussion

3.1. Synthesis and Evaluation of Poly(3-hydroxypropyl ethyleneimine)

L-PEI was synthesized successfully by acidic hydrolysis of PEOZ to remove all amide groups from the side groups. The complete conversion to L-PEI was confirmed by ^{1}H-NMR and FTIR spectroscopies. As illustrated in Figure 2, both PEOZ signals from the side groups, seen at 2.44 ppm and 1.13 ppm were eliminated, while the signal from the two methylene groups within the polymer backbone shifted to 2.75 ppm. FTIR (Figure S2) also confirmed the hydrolysis of the PEOZ amide groups through the loss of the amide carbonyl vibration at 1626 cm^{-1} and the appearance of new strong peaks ~1474 cm^{-1} and 3263 cm^{-1} due to the N-H vibration in PEI. The ^{1}H-NMR and FTIR results from hydrolysis of PEOZ to obtain L-PEI correlated well with earlier reports [18,34].

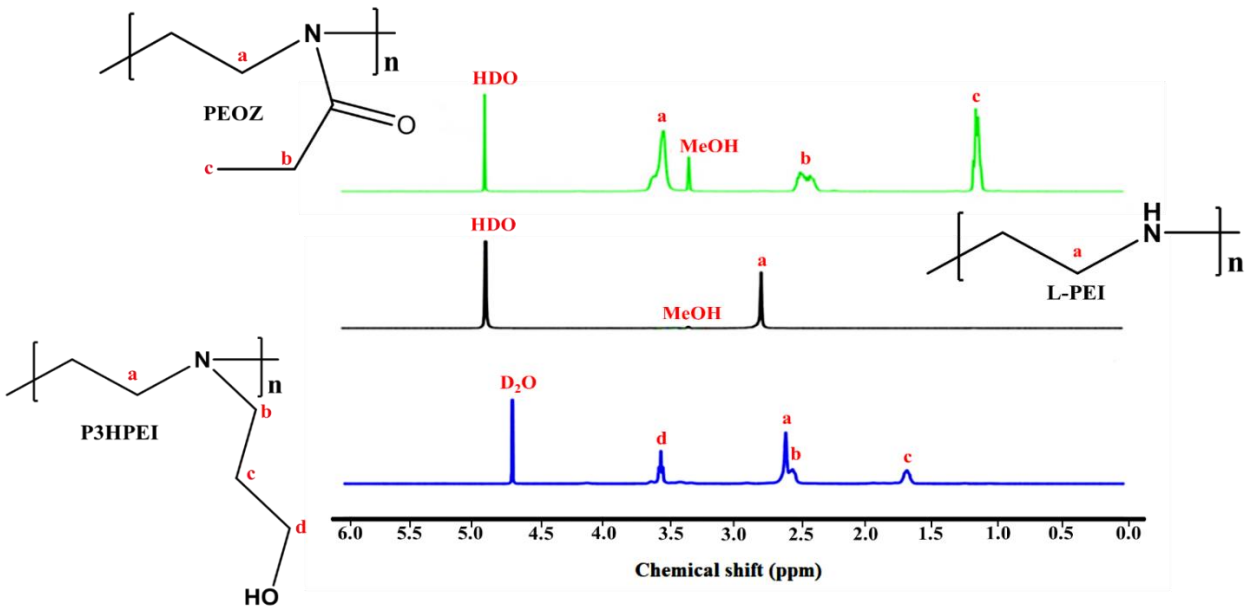

Figure 2. ^{1}H NMR spectra of PEOZ in MeOH-d$_4$, L-PEI in MeOH-d$_4$, and P3HPEI in D$_2$O.

The L-PEI was then alkylated via nucleophilic substitution reaction with 3-bromo-1-propanol in absolute ethanol, with potassium carbonate as a base. The obtained P3HPEI was also characterized using ^{1}H-NMR and FTIR spectroscopies. The ^{1}H NMR spectrum revealed four signals at approximately 2.65 ppm (signal a) due to -CH$_2$CH$_2$- in the polymer backbone, 2.52 ppm (signal b) assigned to the -CH$_2$- in the side chain adjacent to the backbone -CH$_2$CH$_2$-

, 1.66 ppm (signal c) due to the -CH_2- further down the side chain, and 3.54 ppm (signal d) arising from the terminal -CH_2- in the side group, adjacent to a hydroxyl group (-OH).

The degree of substitution (DS) of P3HPEI was determined by comparing the area under the peak from the methylene group on the side group to the area under the peak corresponding to the two methylene groups on the main backbone. The result indicated that the DS of P3HPEI was 97%, 99%, and 99%, as calculated based on signal b, c, and d, respectively. In addition, FTIR data (Figure S2) confirmed the successful synthesis of the hydroxypropyl substituted L-PEI (P3HPEI) by providing a broad absorption band at 3307 cm^{-1}, assigned as an OH- stretching mode.

Differential scanning calorimetry (DSC) and thermogravimetric analysis (TGA) characterized the thermal properties of PEOZ, L-PEI, and P3HPEI. DSC showed that PEOZ, L-PEI, and P3HPEI had glass transition temperatures (T_g) of 60.1, −21.5, and −38.6 °C, respectively (Figure 3). Furthermore, the DSC thermogram of L-PEI gave a melting point of 61.8 °C, consistent with the literature [22,35]. The conversion of L-PEI to P3HPEI, with the inclusion of the side group containing a hydroxyl group, increases chain mobility and polymer flexibility, resulting in a change from a semi-crystalline to an essentially amorphous polymer; X-ray diffractometry confirmed that L-PEI is semi-crystalline, whereas the diffraction pattern from P3HPEI showed no evidence for crystallinity (Figure S3).

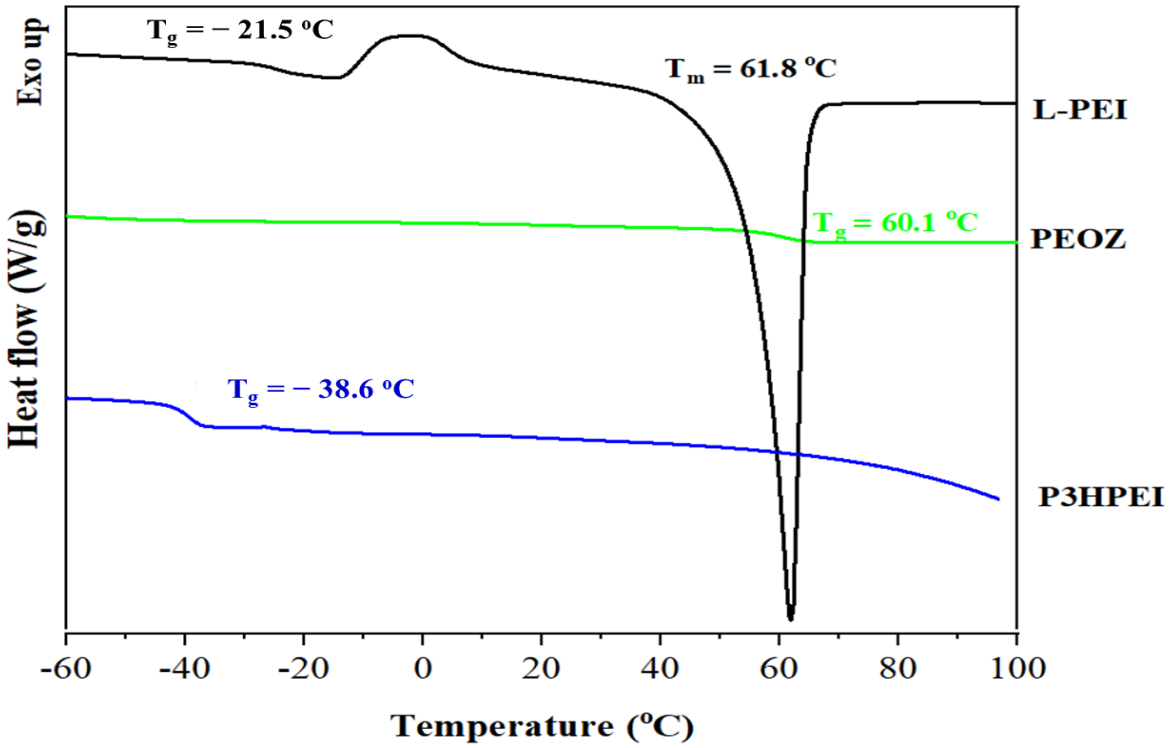

Figure 3. DSC thermograms of PEOZ, L-PEI, and P3HPEI.

TGA was used to compare the thermal stability of P3HPEI to PEOZ and L-PEI (Figure S4). It is noticed that there are two distinct stages for the lost mass of PEOZ, L-PEI, and P3HPEI. The initial decrease was caused by the loss of free and physically bound water between 30 and 150 °C; the proportion of physically bound water was approximately 2.0% for PEOZ, 4.2% for L-PEI, and 8.0% for P3HPEI. The second weight loss of these were related to thermal decomposition, and the onset of decomposition was at 390 °C for PEOZ, 380 °C for L-PEI, and 235 °C for P3HPEI, indicating that the new polymer has lower thermal stability than its parent components.

The cytotoxicity of P3HPEI, in comparison to PEOZ and L-PEI, was assessed using an MTT assay with human dermal fibroblast cells, as shown in Figure 4. L-PEI is highly cytotoxic between 50 to 5000 μg/mL, with less than 50% cell viability when dosed at 50 μg/mL and less than 20% viability when dosed at 500 μg/mL or above. Our modification radically reduces the cytotoxicity with P3HPEI showing no significant ($p < 0.05$) effects when dosed at 5 and 50 μg/mL (viability 97.4 and 95.5%, respectively). At higher doses, a gradual decline in viability from 84.9% to 75.7% was seen as P3HPEI dosing increases from 500 to 5000 μg/mL. Consistent with the literature [36], PEOZ had no adverse effects on dermal fibroblasts as assessed by the MTT assay, with viabilities maintained above 94% for all concentrations tested. The literature contained several reports that L-PEI can cause cytotoxicity when assessed using the MTT assay [24] and that the polymer is highly cytotoxic to human dermal fibroblast cells [22]. Moghimi et al. [24] reported that L-PEI toxicity results from: (1) the disruption of cell membranes, causing necrotic cell death, and (2) the disruption of mitochondrial membranes, resulting in cell apoptosis. Furthermore, L-PEI is a cationic polymer that accumulates on the outer cell membrane, causing necrosis [37]. Fischer et al. [38] reported that the positive charge on the L-PEI surface can bind to the negative charge of cell membrane phospholipids, cell membrane proteins, and blood proteins, contributing to the interaction with the cell membrane that results in cell damage.

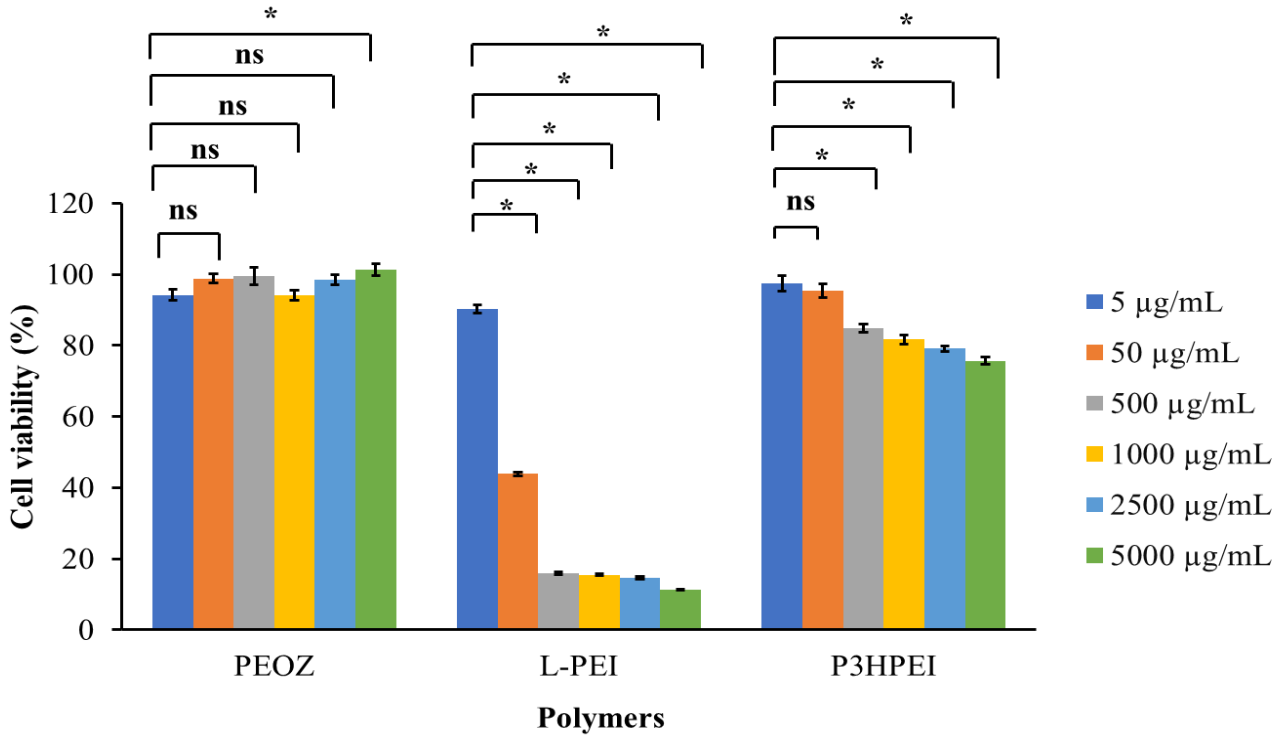

Figure 4. Cytotoxicity test of PEOZ, LPEI, and P3HPEI on human dermal fibroblast using an MTT assay. Statistically significant differences are given as: *—$p < 0.05$; ns—no significance.

3.2. Novel Elastic Films based on Blends of Chitosan and Poly(3-hydroxypropyl ethyleneimine): Formulation, Miscibility, and Mechanical Properties

P3HPEI exhibits good solubility in water, low toxicity, and has a low glass transition temperature (−38.6 °C). Therefore, it was blended with chitosan in aqueous solutions and cast into films to improve their mechanical properties for rapid drug delivery.

Figure 5 and Table 1 show the FTIR data from CHI films and films from blends of CHI/P3HPEI and pure P3HPEI. The FTIR spectrum of pure CHI film revealed the presence of a broad peak above 3247 cm^{-1} due to OH- stretching, which overlaps with NH- stretching in the same region. Absorption bands at 2917 and 2878 cm^{-1} correspond to -CH_2- and -CH- stretching vibrations, respectively. The absorption bands at 1625 and 1514 cm^{-1} are consistent with C=O stretching (amide I) and NH bending (amide II). CH- and OH- vibrations give the absorption band at 1412 cm^{-1}. The band at 1376 cm^{-1} represents acetamide groups, indicating that chitosan was not completely deacetylated [9], and the band at 1311 cm^{-1} was caused by C-N stretching (amide III) [39]. The band at 1250 cm^{-1} is attributable to amino groups, as reported previously [12]. The absorption bands at 1152 and 1062 cm^{-1} correspond to the anti-symmetric stretching of the C-O-C bridge and the skeletal vibrations involving the C-O

stretching, which are characteristic of the chitosan polysaccharide structure [40]. The broad absorption band at 3291 cm^{-1} in the FTIR spectrum of P3HPEI likewise indicates the presence of -OH stretching, as well as bound water. Absorption bands at 2940 and 2827 cm^{-1} are attributed to -CH_2- stretching vibrations. The absorption bands at 1464, 1371, and 1340 cm^{-1} are -CH- bending modes, whereas the absorption bands at 1297, 1260, and 1054 cm^{-1} are assigned to C-C stretching. Furthermore, P3HPEI provided an absorption band at around 1675 cm^{-1} corresponding to water, since P3HPEI is a highly viscous liquid at room temperature, supported by the -OH stretching mode at 3291 cm^{-1}. All characteristic bands of the component polymers were present in the spectra of their blends, and the intensities and shapes of the bands depended on the polymer ratio in the blends. The hydroxyl region of the spectra of the miscible CHI/P3HPEI blends changed gradually, indicating a redistribution of hydroxyl group associations. In short, the -OH stretching mode shifted to higher wavenumbers (3247 to 3348 cm^{-1}) as the amount of P3HPEI increased from 0 to 80%, possibly due to interactions between the polymers and water or arising from interactions between the hydroxyl and amine groups of CHI and the hydroxyl groups of P3HPEI.

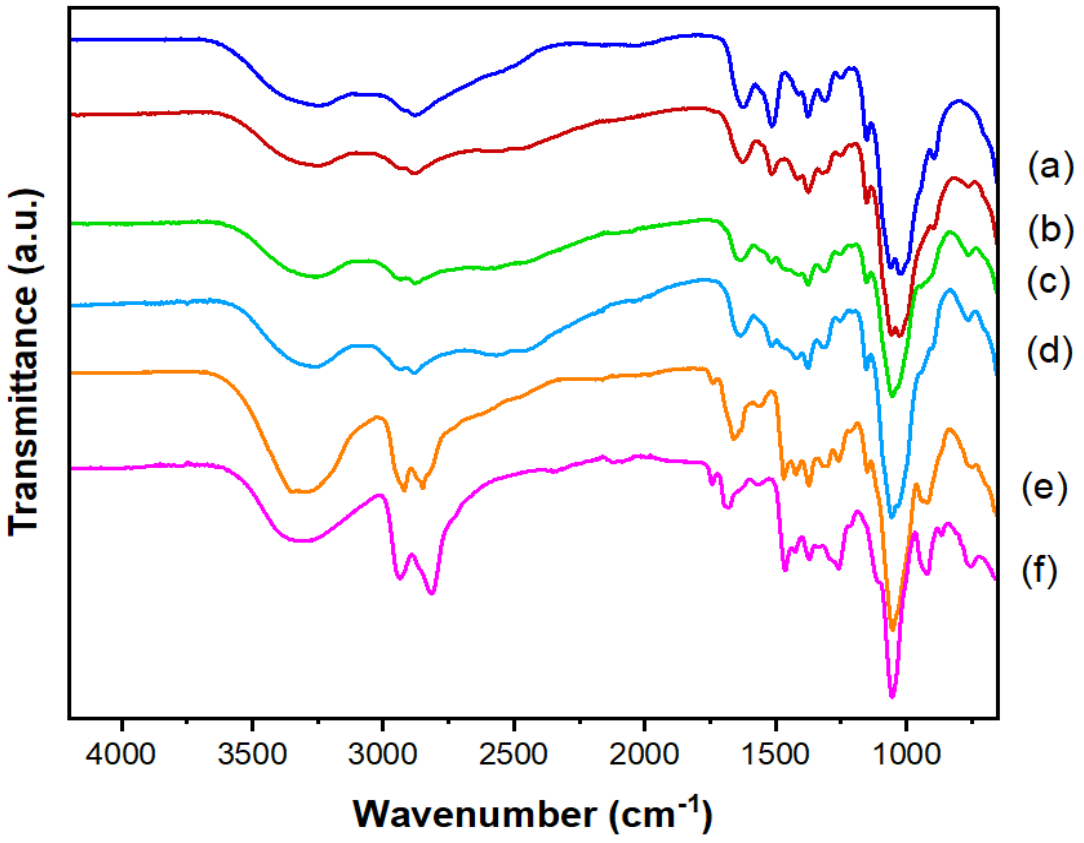

Figure 5. FTIR spectra of CHI (a), their blends (b–e), and P3HPEI (f). Content of P3HPEI in the blends: 20 (b), 40 (c), 60 (d), and 80% (e).

Table 1. FTIR absorption bands in CHI/ P3HPEI blends and their assignment.

FTIR Absorption of Blends (cm^{-1})						Assignment
100:0	**80:20**	**60:40**	**40:60**	**20:80**	**0:100**	
3247	3248	3258	3259	3348	3291	-OH and NH stretching
2917	2928	2929	2928	2920	2940	CH stretching
2878	2879	2880	2880	2849	2827	CH stretching
1625 [1,2]	1624 [1,2]	1635 [1,2]	1631 [1,2]	1633 [1,2]	1675 [2]	C=O stretching (amide I) [1], water region [2]
1514 [3,4]	1514 [3,4]	1515 [3,4]	1515 [3,4]	1468 [3,4]	1464 [4]	NH bending (amide II) [3], CH_2 vibration [4]
1412	1416	1418	1410	1422	1424	CH and OH vibration
1376 [5,6]	1375 [5,6]	1376 [5,6]	1376 [5,6]	1372 [5,6]	1371 [6]	Acetamide groups [5], CH vibration [6]
1311	1321	1317	1315	1302	-	CN stretching (amide III)
1152	1151	1152	1152	1150	-	Anti-symmetric stretching of the C-O-C bridge
1060 [7,8]	1056 [7,8]	1055 [7,8]	1053 [7,8]	1053 [7,8]	1054 [8]	Skeletal vibration involving the C-O stretching [7], C-C stretching [8]

As shown in Figure 6, thermogravimetric analysis (TGA) was used to investigate the thermal stability of pure CHI film, P3HPEI, and films based on blends of CHI and P3HPEI. The results demonstrated that pure CHI film lost mass in two stages. The initial decline was due to the loss of free- and physically bound water between 30 °C and 150 °C; the proportion of physically bound water in pure CHI film was approximately 6%. The second weight loss occurred between 250 and 400 °C as the CHI film degraded by thermal decomposition; the maximum degradation rate was observed at 320 °C, resulting in a 58.3% loss in weight. Chitosan decomposes by depolymerization of its chains and pyranose rings via dehydration, deamination, and ring-opening reaction [9].

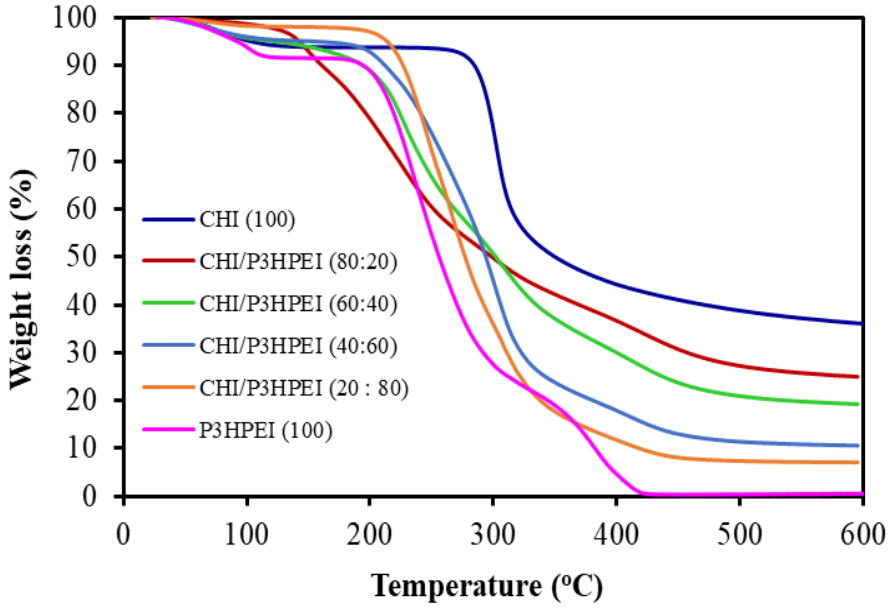

Figure 6. TGA thermograms of CHI film, CHI/P3HPEI blend films, and P3HPEI.

In contrast, three phases of weight loss were seen with P3HPEI. The first thermal event is evaporation of free- and bound water (approximately 8.0%) between 30 and 150 °C. Subsequently, the thermal degradation of P3HPEI is seen >235 °C (40%), followed by a further decomposition event >380 °C (89%).

The blends of CHI/P3HPEI show four weight loss events: (1) 30–150 °C, again due to loss of free and bound water, (2) 200–250 °C consistent with the early degradation of P3HPEI, (3) 275–380 °C where the later degradation of P3HPEI is seen, and (4) 350–450 °C, which correlates with the degradation of CHI. In addition, the residue of CHI/P3HPEI blends tended to decrease (34.5 to 7.1%) as the P3HPEI content in the blends increased up to 80%, with a linear correlation ($R^2 = 0.9853$) confirming the miscibility of polymer blends (Figure S5).

Generally, a single glass-transition temperature (T_g) is taken as evidence for homogeneity (miscibility) in polymeric blend systems. Figure 7 shows DSC thermograms for CHI/P3HPEI blends, illustrating the presence of a single T_g in all compositions. As expected, the T_g of the CHI/P3HPEI blends all fell between the T_g values of the individual components (P3HPEI, −38.6 °C; chitosan, 131.9 °C) and the blends T_g shifted systematically to lower temperatures as the proportion of P3HPEI rose in the blends. The addition of P3HPEI, as a water soluble component, appears to have acted as a plasticizer [41,42].

Figure 8 shows the correlation between the weight fraction of P3HPEI in the blends and T_g using the above experimental result and those calculated theoretically; the T_g of miscible blends can be predicted using Fox [43] and Gordon–Taylor [44] equations, as shown in Equations (5) and (6):

$$\frac{1}{T_g} = \frac{W_{CHI}}{T_{g,\,CHI}} + \frac{W_{P3HPEI}}{T_{g,\,P3HPEI}} \qquad \text{(Fox equation)} \qquad (5)$$

$$T_g = \frac{W_{CHI}T_{g,\,CHI} + kW_{P3HPEI}T_{g,\,P3HPEI}}{W_{CHI} + kW_{P3HPEI}} \qquad \text{(Gordon–Taylor equation)} \qquad (6)$$

where W_{CHI} and W_{P3HPEI} were the weight fractions of chitosan and P3HPEI, respectively; and $T_{g,CHI}$ and $T_{g,P3HPEI}$ are the glass transition temperatures of chitosan and P3HPEI, respectively; k is the ratio of heat capacity change in P3HPEI over chitosan [$k = \Delta C_{p2}/C_{p1}$)] [45].

The predicted glass transition temperatures of the blends were in close agreement, as shown in Figure 7, with the T_g decreasing as P3HPEI content increased. The experimental data sit above the theoretical curves and are commonly seen when there are interactions between the blend components [46–48]. The results suggest that chitosan and P3HPEI are miscible and that the chitosan and P3HPEI molecules interact, probably through intermolecular hydrogen

bonds between the hydroxyl and amine groups of chitosan molecules and the hydroxyl groups of P3HPEI molecules.

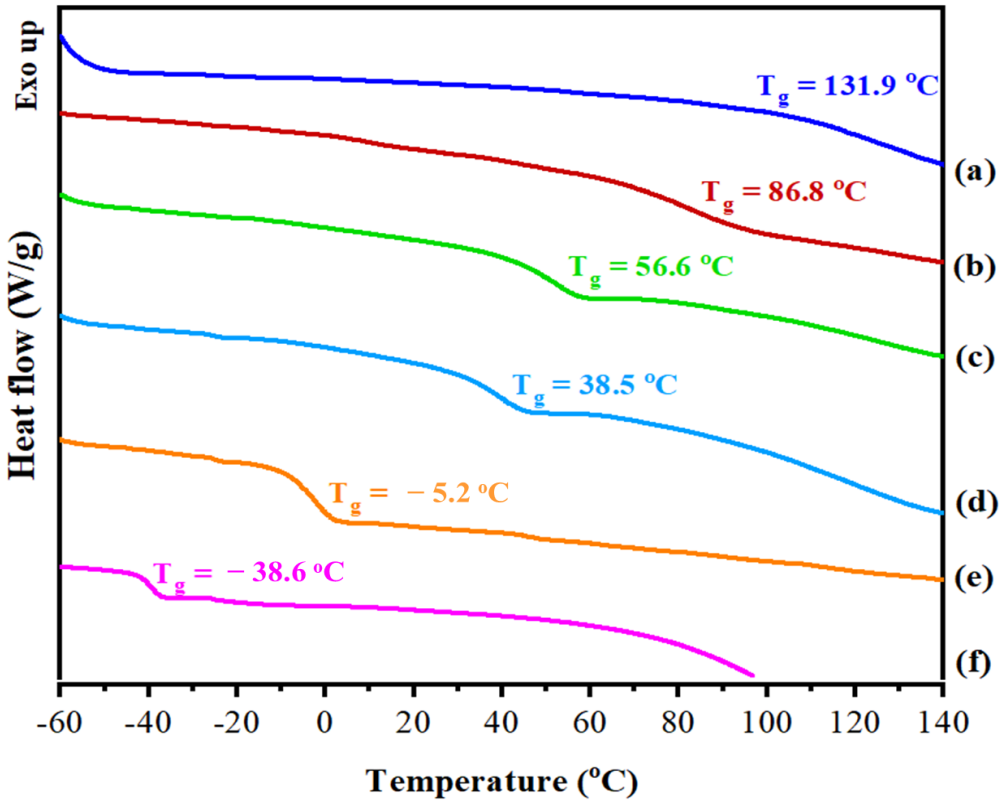

Figure 7. DSC thermogram of CHI (a), their blends (b–e), and P3HPEI (f). Content of P3HPEI in the blends: 20 (b), 40 (c), 60 (d), and 80% (e).

Further, the interaction and miscibility of CHI and P3HPEI blends correlates with X-ray diffraction patterns from the CHI/P3HPEI films (Figure S6). CHI films show the presence of crystalline domains in this polysaccharide, which was correlated well with previous reports [9,49]. The diffraction pattern from pure P3HPEI shows no clear crystalline features but only a broad amorphous “halo”, indicating that the polymer was essentially non-crystalline. The X-ray diffractograms of CHI/P3HPEI films also reveal a broad halo, characteristic of polymers that are predominantly amorphous though some chitosan-typical diffraction peaks, could be detected in the blend films. Further, as P3HPEI content in the films increased, the sharper chitosan diffraction peaks were lost, suggesting molecular interactions between the components and their resultant miscibility.

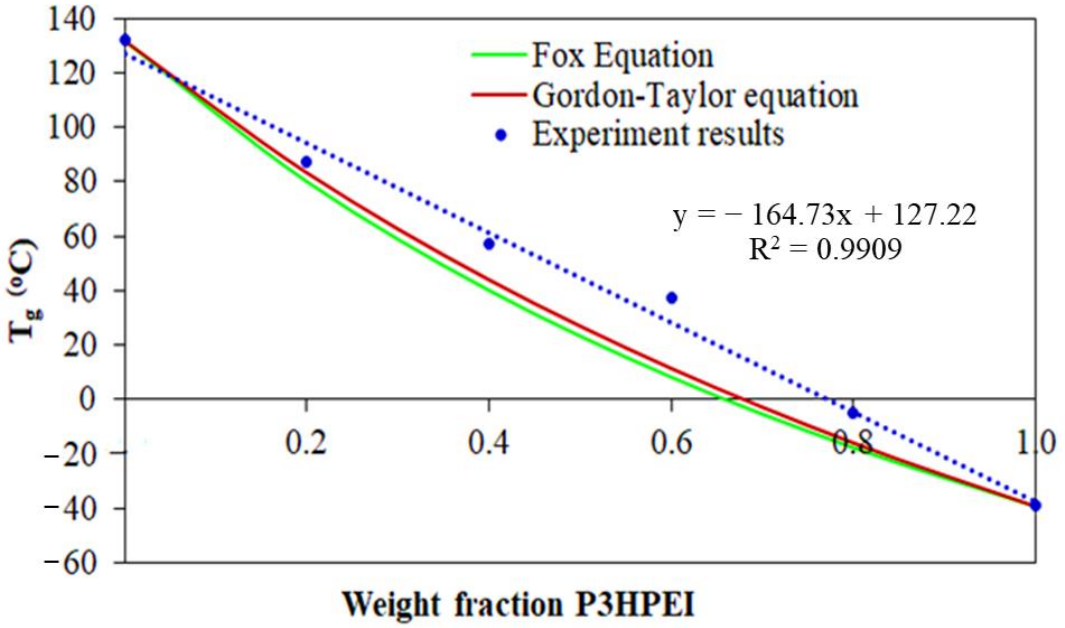

Figure 8. Correlation between weight fraction of P3HPEI and T_g of experimental results, compared with theoretical results.

Fluorescence microscopy was used to examine the morphology of the polymer film surfaces. Initially, fluorescein isothiocyanate (FITC)-labeled chitosan was synthesized and then blended with P3HPEI to form films. The images show no evidence of phase separation or interface boundaries and that all films appear homogeneous (Figure 9). Thus, the fluorescent microscope images data lend further support for miscibility of CHI and P3HPEI in the solid state at the ratios used here. The fluorescent microscope images correlated well with the scanning electron microscope (SEM) image of film surface and cross-sections (Figure S7).

The mechanical properties of pure CHI film and its blends with P3HPEI are illustrated in Figure 10, including puncture strength, elongation, and modulus at puncture. Pure chitosan films (100%) had a higher puncture strength (0.38 N/mm^2) but a lower percentage of elongation (5.62%) than the other films tested. The puncture strength of CHI/P3HPEI films decreased, compared to chitosan alone, whereas the flexibility (% elongation) increased with increasing P3HPEI content. The puncture strengths of CHI/P3HPEI films at 80:20, 60:40, 40:60, and 20:80 were 0.27, 0.24, 0.16, and 0.03 N/mm^2, while elongation was 7.85, 7.94, 11.97, and 15.12%, respectively. The modulus at puncture was calculated from the puncture strength and elongation to predict the rigidity or stiffness of the films; the data show a similar trend to that of the puncture strength.

Clearly, increasing the P3HPEI content in the films results in more elastic materials. As shown above, P3HPEI has a low glass transition temperature (−38.6 °C) and is a water-soluble

polymer, so may function as a plasticizer. Plasticizers are typically relatively small molecules, such as low molecular weight polyethylene glycol (PEG), that intersperse and intercalate between polymer chains, thereby disrupting hydrogen bonding and spreading the chains apart to increase flexibility by increasing the percentage of elongation while decreasing the strength and modulus [50]. Here, increasing the P3HPEI content in CHI/P3HPEI films probably decreases intermolecular hydrogen bonding between CHI chains, resulting in enhanced chain mobility and film flexibility [51], in agreement with the thermal analysis data above.

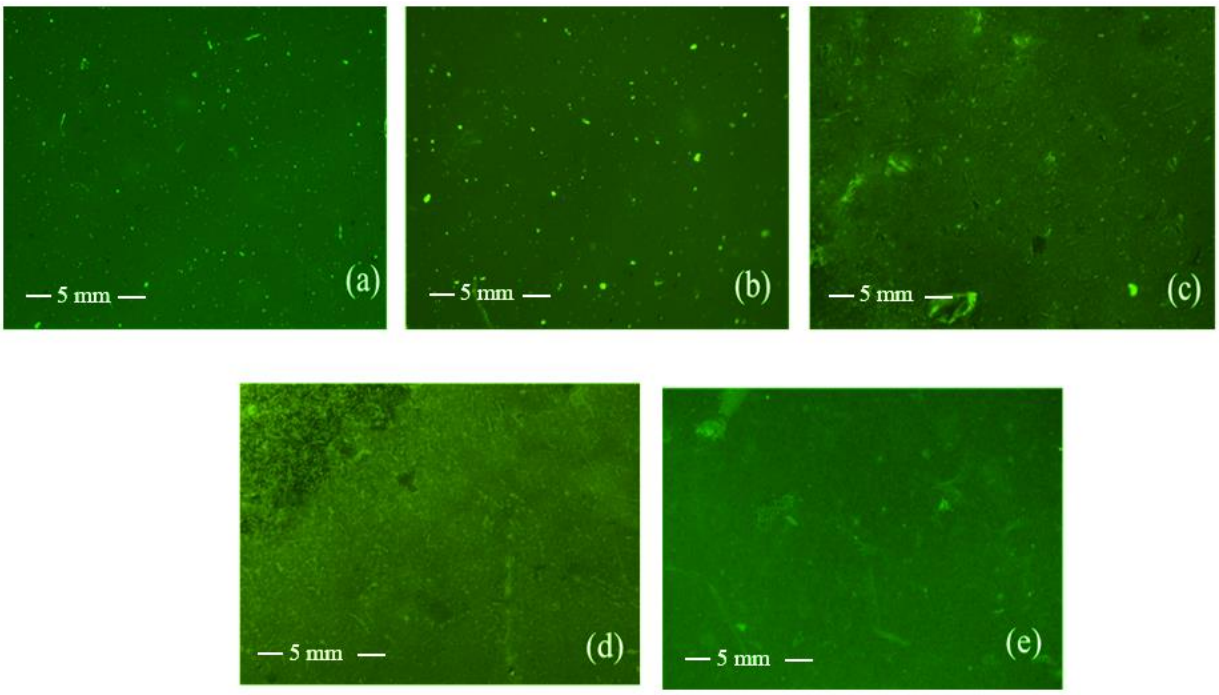

Figure 9. Fluorescent microscopy images of film surfaces of CHI (**a**) and their blends (**b**–**e**). Content of P3HPEI in the blends: 20 (**b**), 40 (**c**), 60 (**d**), and 80% (**e**) at 20x magnification.

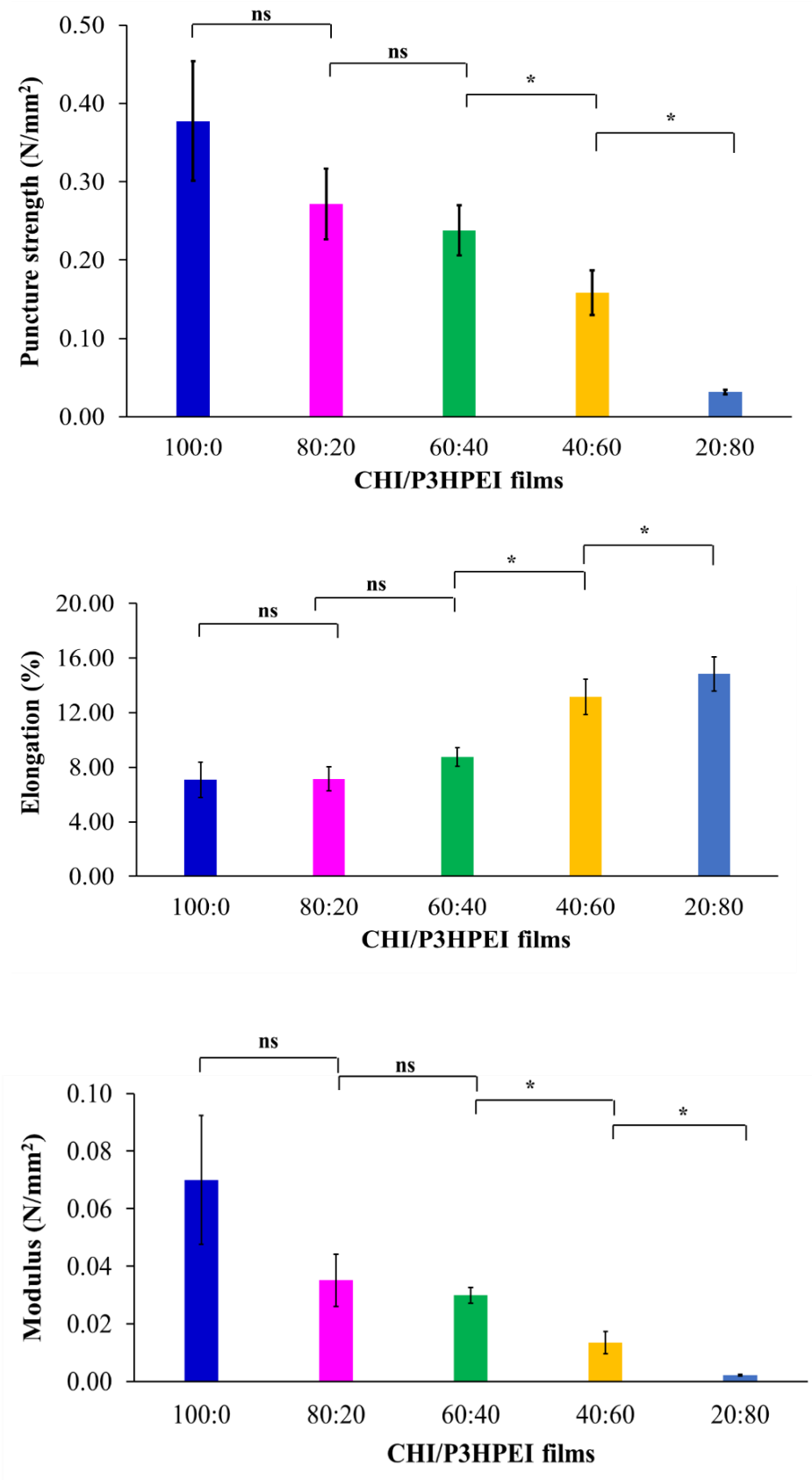

Figure 10. Mechanical properties of CHI and their blends with P3HPEI. Statistically significant differences are given as: *—$p < 0.05$; ns—no significance.

3.3. Chitosan/Poly(3-hydroxypropyl ethyleneimine) Film Formulations for Loading and Delivery of Haloperidol: X-ray, Microscopic, and Drug Release Studies

Drug-loaded films have been used as drug delivery systems for administration via the transdermal, buccal, nasal, and ocular routes, which have advantages over oral and intravenous administration [52,53]. In particular, non-oral delivery methods are noninvasive or minimally invasive, painless, and simple for patients to utilize, especially those with swallowing difficulties. However, control over drug delivery is problematic with formulations, such as creams or gels [54,55]. Moreover, it was suggested that they can increase the bioavailability of various drugs [56]. Drug-loaded films have thus been developed for drug delivery systems via the topical [57], buccal [58], nasal [56], and ocular [9] routes.

Polymeric films, and, in particular, their blends, can be selected to optimize both mechanical properties and drug release [59]. The glass transition temperature (T_g) of a polymer is an important factor when considering their use in drug delivery systems as this impacts the drug release profile; at temperatures greater than T_g, polymer chains become flexible, and thus promote drug release [10]. Since the physiological temperature of mucosal membranes is ~35–37 °C (and skin ranges from 32 °C at the outer surface to body temperature in the inner layers) [11], a CHI/P3HPEI blend with a T_g ~20 °C was selected. To meet this criterion, the appropriate composition of CHI/P3HPEI was calculated from the data in Figure 7 as 35:65% (*w/w*); the T_g of this blend was then confirmed by DSC (Figure S8).

Haloperidol (HP) was chosen as a model poorly soluble drug for inclusion in the film patch. Generally, HP, an antipsychotic, is associated with side effects of drug-induced extrapyramidal syndrome (EPS) in conventional monotherapy [27]. HP is a BCS class 2 drug, characterized by low solubility but high permeability, and has poor oral bioavailability [29]. In this study, CHI/P3HPEI films loaded with haloperidol (HP) at various% drug loading from 1.0 to 5.0% were prepared. X-ray, microscopic, and drug-release studies of HP from CHI/P3HPEI films are shown in Figures 11–13.

The X-ray diffraction (XRD) pattern of HP (Figure 11) is in agreement with literature [18]; a single crystalline polymorphic form was identified. The XRD pattern of the drug-free film showed a predominantly amorphous material with a pattern additive of those from CHI and P3HPEI. Peaks in the XRD patterns from drug-loaded films are attributable to HP crystals. However, the diffraction peaks of HP-loaded CHI/P3HPEI films exhibit a different pattern than that of HP as the free base, with peaks at $2\theta = 17, 23, 25$, and 31°. This is attributable to loading HP into a CHI/P3HPEI solution containing 0.1 M HCl (to solubilize chitosan), which then

converts HP to its hydrochloride salt; our data is consistent with the HP-HCl reported by Al Omari et al. [60].

As expected, HP peak intensity fell with reducing drug content in the films and no crystalline materials were detected below 1.5%. This may be below the limit of detection for the instrument or, alternatively, could reflect the solubility of HP in the polymer blend.

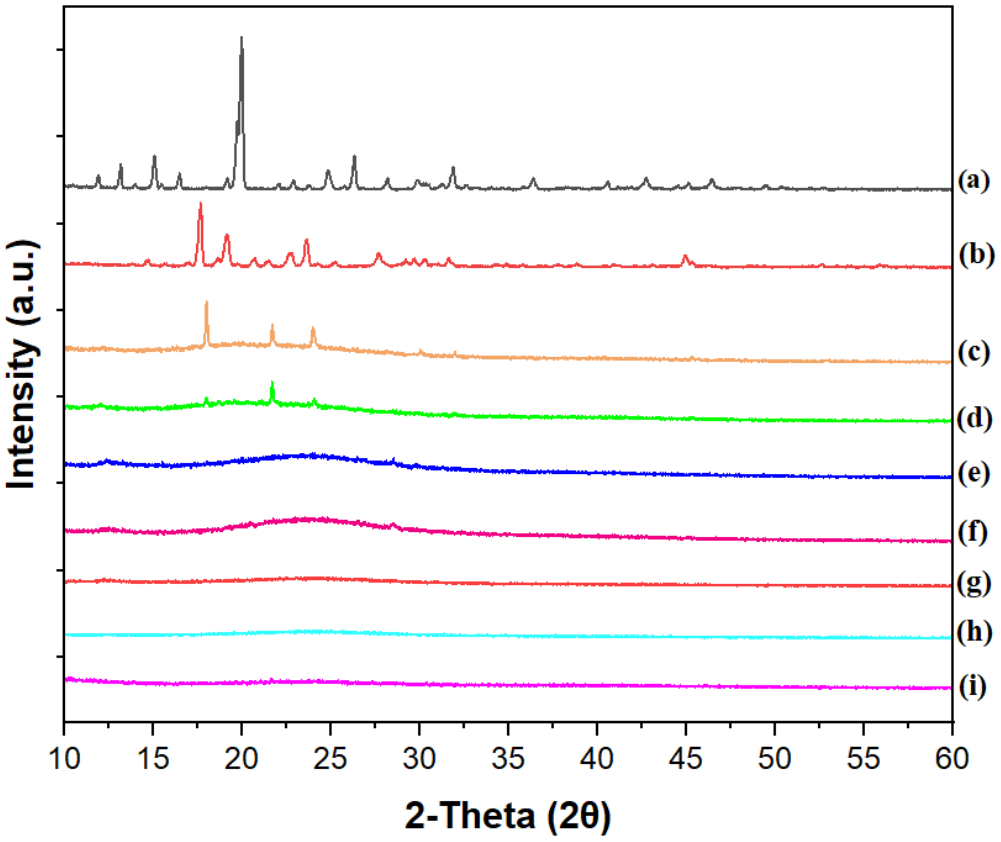

Figure 11. XRD diffractograms of haloperidol (a), haloperidol HCl (b), CHI/P3HPEI films loaded with haloperidol at various% drug loading, 5.0% (c), 2.5% (d), 2.0% (e), 1.75% (f), 1.5% (g), and 1.25% HP films (h) and drug-free CHI/P3HPEI film (i).

Polarized light microscopic examination, as shown in Figure 12, provides direct visual evidence for the presence or absence of solid HP in the CHI/P3HPEI films with large crystals evident at high HP loading (2.0–5.0%), corresponding to the presence of the crystalline peaks shown by XRD. As the HP loading fell below 1.5%, the morphology of HP-loaded film altered, again reflecting the solubility of HP in the polymer blends and consistent with the XRD data. Based on these observations, HP solubility in the CHI/P3HPEI film is approximately 1.5%.

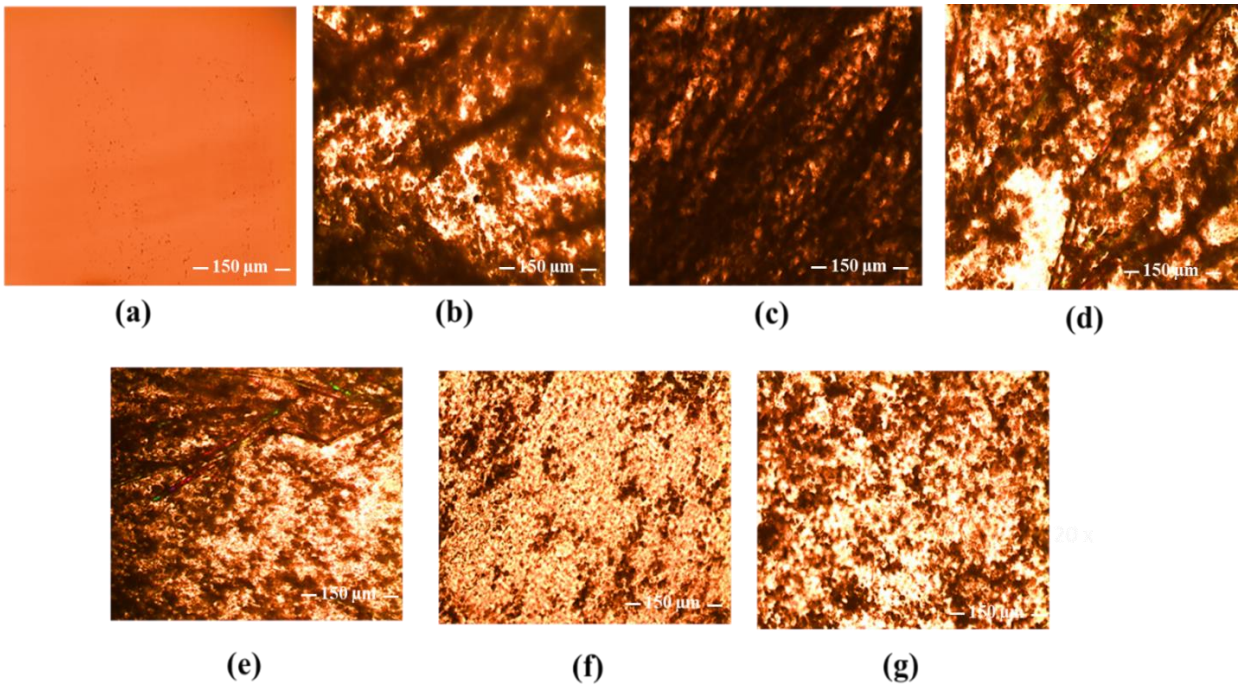

Figure 12. Polarized light microscope images of drug-free CHI/P3HPEI film (**a**) and CHI/P3HPEI films loaded with haloperidol (HP) at various% drug loading, 5.0% (**b**), 2.5% (**c**), 2.0% (**d**), 1.75% (**e**), 1.5% (**f**), and 1.25% (**g**) (20× magnification). Scale bars are 150 µm.

Figure 13 illustrates the cumulative release of HP (1.25, 2.5, and 5%) loaded into CHI/P3HPEI films using the Franz diffusion cell technique and a 20% PEG 400-PBS receiver solution at pH = 7.4 and 37 °C to maintain sink conditions [23]. The data show rapid release from the films, irrespective of drug loading. Drug release from films is dependent on both the physicochemical and mechanical properties of the polymers and also the nature and state of the drug, and whether encapsulated in a carrier. For the polymer matrix, the diffusion of water into the film, relaxation of the polymer chains, swelling, and erosion are important factors to consider [61, 62]. Here, the hydrophilic nature of our CHI/P3HPEI films permits rapid water diffusion, swelling, and erosion whilst the low T_g facilitates the relaxation of the polymer chains, resulting in rapid drug release followed by disintegration of the films. In addition, release increased with drug loading, allowing dose optimization from the films. Similar loading-related release has been described by Budhian et al. [63] when HP was encapsulated in PLGA nanoparticles; here, a simple dispersion of HP in our novel polymer-blended film provides rapid release, as is desired for administration in buccal or ocular delivery.

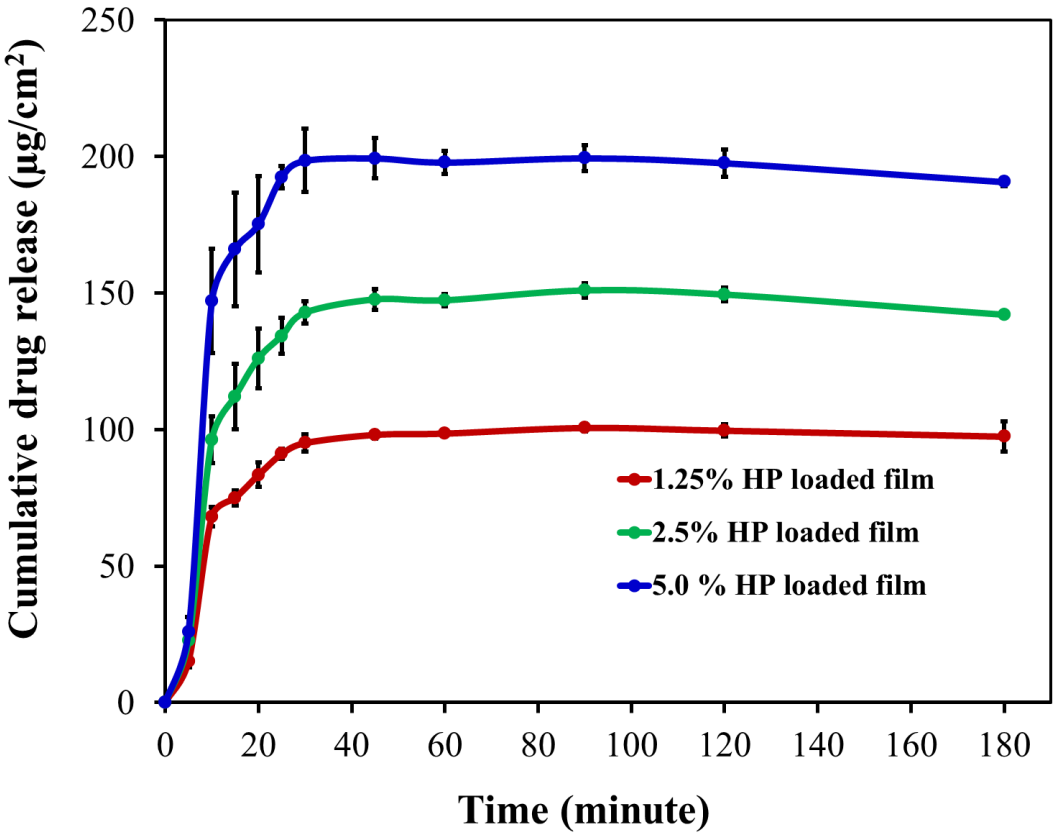

Figure 13. Cumulative drug release per unit area of CHI/P3HPEI films loaded with haloperidol (HP) at various% drug loading (5.0, 2.5 and 1.25%).

4. Conclusions

Poly(3-hydroxypropyl ethyleneimine), or P3HPEI, has been successfully synthesized and its physicochemical and cytotoxic properties have been described. The polymer demonstrated good solubility in water, low toxicity, and a low glass transition temperature. P3HPEI was subsequently blended with chitosan to generate novel flexible films by casting from aqueous solutions and evaporating the solvent. The polymers in the blends were fully miscible in the solid state. Blending chitosan with P3HPEI significantly affected the elasticity and strength of films (increased elongation at the break but reduced puncture strength). P3HPEI has a low glass transition temperature (−38.6 °C) and it is a water-soluble polymer, so may function as a plasticizer. Here, increasing the P3HPEI content in CHI/P3HPEI films probably decreases intermolecular hydrogen bonding between CHI chains, resulting in enhanced chain mobility and film flexibility. A 35:65 (%*w/w*) blend of chitosan/P3HPEI provided the optimum glass transition temperature for the delivery of haloperidol through mucosal membranes. Microscopic and XRD analyses were consistent and indicated that the solubility of the drug in the films was ~1.5%. The inclusion of the hydrophilic polymer P3HPEI allowed rapid drug

release followed by disintegration due to rapid water diffusion into the films, swelling, and erosion, supported by the relaxation of the polymer chains. The drug release profiles are consistent with the physicochemical properties of P3HPEI as a hydrophilic polymer with a low T_g. Hence, blending P3HPEI with chitosan allows the selection of desirable physicochemical and mechanical properties of the films for the loading and rapid delivery of haloperidol, a model poorly water-soluble drug for transmucosal drug delivery, such as buccal or ocular administration.

Supplementary Materials: The following supporting information can be downloaded at: www.mdpi.com/xxx/s1, Figure S1. Synthesis scheme of P3HPEI.; Figure S2. FTIR spectra of PEOZ, LPEI and P3HPEI.; Figure S3. X-ray diffractograms of PEOZ, LPEI and P3HPEI.; Figure S4.TGA thermograms of PEOZ, LPEI and P3HPEI.; Table S1. thickness of films.; Table S2. Water loss of CHI, P3HPEI and their blends detected by TGA analysis.; Figure S5. Correlation between residue and amount of P3HPEI in CHI/P3HPEI blends.; Figure S6. X-ray diffractograms of CHI (a), their blends (b–e) and P3HPEI (f). Content of P3HPEI in the blends: 20 (b), 40 (c), 60 (d) and 80% (e).; Figure S7. SEM images of film surfaces (A) and cross section (B) of CHI (a) and their blends (b–e). Content of P3HPEI in the blends: 20 (b), 40 (c), 60 (d) and 80% (e).; Figure S8. DSC and TGA thermogram of CHI/P3HPEI (35:65).; Figure S9. FTIR of haloperidol HCl (a), haloperidol HCl with different concentrations: 5% (b), 2.5% (c), 1.5% (d) and 1.25% (e) loaded in CHI/P3HPEI films and drug free CHI/P3HPEI film (f).; Table S3. Solubility of haloperidol in various medias; Figure S10. Standard curve of haloperidol.

Author Contributions: Conceptualization, A.C.W. and V.V.K.; methodology, S.S. and P.K.; software, S.S.; validation, S.S., A.C.W. and V.V.K.; formal analysis, S.S. and P.K.; investigation, S.S. and P.K.; resources, A.C.W. and V.V.K.; data curation, S.S., A.C.W. and V.V.K.; writing—original draft preparation, S.S.; writing—review and editing, A.C.W. and V.V.K.; visualization, S.S.; supervision, A.C.W. and V.V.K.; project administration, A.C.W. and V.V.K.; funding acquisition, S.S. All authors have read and agreed to the published version of the manuscript.

Funding: This research received funding from Thailand Institute of Scientific and Technological Research, Ministry of Higher Education, Science, Research and Innovation, Thailand.

Institutional Review Board Statement: Not applicable.

Informed Consent Statement: Not applicable.

Data Availability Statement: All raw data are included in Supporting Information or from the authors.

Acknowledgments: The authors are grateful to the Thailand Institute of Scientific and Technological Research, Ministry of Higher Education, Science, Research and Innovation for funding the PhD studentship of Sitthiphong Soradech. The assistance of staff at the Chemical Analysis Facility (CAF, University of Reading) with ^{1}H-NMR, FTIR, TGA, DSC, SEM, and XRD experiments is also acknowledged.

Conflicts of Interest: The authors declare that they have no known competing financial interests or personal relationships that could have appeared to influence the work reported in this paper.

References

1. Ferreira, P.G.; Ferreira, V.F.; da Silva, F.d.C.; Freitas, C.S.; Pereira, P.R.; Paschoalin, V.M.F. Chitosans and Nanochitosans: Recent Advances in Skin Protection, Regeneration, and Repair. *Pharmaceutics* **2022**, *14*, 1307. https://doi.org/10.3390/pharmaceutics14061307.
2. Li, B.; Wang, J.; Gui, Q.; Yang, H. Drug-Loaded Chitosan Film Prepared via Facile Solution Casting and Air-Drying of Plain Water-Based Chitosan Solution for Ocular Drug Delivery. *Bioact. Mater.* **2020**, *5*, 577–583. https://doi.org/10.1016/j.bioactmat.2020.04.013.
3. Xiao, C.; Zhang, J.; Zhang, Z.; Zhang, L. Study of Blend Films from Chitosan and Hydroxypropyl Guar Gum. *J. Appl. Polym. Sci.* **2003**, *90*, 1991–1995. https://doi.org/10.1002/app.12766.
4. Irikura, K.; Ekapakul, N.; Choochottiros, C.; Chanthaset, N.; Yoshida, H.; Ajiro, H. Fabrication of Flexible Blend Films Using a Chitosan Derivative and Poly(Trimethylene Carbonate). *Polym. J.* **2021**, *53*, 823–833. https://doi.org/10.1038/s41428-021-00470-6.
5. Hao, J.Y.; Mi, F.L.; Shyu, S.S.; Wu, Y.B.; Schoung, J.Y.; Tsai, Y.H.; Huang, Y. Bin Control of Wound Infections Using a Bilayer Chitosan Wound Dressing with Sustainable Antibiotic Delivery. *J. Biomed. Mater. Res.* **2002**, *59*, 438–449. https://doi.org/10.1002/jbm.1260.

6. Can, A.S.; Erdal, M.S.; Güngör, S.; Özsoy, Y. Optimization and Characterization of Chitosan Films for Transdermal Delivery of Ondansetron. *Molecules* **2013**, *18*, 5455–5471. https://doi.org/10.3390/molecules18055455.
7. Michailid, G.; OuBikiaris, D.N. Novel 3D-Printed Dressings of Chitosan–Vanillin-Modified Chitosan Blends Loaded with Fluticasone Propionate for Treatment of Atopic Dermatitis. *Pharmaceutics* **2022**, *14*, 1966. https://doi.org/10.3390/pharmaceutics14091966.
8. Sogias, I.A.; Williams, A.C.; Khutoryanskiy, V.V. Why Is Chitosan Mucoadhesive? *Biomacromolecules* **2008**, *9*, 1837–1842. https://doi.org/10.1021/bm800276d.
9. Abilova, G.K.; Kaldybekov, D.B.; Ozhmukhametova, E.K.; Saimova, A.Z.; Kazybayeva, D.S.; Irmukhametova, G.S.; Khutoryanskiy, V.V. Chitosan/Poly(2-Ethyl-2-Oxazoline) Films for Ocular Drug Delivery: Formulation, Miscibility, in Vitro and in Vivo Studies. *Eur. Polym. J.* **2019**, *116*, 311–320. https://doi.org/10.1016/j.eurpolymj.2019.04.016.
10. Lappe, S.; Mulac, D.; Langer, K. Polymeric Nanoparticles—Influence of the Glass Transition Temperature on Drug Release. *Int. J. Pharm.* **2017**, *517*, 338–347. https://doi.org/10.1016/j.ijpharm.2016.12.025.
11. Akash, S.Z.; Lucky, F.Y.; Hossain, M.; Bepari, A.K.; Sayedur Rahman, G.M.; Reza, H.M.; Sharker, S.M. Remote Temperature-Responsive Parafilm Dermal Patch for on-Demand Topical Drug Delivery. *Micromachines* **2021**, *12*, 975. https://doi.org/10.3390/mi12080975.
12. Luo, K.; Yin, J.; Khutoryanskaya, O.V.; Khutoryanskiy, V.V. Mucoadhesive and Elastic Films Based on Blends of Chitosan and Hydroxyethylcellulose. *Macromol. Biosci.* **2008**, *8*, 184–192. https://doi.org/10.1002/mabi.200700185.
13. Yin, J.; Luo, K.; Chen, X.; Khutoryanskiy, V.V. Miscibility Studies of the Blends of Chitosan with Some Cellulose Ethers. *Carbohydr. Polym.* **2006**, *63*, 238–244. https://doi.org/10.1016/j.carbpol.2005.08.041.
14. Marsano, E.; Vicini, S.; Skopińska, J.; Wisniewski, M.; Sionkowska, A. Chitosan and Poly(Vinyl Pyrrolidone): Compatibility and Miscibility of Blends. *Macromol. Symp.* **2004**, *218*, 251–260. https://doi.org/10.1002/masy.200451426.
15. Mohd Nasir, N.F.; Zain, N.M.; Raha, M.G.; Kadri, N.A. Characterization of Chitosan-Poly (Ethylene Oxide) Blends as Haemodialysis Membrane. *Am. J. Appl. Sci.* **2005**, *2*, 1578–1583. https://doi.org/10.3844/ajassp.2005.1578.1583.

16. Yeh, J.T.; Chen, C.L.; Huang, K.S.; Nien, Y.H.; Chen, J.L.; Huang, P.Z. Synthesis, Characterization, and Application of PVP/Chitosan Blended Polymers. *J. Appl. Polym. Sci.* **2006**, *101*, 885–891. https://doi.org/10.1002/app.23517.
17. Soradech, S.; Williams, A.C.; Khutoryanskiy, V.V. Physically Cross-Linked Cryogels of Linear Polyethyleneimine : Influence of Cooling Temperature and Solvent Composition. *Macromolecules* **2022**, *55*, 9537–9546. https://doi.org/10.1021/acs.macromol.2c01308.
18. Shan, X.; Williams, A.C.; Khutoryanskiy, V.V. Polymer Structure and Property Effects on Solid Dispersions with Haloperidol: Poly(N-Vinyl Pyrrolidone) and Poly(2-Oxazolines) Studies. *Int. J. Pharm.* **2020**, *590*, 119884. https://doi.org/10.1016/j.ijpharm.2020.119884.
19. Mees, M.A.; Hoogenboom, R. Full and Partial Hydrolysis of Poly(2-Oxazoline)s and the Subsequent Post-Polymerization Modification of the Resulting Polyethylenimine (Co)Polymers. *Polym. Chem.* **2018**, *9*, 4968–4978. https://doi.org/10.1039/c8py00978c.
20. Lungu, C.N.; Diudea, M.V.; Putz, M.V.; Grudziński, I.P. Linear and Branched PEIs (Polyethylenimines) and Their Property Space. *Int. J. Mol. Sci.* **2016**, *17*, 555. https://doi.org/10.3390/ijms17040555.
21. Chatani, Y.; Tadokoro, H.; Saegusa, T.; Ikeda, H. Structural Studies of Poly (Ethylenimine). 1. Structures of Two Hydrates of Poly (Ethylenimine): Sesquihydrate and Dihydrate. *Macromolecules* **1981**, *14*, 315–321. https://doi.org/10.1021/ma50003a017.
22. Van Kuringen, H.P.C.; Lenoir, J.; Adriaens, E.; Bender, J.; De Geest, B.G.; Hoogenboom, R. Partial Hydrolysis of Poly(2-Ethyl-2-Oxazoline) and Potential Implications for Biomedical Applications? *Macromol. Biosci.* **2012**, *12*, 1114–1123. https://doi.org/10.1002/mabi.201200080.
23. Yuan, J.J.; Jin, R.H. Fibrous Crystalline Hydrogels Formed from Polymers Possessing a Linear Poly(Ethyleneimine) Backbone. *Langmuir* **2005**, *21*, 3136–3145. https://doi.org/10.1021/la047182l.
24. Moghimi, S.M.; Symonds, P.; Murray, J.C.; Hunter, A.C.; Debska, G.; Szewczyk, A. A Two-Stage Poly(Ethylenimine)-Mediated Cytotoxicity: Implications for Gene Transfer/Therapy. *Mol. Ther.* **2005**, *11*, 990–995. https://doi.org/10.1016/j.ymthe.2005.02.010.
25. Taranejoo, S.; Liu, J.; Verma, P.; Hourigan, K. A Review of the Developments of Characteristics of PEI Derivatives for Gene Delivery Applications. *J. Appl. Polym. Sci.* **2015**, *132*, 1-8. https://doi.org/10.1002/app.42096.

26. Patil, S.; Lalani, R.; Bhatt, P.; Vhora, I.; Patel, V.; Patel, H.; Misra, A. Hydroxyethyl Substituted Linear Polyethylenimine for Safe and Efficient Delivery of SiRNA Therapeutics. *RSC Adv.* **2018**, *8*, 35461–35473. https://doi.org/10.1039/C8RA06298F.
27. Samanta, M.K.; Dube, R.; Suresh, B. Transdermal Drug Delivery System of Haloperidol to Overcome Self-Induced Extrapyramidal Syndrome. *Drug Dev. Ind. Pharm.* **2003**, *29*, 405–415. https://doi.org/10.1081/DDC-120018376.
28. Abruzzo, A.; Cerchiara, T.; Luppi, B.; Bigucci, F. Transdermal Delivery of Antipsychotics: Rationale and Current Status. *CNS Drugs* **2019**, *33*, 849–865. https://doi.org/10.1007/s40263-019-00659-7.
29. Sushmita, G.; Maha Lakshmi, J.; Prathyusha, K.S.S.; Srinivasa Rao, Y. Formulation and Evaluation of Haloperdiol-Carrier Loaded Buccal Film. *Int. J. Curr. Adv. Res.* **2018**, *7*, 5–10. http://dx.doi.org/10.24327/ijcar.2018.15700.2875
30. Sedlacek, O.; Janouskova, O.; Verbraeken, B.; Richard, H. Straightforward Route to Superhydrophilic Poly(2-Oxazoline)s via Acylation of Well-Defined Polyethylenimine. *Biomacromolecules* **2018**, *20*, 222–230. https://doi.org/10.1021/acs.biomac.8b01366.
31. Cook, M.T.; Tzortzis, G.; Charalampopoulos, D.; Khutoryanskiy, V.V. Production and Evaluation of Dry Alginate-Chitosan Microcapsules as an Enteric Delivery Vehicle for Probiotic Bacteria. *Biomacromolecules* **2011**, *12*, 2834–2840. https://doi.org/10.1021/bm200576h.
32. Soradech, S.; Limatvapirat, S.; Luangtana-anan, M. Stability Enhancement of Shellac by Formation of Composite Film: Effect of Gelatin and Plasticizers. *J. Food Eng.* **2013**, *116*, 572–580. https://doi.org/10.1016/j.jfoodeng.2012.12.035.
33. Soradech, S.; Nunthanid, J.; Limmatvapirat, S.; Luangtana-Anan, M. An Approach for the Enhancement of the Mechanical Properties and Film Coating Efficiency of Shellac by the Formation of Composite Films Based on Shellac and Gelatin. *J. Food Eng.* **2012**, *108*, 94–102. https://doi.org/10.1016/j.jfoodeng.2011.07.019.
34. Shan, X.; Aspinall, S.; Kaldybekov, D.B.; Buang, F.; Williams, A.C.; Khutoryanskiy, V.V. Synthesis and Evaluation of Methacrylated Poly(2-Ethyl-2-Oxazoline) as a Mucoadhesive Polymer for Nasal Drug Delivery. *ACS Appl. Polym. Mater.* **2021**, *3*, 5882–5892. https://doi.org/10.1021/acsapm.1c01097.
35. Saegusa, T.; Ikeda, H.; Fujii, H. Crystalline Polyethylenimine. *Macromolecules* **1972**, *5*, 108. https://doi.org/10.1021/ma60025a029.
36. Lorson, T.; Lübtow, M.M.; Wegener, E.; Haider, M.S.; Borova, S.; Nahm, D.; Jordan, R.; Sokolski-Papkov, M.; Kabanov, A.V.; Luxenhofer, R. Poly(2-Oxazoline)s Based

Biomaterials: A Comprehensive and Critical Update. *Biomaterials* **2018**, *178*, 204–280. https://doi.org/10.1016/j.biomaterials.2018.05.022.

37. Gholami, L.; Sadeghnia, H.R.; Darroudi, M.; Kazemi Oskuee, R. Evaluation of Genotoxicity and Cytotoxicity Induced by Different Molecular Weights of Polyethylenimine/DNA Nanoparticles. *Turkish J. Biol.* **2014**, *38*, 380–387. https://doi.org/10.3906/biy-1309-51.
38. Fischer, D.; Li, Y.; Ahlemeyer, B.; Krieglstein, J.; Kissel, T. In Vitro Cytotoxicity Testing of Polycations: Influence of Polymer Structure on Cell Viability and Hemolysis. *Biomaterials* **2003**, *24*, 1121–1131. https://doi.org/10.1016/S0142-9612(02)00445-3.
39. Leceta, I.; Guerrero, P.; Ibarburu, I.; Dueñas, M.T.; De La Caba, K. Characterization and Antimicrobial Analysis of Chitosan-Based Films. *J. Food Eng.* **2013**, *116*, 889–899. https://doi.org/10.1016/j.jfoodeng.2013.01.022.
40. Silva, C.L.; Pereira, J.C.; Ramalho, A.; Pais, A.A.C.C.; Sousa, J.J.S. Films Based on Chitosan Polyelectrolyte Complexes for Skin Drug Delivery: Development and Characterization. *J. Membr. Sci.* **2008**, *320*, 268–279. https://doi.org/10.1016/j.memsci.2008.04.011.
41. Matveev, Y.I.; Grinberg, V.Y.; Tolstoguzov, V.B. The Plasticizing Effect of Water on Proteins, Polysaccharides and Their Mixtures. Glassy State of Biopolymers, Food and Seeds. *Food Hydrocoll.* **2000**, *14*, 425–437. https://doi.org/10.1016/S0268-005X(00)00020-5.
42. Khutoryanskiy, V.V.; Cascone, M.G.; Lazzeri, L.; Barbani, N.; Nurkeeva, Z.S.; Mun, G.A.; Bitekenova, A.B.; Dzhusupbekova, A.B. Hydrophilic Films Based on Blends of Poly(Acrylic Acid) and Poly(2-Hydroxyethyl Vinyl Ether): Thermal, Mechanical, and Morphological Characterization. *Macromol. Biosci.* **2003**, *3*, 117–122. https://doi.org/10.1002/mabi.200390017.
43. Sakurai, K.; Maegawa, T.; Takahashi, T. Glass Transition Temperature of Chitosan and Miscibility of Chitosan/Poly(N-Vinyl Pyrrolidone) Blends. *Polymer* **2000**, *41*, 7051–7056. https://doi.org/10.1016/S0032-3861(00)00067-7.
44. Brostow, W.; Chiu, R.; Kalogeras, I.M.; Vassilikou-Dova, A. Prediction of Glass Transition Temperatures: Binary Blends and Copolymers. *Mater. Lett.* **2008**, *62*, 3152–3155. https://doi.org/10.1016/j.matlet.2008.02.008.
45. Seong, D.W.; Yeo, J.S.; Hwang, S.H. Fabrication of Polycarbonate Blends with Poly(Methyl Methacrylate-Co-Phenyl Methacrylate) Copolymer: Miscibility and Scratch

Resistance Properties. *J. Ind. Eng. Chem.* **2016**, *36*, 251–254. https://doi.org/10.1016/j.jiec.2016.02.005.

46. Rao, V.; Ashokan, P.V.; Shridhar, M.H. Studies on the Compatibility and Specific Interaction in Cellulose Acetate Hydrogen Phthalate (CAP) and Poly Methyl Methacrylate (PMMA) Blend. *Polymer* **1999**, *40*, 7167–7171. https://doi.org/10.1016/S0032-3861(99)00311-0.
47. Rao, V.; Ashokan, P.V.; Shridhar, M.H. Miscible Blends of Cellulose Acetate Hydrogen Phthalate and Poly(Vinyl Pyrollidone) Characterization by Viscometry, Ultrasound, and DSC. *J. Appl. Polym. Sci.* **2000**, *76*, 859–867. https://doi.org/10.1002/(SICI)1097-4628(20000509)76:6<859::AID-APP12>3.0.CO;2-2.
48. Mujaheddin; Jagadish, R.; Sheshappa, R.; Guru, G. Miscibility Studies of Agar-Agar/Starch Blends Using Various Techniques. *Int. J. Res. Pharm. Chem.* **2012**, *2*, 1049–1056.
49. Shubha, A.; Manohara, S.R.; Gerward, L. Influence of Polyvinylpyrrolidone on Optical, Electrical, and Dielectric Properties of Poly(2-Ethyl-2-Oxazoline)-Polyvinylpyrrolidone Blends. *J. Mol. Liq.* **2017**, *247*, 328–336. https://doi.org/10.1016/j.molliq.2017.09.086.
50. Rodríguez-Núñez, J.R.; Madera-Santana, T.J.; Sánchez-Machado, D.I.; López-Cervantes, J.; Soto Valdez, H. Chitosan/Hydrophilic Plasticizer-Based Films: Preparation, Physicochemical and Antimicrobial Properties. *J. Polym. Environ.* **2014**, *22*, 41–51. https://doi.org/10.1007/s10924-013-0621-z.
51. Vieira, M.G.A.; Da Silva, M.A.; Dos Santos, L.O.; Beppu, M.M. Natural-Based Plasticizers and Biopolymer Films: A Review. *Eur. Polym. J.* **2011**, *47*, 254–263. https://doi.org/10.1016/j.eurpolymj.2010.12.011.
52. Jumelle, C.; Gholizadeh, S.; Annabi, N.; Dana, R. Advances and Limitations of Drug Delivery Systems Formulated as Eye Drops. *J. Control. Release* **2020**, *321*, 1–22. https://doi.org/10.1016/j.jconrel.2020.01.057.
53. Jeong, W.Y.; Kwon, M.; Choi, H.E.; Kim, K.S. Recent Advances in Transdermal Drug Delivery Systems: A Review. *Biomater. Res.* **2021**, *25*, 1–15. https://doi.org/10.1186/s40824-021-00226-6.
54. Latif, M.S.; Al-Harbi, F.F.; Nawaz, A.; Rashid, S.A.; Farid, A.; Al Mohaini, M.; Alsalman, A.J.; Al Hawaj, M.; Alhashem, Y.N. Formulation and Evaluation of Hydrophilic Polymer Based Methotrexate Patches: In Vitro and In Vivo Characterization. *Polymers* **2022**, *14*, 1310. https://doi.org/10.3390/polym14071310.

55. Brown, M.; Williams, A. *The Art and Science of Dermal Formulation Development*; CRC Press: Boca Raton, FL, USA, 2019; ISBN 9780429059872.
56. Berillo, D.; Zharkinbekov, Z.; Kim, Y.; Raziyeva, K.; Temirkhanova, K.; Saparov, A. Stimuli-Responsive Polymers for Transdermal, Transmucosal and Ocular Drug Delivery. *Pharmaceutics* **2021**, *13*, 1–30. https://doi.org/10.3390/pharmaceutics13122050.
57. Williams, A. Controlled Drug Delivery into and Through Skin. In: *Fundamentals of Drug Delivery*, Benson H.A.E,, Roberts, M.S., Williams, A.C. and Liang, X, Eds, Wiley, NJ, USA. **2021**, Chapter 20, 507–534. ISBN 9781119769675
58. Trastullo, R.; Abruzzo, A.; Saladini, B.; Gallucci, M.C.; Cerchiara, T.; Luppi, B.; Bigucci, F. Design and Evaluation of Buccal Films as Paediatric Dosage Form for Transmucosal Delivery of Ondansetron. *Eur. J. Pharm. Biopharm.* **2016**, *105*, 115–121. https://doi.org/10.1016/j.ejpb.2016.05.026.
59. Ahsan, A.; Tian, W.X.; Farooq, M.A.; Khan, D.H. An Overview of Hydrogels and Their Role in Transdermal Drug Delivery. *Int. J. Polym. Mater. Polym. Biomater.* **2021**, *70*, 574–584. https://doi.org/10.1080/00914037.2020.1740989.
60. Al Omari, M.M.; Zughul, M.B.; Davies, J.E.D.; Badwan, A.A. A Study of Haloperidol Inclusion Complexes with β-Cyclodextrin Using Phase Solubility, NMR Spectroscopy and Molecular Modeling Techniques. *J. Solution Chem.* **2009**, *38*, 669–683. https://doi.org/10.1007/s10953-009-9404-5.
61. Kraisit, P.; Limmatvapirat, S.; Luangtana-Anan, M.; Sriamornsak, P. Buccal Administration of Mucoadhesive Blend Films Saturated with Propranolol Loaded Nanoparticles. *Asian J. Pharm. Sci.* **2018**, *13*, 34–43. https://doi.org/10.1016/j.ajps.2017.07.006.
62. Giovino, C.; Ayensu, I.; Tetteh, J.; Boateng, J.S. An Integrated Buccal Delivery System Combining Chitosan Films Impregnated with Peptide Loaded PEG-b-PLA Nanoparticles. *Colloids Surfaces B Biointerfaces* **2013**, *112*, 9–15. https://doi.org/10.1016/j.colsurfb.2013.07.019.
63. Budhian, A.; Siegel, S.J.; Winey, K.I. Controlling the in Vitro Release Profiles for a System of Haloperidol-Loaded PLGA Nanoparticles. *Int. J. Pharm.* **2008**, *346*, 151–159. https://doi.org/10.1016/j.ijpharm.2007.06.011.

Supplementary information to

Synthesis and Evaluation of Poly(3-hydroxypropyl Ethyleneimine) and Its Blends with Chitosan Forming Novel Elastic Films for Delivery of Haloperidol

Sitthiphong Soradech [1, 2], Pattarawadee Kengkwasingh[2], Adrian C. Williams [1], and Vitaliy V. Khutoryanskiy [1*]

[1] Reading School of Pharmacy, University of Reading, Whiteknights, Reading RG6 6DX, UK

[2] Expert Centre of Innovative Herbal Products, Thailand Institute of Scientific and Technological Research, Pathum Thani, 12120, Thailand

*v.khutoryanskiy@reading.ac.uk; Tel.: +44-(0)118-378-6119

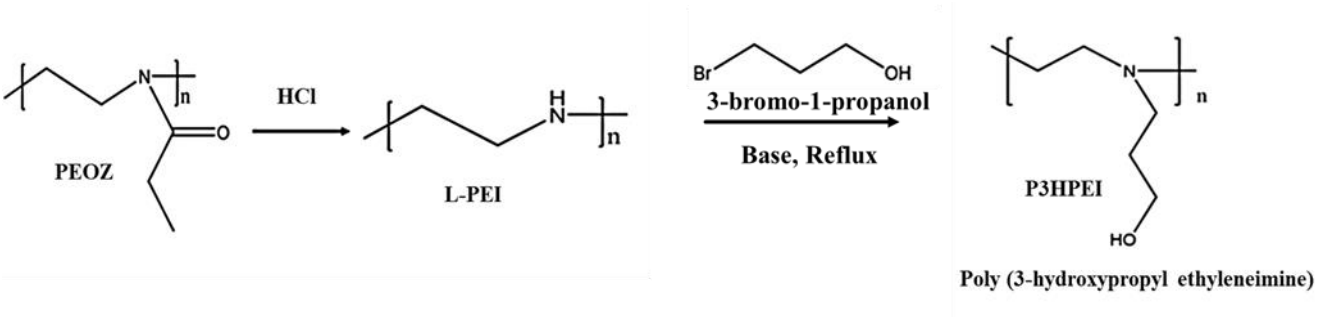

Figure S1. Synthesis scheme of P3HPEI.

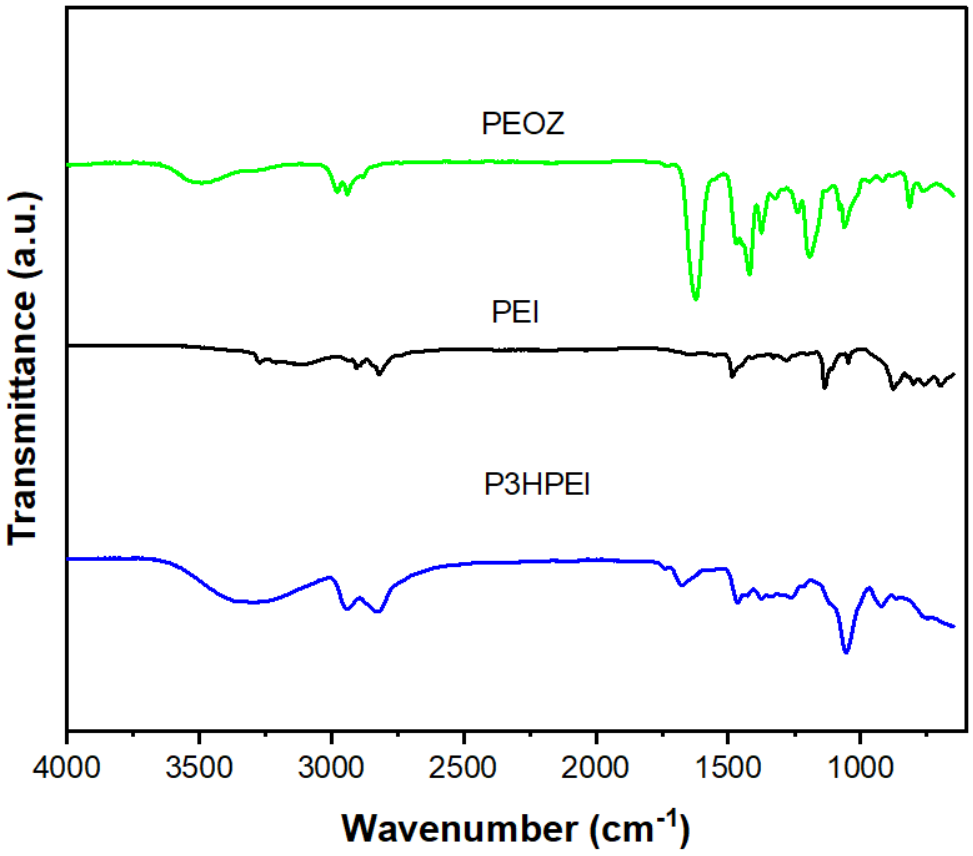

Figure S2. FTIR spectra of PEOZ, LPEI and P3HPEI.

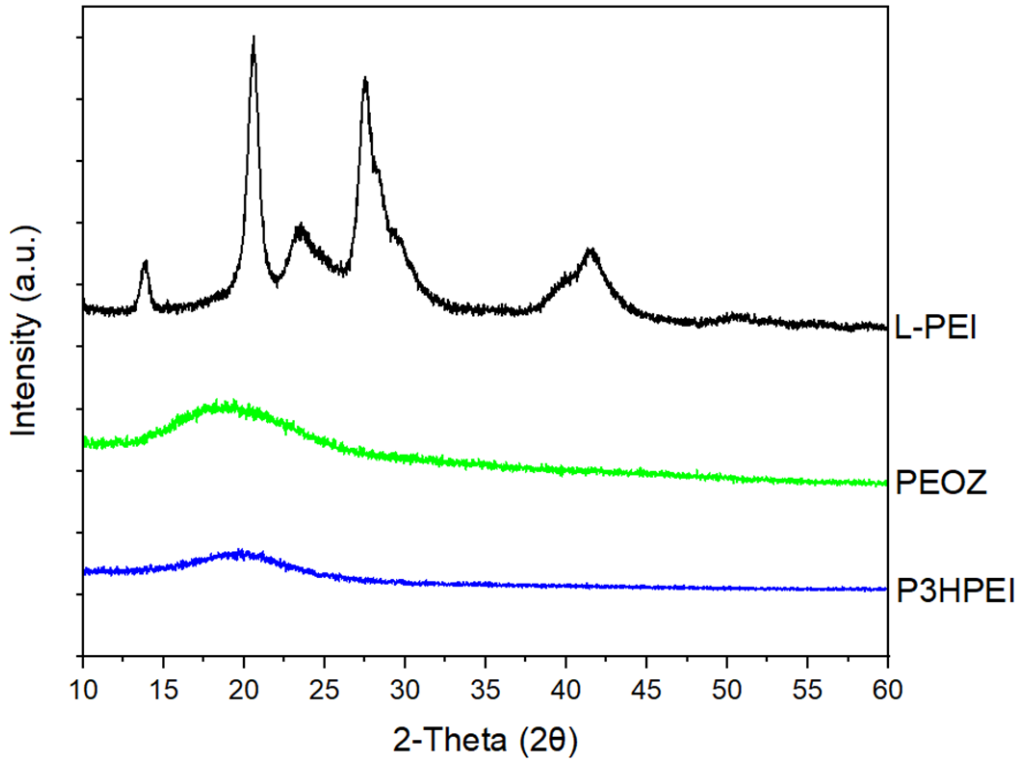

Figure S3. X-ray diffractograms of PEOZ, LPEI and P3HPEI.

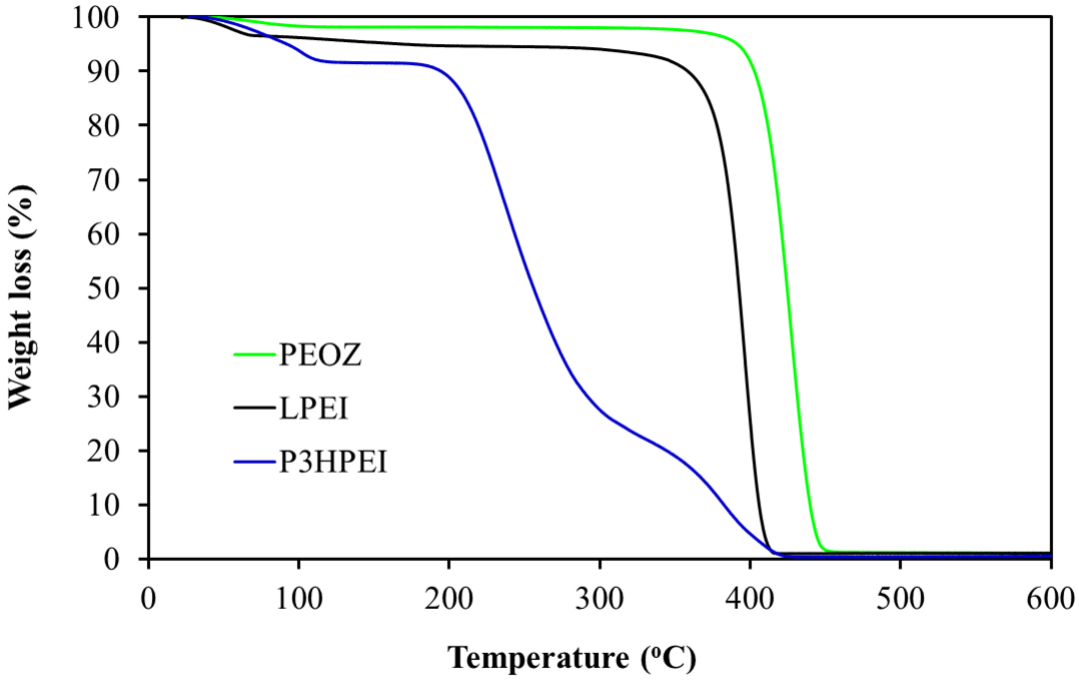

Figure S4. TGA thermograms of PEOZ, LPEI and P3HPEI.

Table S1. Thickness of CHI and CHI/P3HPEI films.

Films	Thickness (mm)
CHI (100)	0.06 ± 0.01
CHI/P3HPEI (80:20)	0.06 ± 0.02
CHI/P3HPEI (60:40)	0.07± 0.02
CHI/P3HPEI (40:60)	0.06 ± 0.01
CHI/P3HPEI (20:80)	0.06 ± 0.01

Table S2. Water loss of CHI, P3HPEI and their blends detected by TGA analysis

CHI/P3HPEI	Water loss (%)
CHI (100)	6.0
CHI/P3HPEI (80:20)	2.5
CHI/P3HPEI (60:40)	4.9
CHI/P3HPEI (40:60)	4.6
CHI/P3HPEI (20:80)	2.4
P3HPEI	8.0

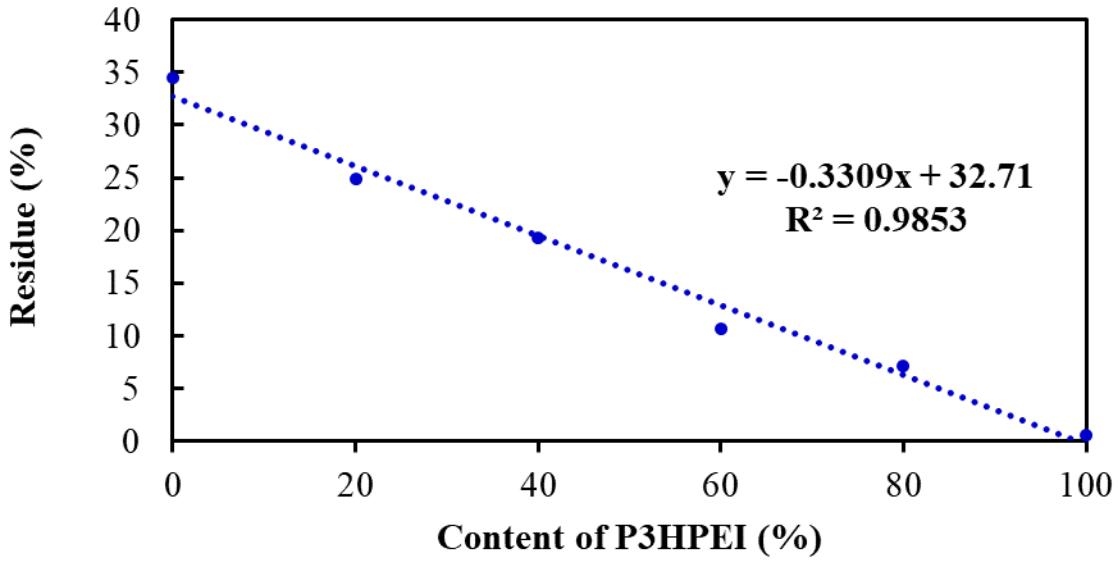

Figure S5. Correlation between residue and amount of P3HPEI in CHI/P3HPEI blends.

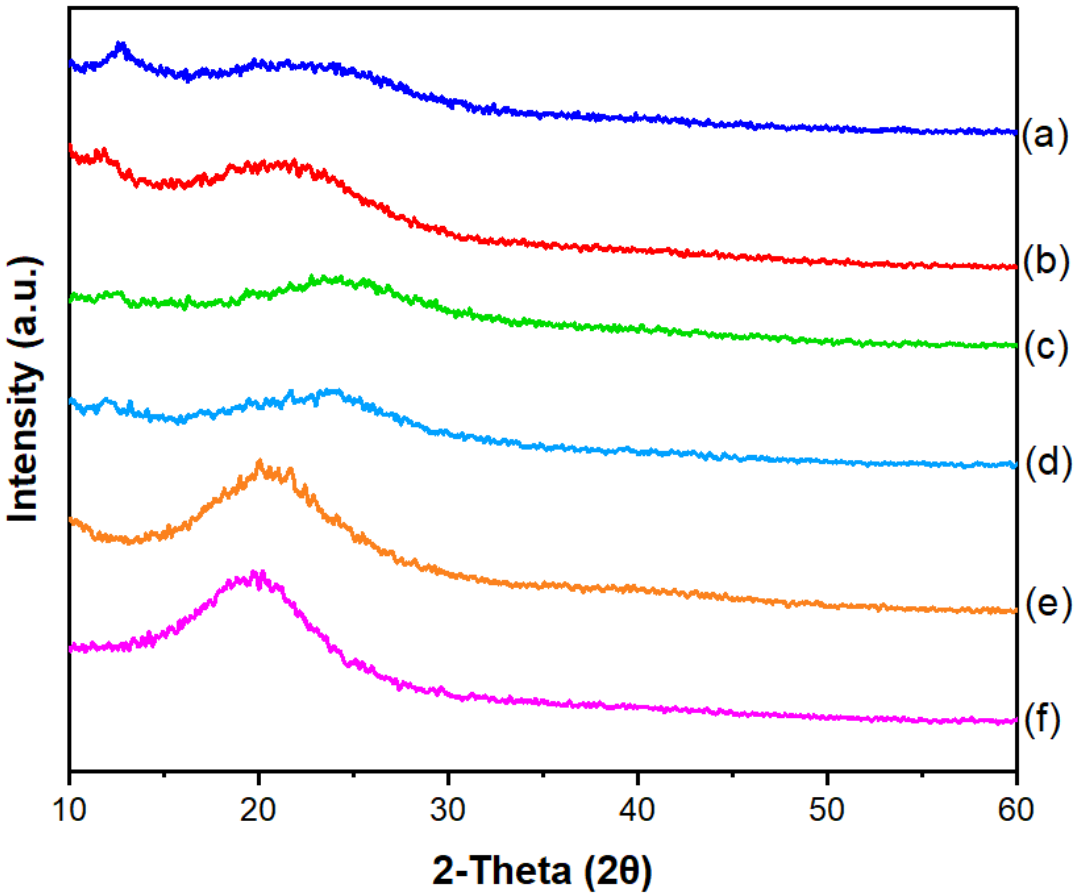

Figure S6. X-ray diffractograms of CHI (a), their blends (b, c, d and e) and P3HPEI (f). Content of P3HPEI in the blends: 20 (b), 40 (c), 60 (d) and 80 % (e).

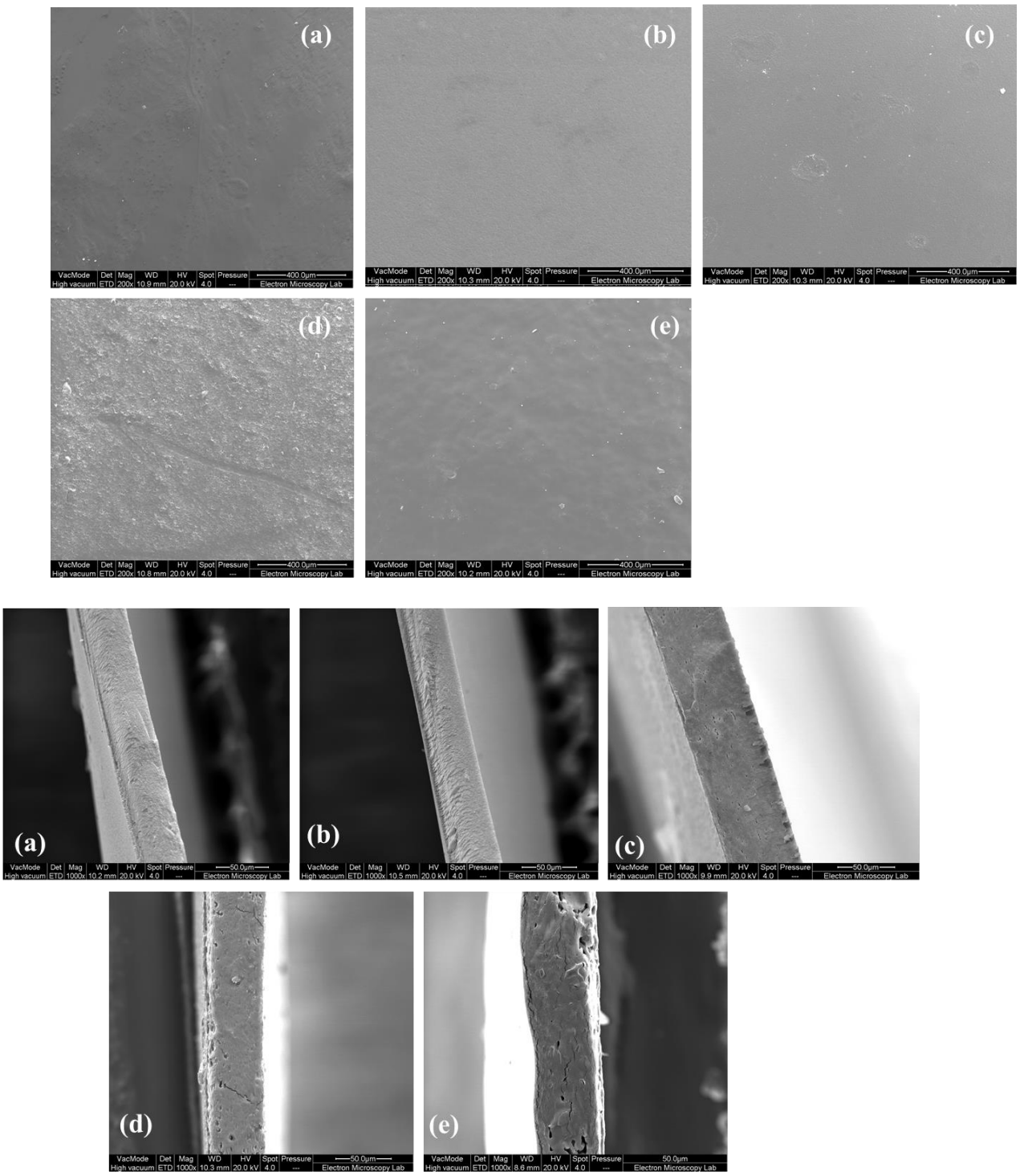

Figure S7. SEM images of film surfaces (A) and cross section (B) of CHI (a) and their blends (b, c, d, and e). Content of P3HPEI in the blends: 20 (b), 40 (c), 60 (d) and 80 % (e).

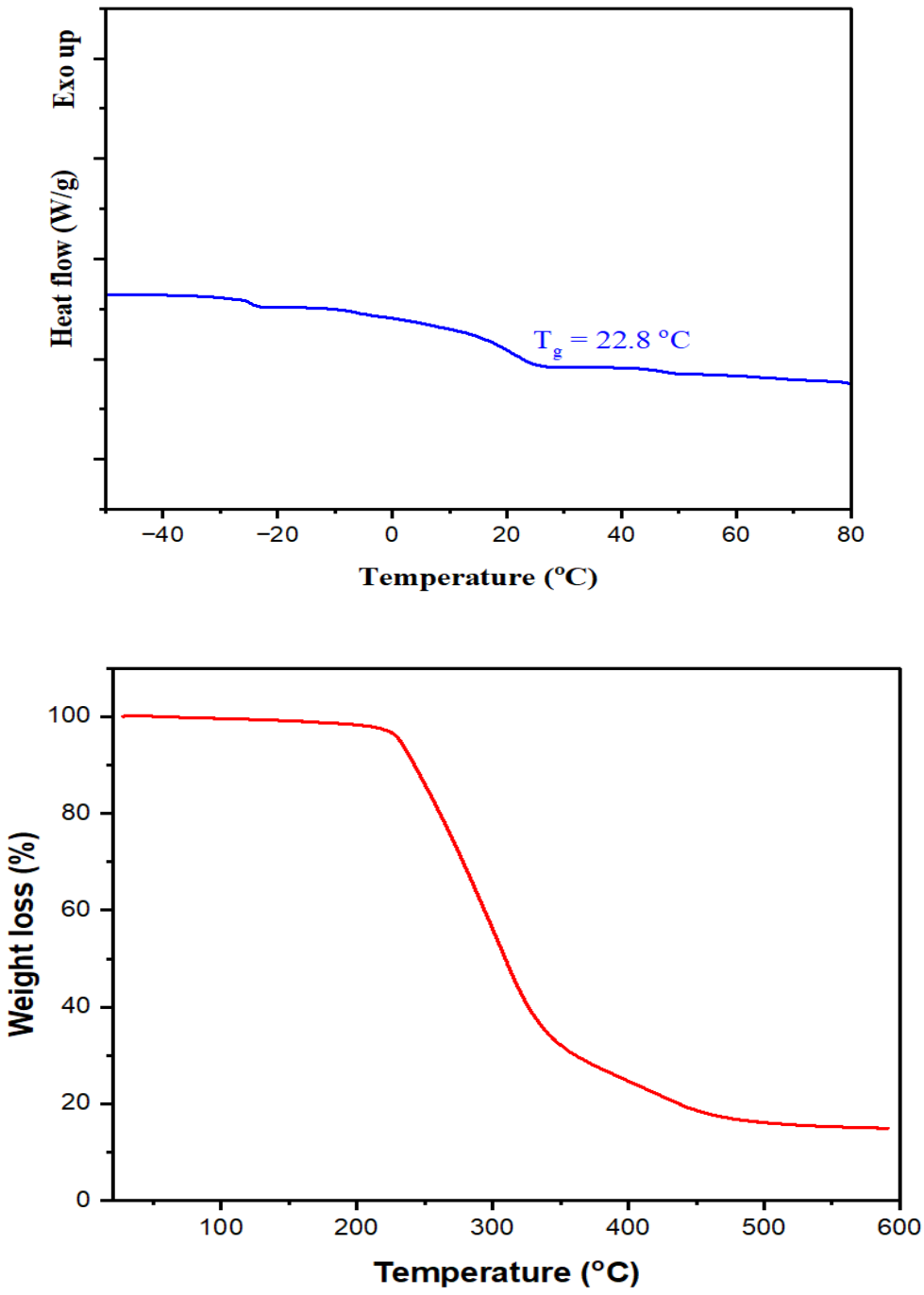

Figure S8. DSC and TGA thermogram of CHI/P3HPEI (35:65).

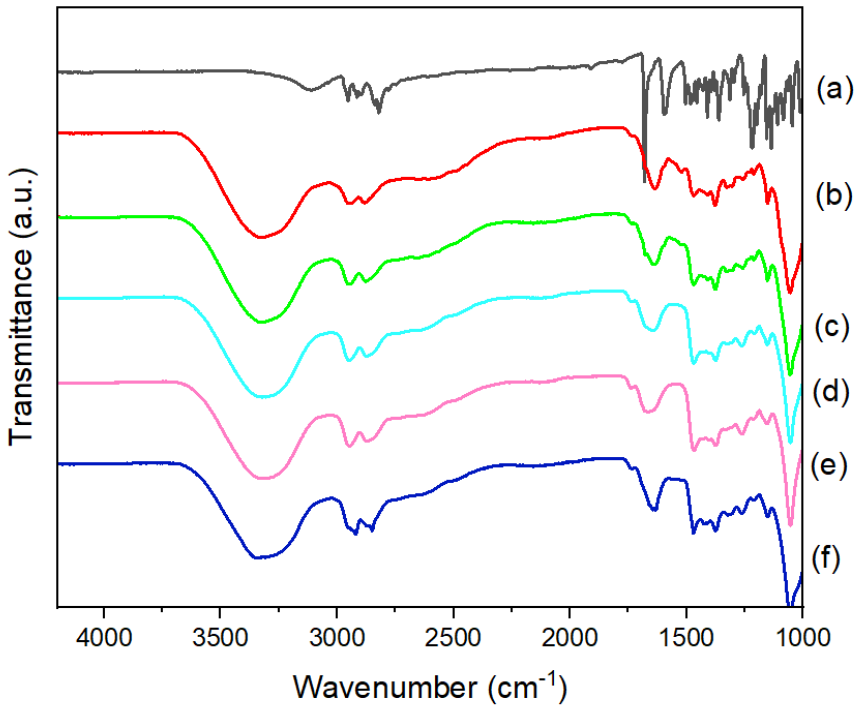

Figure S9. FTIR of haloperidol HCl (a), haloperidol HCl with different concentrations : 5% (b), 2.5% (c), 1.5% (d) and 1.25% (e) loaded in CHI/P3HPEI films and drug free CHI/P3HPEI film (f).

Table S3. Solubility of haloperidol in various media.

Medium	Solubility (mg/mL)
Distilled water	0.01
20% PEG 400-PBS pH 7.4	0.22
50% EtOH-PBS pH 7.4	0.03
95% EtOH	5.00
0.1 M HCl	3.00

Preparation of stock solution

Haloperidol (100 mg) was weighed accurately and dissolved in methanol and the volume was made up to 100 mL with the same solvent in a volumetric flask.

Preparation of phosphate buffer solution (pH 7.4)

Phosphate buffer solution pH 7.4 was prepared by dissolving 10 tablets of phosphate buffered saline in 500 mL of deionized water and then added solution into 1000 mL of

volumetric flask. Subsequently, the total volume of PBS solution was adjusted to 1000 mL. The pH 7.4 of PBS was adjusted by adding 0.1 M HCl.

Preparation of working standard solutions

From the stock solution, 0.5, 1, 1.5, 2, 3, 3.5, 4.0, 4.5 and 5.0 mL were pipette out and the volume was made up to 100 mL with 20% PEG 400 in phosphate-buffered saline (pH = 7.4) to produce concentrations of 5, 10, 15, 20, 25, 30, 35, 40, 45 and 50 µg/mL respectively. A scan was performed in order to determine the λ_{max} and the absorbance of diluted solution was measured at the λ_{max} obtained using spectrophotometer against blank buffer solution of pH 7.4 as the blank. A calibration curve **(Figure S10)** was constructed by plotting the absorbance against the concentration of haloperidol. A regression equation was derived from the plot, which was used for the estimation of haloperidol in 20% PEG 400 in phosphate buffer solution (pH = 7.4).

The method obeyed Beer's law in concentration range of 5 - 50 µg/mL and is suitable for the estimation of haloperidol from different sample solutions. The correlation coefficient value (r) was found to be 0.9991 indicating a positive correlation between the concentration of haloperidol and the corresponding absorbance values. The regression line describes the relation between the concentration and absorbance was as follows.

$$Y = 0.0153\ X + 0.0131$$

Where, Y is the absorbance and X is the concentration of haloperidol in µg/mL.

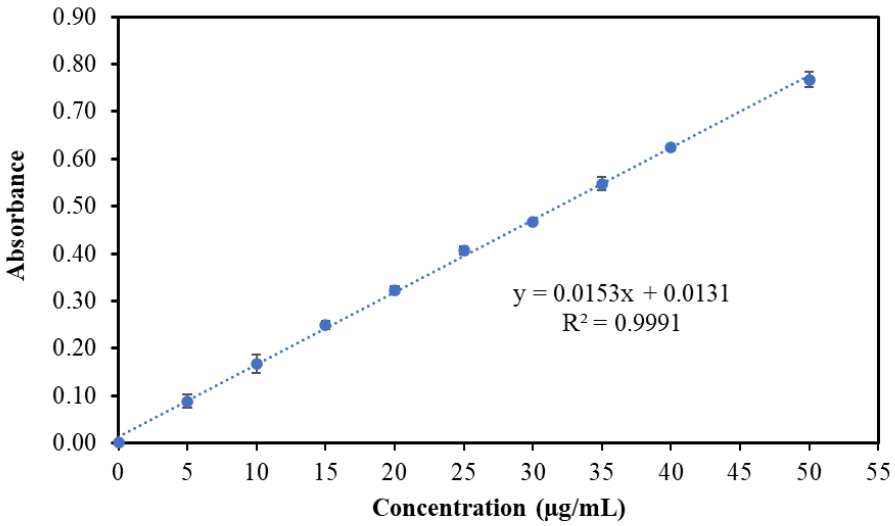

Figure S10. Standard curve of haloperidol.

Chapter 4

Synthesis of poly(2-hydroxyethyl ethyleneimine) and its mucoadhesive film formulations based on blends with chitosan for buccal delivery of haloperidol

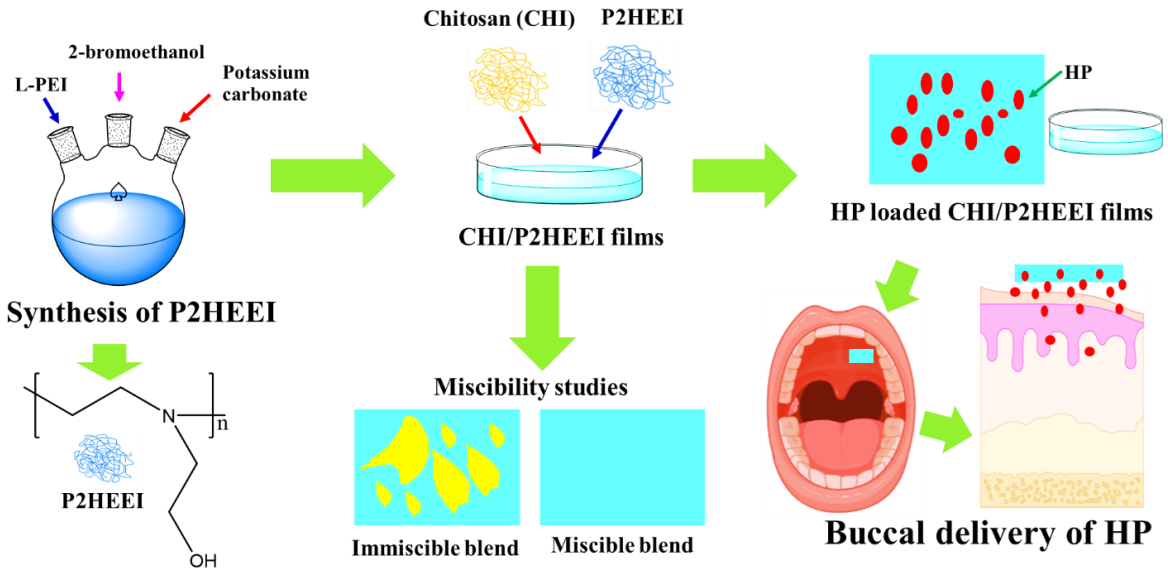

This chapter was prepared for submission as: Sitthiphong Soradech, Pattarawadee Kengkwasingh, Adrian C. Williams, and Vitaliy V. Khutoryanskiy, Synthesis of Poly(2-hydroxyethyl ethyleneimine) and Its Mucoadhesive Film Formulations Based on Blends with Chitosan for Buccal Delivery of Haloperidol.

Chapter 4

Synthesis of poly(2-hydroxyethyl ethyleneimine) and its mucoadhesive film formulations based on blends with chitosan for buccal delivery of haloperidol

Sitthiphong Soradech [1, 2], Pattarawadee Kengkwasingh [2], Adrian C. Williams [1], and Vitaliy V. Khutoryanskiy [1*]

[1]Reading School of Pharmacy, University of Reading, Whiteknights, Reading, RG6 6AD, UK.

[2]Expert Centre of Innovative Herbal Products, Thailand Institute of Scientific and Technological Research, Pathum Thani, 12120, Thailand.

*__Corresponding author:__
Postal address: Reading School of Pharmacy, University of Reading, Whiteknights, PO Box 224, RG6 6AD, Reading, United Kingdom
E-mail address: v.khutoryanskiy@reading.ac.uk
Telephone: +44(0) 118 378 6119
Fax: +44(0) 118 378 4703

Abstract

Mucoadhesive films are one of commercially relevant formulations for buccal drug delivery due to their adaptability and ease of use. Additionally, the use of these films can prolong the time spent on the mucosa, directly delivering a precise dose of the drug to the tissue. Hence, this study aimed to synthesize poly(2-hydroxyethyl ethyleneimine) or P2HEEI and its mucoadhesive film formulations based on blends with chitosan for buccal delivery of haloperidol. Initially, P2HEEI was synthesized via nucleophilic substitution of linear polyethyleneimine (L-PEI) with 2-bromoethanol. P2HEEI exhibited good solubility in water, low toxicity in human dermal skin fibroblast cells, and low glass transition temperature (-31.6 °C). This polymer was then blended with chitosan to improve mechanical properties and these materials were used for the buccal delivery of haloperidol. Polymeric films based on chitosan and its blends with P2HEEI were prepared by casting from aqueous solutions. The investigation of these films using differential scanning calorimetry and scanning electron microscopy confirmed that chitosan and P2HEEI form completely miscible blends. Blending chitosan with P2HEEI improved the mechanical properties of the films, resulting in more elastic materials. Blend films were also prepared loaded with haloperidol as a model poorly water-soluble drug. The cumulative release of haloperidol from the films increased when the blends were prepared with greater P2HEEI content. Mucoadhesive properties of these films with respect to freshly excised sheep buccal mucosa were evaluated using a tensile method. It was found that all films are mucoadhesive; however, an increase in P2HEEI content in the blend resulted in a gradual reduction of their ability to adhere to the buccal mucosa. These films could potentially find applications in buccal drug delivery.

Keywords: Chitosan, poly(2-hydroxyethyl ethyleneimine), mucoadhesive films, miscibility, buccal drug delivery.

1. Introduction

Buccal drug delivery is commonly used to administer drugs through the buccal mucosa to provide local or systemic pharmacological effects [1]. It has generated interest as a potential alternative to gastrointestinal drug delivery. The market for buccal drug delivery is anticipated to grow at a CAGR of 9.8%. In 2022, the market's worth is estimated to be $3.38 billion, and by 2030, it will have increased to $7.13 billion. Numerous dosage forms such as buccal tablets, wafers, lozenges, liquids, patches, and films are available on the market [2]. The advantages of the buccal route include direct access to the systemic circulation via the internal jugular vein, rapid onset of action, possibility to by-pass hepatic first-pass metabolism, avoidance of gastrointestinal acid-related hydrolysis, increased patient compliance, and suitability for drugs or excipients that cause mild and reversible mucosal damage or irritation [3]. Mucoadhesive films are one of commercially relevant formulations for buccal drug delivery due to their adaptability and ease of use. Additionally, the use of these films can prolong the time spent on the mucosa, directly delivering a precise dose of the drug to the tissue [3].

Chitosan is a natural cationic polysaccharide that has been widely used in a variety of applications, including drug delivery systems, artificial skin, cosmetics, nutrition, and food additives, due to its nontoxicity, biocompatibility, biodegradability, mucoadhesive and antimicrobial properties, and film forming ability [4, 5]. Furthermore, chitosan could improve skin penetration and wound healing by increasing the function of inflammatory and repair cells [6,7]. Chitosan can be chosen for buccal drug delivery due to its ability to enhance drug penetration by opening tight junctions and increasing the paracellular permeability of mucosal membranes. This polymer can also control drug release in buccal drug delivery systems and has excellent mucoadhesive properties [8]. The mucoadhesive properties and percutaneous penetration of chitosan are due to the interaction between positive charges of this polymer and negative charges of the mucosal membrane [7, 8]. However, the use of pure chitosan mucoadhesive films has limitations due to their brittleness, resulting from its relatively high glass transition temperature (~131 ^{o}C) [9, 10].

The characteristics of chitosan could be further enhanced by blending it with other water-soluble polymers [8]. Polymer blending may provide a simple and low-cost technique for the development of novel materials with a variety of valuable properties. For instance, good mechanical and mucoadhesive properties of chitosan were achieved through combination with cellulose ethers [11]. Chitosan was also blended with poly(N-vinyl pyrrolidone) [12],

poly(ethylene oxide)[13, 14] and poly(vinyl alcohol) [15] to improve physicochemical properties. Luo et al. [8] developed mucoadhesive polymeric films using chitosan-hydroxyethylcellulose blends (HEC). While blending chitosan with HEC improves the mechanical properties of materials, the mucoadhesion of films to the buccal mucosa decreased as the HEC content in the blends increased. Abilova et al.[9] developed films using chitosan and poly(2-ethyl-2-oxazoline) blends. The T_g of the blends based on chitosan and PEOZ decreased from 131 to 63 ^oC, but the mechanical properties declined with the increase in PEOZ content in the samples.

Linear polyethyleneimine (L-PEI) is a cationic polymer comprised of two methylene (-CH_2CH_2-) groups and secondary amino group in each repeating unit. It was synthesized by hydrolysis of poly(2-ethyl-oxazolines) to remove all amide side chains[16, 17]. Generally, L-PEI has a semi-crystalline structure[18, 19] and a glass transition temperature (T_g) around -29.5 ^{o} [20]; hence, it can be blended with chitosan to improve mechanical properties. However, L-PEI can dissolve in water only at high temperatures [18] and forms a gel at room temperature [21]. Additionally it is known to be cytotoxic [20, 22]. The solubility and toxicity of L-PEI is a significant concern when considering its pharmaceutical and biomedical applications [23]. Thus, modification of L-PEI is one of the methods for increasing its water solubility and decreasing toxicity. Patil et al. [24] used nucleophilic substitution to synthesize hydroxyethyl substituted linear polyethyleneimine (HELPEI) for the safe and efficient delivery of siRNA therapeutics. The percentage of linear polyethyleneimine substitution with hydroxyethyl groups was between 11.8 and 43.3 %. Additionally, the cytotoxicity of HELPEI on human bronchial epithelial cells decreased as the degree of substitution increased. However, the degree of hydroxyethyl substitution in linear polyethyleneimine was less than 50%, and there was no information available about the physicochemical properties of this polymer. Previously, we modified L-PEI using nucleophilic substitution reaction with 3-bromo-1-propanol to form poly(3-hydroxypropyl ethyleneimine) or P3HPEI. It exhibited a good water solubility and was significantly less toxic in human dermal skin fibroblast cells than L-PEI. This polymer also had a low glass transition temperature (T_g = -38.6 ^oC). P3HPEI was then blended with chitosan to enhance its mechanical properties, and these materials were also used for rapid delivery of haloperidol. According to microscopic and X-ray diffraction (XRD) measurements, the solubility of haloperidol in CHI/P3HPEI films was ~1.5%. The incorporation of the hydrophilic polymer P3HPEI also facilitated rapid drug release within 30 minutes, after which the films

disintegrated, indicating that the formulations are acceptable for application to mucosal surfaces, such as buccal or ocular drug administration[10].

The present work aimed to synthesize poly(2-hydroxyethyl ethyleneimine) or P2HEEI and to prepare mucoadhesive blends with chitosan as a potential platform for buccal delivery of haloperidol. Firstly, a P2HEEI derivative with high degree of hydroxyethyl substitution was synthesized by reaction of linear polyethyleneimine with 2-bromoethanol. The physicochemical and toxicological properties of this polymer were then assessed. This polymer was blended subsequently with chitosan to fabricate novel elastic and mucoadhesive films for buccal delivery of haloperidol. Miscibility between polymers, mucoadhesive properties of the blend films, and drug release from these formulations were investigated.

2. Materials and Methods

2.2. Materials

A high molecular weight of chitosan (CHI, MW∼310–375 kDa, degree of deacetylation: 75–85%), poly(2-ethyl-2-oxazoline) (PEOZ, MW∼50 kDa and PDI 3–4), 2-bromoethanol, 37% hydrochloric acid solution, fluorescein isothiocyanate (FITC) and haloperidol were purchased from Merck (Gillingham, UK), while phosphate-buffered saline (PBS) tablets and sodium hydroxide were ordered from Fisher Chemical (Fisher Scientific, UK). All other chemicals were of analytical grade and used without further purification.

2.2. Synthesis of linear polyethyleneimine

L-PEI was synthesized by hydrolysis of poly(2-ethyl-2-oxazoline) as described by our previous studies [25, 26]. Briefly, 10 g of poly(2-ethyl-2-oxazolines) (PEOZ) was dissolved in 100 mL of 18.0 % (w/w) hydrochloric acid and then refluxed at 100 ^{o}C, 14 h to remove all amide groups in the side chains**.** The L-PEI solution obtained in hydrochloric acid was then diluted with cold deionized water (500 mL). Cold aqueous sodium hydroxide (4M) was added dropwise to the suspension until the base form of L-PEI precipitated at pH 10 - 11 [27]. The precipitate was recovered by filtration, washed with deionized water, and re-precipitated twice before drying under vacuum to obtain L-PEI as a white power (yielding 3.8 g (89 %)).

2.3. Synthesis of poly(2-hydroxyethyl ethyleneimine)

P2HEEI was synthesized by nucleophilic substitution reaction, using the protocol adapted from our previous study [25]. Briefly, L-PEI (0.02 moles, 1.0 g) was dissolved in absolute ethanol (60 mL) in a three-necked round bottom flask and different quantities of 2-bromoethanol (0.02, 0.03, 0.05 and 0.06 moles) were added. Then different quantities of potassium carbonate (0.02, 0.03, 0.05 and 0.06 moles) were added to this solution. The amounts of 2-bromoethanol and potassium carbonate used are shown in **Table 1**. The reaction mixture was refluxed at 78 ^{o}C with varied time between 24 and 48 h. After completion, the reaction mixture was centrifuged, subsequently, supernatant was collected and evaporated using rotary evaporator at 40 ^{o}C (280 rpm). The obtained mixture was then diluted with deionized water and purified by dialysis using cellulose membrane with MWCO 3.5 kDa at room temperature. P2HEEI was recovered by freeze-drying as a dry residue for several days. The ^{1}H-NMR and FTIR spectroscopies were used to confirm the successful conversion of L-PEI to P2HEEI.

Table 1. Different amount of L-PEI, 2-bromoethanol and potassium carbonate (base) to synthesize poly(2-hydroxyethyl ethyleneimine).

L-PEI: 2-bromoethanol: base (moles)	L-PEI (g)	2-bromoethanol (mL)	Potassium carbonate (g)
0.02: 0.02: 0.02	1.0	1.7	3.2
0.02: 0.03: 0.03	1.0	2.5	4.8
0.02: 0.05: 0.05	1.0	3.3	6.4
0.02: 0.06: 0.06	1.0	4.1	8.1

2.4. Preparation of films

Films were prepared based on chitosan (CHI) and its blends with P2HEEI by casting polymer solutions with subsequent evaporation of solvent. Initially, 1% w/v aqueous solutions of CHI and P2HEEI were prepared by dissolving pre-weighed amount of dry polymers at room temperature. CHI solution (pH~2.0) was prepared in 0.1 M hydrochloric acid by stirring magnetically for 24 h prior to casting, while P2HEEI solutions (pH~6.8) were prepared in deionised water and allowed to stir continuously for 1 h. The prepared polymer solutions were mixed at different volume ratios and named as CHI (100: 0), CHI/P2HEEI: (80:20), (60:40), (40:60) and (20:80). Subsequently, all CHI/P2HEEI solutions were magnetically agitated for 3 h until homogeneous mixture was formed. The pH of the combined solutions was in the range

of 3.0 – 4.0. Then 45 mL of each mixture was poured into Petri dishes with 90 mm diameter and dried at 30 ± 2 ^{o}C in an oven for several days.

2.5. Preparation of haloperidol loaded films

A stock solution of haloperidol (5 mg/mL) was prepared by dissolving 50 mg of the drug in 5 mL of absolute ethanol and then making the total volume up to 10 mL. Then, 1 mL of haloperidol solution was aspirated and mixed with 9 mL of CHI and CHI/P2HEEI solutions for 2 h to generate the final 5 mg of haloperidol on films. The preparation of 1 % CHI solution and 1% CHI/P2HEEI solution was described as above. Subsequently, prepared solution was casted and dried as mentioned above but using 10 mL of solution decanted into 35 mm diameter Petri dishes.

2.6. Characterisation of polymer and films

2.6.1. ^{1}H-Nuclear magnetic resonance spectroscopy (^{1}H-NMR)

^{1}H NMR spectra were recorded for 20 mg/mL PEOZ and L-PEI prepared in methanol-d_4 and 20 mg/mL P2HEEI prepared in D_2O using a 400 MHz ULTRASHIELD PLUSTM B-ACS 60 spectrometer (Bruker, UK). The degree of substitution (DS) of P2HEEI was determined using peak integration with the following equation (1):

$$\% \text{ DS} = \frac{\int \text{Peak b}/n_b}{\int \text{Peak a}/n_a} \text{x } 100 \qquad (1)$$

Where Peak a is the integral of CH_2CH_2 signal on the main backbone adjacent to nitrogen, Peak b is the integral of CH_2 on side-group signal, n_a is the number of protons of CH_2CH_2 on the main backbone adjacent to nitrogen and n_b is the number of protons in CH_2 on the side-group.

2.6.2. Fourier transformed infrared (FTIR) spectroscopy

Dry polymer and film samples were scanned from 4000 to 400 cm^{-1} at resolution of 4 cm^{-1} using Nicolet iS5-iD5 ATR FT-IR spectrometer (Thermo Scientific, UK).

2.6.3. Differential scanning calorimetry

DSC characterization of polymer and film samples was conducted using a Q100 DSC (TA Instruments, Germany). Polymer and film samples (~ 3 - 5 mg) were loaded into pierced Tzero aluminum pans. The thermal behavior of each sample was investigated in a nitrogen atmosphere with a heating/cooling rate of 10 ^{o}C/min (-70 to 180 ^{o}C). The values of the glass transition temperature (T_g) of polymers were determined from the second heating cycle.

2.6.4. Thermogravimetric analysis (TGA)

Thermogravimetric analysis of polymer and film samples was conducted using Q50 TGA analyser (TA Instruments, UK) from 20 to 600 °C at a heating rate of 10 °C/min under nitrogen atmosphere. Prior to analysis, the films were dried in a vacuum oven (as above) and then were placed in a desiccator over dry silica gel for 3 days. Moisture content in each film was determined from the first step weight loss in their TGA curves (up to about 150 °C).

2.6.5. X-ray diffractometry (XRD)

Dry polymers (~20 mg) or films (2×2 cm^2) were placed on a silica slide and analyzed in a Bruker D8 ADVANCE PXRD equipped with a LynxEye detector and monochromatic Cu $K\alpha_1$ radiation (λ = 1.5406 Å). Samples were rotated at 30 rpm and data collected over an angular range (2θ) of 5 - 60 ^{o} for 1 h, with a step of 0.05^{o} (2θ) and count time of 1.2 s. The results were analyzed using Origin software.

2.6.6. Cytotoxicity of polymers

Polymer cytotoxicity was evaluated using an MTT assay. Briefly, L-PEI was dissolved in 95% ethanol and then diluted with Dulbecco's modified eagle medium (DMEM) to obtain polymer concentrations between 5–5000 µg/mL, whereas PEOZ and P2HEEI were dissolved directly in Dulbecco's modified eagle medium (DMEM) and then diluted with DMEM to prepare solutions with polymer concentrations ranging between 5–5000 µg/mL. The amount of formazan produced quantitatively was determined by monitoring the absorbance at 570 nm, which is proportional to the number of living cells. Human dermal fibroblasts (ATCC CRL-2522) were seeded at a density of 1×10^5 cells/mL cells per well in a

96 well plate and allowed to attach overnight before being incubated with the respective polymer solutions at 5, 50, 500, 1000, 2500, and 5000 µg/mL for 24 h. 10% DMSO (v/v) in Dulbecco's modified eagle medium (DMEM) was used as a positive control and, and 10% Fetal bovine serum in DMEM was used as a negative control. 100 µL of 3-(4, 5-dimethylthiazol-2-yl)-2, 5-diphenyl tetrazolium bromide solution (MTT) solution was then pipetted into each well and the plate incubated at 37 ^{o}C in a CO_2 incubator for 3 h. Finally, the absorbance at 570 nm was measured using a standard plate reader (Thermo Scientific™ Multiskan™ GO, Finland).

2.6.7. Film thickness

The film thickness was measured with a digital micrometer (Mitutoyo, Japan) with 0.001 mm resolution. Several thickness measurements were taken at different points of each film and then, the mean values ± standard deviations were calculated **(Table S1)**.

2.6.8. Scanning electron microscopy (SEM)

SEM experiments used a FEI Quanta 600 FEG Environmental Scanning Electron Microscope instrument (FEI UK Ltd., UK) with an acceleration voltage of 20 kV. The images were taken from the fracture surface of the films, which were preliminary frozen in liquid nitrogen and coated with gold (a diode sputter) to facilitate high resolution imaging.

2.6.9. Fluorescence microscopy

The fluorescein isothiocyanate (FITC)-labeled chitosan was synthesized according to Cook and co-workers [28]. Chitosan solution (1% w/v in 0.1 M hydrochloric acid, 100 mL) was prepared, followed by the addition of anhydrous methanol (100 mL) and FITC (2 mg/mL in methanol, 50 mL). The reaction was carried out in the dark at room temperature for 3 h before precipitation in 1 L of 0.1 M NaOH. The resulting precipitate was filtered and dialyzed in deionized water until FITC traces were not detectible in water. The dialyzed product was then freeze-dried. Initially, 1% w/v aqueous solutions of FITC-labeled chitosan and P2HEEI were prepared by dissolving pre-weighed amount of dry polymers at room temperature. FITC-labeled chitosan solution was prepared in 0.1 M hydrochloric acid by stirring magnetically for 24 h prior to casting. P2HEEI solutions were prepared in deionised water and allowed to stir continuously for 1 h. The prepared polymer solutions were mixed at different volume ratios and named as FITC-labeled chitosan (100: 0), FITC-labeled chitosan

/P2HEEI: (80:20), (60:40), (40:60) and (20:80). Subsequently, FITC-labeled chitosan /P2HEEI solutions were magnetically agitated for 3 h until total homogeneous mixture was formed. After that, 10 mL of each solution was poured into Petri dishes (30 mm in diameter) and dried at 30 ^{o}C in an oven for several days. The morphology of film samples was analysed using fluorescence microscope.

2.6.10. Mechanical properties of films

The mechanical properties of films, including puncture strength, elongation at puncture and modulus at puncture were evaluated using a TA.XT Plus Texture Analyser (Stable Micro Systems Ltd., UK) in a compression mode, which was adapted from our previous studies [9, 29, 30]. Film thickness was measured in five different places using a hand-held micrometre. Square shaped film samples (30×30 mm) were fixed between two plates with a cylindrical hole of 10 mm diameter (area of the sample holder hole: Ar_s = 78.57 mm^2) and compressed by the upper load 5 mm stainless steel spherical ball probe (P/5S) at a test speed of 1.0 mm/sec. The plate was stabilised to avoid movements using two pins. The measurements started after the probe was in contact with the sample surface. The probe was moved at a constant speed until each film sample was broken. These tests were performed with the following settings: pre-speed test 2.0 mm/sec; test-speed 1.0 mm/sec; post-test speed 10.0 mm/sec; target mode-distance; distance 5 mm; trigger type auto; and trigger force 0.049 N. The film samples were punctured and the force required in Newtons was recorded and puncture strength was calculated using the following equations (2-4):

$$\text{Puncture strength} = \frac{F_{max}}{Ar_s} \qquad (2)$$

where F_{max} is the maximum applied force, Ar_s is the area of the sample holder hole, with $Ar_s = \pi r^2$, where r is the radius of the hole.

$$\text{Elongation (\%)} = \left(\frac{\sqrt{r^2+d^2}-r}{r}\right) \text{x } 100 \qquad (3)$$

where r is the radius of the film exposed in the cylindrical hole of the film holder and d represents the displacement of the probe from the point of contact to the point of puncture.

$$\text{Modulus at puncture} = \frac{\text{Puncture strength}}{\text{Elongation (\%)}} \qquad (4)$$

2.7. *In vitro* drug release study

Haloperidol release from films was carried out using a Franz diffusion cell and a methodology adapted from Samanta et al. [31] and Soradech et al. [10]. The receptor compartment was filled with 20 mL of 20% PEG 400 in phosphate-buffered saline (pH = 7.4) as a medium [31] and then it was stirred at 600 rpm and maintained at 37 °C throughout the experiment. 5% haloperidol loaded films were placed between the donor and receptor compartments. 1 mL aliquots were taken from the receptor compartment at predetermined time intervals and replaced with 1 mL fresh medium (20 % PEG 400 in phosphate-buffered saline) to maintain a constant volume. All release experiments were carried out for 180 minutes. The drug concentration in the aliquot was measured spectrophotometrically at 254 nm and calculated using a standard calibration curve ranging from 5–50 µg/mL. The protocol used for the preparation of stock solution of haloperidol and stand curve was followed from our previous study [10]. For each type of films, three replicate experiments were performed.

2.8. *Ex vivo* mucoadhesive properties of film with and without haloperidol

Sheep buccal mucosal tissues were used for *ex vivo* assessment of mucoadhesive properties. The mucosal adhesion of the polymeric films with and without haloperidol was determined using a TA XT plus Texture Analyser (Stable Microsystems, UK) in a tensile mode at room temperature, as followed from the previous studies [32]. The scheme of *ex vivo* mucoadhesive test using texture analyzer is shown in **Fig.S1** (Supporting information). Using double-sided adhesive tape, the square-shaped films (1×1 cm) were manually attached to the texture analyzer probe. The mucosal tissue was affixed on the mucoadhesion rig and moisturized with 1 mL of phosphate buffer saline solution. The films were brought in contact with mucosa and a downward force of 0.1 N was applied for 60 s. The probe was then withdrawn from the mucosa at 1 mm/s. Data acquired from the detachment experiments were then used to evaluate the maximal force required for the detachment (F_{adh}) and the total work of adhesion (the area under the force-distance curve, W_{adh}) values. For each type of films, five replicate experiments were performed.

2.9. Statistical analysis

The results of our measurements were shown as mean values ± standard deviation, which were calculated as a result of three independent experiments. One-way ANOVA and

Student's t-test were used for the analysis of the data to determine the extent of any differences between the results.

3. Results and discussion

3.1. Synthesis and evaluation of poly(2-hydroxyethyl ethyleneimine), P2HEEI

L-PEI was synthesized successfully by acidic hydrolysis of PEOZ to remove all amide groups from the side moieties. The complete conversion of PEOZ into L-PEI was confirmed using ^{1}H-NMR and FTIR spectroscopies. As illustrated in **Fig. S2**, both PEOZ signals at side moieties around 2.44 ppm and 1.13 ppm disappeared, while the signal of two methylene groups at the backbone was shifted to 2.75 ppm. FTIR **(Fig. S3)** confirmed the complete hydrolysis of the amide groups in PEOZ showing the disappearance of the amide carbonyl vibration at 1626 cm^{-1} and the appearance of new strong bands at around 1474 cm^{-1} and 3263 cm^{-1} due to the N-H vibration of PEI. The ^{1}H-NMR and FTIR results correlated well with other reports [26][16]. L-PEI was then alkylated via nucleophilic substitution with 2-bromoethanol in absolute ethanol in the presence of potassium carbonate as a base. The ^{1}H-NMR and FTIR spectroscopies were used to confirm the structure of the resulting P2HEEI (**Fig. S2** and **Fig.S3**). The result indicated the presence of two signals in the spectrum of P2HEEI. One signal is observed at 2.62 ppm (signal a) due to the methylene groups in the backbone and also methylene group in the side group adjacent to nitrogen. The second signal at 3.60 ppm (signal b) is due to the methylene group (CH_2) adjacent to the hydroxyl group (-OH) at the side moiety. The downfield shift of signal b was caused by de-shielding effect of the -OH group. The from methylene group (CH_2) on the side group adjacent to the nitrogen overlapped with the signal from the methylene groups of the backbone. P2HEEI was synthesized by varying the moles of 2-bromoethanol (0.02 to 0.06 mol to 1 unit-mole of L-PEI repeating unit) and the reaction time (24 and 48 h). **Fig.1** shows the scheme of chemical transformations from PEOZ through L-PEI and then to P2HEEI.

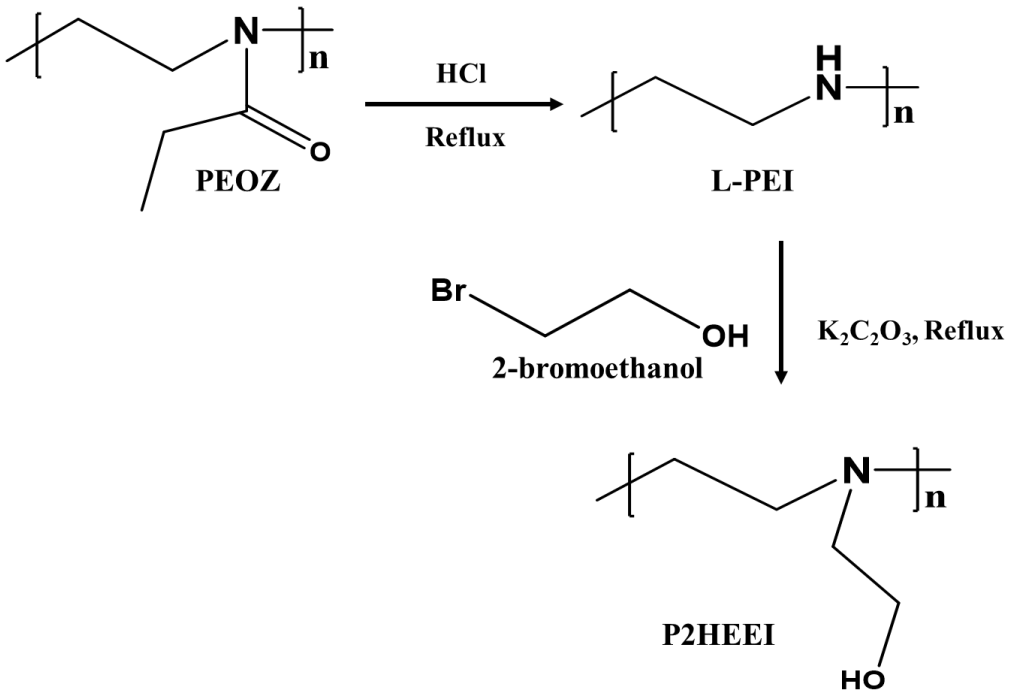

Fig. 1. Scheme of chemical transformations from PEOZ through L-PEI and then to P2HEEI.

Fig. 2 and **Table 2** summarise ^{1}H NMR spectra and the values of the degrees of substitution (DS). The result indicated that increasing the amount of 2-bromoethanol from 0.02 to 0.06 moles to react with L-PEI at 24 h reflux time resulted in increase of the DS from 59.2 to 84.3 %. The effect of reflux time on the DS was also investigated using the moles of L-PEI: 2-bromoethanol of 0.02 : 0.06. A longer time to reflux (24 to 48 h) resulted in a higher DS, increasing from 84.3 to 97.1 %. FTIR **(Fig. S3)** also confirmed the successful synthesis of the hydroxyethyl substituted L-PEI derivative (P2HEEI) by observing the broad absorption peak at 3414 cm^{-1} in the FTIR spectrum of P2HEEI indicating the presence of OH- stretching.

Table 2. Degrees substitution of hydroxyethyl polyethyleneimine prepared at different mole ratios of L-PEI : 2-bromoethanol : base and reflux time.

L-PEI: 2-bromoethanol : base (moles)	Reflux time (h)	Degree substitution (%)
0.02 : 0.02 : 0.02	24	59.2
0.02 : 0.03 : 0.03	24	72.5
0.02 : 0.05 : 0.05	24	77.6
0.02 : 0.06 : 0.06	24	84.3
0.02 : 0.06 : 0.06	48	97.1

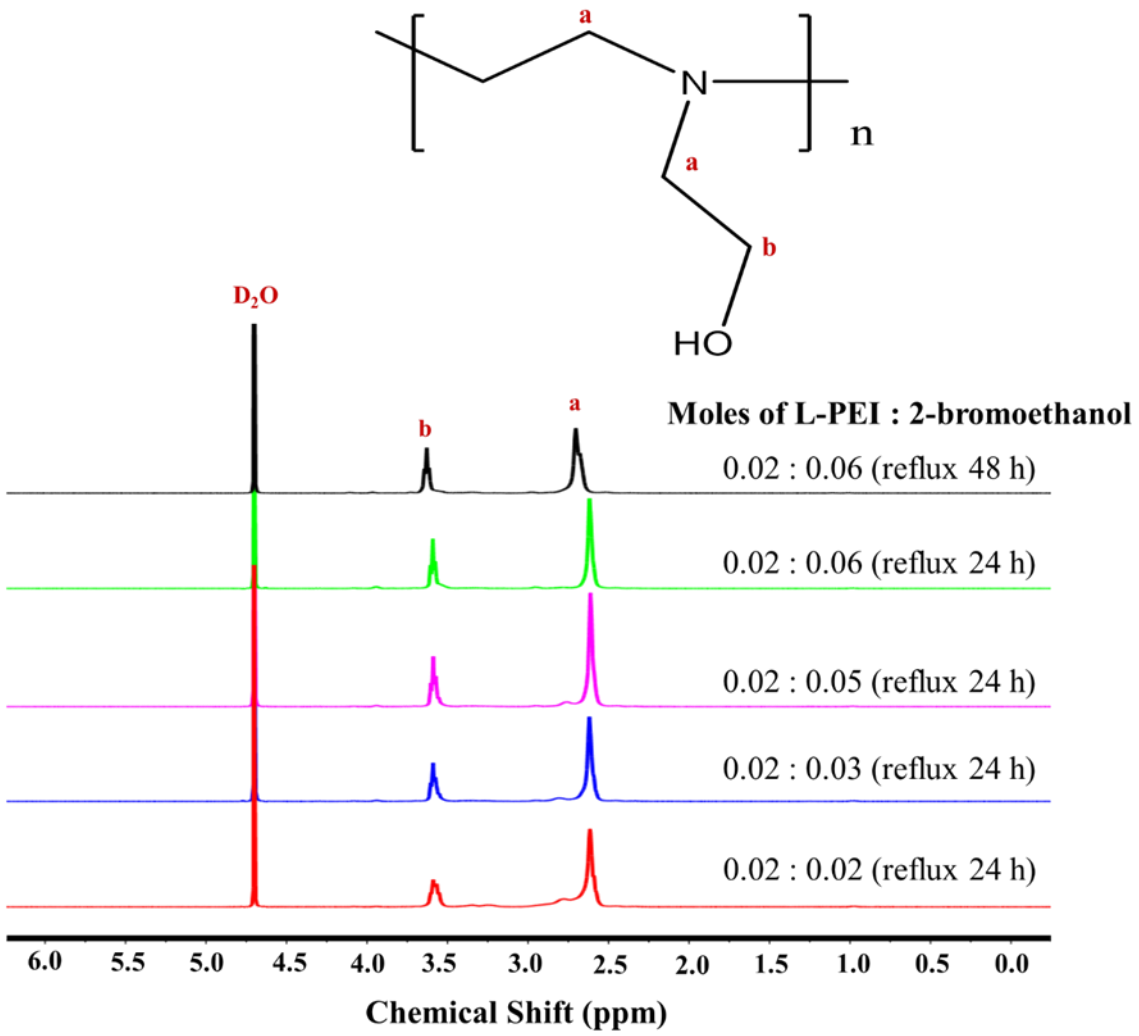

Fig. 2. ^{1}H NMR spectra of hydroxyethyl substituted linear polyethyleneimine prepared at different moles of L-PEI: 2-bromoethanol and reflux time.

PEOZ, L-PEI and P2HEEI were characterized using differential scanning calorimetry (DSC) and thermogravimetric analysis (TGA). The glass transition temperatures (T_g) of PEOZ, L-PEI, and P2HEEI were 60.1, -21.5, and -31.6 ^oC, respectively **(Fig. 3).** Moreover, the DSC thermogram of L-PEI indicated a melting point of 61.8 ^oC, which is in a good agreement with the literature[20, 33]. P2HEEI, in contrast to L-PEI, exhibited a fully amorphous behavior. The high chain flexibility of P2HEEI and very low value of T_g is consistent with the properties of some other water-soluble polymers that have hydroxyl pendant groups, for example, poly(2-hydroxyethyl vinyl ether) was reported to have T_g < -30 °C [34] or poly(3-hydroxypropyl ethyleneimine) has a T_g = -38.6 ^oC [10]. The change from semi-crystalline L-PEI to fully amorphous P2HEEI was confirmed by X-ray diffractometry (**Fig. S4)**.

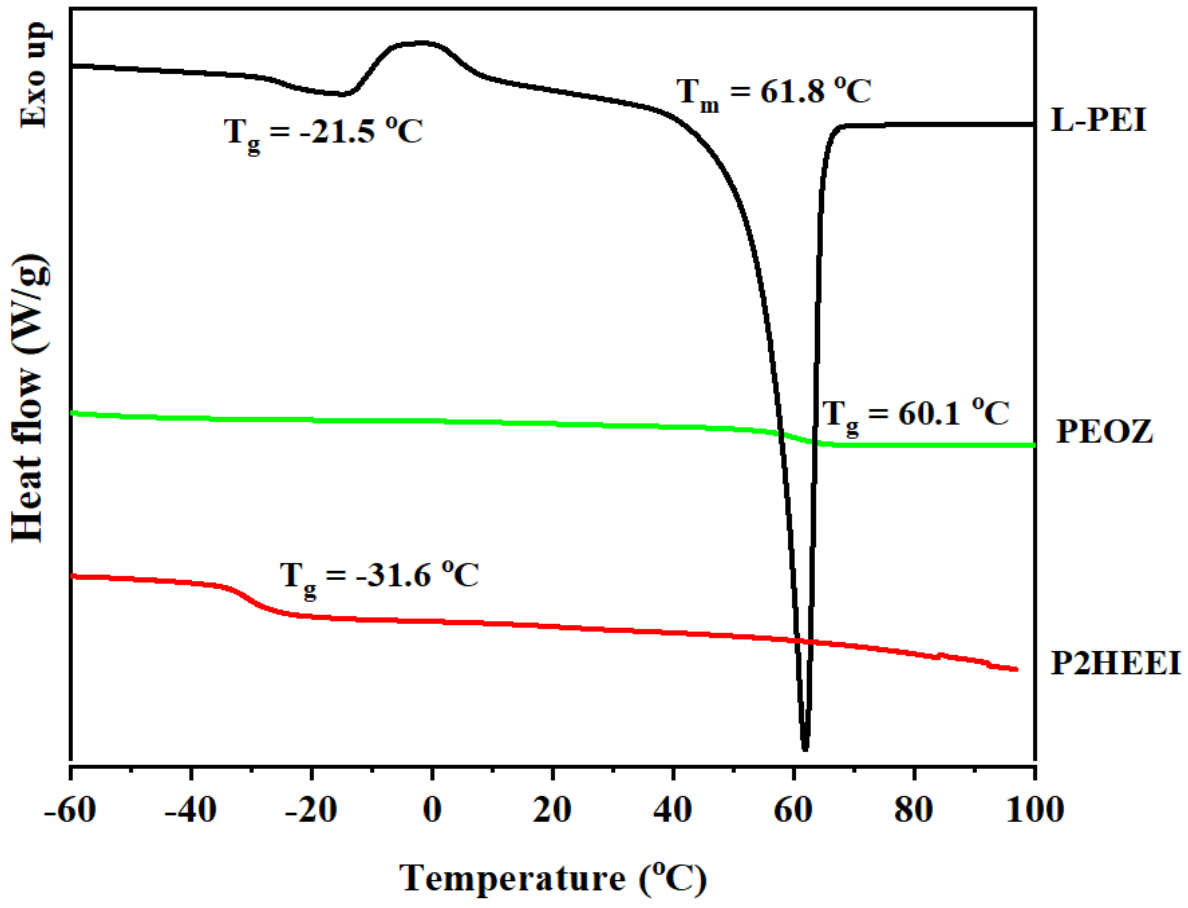

Fig. 3. DSC thermograms of PEOZ, LPEI and P2HEEI.

TGA was used to characterize the thermal stability of P2HEEI in comparison to PEOZ and L-PEI **(Fig. S5)**. It is seen that there are two distinct degradation stages for PEOZ, L-PEI and P3HPEI. The initial decrease was caused by the loss of free and physically-bound water between 30 and 150 ^{o}C; the proportion of physically-bound water was approximately 2.0 % for PEOZ, 4.2 % for L-PEI and 5.0 % for P2HEEI. The maximum temperature reached during the second stage of thermal degradation of P2HEEI was over 250 °C (42.0 %), while the maximum temperature reached during the third stage was approximately 300 °C (70.1 %), indicating that this polymer has lower thermal stability than its parent components.

As this is the first report of the synthesis of P2HEEI with high degree of hydroxyethylation it was of interest to study its toxicological properties in comparison with PEOZ and L-PEI. These were evaluated using MTT assay with human dermal fibroblast cells (**Fig. 4).** P2HEEI was found to have relatively good biocompatibility. The human dermal fibroblast cells were >80 % viable even at 5000 μg/mL. On the contrary, L-PEI was found to be highly cytotoxic at concentrations ranging from 50 to 5000 μg/mL, with less than 50% cell viability. This is in good agreement with the literature, reporting cytotoxic properties of L-PEI [22, 35]. PEOZ exhibited excellent biocompatibility, which did not cause any substantial levels of cell death in a broad range of concentrations (5-5000 μg/mL), which is also in good agreement with the literature [36]. Soradech and co-workers [10] reported that L-PEI can cause cytotoxicity when assessed using the MTT assay and that the polymer is highly cytotoxic to human dermal fibroblast cells. In comparison to P3HPEI [10], the percentage of cell viability of all concentrations of P2HEEI (5-5000 μg/mL) was higher than P3HPEI, indicating that P2HEEI was less toxic than P3HPEI. This finding demonstrated that a longer alkyl chain led to an increase in the toxicity of modified L-PEI in human dermal skin fibroblast cells; however, both polymers were still low toxic in human dermal skin fibroblast cells.

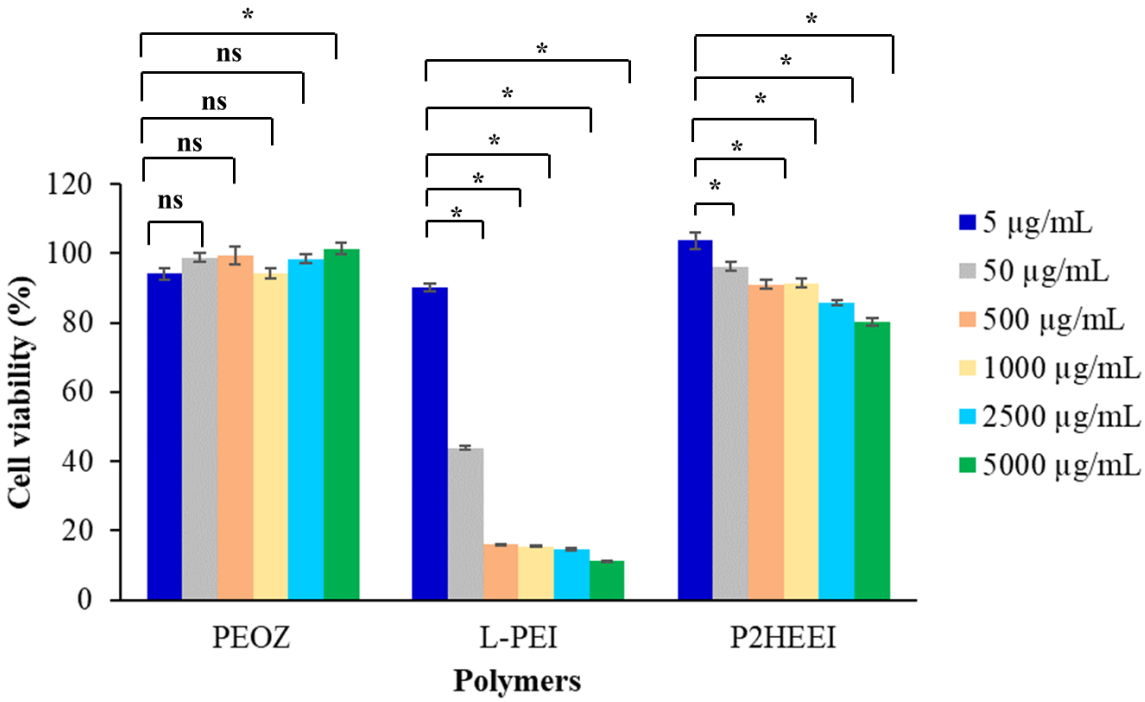

Fig. 4. Human dermal fibroblasts viability in the presence of PEOZ, LPEI and P2HEEI assessed using MTT assay. Statistically significant differences are given as: * - $p < 0.05$; ns - no significance.

3.2. Preparation and evaluation of films based on blends of chitosan and poly(2-hydroxyethyl ethyleneimine)

Low glass transition temperature (-31.6 ºC) of P2HEEI may be of interest for application in the preparation of polymeric blends with other polymers, exhibiting more rigid properties. In this case, P2HEEI may act as a plasticiser and will help to improve the mechanical properties of the resulting blends.

In this study, polymeric films based on chitosan and its blends with P2HEEI were prepared by casting from aqueous solutions with subsequent drying. **Fig. 5** and **Table 3** show the FTIR spectra of films based on pure CHI, CHI/P2HEEI blends and pure P2HEEI. The FTIR spectrum of pure CHI film revealed the presence of a broad peak above 3247 cm^{-1}, which belonged to OH- stretching and also overlaps with NH- stretching. Absorption bands at 2917 and 2878 cm^{-1} corresponded to CH_2- and CH- stretching vibrations, respectively. C=O stretching (amide I) and NH-bending (amide II) were the absorption bands at 1625 and 1514 cm^{-1}, respectively. CH- and OH- vibrations were responsible for the absorption band at 1412 cm^{-1}. The band at

1376 cm^{-1} was attributed to acetamide groups, confirming that chitosan was not completely deacetylated [9], and the band at 1311 cm^{-1} could be due to C-N stretching (amide III) [37]. The band at 1250 cm^{-1} corresponds to amino groups, which is consistent with the literature [8]. The absorption bands at 1152 and 1062 cm^{-1} correspond to the anti-symmetric stretching of the C-O-C bridge and the skeletal vibrations involving the C-O stretching, which are typical for FTIR spectra of all polysaccharides [38]. The FTIR spectra pattern of CHI agreed well with other reports [9, 10]. The broad absorption band at 3314 cm^{-1} in the FTIR spectrum of P2HEEI indicated the presence of OH- stretching as well as bound water. CH_2- stretching vibrations are represented by absorption bands at 2940 and 2818 cm^{-1}. The absorption bands at 1459, 1361, and 1361 cm^{-1} are due to CH-bending, while the absorption bands at 1288, 1112, and 1029 cm^{-1} are owing to C-C stretching. In addition, P2HEEI demonstrated the absorption band at around 1648 cm^{-1} corresponding to the water of amorphous region because P2HEEI is in liquid state at room temperature, which correlated to OH- stretching at 3314 cm^{-1}. All of the characteristic bands of the component polymers were present in the spectra of their blends, and the intensities of the bands and the shape of the bands depended on the polymer ratio in the blends. The spectra of the CHI/P2HEEI blends showed significant changes in the hydroxyl region, indicating a redistribution of the hydroxyl group associations. When comparing the spectra of the blends as a function of the polymer composition, it was noticed that this band shifted towards higher wavenumbers (3247 to 3285 cm^{-1}) as the amount of P2HEEI increased from 0 to 80 % w/v. This behavior suggests that a significant portion of the hydroxyl and amine groups in chitosan are hydrogen-bonded to hydroxyl groups in P2HEEI or the interactions between the polymers and water are present.

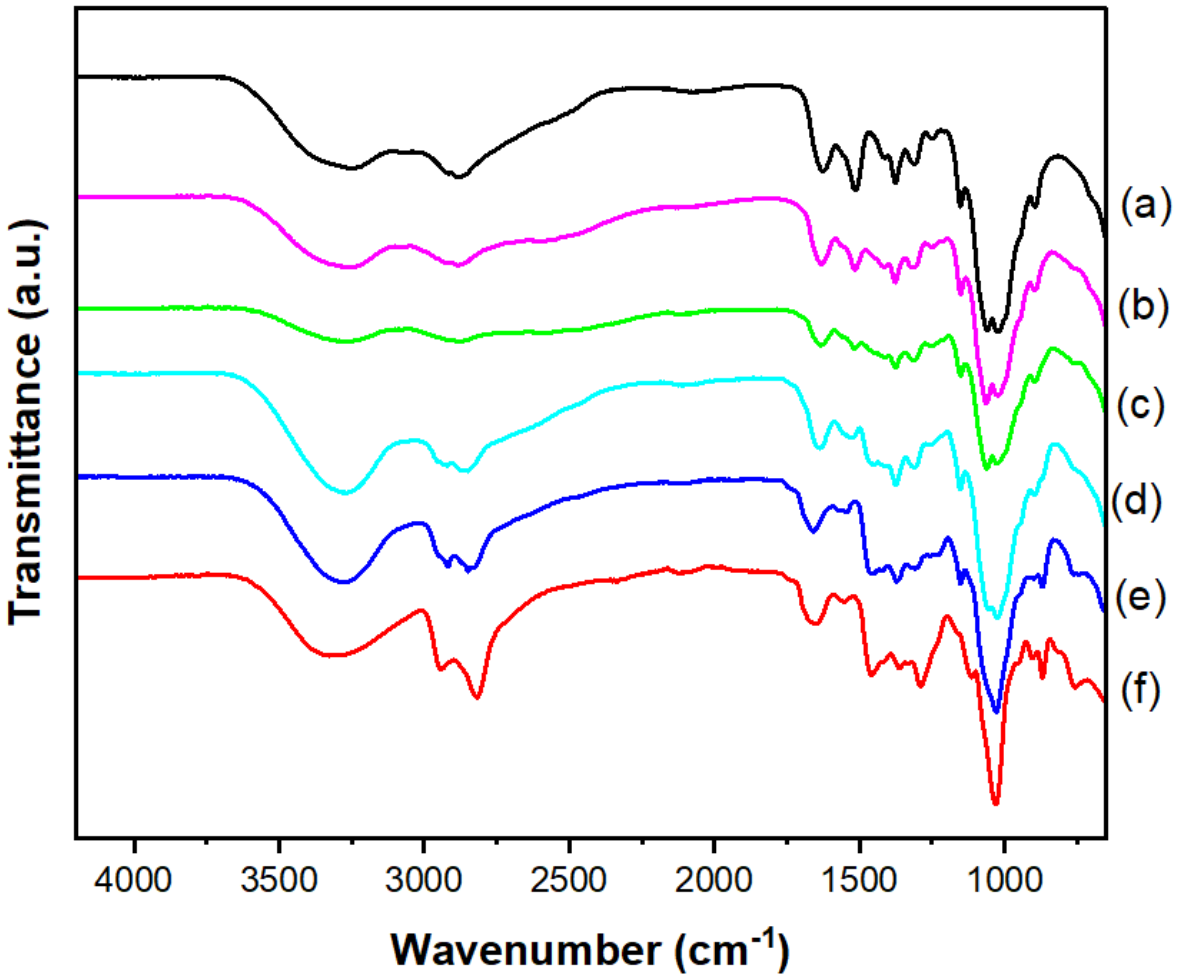

Fig. 5. FTIR spectra of CHI (a), their blends (b, c, d and e) and P2HEEI (f). Content of P2HEEI in the blends: 20 (b), 40 (c), 60 (d) and 80 % (e).

Table 3. FTIR absorption bands in CHI/P2HEEI blends and their assignment.

FTIR absorption of blends (cm^{-1})						Assignment
100:0	**80:20**	**60:40**	**40:60**	**20:80**	**0:100**	
3247	3259	3266	3270	3285	3314	OH- and NH-stretching
2917	2923	2920	2912	2918	2940	CH-stretching
2878	2883	2891	2880	2832	2818	CH-stretching
1625[1,2]	1630[1,2]	1633[1,2]	1638[1,2]	1639[1,2]	1648[2]	C=O stretching (amide I)[1], water region[2]
1514[3,4]	1514[3,4]	1516[3,4]	1513[3,4]	1455[3,4]	1459[4]	NH-bending (amide II)[3], CH_2 vibration[4]
1412	1414	1413	1412	1422	1424	CH- and OH vibration
1376[5,6]	1377[5,6]	1376[5,6]	1376[5,6]	1370[5,6]	1361[6]	Acetamide groups[5], CH-vibration[6]
1311	1317	1311	1316	1306	-	CN- stretching (amide III)
1152	1151	1152	1152	1150	-	Anti-symmetric stretching of the C-O-C bridge
1060[7,8]	1063[7,8]	1061[7,8]	1062[7,8]	1028[7,8]	1029[8]	Skeletal vibration involving the C-O stretching[7], C-C stretching[8]

The thermal stability of CHI, CHI/P2HEEI and P2HEEI was investigated using thermogravimetric analysis (TGA) as shown in **Fig. 6**. The results demonstrated that there were two main stages of degradation of CHI. The first stage of degradation of CHI was due to loosing of free water and physically-bound water between 30 °C to 150 °C and the amount of physically bound water in pure CHI film was around 6.0 %. The next degradation stage of CHI was due to the thermal decomposition which appeared between 250 to 400 °C (the maximum degradation rate was observed at ~320 °C as well as this degradation resulted in 58.3 % loss of sample weight). The decomposition of chitosan was a result of the depolymerisation of chitosan chains and pyranose rings through dehydration and deamination and finally ring-opening reaction[9]. There were three main stages of degradation of P2HEEI. The first thermal event occurs between 30 °C to 150 °C, which is likely associated with the evaporation of physically bound water (approximately 5.0 %). The maximum temperature reached during the second stage of thermal degradation of P2HEEI was over 250 °C (42.0 %), while the maximum temperature reached during the third stage was approximately 300 °C (70.1 %). The decomposition profiles of CHI/P2HEEI blends are characterised by four stages: (1) 30 - 150 °C, corresponding to the loss of physically bound water; (2) 200–250 °C, due to the first stage of P2HEEI degradation; and (3) 275–350 °C, due to the second stage of P2HEEI degradation and (4) 300 - 450 °C, corresponding to the degradation of CHI. In addition, the solid residue

of CHI/P2HEEI blends tended to decrease (34.5 to 2.5 % w/w) when rising P2HEEI content in the blends, with a linear correlation (R^2=0.9515) **(Fig. S6)** indicating the miscibility of polymer blends.

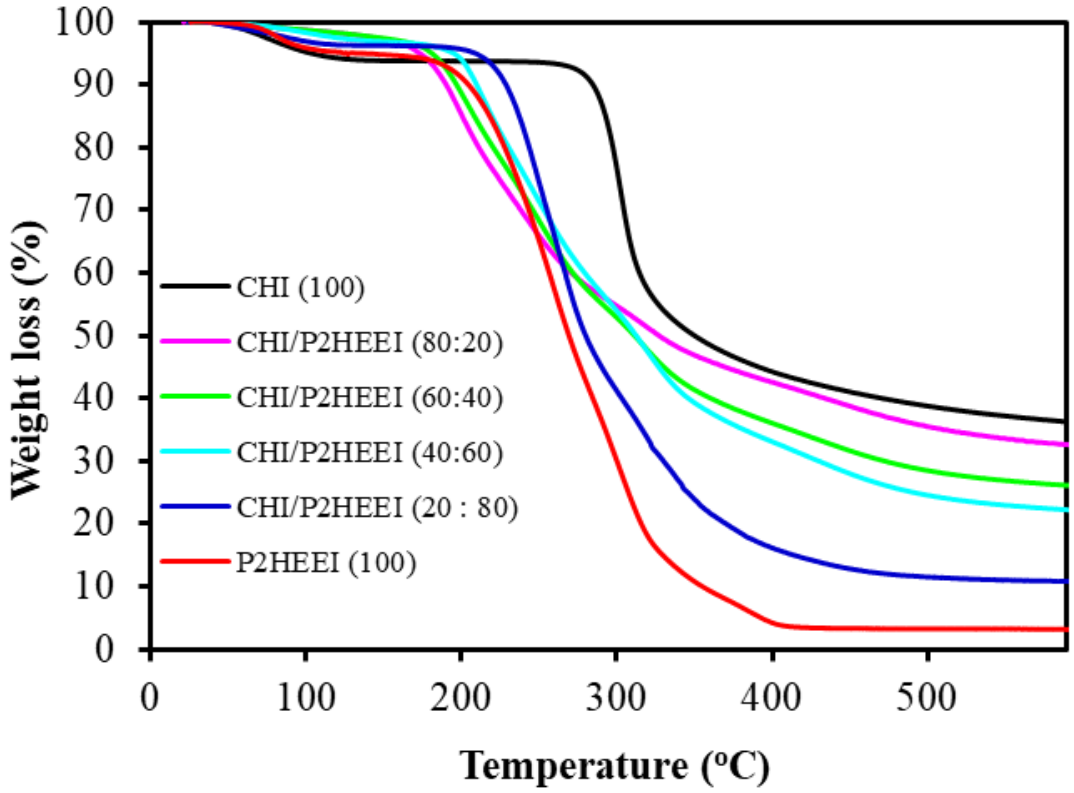

Fig. 6. TGA thermograms of CHI, CHI/P2HEEI blends and P2HEEI.

The miscibility of the polymer blends was studied using differential scanning calorimetry (DSC). Generally, the presence of a single glass transition temperature between the T_g values of individual polymer components strongly suggests complete miscibility of the blend components. **Fig. 7a** shows the presence of a single glass transition in the blends, which is dependent on the polymer mixture composition. Depending on the amount of P2HEEI in the blends, T_g of CHI/P2HEEI blends were between the T_g values of individual P2HEEI (-31.6 °C) and chitosan (131.9 °C). P2HEEI appeared to have acted as a plasticizer for these blends. It is well known that traces of water can act as a plasticizer for water-soluble polymers, significantly lowering the glass transition temperature [34][39]. P2HEEI has a structural similarity to poly(2-hydroxyethyl vinyl ether), which has a T_g < -30 °C [34]. Blending of of poly(acrylic acid) with poly(2-hydroxyethyl vinyl ether) also resulted in a substantial reduction of T_g of the films [34].

Fig. 7b shows the correlation between weight fraction of P2HEEI and T_g of experimental result compared with theoretical calculations. The T_g of miscible blends can be predicted by using Fox [40] and Gordon–Taylor [41] expressed by the following equations (5) and (6):

$$\frac{1}{T_g} = \frac{W_{CHI}}{T_{g,\,CHI}} + \frac{W_{P2HEEI}}{T_{g,\,P2HEI}} \qquad \text{(Fox equation)} \quad (5)$$

$$T_g = \frac{W_{CHI}T_{g,\,CHI} + kW_{P2HEEI}T_{g,\,P2HEEI}}{W_{CHI} + kW_{P2HEEI}} \qquad \text{(Gordon–Taylor equation)} \quad (6),$$

where W_{CHI} and W_{P2HEEI} are the weight fractions of chitosan and P2HEEI, respectively; and $T_{g,CHI}$ and $T_{g,P2HEEI}$ are the glass transition temperatures of chitosan and P2HEEI, respectively; k is the ratio of heat capacity change of P2HEEI over chitosan [$k = \Delta C_{p2}/ C_{p1}$)][42].

The T_g of the blends tended to decrease as the P2HEEI concentration increased, and their relation was well expressed by the theoretical curves. The correlation curve between the weight fraction of P2HEEI and the T_g of CHI/P2HEEIl blends obtained from experimental data was observed to be higher than that obtained from the Fox and Gordon-Taylor equations, demonstrating greater interaction between the components and thus compatibility [43]. These findings suggested that a miscible phase was formed at the molecular level in these blends, and that intermolecular hydrogen bonds could probably form between the hydroxyl and amine groups of chitosan and the hydroxyl groups of P2HEEI.

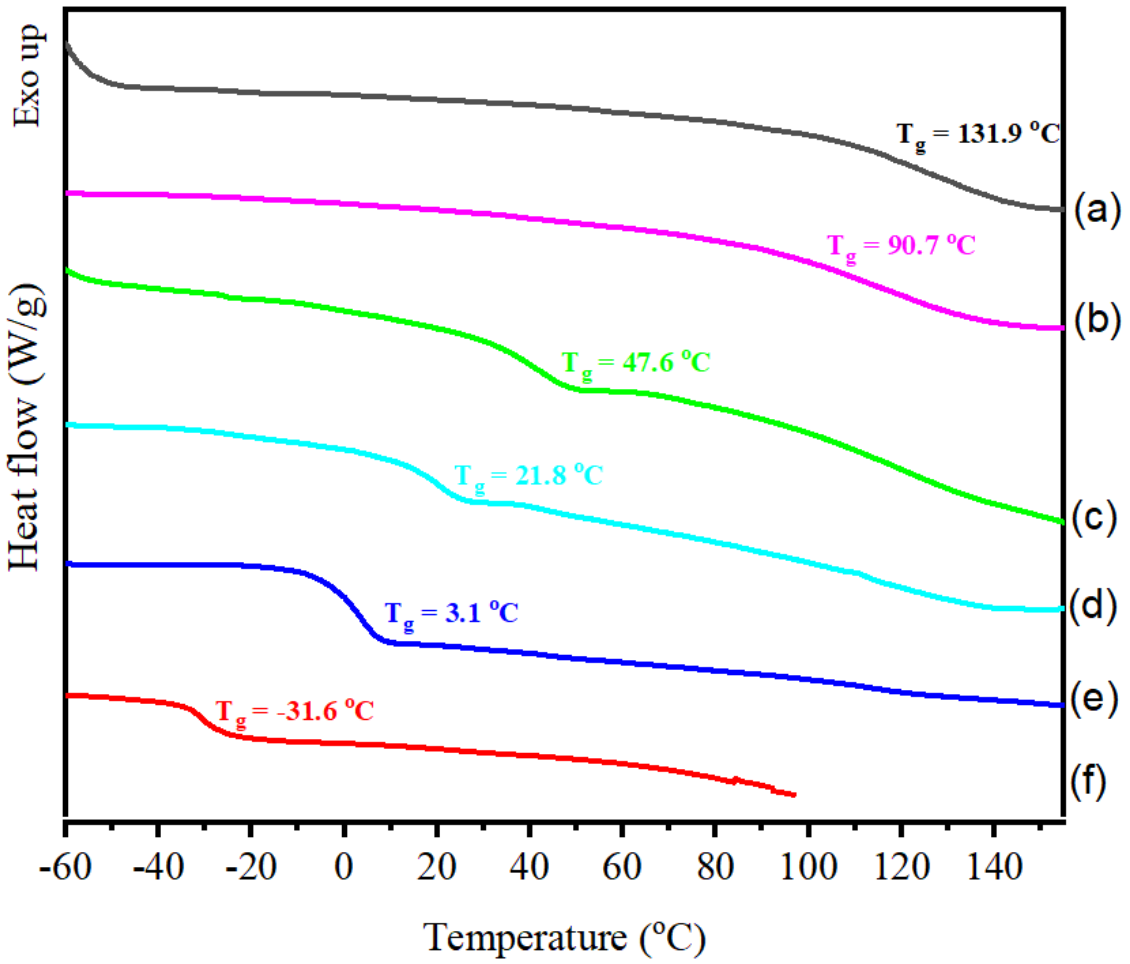
Exo up
Heat flow (W/g)
T_g = 131.9 °C
T_g = 90.7 °C
T_g = 47.6 °C
T_g = 21.8 °C
T_g = 3.1 °C
T_g = -31.6 °C
(a)
(b)
(c)
(d)
(e)
(f)
-60 -40 -20 0 20 40 60 80 100 120 140
Temperature (°C)

(a)

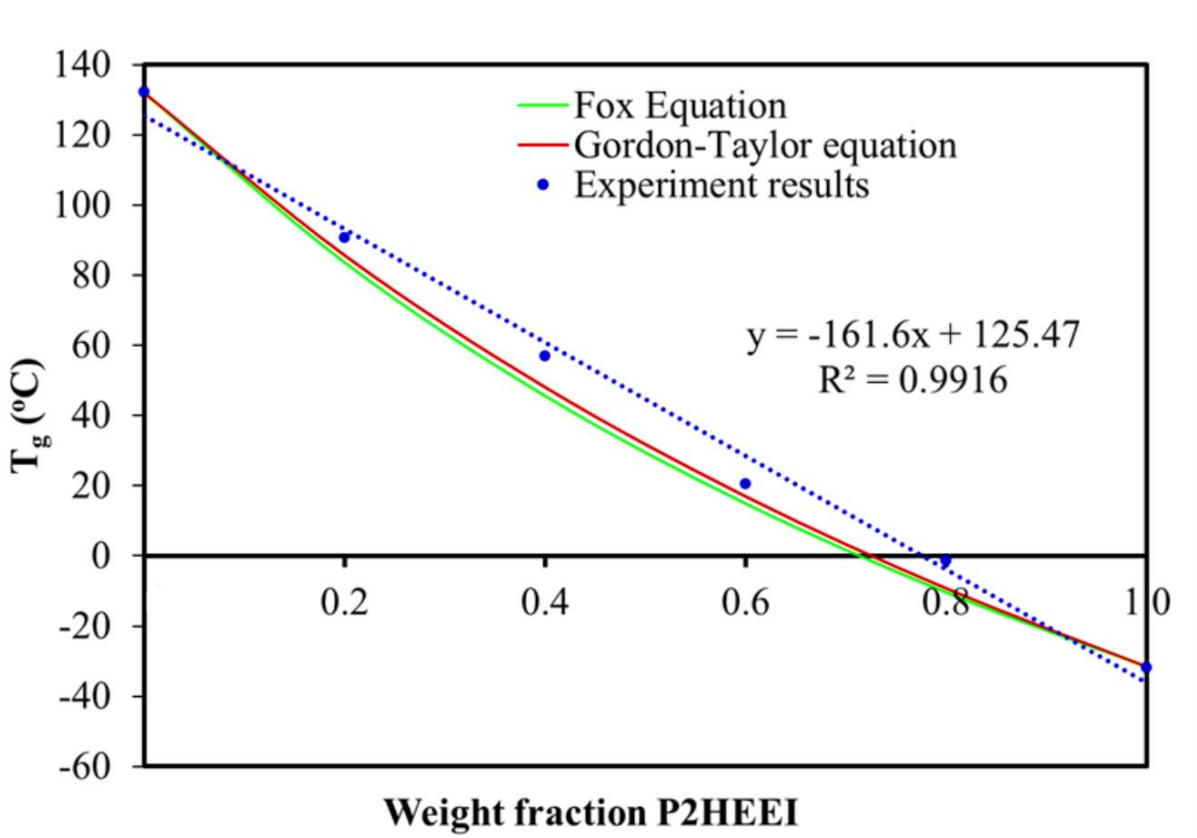

(b)

Fig. 7. DSC thermogram of CHI (a), their blends (b, c, d and e) and P2HEEI (f). Content of P2HEEI in the blends: 20 (b), 40 (c), 60 (d) and 80 % (e) (7a) and Correlation between the weight fraction of P2HEEI in P2HEEI-chitosan blends and Tg of experimental result compared with theoretical results (7b).

The morphology of the polymer films in cross-section and surface was studied using scanning electron microscopy (SEM). The investigation of the sample cross-sections at high magnification (1000x) reveals that the films have a fully homogeneous morphology with no signs of phase separation and interface boundaries **(Fig. 8)**. Similar lack of phase separation is observed on the film surfaces. Thus, the SEM data provided another evidence for miscibility between CHI and P2HEEI in the solid-state at different polymer ratios. The SEM results correlated well with the fluorescent microscopy evaluation of the films prepared using fluorescently-labelled chitosan **(Fig. S7)**. The fluorescence images also show lack of phase separation in these blends.

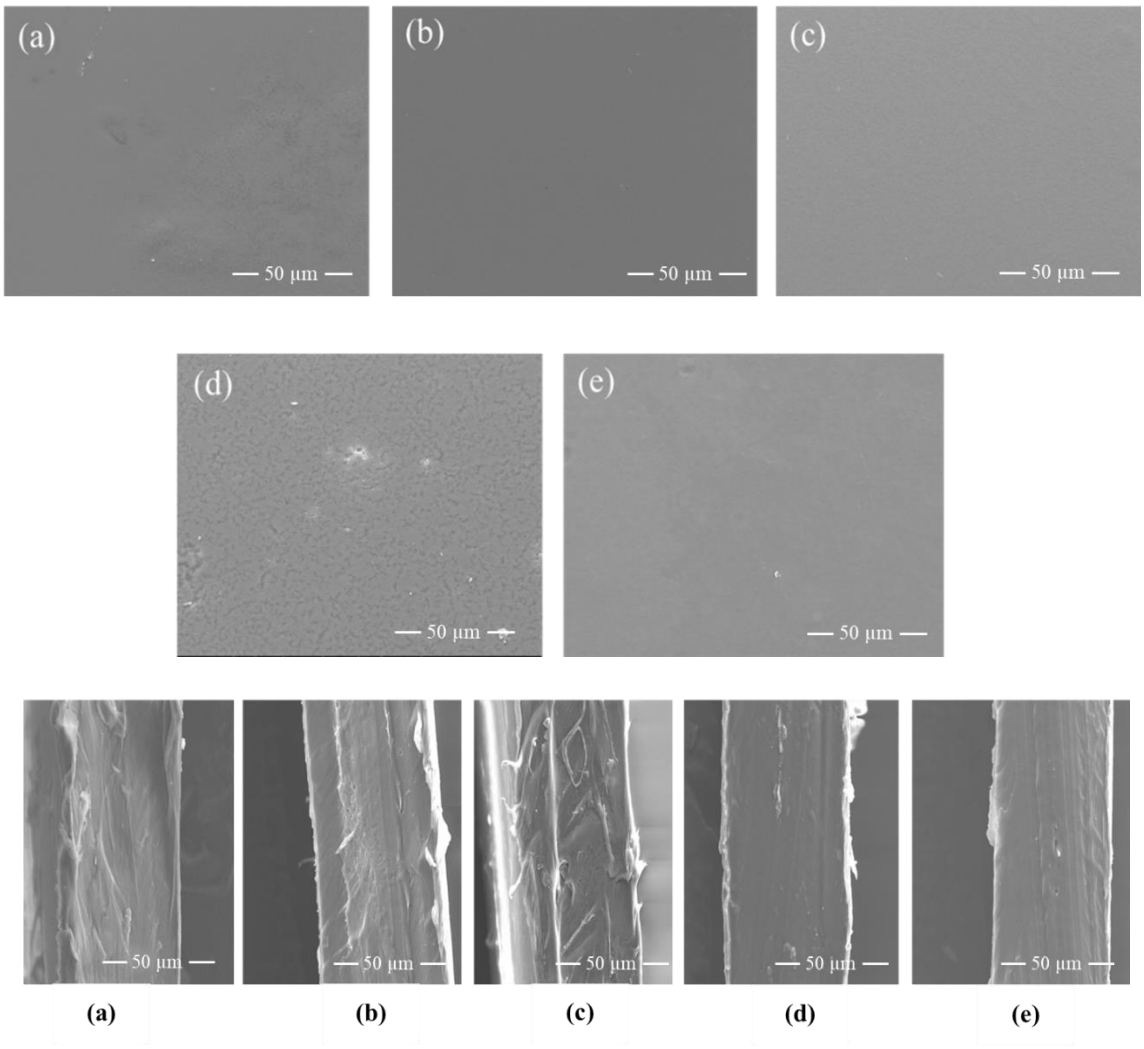

Fig. 8. SEM images of film surfaces (A) and cross-sections (B) of CHI (a) and their blends with P2HEEI (b, c, d, and e). Content of P2HEEI in the blends: 20 (b), 40 (c), 60 (d) and 80 % (e).

Further, X-ray diffraction patterns recorded for CHI/P2HEEI films also indicate the possibility of interactions between CHI and P2HEEI and miscibility of these polymers in the blends **(Fig. S8)**. CHI as a semi-crystalline polysaccharide has crystalline domains that typically show several diffraction peaks [44]. The diffraction pattern of pure chitosan film recorded in the current study has relatively low signal-to-noise ratio, which is possibly related to lower thickness of films used compared to Abilova et al. [9]. However, the diffraction peak at 12.9 ° typical for CHI is still clearly visible. The absence of different crystalline characteristics in the diffraction pattern of pure P2HEEI and the presence of a broad amorphous "halo" indicate that the polymer was essentially non-crystalline. The X-ray diffractograms of

CHI/P2HEEI films similarly display a large halo, which is characteristic of polymers that are predominately amorphous, despite the fact that chitosan-typical diffraction peaks were observed in the blend films. In addition, when the amount of P2HEEI in the films increased, the sharper chitosan diffraction peaks disappeared, resulting in their miscibility.

Fig. 9 illustrates the mechanical properties of pure CHI film and its blends with P2HEEI, including the puncture strength, elongation, and modulus at puncture. The results indicated that pure chitosan films (100%) had a greater puncture strength (0.38 N/mm^2) but it presented a lower percentage of elongation (5.6 %). When the P2HEEI content increased, the puncture strength of CHI/P2HEEI films decreased significantly ($p < 0.05$), whereas the flexibility of CHI/P2HEEI films tended to increase as seen from greater values of the percentage of elongation ($p < 0.05$). The puncture strengths of 80:20, 60:40, 40:60, and 20:80 CHI/P2HEEI films were 0.19, 0.12, and 0.08 N/mm^2, respectively, while percentages of elongation were 8.7, 11.9, 18.6, and 35.3 %. The modulus at puncture could be calculated by using the correlation between puncture strength over elongation, which had previously been used to calculate the rigidity or stiffness of materials. Because of the high strength and low percentage of elongation, the modulus was high. This study found that increasing the P2HEEI content in CHI/P2HEEI films resulted in a decrease in modulus at puncture, indicating that increasing the P2HEEI content results in more elastic materials. The decrease in modulus was caused by P2HEEI properties. According to the DSC results, P2HEEI had a low glass transition temperature (-31.6 ^oC) , hence it acts as a plasticizer [34]. Plasticizers are typically small or oligomeric molecules, such as low molecular weight of polyethylene glycol (PEG), that intersperse and intercalate between polymer chains, thereby disrupting hydrogen bonding and spreading the chains apart to increase flexibility [45]. As a result, increasing the P2HEEI concentration in CHI/P2HEEI films probably reduced intermolecular hydrogen interactions between CHI chains, resulting in improved chain mobility and film flexibility [45]. This result correlates with DSC data, as the higher elasticity of CHI/P2HEEI films with an increasing P2HEEI content is associated with a decrease in the glass transition temperature of CHI/P2HEEI films.

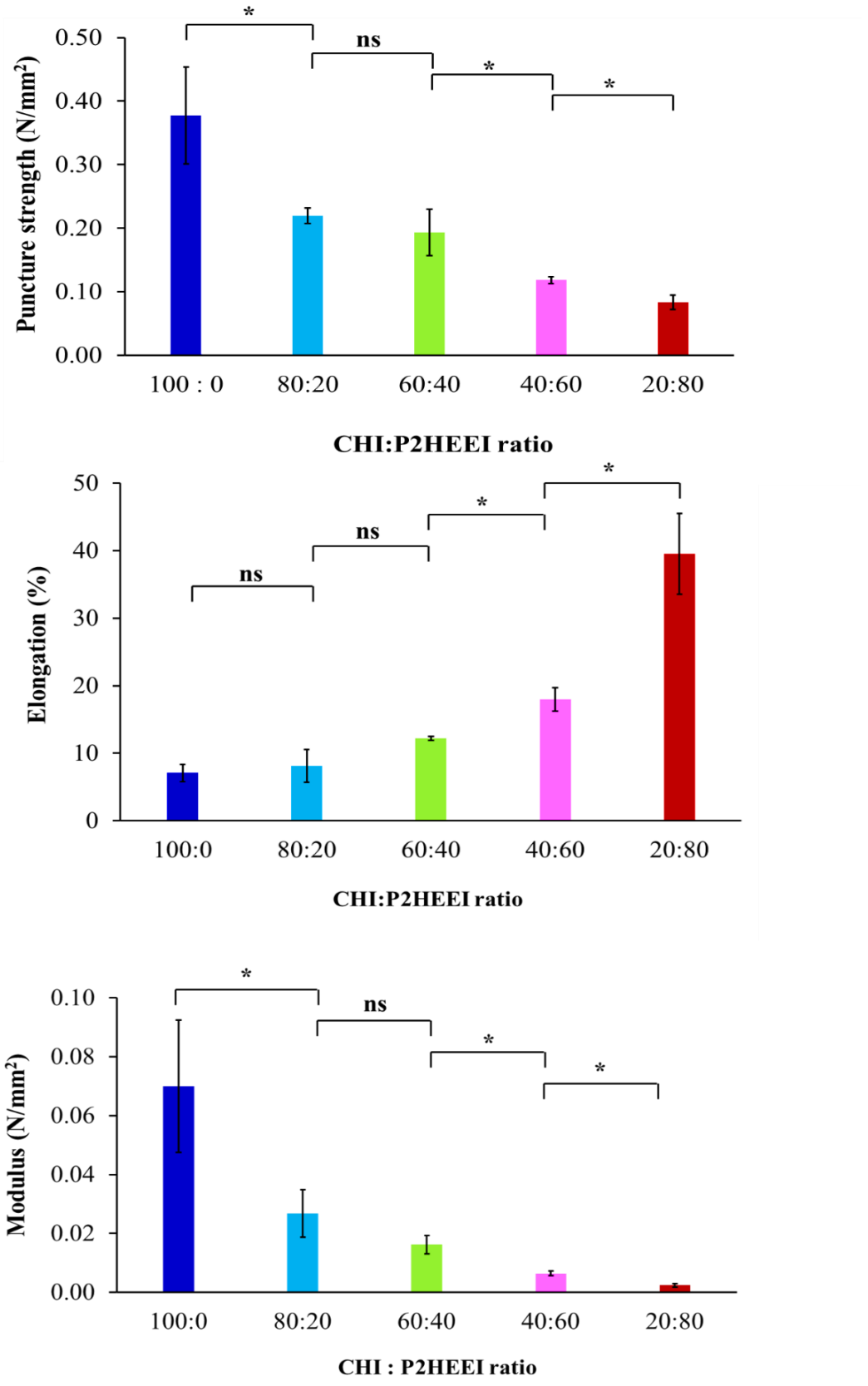

Fig. 9. Mechanical properties of CHI and their blends with P2HEEI. Statistically significant differences are given as: * - $p < 0.05$; ns - no significance.

3.3. Chitosan and poly(2-hydroxyethyl ethyleneimine) films for buccal delivery of haloperidol: *In vitro* drug release and *Ex vivo* mucoadhesion studies

In this study, haloperidol (HP) was chosen as a model poorly water-soluble drug for buccal drug delivery. HP is an antipsychotic drug and, its use is often associated with extrapyramidal syndrome side effect manifested as involuntary body movements that cannot be easily controlled [31]. It is a poorly water-soluble drug and is commonly formulated as solutions for oral administration or injections, and as tablets [26]. The average oral dose of haloperidol ranges from 0.5 to 30 mg per day [46]. Further, HP is a BCS class 2 drug, characterized by low solubility but high permeability[47] and has poor oral bioavailability (59%)[46]. Hence, developing a haloperidol formulation for buccal administration is of interest and the drug-loaded films based on blends of chitosan and P2HEEI were prepared for this purpose.

The drug release from these films was studied using a Franz diffusion cell technique in a 20 % PEG 400-PBS solution at pH = 7.4 (37 ^{o}C). **Fig. 10** illustrates the cumulative release profiles from HP-loaded CHI/P2HEEI films prepared at different polymer ratios It is seen that the drug release varied significantly ($p < 0.05$) when the CHI-P2HEEI ratio is changed in the films. The films based on pure CHI showed the lowest drug release (no more than ~125 µg/cm^2) within 180 minutes. The addition of P2HEEI to CHI in the films from 0 to 80 % (w/v) resulted in an increase in the drug release from ~135 to ~207 µg/cm^2. This faster release of haloperidol from the films plasticized with P2HEEI is likely related from their better flexibility that facilitates better diffusion of drug molecules.

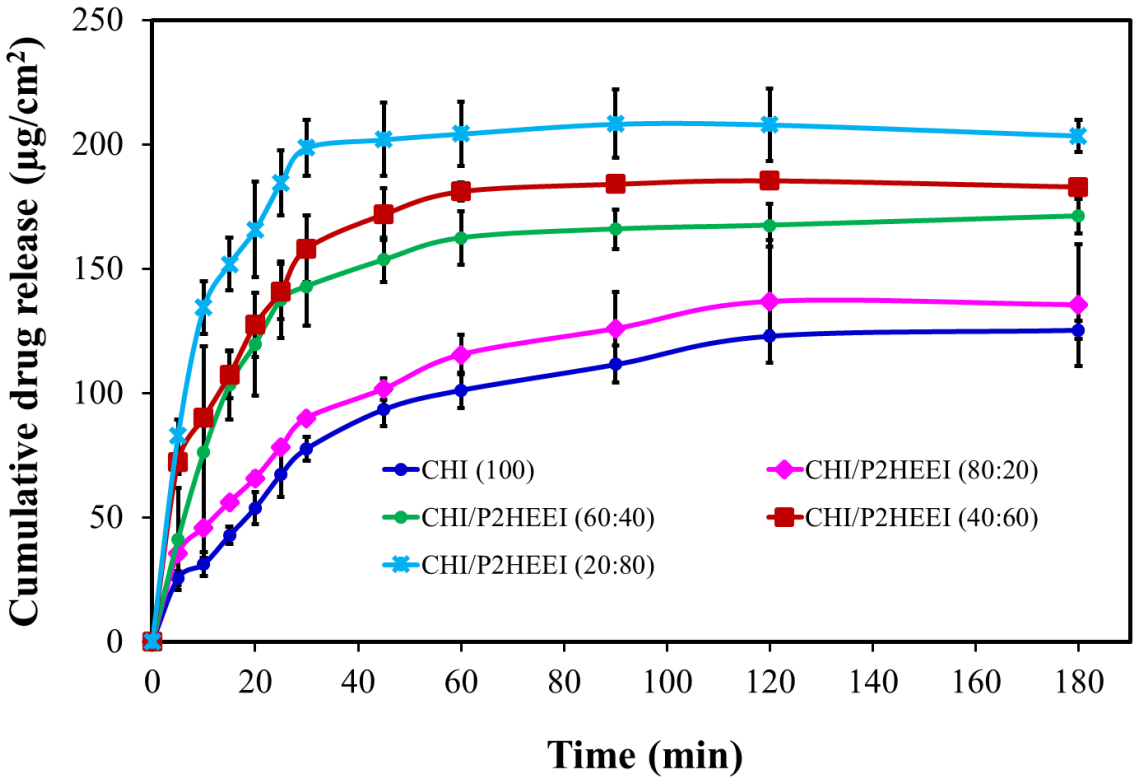

Fig. 10. Cumulative drug release per unit area of haloperidol loaded CHI and their blends with P2HEEI.

The mucoadhesive characteristics of films is an important property that will determine their applicability for buccal drug delivery. Good mucoadhesiveness of the films helps to achieve their longer residence on the buccal mucosa and to maintain high drug concentrations at the site of administration [48]. The tensile method is one of the approaches commonly utilized to examine the mucoadhesive characteristics of various formulations (films, tablet and granule) [49]. In this work, sheep buccal tissues were used as a substrate for mucoadhesion experiments. When CHI and CHI/P2HEEI films with and without haloperidol were placed on and then detached from the buccal tissue, the maximum detachment force (F_{adh}) and total work of adhesion (W_{adh}) were determined **(Fig. 11)**. The results clearly indicated that the films based on pure chitosan exhibited greatest mucoadhesive properties with the highest F_{adh} (0.42 ± 0.09 N) and W_{adh} (0.45 ± 0.13 N·Mm). This was expected as chitosan is known for its strong mucoadhesive properties due to its cationic nature and resulting electrostatic attraction to negatively charged mucosa. According to the literature, the chitosan's hydroxyl groups may form hydrogen bonds with mucin, contributing to excellent mucoadhesive properties further [50]. As the amount of P2HEEI in the films increased, the values for detachment force and

total effort of adhesion tended to decrease progressively, which was consistent with the reduction in mucoadhesive properties. The F_{adh} declined significantly ($P < 0.05$) from 0.42 to 0.12 N and the W_{adh} fall significantly ($P < 0.05$) from 0.45 to 0.16 N·Mm when P2HEEI content in the blends was up to 80% (w/v). This trend was also consistent with our previous research on the mucoadhesive properties of chitosan blends containing hydroxyethylcellulose (HEC) with porcine buccal mucosa [8], which demonstrated that the mucoadhesive properties decreased with increase in the content of HEC. In addition, Abilova et al.[32] developed mucoadhesive films based on chitosan and poly(2-ethyl-2-oxazoline). The result showed that an increase in poly(2-ethyl-2-oxazoline) content in the films showed a gradual reduction in the detachment force and total work of adhesion values [32]. In addition, the mucoadhesiveness of 5% haloperidol-loaded CHI and CHI/P2HEEI films was lower compared to the films without haloperidol. 5% haloperidol loading in films exhibited some loss of mucoadhesive properties when compared to drug-free blends, probably due to the inability of small drug molecules to contribute to mucosal adhesion. This trend was previously observed in chitosan/poly(2-ethyl-2-oxazoline) films loaded with ciprofloxacin [32].

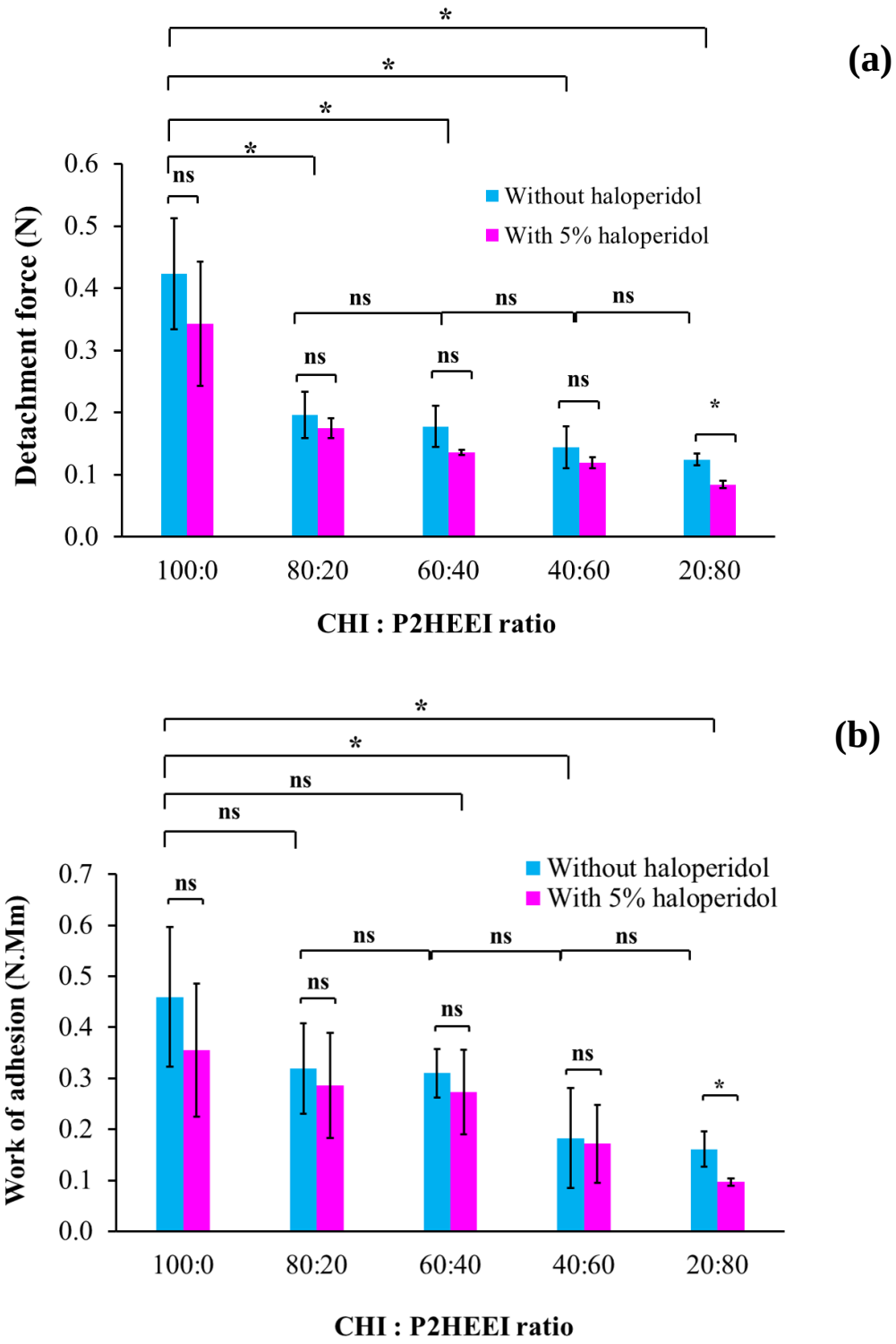

Fig. 11. Detachment force (a) and work of adhesion (b) of CHI/P2HEEI films with and without haloperidol to sheep buccal mucosa as a function of P2HEEI content in the blends. Statistically significant differences are given as: * - $p < 0.05$; ns - no significance.

4. Conclusions

Poly(2-hydroxyethyl ethyleneimine) or P2HEEI was synthesized successfully via nucleophilic substitution reaction of linear polyethyleneimine (L-PEI) with 2-bromoethanol. P2HEEI exhibited good solubility in water, low toxicity in human dermal skin fibroblast cells, and low glass transition temperature (-31.6 °C). The increase in the molar ratio of 2-bromoethanol to L-PEI and increase in the reflux time resulted in higher degree of substitution of P2HEEI. P2HEEI was then blended with chitosan providing novel flexible films, which were prepared by casting in aqueous solutions and then evaporating the solvent. Miscibility and physicochemical properties of these films were investigated. These investigations revealed that the polymers in the blends were completely miscible. Chitosan and P2HEEI based on blends significantly improved the elasticity and mechanical strength of the films. An increase in the amount of P2HEEI in the blends resulted in a greater cumulative release of haloperidol from the films. For *ex vivo* mucoadhesion study with sheep buccal tissue, films based on pure chitosan and its blends with poly(2-hydroxyethyl ethyleneimine) demonstrated mucoadhesive properties; however, this property decreased significantly when the amount of P2HEEI in the films was increased. Therefore, blending chitosan with P2HEEI offers a simple way of modulating the mucoadhesive properties and these formulations have the potential to be used as elastic films for the buccal drug delivery.

CRediT authorship contribution statement

Sitthiphong Soradech: Methodology, Investigation, Validation, Writing an original draft.
Adrian C. Williams: Writing - review & editing, Supervision.
Pattarawadee Kengkwasingh: Performed experiment and analyze data in the part of the cytotoxicity test
Vitaliy V. Khutoryanskiy: Conceptualization, Writing –review & editing, Supervision.

Declaration of Competing Interest

The authors declare that they have no known competing financial interests or personal relationships that could have appeared to influence the work reported in this paper.

Acknowledgments

The authors are grateful to Thailand Institute of Scientific and Technological Research, Ministry of Higher Education, Science, Research and Innovation for funding the PhD studentship of S.S. The assistance of staff at the Chemical Analysis Facility (CAF, University of Reading) with ^{1}H-NMR, FTIR, TGA, DSC, SEM and XRD experiments is also acknowledged.

References

[1] J. Hao, P.W.S. Heng, Buccal delivery systems, Drug Dev. Ind. Pharm. 29 (2003) 821–832. https://doi.org/10.1081/DDC-120024178.

[2] Buccal Drug Delivery System Global Market Report 2023. https://www.globenewswire.com/news-release/2023/05/08/2663585/28124/en/Buccal-Drug-Delivery-System-Global-Market-Report-2023.html#:~:text=The global buccal drug delivery,at a CAGR of 9.7%25. (accessed 2023-07-01).

[3] D.M. Park, Y.K. Song, J.P. Jee, H.T. Kim, C.K. Kim, Development of chitosan-based ondansetron buccal delivery system for the treatment of emesis, Drug Dev. Ind. Pharm. 38 (2012) 1077–1083. https://doi.org/10.3109/03639045.2011.639076.

[4] B. Li, J. Wang, Q. Gui, H. Yang, Drug-loaded chitosan film prepared via facile solution casting and air-drying of plain water-based chitosan solution for ocular drug delivery, Bioact. Mater. 5 (2020) 577–583. https://doi.org/10.1016/j.bioactmat.2020.04.013.

[5] C. Xiao, J. Zhang, Z. Zhang, L. Zhang, Study of blend films from chitosan and hydroxypropyl guar gum, J. Appl. Polym. Sci. 90 (2003) 1991–1995. https://doi.org/10.1002/app.12766.

[6] J.Y. Hao, F.L. Mi, S.S. Shyu, Y.B. Wu, J.Y. Schoung, Y.H. Tsai, Y. Bin Huang, Control of wound infections using a bilayer chitosan wound dressing with sustainable antibiotic delivery, J. Biomed. Mater. Res. 59 (2002) 438–449. https://doi.org/10.1002/jbm.1260.

[7] A.S. Can, M.S. Erdal, S. Güngör, Y. Özsoy, Optimization and characterization of chitosan films for transdermal delivery of ondansetron, Molecules. 18 (2013) 5455–

5471. https://doi.org/10.3390/molecules18055455.

[8] K. Luo, J. Yin, O. V. Khutoryanskaya, V. V. Khutoryanskiy, Mucoadhesive and elastic films based on blends of chitosan and hydroxyethylcellulose, Macromol. Biosci. 8 (2008) 184–192. https://doi.org/10.1002/mabi.200700185.

[9] G.K. Abilova, D.B. Kaldybekov, E.K. Ozhmukhametova, A.Z. Saimova, D.S. Kazybayeva, G.S. Irmukhametova, V. V. Khutoryanskiy, Chitosan/poly(2-ethyl-2-oxazoline) films for ocular drug delivery: Formulation, miscibility, in vitro and in vivo studies, Eur. Polym. J. 116 (2019) 311–320. https://doi.org/10.1016/j.eurpolymj.2019.04.016.

[10] S. Soradech, P. Kengkwasingh, A.C. Williams, V. V Khutoryanskiy, Synthesis and Evaluation of Poly (3-hydroxypropyl Ethylene-imine) and Its Blends with Chitosan Forming Novel Elastic Films for Delivery of Haloperidol, Pharmaceutics. 14 (2022) 1–22. https://doi.org/https://doi.org/10.3390/pharmaceutics14122671.

[11] J. Yin, K. Luo, X. Chen, V. V. Khutoryanskiy, Miscibility studies of the blends of chitosan with some cellulose ethers, Carbohydr. Polym. 63 (2006) 238–244. https://doi.org/10.1016/j.carbpol.2005.08.041.

[12] E. Marsano, S. Vicini, J. Skopińska, M. Wisniewski, A. Sionkowska, Chitosan and poly(vinyl pyrrolidone): Compatibility and miscibility of blends, Macromol. Symp. 218 (2004) 251–260. https://doi.org/10.1002/masy.200451426.

[13] N.F. Mohd Nasir, N.M. Zain, M.G. Raha, N.A. Kadri, Characterization of Chitosan-poly (Ethylene Oxide) Blends as Haemodialysis Membrane, Am. J. Appl. Sci. 2 (2005) 1578–1583. https://doi.org/10.3844/ajassp.2005.1578.1583.

[14] M. Serres-Gómez, G. González-Gaitano, D.B. Kaldybekov, E.D.H. Mansfield, V. V Khutoryanskiy, J.R. Isasi, C.A. Dreiss, Supramolecular Hybrid Structures and Gels from Host-Guest Interactions between α-Cyclodextrin and PEGylated Organosilica Nanoparticles., Langmuir. 34 (2018) 10591–10602. https://doi.org/10.1021/acs.langmuir.8b01744.

[15] J.T. Yeh, C.L. Chen, K.S. Huang, Y.H. Nien, J.L. Chen, P.Z. Huang, Synthesis, characterization, and application of PVP/chitosan blended polymers, J. Appl. Polym. Sci. 101 (2006) 885–891. https://doi.org/10.1002/app.23517.

[16] X. Shan, S. Aspinall, D.B. Kaldybekov, F. Buang, A.C. Williams, V. V. Khutoryanskiy, Synthesis and Evaluation of Methacrylated Poly(2-ethyl-2-oxazoline) as a Mucoadhesive Polymer for Nasal Drug Delivery, ACS Appl. Polym. Mater. (2021). https://doi.org/10.1021/acsapm.1c01097.

[17] M.A. Mees, R. Hoogenboom, Full and partial hydrolysis of poly(2-oxazoline)s and the subsequent post-polymerization modification of the resulting polyethylenimine (co)polymers, Polym. Chem. 9 (2018) 4968–4978. https://doi.org/10.1039/c8py00978c.

[18] C.N. Lungu, M. V. Diudea, M. V. Putz, I.P. Grudziński, Linear and branched PEIs (Polyethylenimines) and their property space, Int. J. Mol. Sci. 17 (2016). https://doi.org/10.3390/ijms17040555.

[19] Y. Chatani, H. Tadokoro, T. Saegusa, H. Ikeda, Structural Studies of Poly (ethylenimine). 1. Structures of Two Hydrates of Poly (ethylenimine): Sesquihydrate and Dihydrate, Macromolecules. 14 (1981) 315–321. https://doi.org/10.1021/ma50003a017.

[20] H.P.C. Van Kuringen, J. Lenoir, E. Adriaens, J. Bender, B.G. De Geest, R. Hoogenboom, Partial Hydrolysis of Poly(2-ethyl-2-oxazoline) and Potential Implications for Biomedical Applications?, Macromol. Biosci. 12 (2012) 1114–1123. https://doi.org/10.1002/mabi.201200080.

[21] J.J. Yuan, R.H. Jin, Fibrous crystalline hydrogels formed from polymers possessing a linear poly(ethyleneimine) backbone, Langmuir. 21 (2005) 3136–3145. https://doi.org/10.1021/la047182l.

[22] S.M. Moghimi, P. Symonds, J.C. Murray, A.C. Hunter, G. Debska, A. Szewczyk, A two-stage poly(ethylenimine)-mediated cytotoxicity: Implications for gene transfer/therapy, Mol. Ther. 11 (2005) 990–995. https://doi.org/10.1016/j.ymthe.2005.02.010.

[23] S. Taranejoo, J. Liu, P. Verma, K. Hourigan, A review of the developments of characteristics of PEI derivatives for gene delivery applications, J. Appl. Polym. Sci. 132 (2015). https://doi.org/10.1002/app.42096.

[24] S. Patil, R. Lalani, P. Bhatt, I. Vhora, V. Patel, H. Patel, A. Misra, Hydroxyethyl

substituted linear polyethylenimine for safe and efficient delivery of siRNA therapeutics, RSC Adv. 8 (2018) 35461–35473. https://doi.org/10.1039/C8RA06298F.

[25] S. Soradech, A.C. Williams, V. V. Khutoryanskiy, Physically Cross-Linked Cryogels of Linear Polyethyleneimine: Influence of Cooling Temperature and Solvent Composition, Macromolecules. 55 (2022) 9537–9546. https://doi.org/10.1021/acs.macromol.2c01308.

[26] X. Shan, A.C. Williams, V. V. Khutoryanskiy, Polymer structure and property effects on solid dispersions with haloperidol: Poly(N-vinyl pyrrolidone) and poly(2-oxazolines) studies, Int. J. Pharm. 590 (2020) 119884. https://doi.org/10.1016/j.ijpharm.2020.119884.

[27] O. Sedlacek, O. Janouskova, B. Verbraeken, H. Richard, Straightforward Route to Superhydrophilic Poly(2-oxazoline)s via Acylation of Well-Defined Polyethylenimine, Biomacromolecules. 20 (2018). https://doi.org/10.1021/acs.biomac.8b01366.

[28] M.T. Cook, G. Tzortzis, D. Charalampopoulos, V. V. Khutoryanskiy, Production and evaluation of dry alginate-chitosan microcapsules as an enteric delivery vehicle for probiotic bacteria, Biomacromolecules. 12 (2011) 2834–2840. https://doi.org/10.1021/bm200576h.

[29] S. Soradech, J. Nunthanid, S. Limmatvapirat, M. Luangtana-Anan, An approach for the enhancement of the mechanical properties and film coating efficiency of shellac by the formation of composite films based on shellac and gelatin, J. Food Eng. 108 (2012) 94–102. https://doi.org/10.1016/j.jfoodeng.2011.07.019.

[30] S. Soradech, S. Limatvapirat, M. Luangtana-anan, Stability enhancement of shellac by formation of composite film: Effect of gelatin and plasticizers, J. Food Eng. 116 (2013) 572–580. https://doi.org/10.1016/j.jfoodeng.2012.12.035.

[31] M.K. Samanta, R. Dube, B. Suresh, Transdermal drug delivery system of haloperidol to overcome self-induced extrapyramidal syndrome, Drug Dev. Ind. Pharm. 29 (2003) 405–415. https://doi.org/10.1081/DDC-120018376.

[32] G.K. Abilova, D.B. Kaldybekov, G.S. Irmukhametova, D.S. Kazybayeva, Z.A. Iskakbayeva, S.E. Kudaibergenov, V. V. Khutoryanskiy, Chitosan/poly(2-ethyl-2-oxazoline) films with ciprofloxacin for application in vaginal drug delivery, Materials

(Basel). 13 (2020). https://doi.org/10.3390/ma13071709.

[33] T. Saegusa, H. Ikeda, H. Fujii, Crystalline Polyethylenimine, Macromolecules. 5 (1972) 108. https://doi.org/10.1021/ma60025a029.

[34] V. V. Khutoryanskiy, M.G. Cascone, L. Lazzeri, N. Barbani, Z.S. Nurkeeva, G.A. Mun, A.B. Bitekenova, A.B. Dzhusupbekova, Hydrophilic films based on blends of poly(acrylic acid) and poly(2-hydroxyethyl vinyl ether): Thermal, mechanical, and morphological characterization, Macromol. Biosci. 3 (2003) 117–122. https://doi.org/10.1002/mabi.200390017.

[35] H.P.C. Van Kuringen, J. Lenoir, E. Adriaens, J. Bender, B.G. De Geest, R. Hoogenboom, Partial Hydrolysis of Poly(2-ethyl-2-oxazoline) and Potential Implications for Biomedical Applications?, Macromol. Biosci. 12 (2012) 1114–1123. https://doi.org/10.1002/mabi.201200080.

[36] J. Kronek, E. Paulovicova, In vitro bio-immunological and cytotoxicity studies of poly (2-oxazolines), (2011). https://doi.org/10.1007/s10856-011-4346-z.

[37] I. Leceta, P. Guerrero, I. Ibarburu, M.T. Dueñas, K. De La Caba, Characterization and antimicrobial analysis of chitosan-based films, J. Food Eng. 116 (2013) 889–899. https://doi.org/10.1016/j.jfoodeng.2013.01.022.

[38] C.L. Silva, J.C. Pereira, A. Ramalho, A.A.C.C. Pais, J.J.S. Sousa, Films based on chitosan polyelectrolyte complexes for skin drug delivery: Development and characterization, J. Memb. Sci. 320 (2008) 268–279. https://doi.org/10.1016/j.memsci.2008.04.011.

[39] Y.I. Matveev, V.Y. Grinberg, V.B. Tolstoguzov, The plasticizing effect of water on proteins, polysaccharides and their mixtures. Glassy state of biopolymers, food and seeds, Food Hydrocoll. 14 (2000) 425–437. https://doi.org/10.1016/S0268-005X(00)00020-5.

[40] K. Sakurai, T. Maegawa, T. Takahashi, Glass transition temperature of chitosan and miscibility of chitosan/poly(N-vinyl pyrrolidone) blends, Polymer (Guildf). 41 (2000) 7051–7056. https://doi.org/10.1016/S0032-3861(00)00067-7.

[41] W. Brostow, R. Chiu, I.M. Kalogeras, A. Vassilikou-Dova, Prediction of glass transition temperatures: Binary blends and copolymers, Mater. Lett. 62 (2008) 3152–

3155. https://doi.org/10.1016/j.matlet.2008.02.008.

[42] D.W. Seong, J.S. Yeo, S.H. Hwang, Fabrication of polycarbonate blends with poly(methyl methacrylate-co-phenyl methacrylate) copolymer: Miscibility and scratch resistance properties, J. Ind. Eng. Chem. 36 (2016) 251–254. https://doi.org/10.1016/j.jiec.2016.02.005.

[43] V. Rao, P. V. Ashokan, M.H. Shridhar, Studies on the compatibility and specific interaction in cellulose acetate hydrogen phthalate (CAP) and poly methyl methacrylate (PMMA) blend, Polymer (Guildf). 40 (1999) 7167–7171. https://doi.org/10.1016/S0032-3861(99)00311-0.

[44] A. Shubha, S.R. Manohara, L. Gerward, Influence of polyvinylpyrrolidone on optical, electrical, and dielectric properties of poly(2-ethyl-2-oxazoline)-polyvinylpyrrolidone blends, J. Mol. Liq. 247 (2017) 328–336. https://doi.org/10.1016/j.molliq.2017.09.086.

[45] M.G.A. Vieira, M.A. Da Silva, L.O. Dos Santos, M.M. Beppu, Natural-based plasticizers and biopolymer films: A review, Eur. Polym. J. 47 (2011) 254–263. https://doi.org/10.1016/j.eurpolymj.2010.12.011.

[46] A. Abruzzo, T. Cerchiara, B. Luppi, F. Bigucci, Transdermal Delivery of Antipsychotics: Rationale and Current Status, CNS Drugs. 33 (2019) 849–865. https://doi.org/10.1007/s40263-019-00659-7.

[47] G. Sushmita, J. Maha Lakshmi, K.S.S. Prathyusha, Y. Srinivasa Rao, Formulation and evaluation of haloperdiol-carrier loaded buccal film, Int. J. Curr. Adv. Res. 7 (2018) 5–10. http://dx.doi.org/10.24327/ijcar.2018.15700.2875.

[48] P. Kraisit, S. Limmatvapirat, M. Luangtana-Anan, P. Sriamornsak, Buccal administration of mucoadhesive blend films saturated with propranolol loaded nanoparticles, Asian J. Pharm. Sci. 13 (2018) 34–43. https://doi.org/10.1016/j.ajps.2017.07.006.

[49] M. Davidovich-Pinhas, H. Bianco-Peled, Mucoadhesion: A review of characterization techniques, Expert Opin. Drug Deliv. 7 (2010) 259–271. https://doi.org/10.1517/17425240903473134.

[50] I.A. Sogias, A.C. Williams, V. V. Khutoryanskiy, Why is chitosan mucoadhesive?, Biomacromolecules. 9 (2008) 1837–1842. https://doi.org/10.1021/bm800276d.

Supporting Information

Synthesis of poly(2-hydroxyethyl ethyleneimine) and its mucoadhesive film formulations based on blends with chitosan for buccal delivery of haloperidol

Sitthiphong Soradech [1, 2], Pattarawadee Kengkwasingh [2], Adrian C. Williams [1], and Vitaliy V. Khutoryanskiy [1*]

[1] Reading School of Pharmacy, University of Reading, Whiteknights, Reading, RG6 6AX, UK

[2] Expert Centre of Innovative Herbal Products, Thailand Institute of Scientific and Technological Research, Pathum Thani, 12120, Thailand.

***Corresponding author:**

Postal address: School of Pharmacy, University of Reading, Whiteknights, RG6 6AX, Reading, United Kingdom

E-mail address: v.khutoryanskiy@reading.ac.uk

Telephone: +44(0) 118 378 6119

Fax: +44(0) 118 378 4703

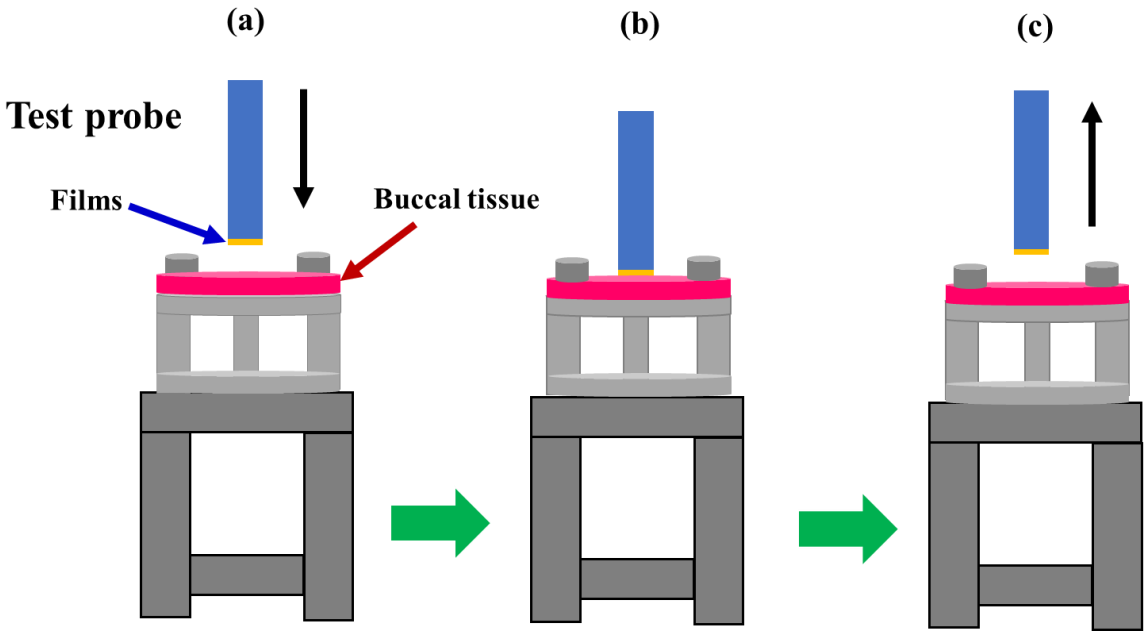

Fig. S1. Scheme process of *ex vivo* mucoadhesive test using texture analyzer with a mucoadhesive holder. (a) The probe with CHI and CHI/P2HEEI films was moved downward. (b) Film was attached to sheep buccal mucosa. (c) The probe is withdrawn at a specified rate.

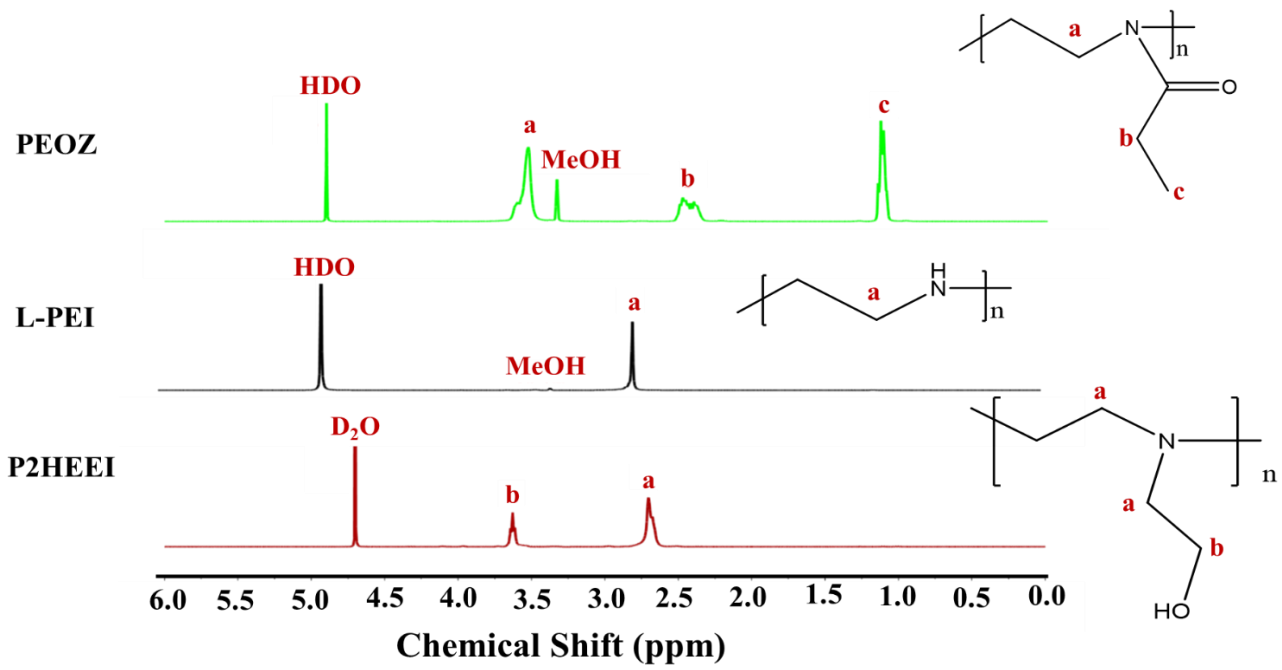

Fig. S2. ^{1}H-NMR spectra of PEOZ and L-PEI (MeOH-d_4) while P2HEEI (D_2O).

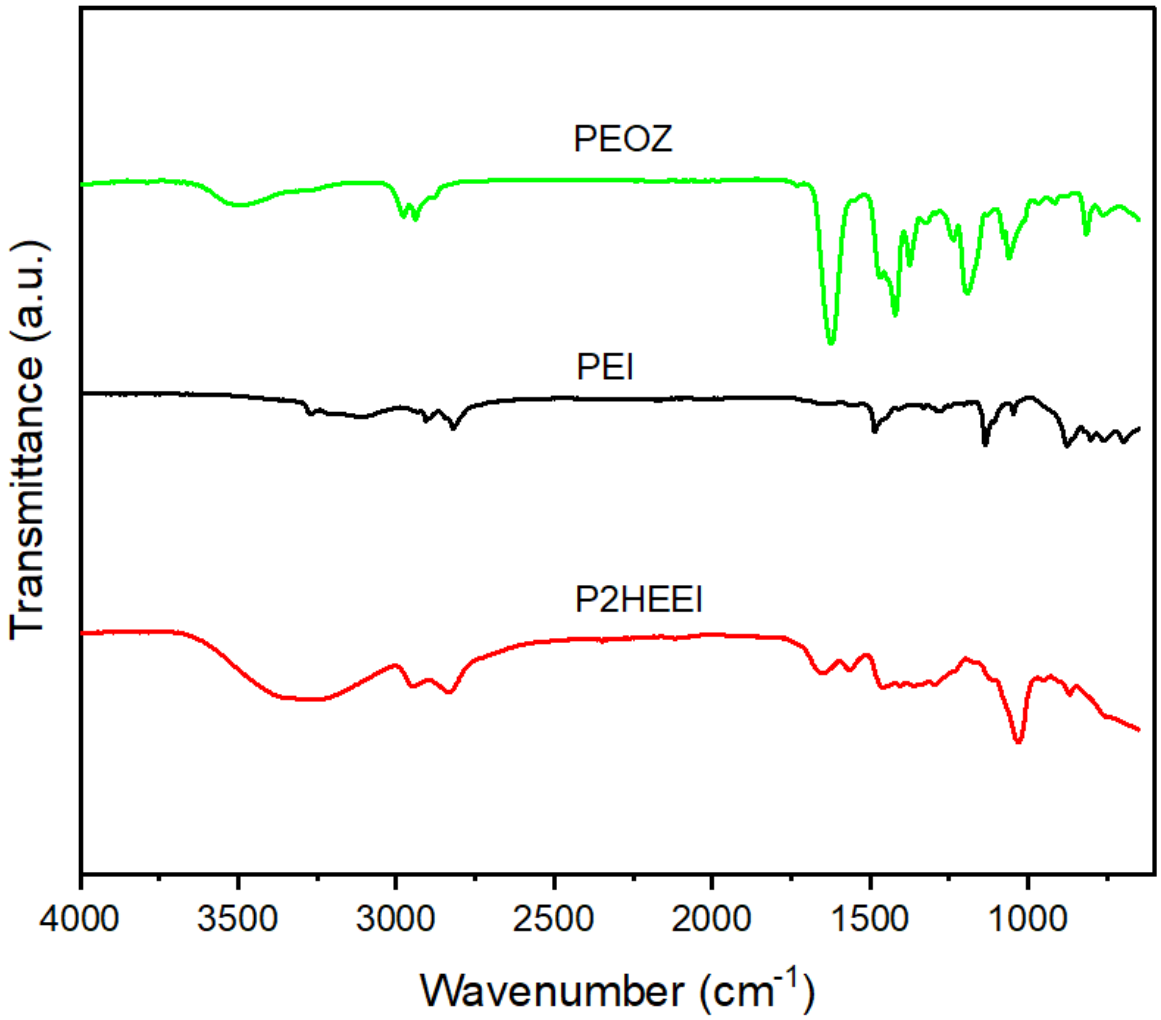

Fig. S3. FTIR spectra of PEOZ, LPEI, and P2HEEI.

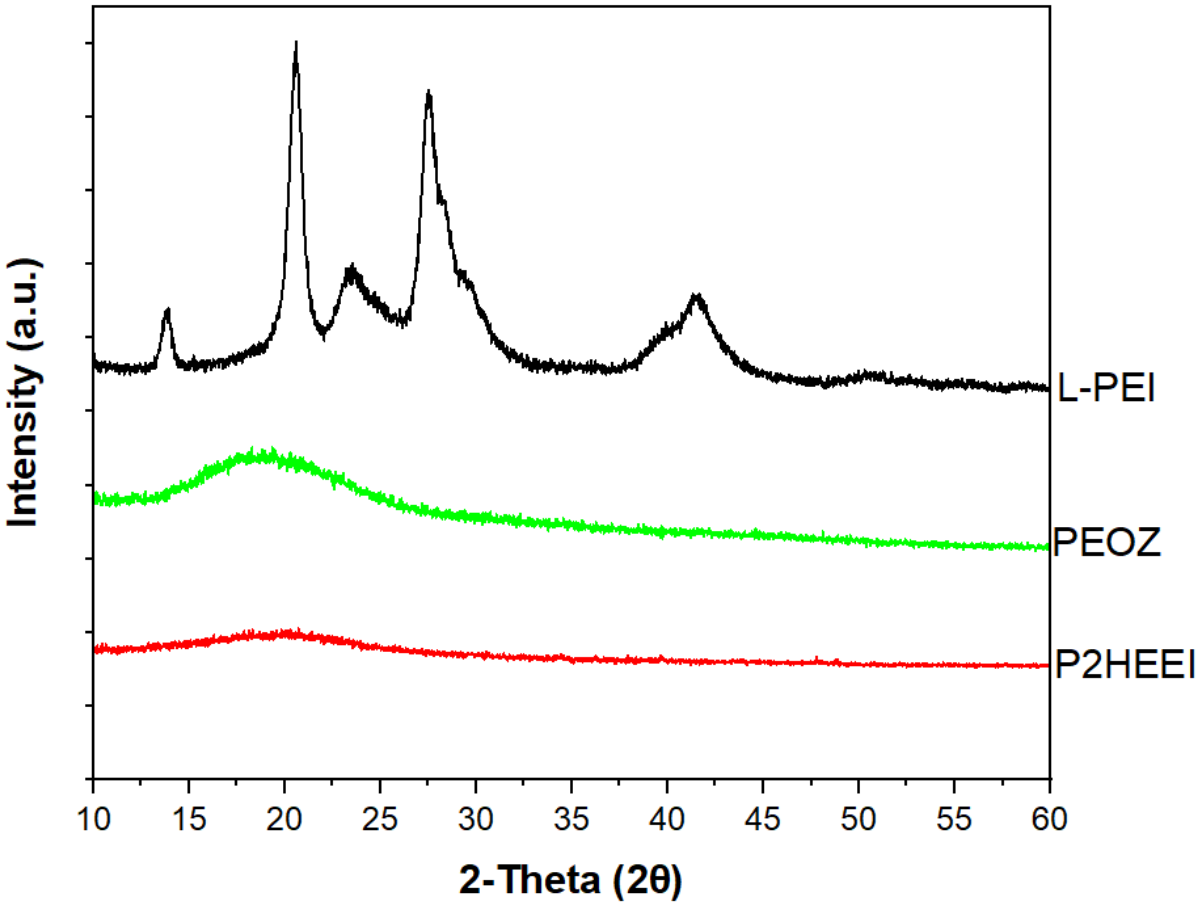

Fig. S4. X-ray diffractograms of PEOZ, LPEI and P2HEEI.

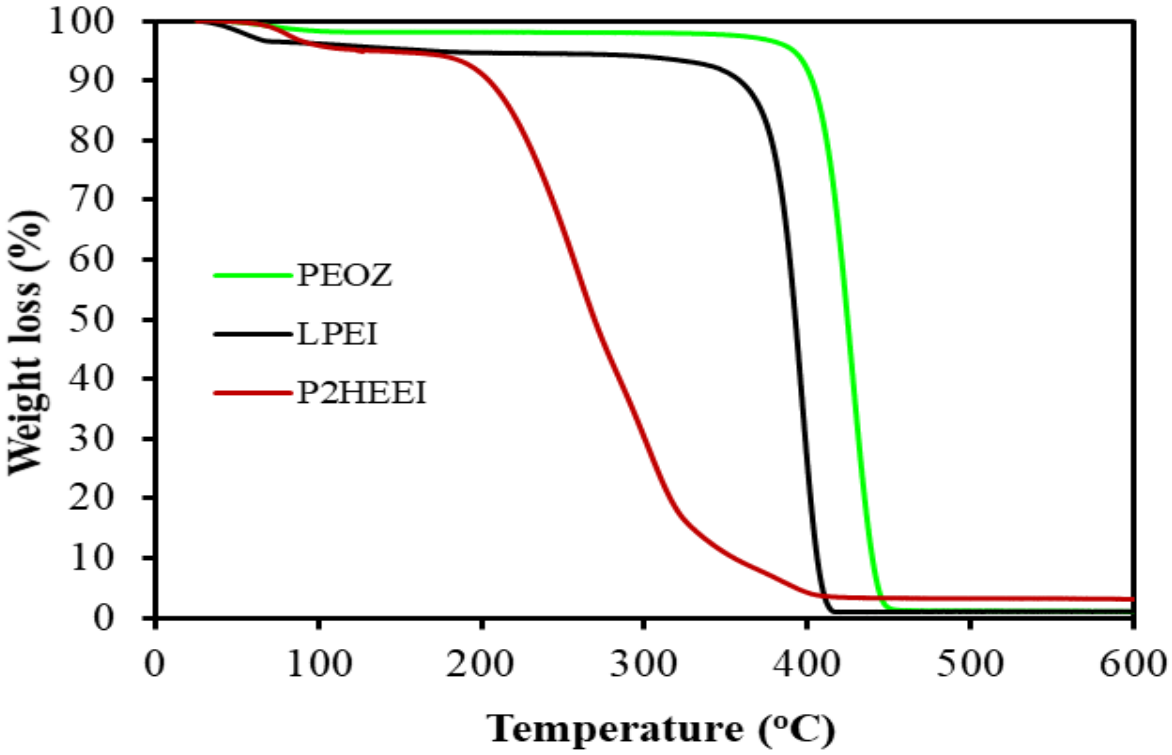

Fig. S5. TGA thermograms of PEOZ, LPEI and P2HEEI.

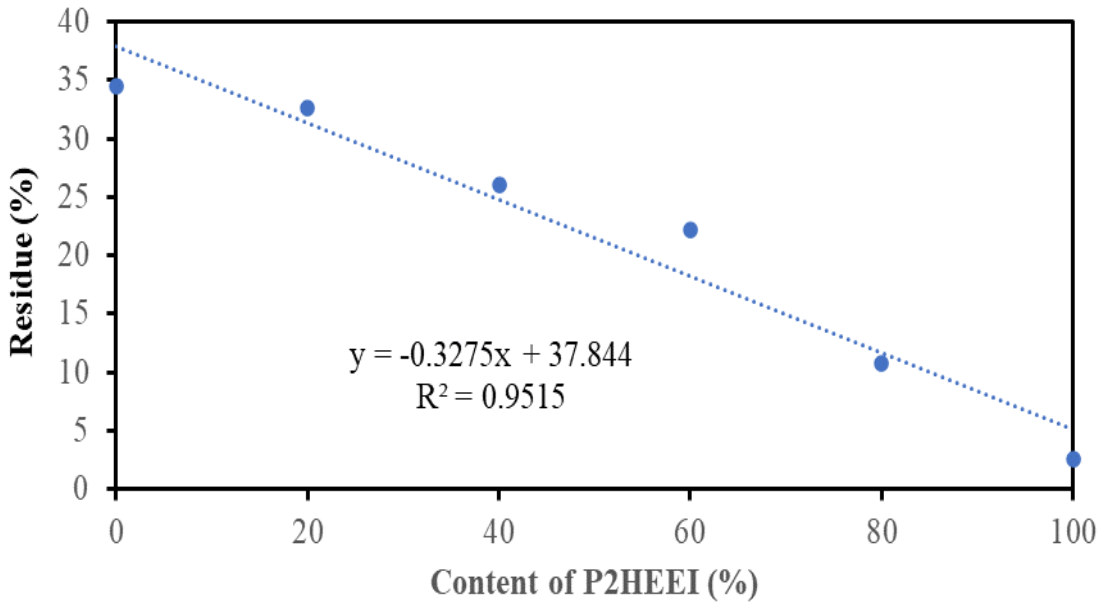

Fig. S6. Correlation between residue and amount of P2HEEI in CHI/P2HEEI blends.

Table S1. Thickness of CHI and CHI/P2HEEI films

Films	**Thickness (mm)**
CHI (100)	0.06 ± 0.01
CHI/P2HEEI (80:20)	0.06 ± 0.01
CHI/P2HEEI (60:40)	0.07± 0.02
CHI/P2HEEI (40:60)	0.07 ± 0.01
CHI/P2HEEI (20:80)	0.07 ± 0.01

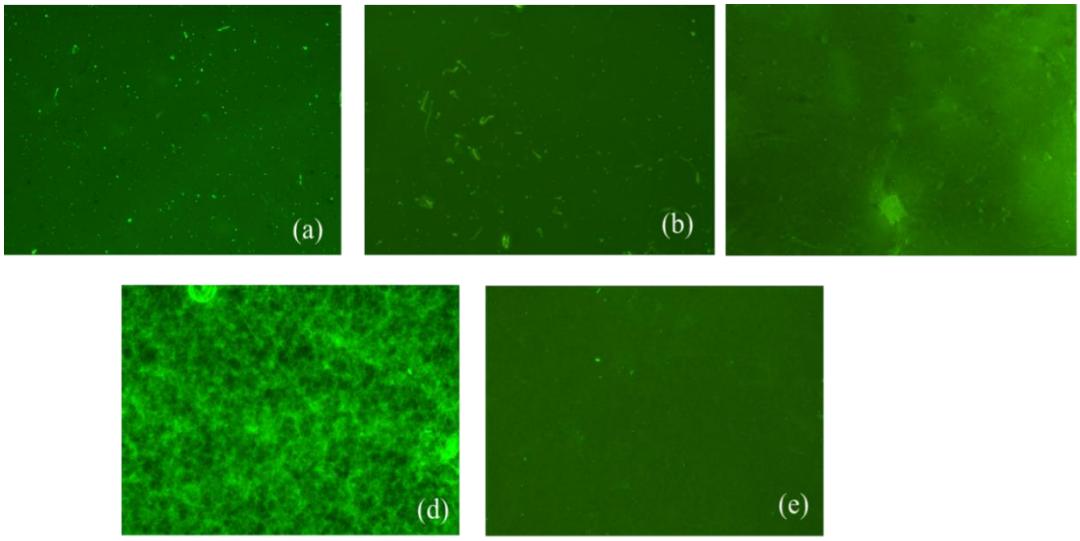

Fig. S7. Fluorescent microscopy images of film surfaces (A) and cross-section (B) of CHI (a) and their blends (b, c, d, and e). Content of P2HPEEI in the blends: 20 (b), 40 (c), 60 (d) and 80 % (e).

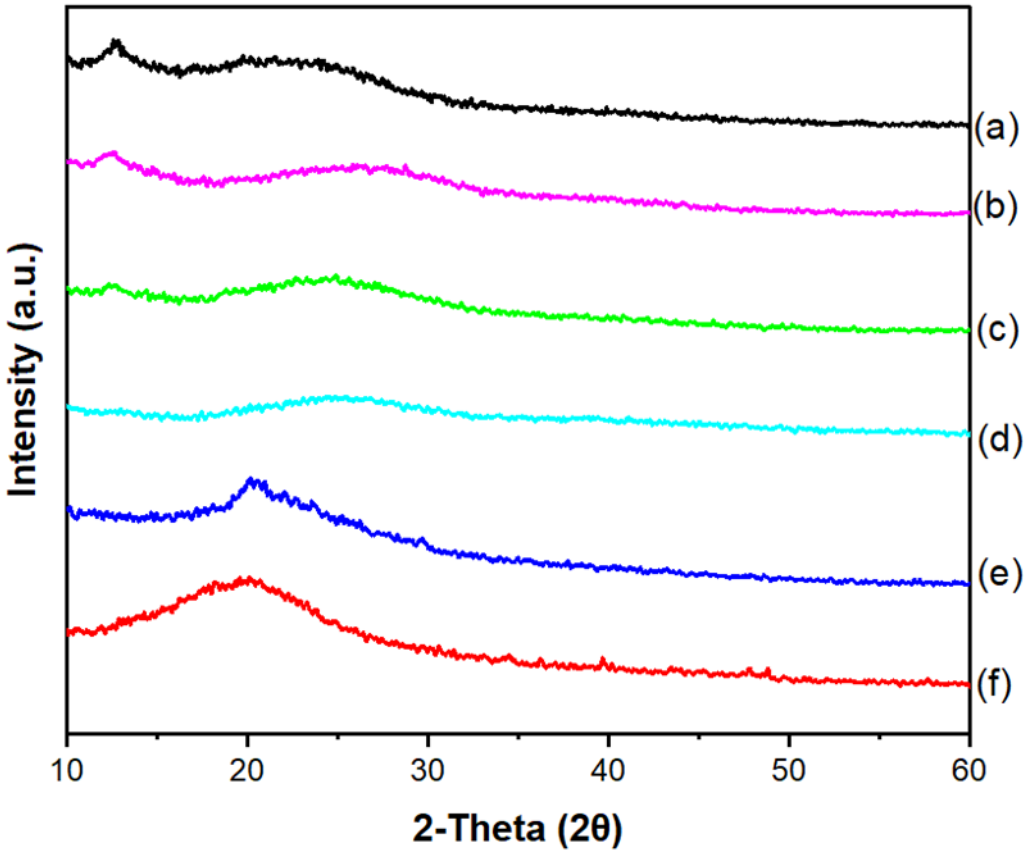

Fig. S8. X-ray diffractograms of CHI (a), their blends (b, c, d and e), and P2HEEI (f).

Content of P2HEEI in the blends: 20 (b), 40 (c), 60 (d) and 80 % (e).

Chapter 5

General Conclusions and Future Work

5.1. General conclusions

The key findings of the PhD project as well as potential future work are detailed in this concluding chapter. This PhD project was focused on the synthesis and evaluation of linear polyethyleneimine and its derivatives as potential biomaterials and excipients for drug delivery.

Polyethyleneimine (PEI) is a cationic polymer consisting of two carbon aliphatic (-CH_2CH_2-) spacer groups and primary, secondary and tertiary amine groups in each repeating unit. PEI is either linear or branched, which differ in structure and some properties [1]. In linear PEI all amine groups are secondary whereas branched PEI has primary, secondary and tertiary amine groups. Branched PEI is usually synthesized by ring-opening polymerization of aziridine and L-PEI can be prepared by hydrolysis of poly(2-ethyl-2-oxazoline) under acidic or basic conditions to eliminate all the amide groups in the side chains[2,3]. Branched PEI is an amorphous polymer that is readily soluble in water [4], whereas L-PEI is semi-crystalline and only dissolves in water at high temperatures. PEI is used in a wide range of applications, including gene delivery[5], pharmaceutical[1], antimicrobial[6, 7] and enviromental applications[8]. Therefore, chapter 1 describes the introduction and literature review about polyethyleneimine and its derivatives for pharmaceutical and biomedical applications. The synthesis methods of linear PEI and branched PEI have been reported in this review. Physical properties of both PEIs including solid-state properties and behavior in aqueous and non-aqueous solutions were also discussed. The studies of complex formation of PEIs and anionic polymers, as well as metal ions, have been described. The toxicity of both PEIs was then assessed using a variety of techniques, including cytotoxicity, slug mucosal irritation (SMI), and cytogenomic testing. Various methods used to synthesize modified PEI have been considered and critically evaluated. When compared to unmodified PEIs, PEI derivatives can improve biocompatibility, transfection efficiency, solubility, and toxicity. PEI and modified PEI can be used in a wide range of pharmaceutical and biomedical applications, including gene delivery, mucoadhesive properties, transdermal drug delivery, antibacterial agents, hydrogels, polymer blends, as well as scaffolds for tissue and stem cell engineering. Therefore, PEI and its derivatives may have future applications in pharmaceutical and biomedical industries.

Chapter 2 focuses on the development of physically crosslinked cryogels based on L-PEI. Polymeric gels are extensively used for biomedical applications due to their flexibility, high water content, biocompatibility, and softness [9]. They are also widely used in drug delivery systems, chromatography, as immobilization matrices, for biomedical scaffolds and in wound healing products. Gels are defined as three-dimensional cross-linked polymer networks, which are swollen in solvents [10, 11]. Networks swollen in water provide hydrogels, whereas those swelling in an organic solvent are organogels. Polymeric gels are broadly classified as physical and chemical gels. Physical gels can be prepared through physical crosslinking of polymer chains via hydrophobic effects, ionic or hydrogen bonds and through the formation of crystallites within the network. Physical gels commonly re-dissolve upon changes in environmental conditions such as temperature, ionic strength, and pH. In contrast, chemical gels form by cross-linking through covalent bonds, leading to irreversibly insoluble networks [12]. The cryogels based on L-PEI were prepared by freeze/thaw processing of concentrated L-PEI solutions in water. The physical nature of their crosslinking was also validated by demonstrating that the cryogels melt and form a clear solution upon heating to 80 ^{o}C due to the melting of the L-PEI crystalline domains. L-PEI cryogels were found to have a higher enthalpy of melting, crystallinity, and strength when cooled to temperatures below 0 ^{o}C. Additionally, increasing ethanol content in water-ethanol mixture used to prepare L-PEI cryogels resulted in a decrease in mechanical strength, crystallinity, and viscosity. This could be because the intermolecular hydrogen bonds between NH-O and OH-N in L-PEI decreased, most likely due to hydrogen bond competition from the solvent molecules. This study demonstrates that the physical properties of L-PEI cryogels can be manipulated by controlling the cooling rate and solvent composition used to form the cryogels. Hence, due to the unique chemical and physical properties of L-PEI, these novel physical cryogels have high potential for biomedical, pharmaceutical, wound healing, and antimicrobial applications. However, L-PEI typically dissolves in water at high temperatures [4] and has been shown to cause cytotoxicity. Hence, there are limitations of L-PEI cryogels for biomedical, pharmaceutical, wound healing, and antimicrobial applications. The solubility and toxicity of L-PEI is naturally a significant concern when considering its use in pharmaceutical and biomedical applications [14]. Next a study, we attempted to synthesize poly(2-hydroxyethyl ethyleneimine), P2HEEI and poly(3-hydroxypropyl ethyleneimine), P3HPEI as potential biomaterials and excipients for drug delivery.

Chemical modification of L-PEI is one approach to increase its water solubility and decrease its toxicity[15]. P2HEEI and P3HPEI were synthesized via nucleophilic substitution reaction between L-PEI and 2-bromoethanol and 3-bromo-1-propanol, respectively. Both polymers had a good water solubility, low toxicity, and a low glass transition temperature. However, neither polymer would be capable of freezing and thawing to form cryogels. Therefore, due to the lower glass transition below 0 ^{o}C, these novel polymers were blended with chitosan for improving mechanical properties and the resulting polymeric films were evaluated for their applicability in transmucosal drug delivery. Here, we selected poly(3-hydroxypropyl ethyleneimine) as a suitable candidate to blend with chitosan to produce films to deliver haloperidol and report, for the first time, its synthesis using nucleophilic substitution reaction of linear polyethyleneimine with 3-bromo-1-propanol. ^{1}H-NMR and FTIR spectroscopies confirmed the successful conversion of L-PEI to P3HPEI. P3HPEI had good solubility in water and was significantly less toxic than the parent L-PEI. It had a low glass transition temperature (T_g = −38.6 °C). Consequently, this new polymer was blended with chitosan to improve mechanical properties, and these materials were used for the rapid delivery of haloperidol. Films were prepared by casting from aqueous solutions and then evaporating the solvent. The blends of chitosan and P3HPEI were miscible in the solid state and the inclusion of P3HPEI improved the mechanical properties of the films, producing more elastic materials. A 35:65 (%w/w) blend of chitosan–P3HPEI provided the optimum glass transition temperature for transmucosal drug delivery and so was selected for further investigation with haloperidol, which was chosen as a model hydrophobic drug. Microscopic and X-ray diffractogram (XRD) data indicated that the solubility of the drug in the films was ~1.5%. The inclusion of the hydrophilic polymer P3HPEI allowed rapid drug release within ~30 min, after which films disintegrated, demonstrating that the formulations are suitable for application to mucosal surfaces, such as in buccal drug delivery. Higher release with increasing drug loading allows flexible dosing. Blending P3HPEI with chitosan thus allows the selection of desirable physicochemical and mechanical properties of the films for delivery of haloperidol as a poorly water-soluble drug. However, the preparation of novel films based on P3HPEI and chitosan resulted in cloudy materials, and the elasticity of this composite film remained low due to the long alkyl side chain. In a subsequent study, we attempted to develop novel films based on P2HEEI and chitosan to obtain transparent films with excellent mechanical properties that were suitable for buccal administration of haloperidol.

Buccal drug delivery is commonly used to administer drugs through the buccal mucosa to provide local or systemic pharmacological effects [16]. It has generated interest as a potential

alternative to gastrointestinal drug delivery. The advantages of the buccal route include direct access to the systemic circulation via the internal jugular vein, rapid onset of action, possibility to by-pass hepatic first-pass metabolism, avoidance of gastrointestinal acid hydrolysis, increased patient compliance, and suitability for drugs or excipients that cause mild and reversible mucosal damage or irritation [17]. Mucoadhesive films are one of commercially relevant formulations for buccal drug delivery due to their adaptability and ease of use. Additionally, it can prolong the time spent on the mucosa, increasing the permeability of the buccal epithelial lining as well as it is capable of directly delivering a precise dose of the drug to the mucosa [17, 18]. Hence, chapter 4 focuses on the development of novel flexible and mucoadhesive films based on blends of chitosan and poly (2-hydroxyethyl ethyleneimine) as potential platform for buccal delivery of haloperidol. Initially, P2HEEI was synthesized via nucleophilic substitution of linear polyethyleneimine (L-PEI) with 2-bromoethanol. P2HEEI exhibited good solubility in water, low toxicity in human dermal skin fibroblast cells, and low glass transition temperature (-31.6 ^{o}C). This polymer was then blended with chitosan to improve mechanical properties and these materials were used for the buccal delivery of haloperidol. Polymeric films based on chitosan and its blends with P2HEEI were prepared by casting from aqueous solutions that the investigation of these films using differential scanning calorimetry and scanning electron microscopy confirmed that chitosan and P2HEEI form completely miscible blends with good transparency. Blending chitosan with P2HEEI improved the mechanical properties of the films, resulting in more elastic materials that were superior to those based on P3HPEI and chitosan. Blend films were also prepared loaded with haloperidol as a model poorly water-soluble drug. The cumulative release of haloperidol from the films increased when the blends were prepared with greater P2HEEI content. Mucoadhesive properties of these films with respect to freshly excised sheep buccal mucosa were evaluated using a tensile method. It was found that all films are mucoadhesive; however, an increase in P2HEEI content in the blend resulted in a gradual reduction of their ability to adhere to the buccal mucosa. These films could potentially find applications in buccal drug delivery. Further, this research will be conducted on *in vivo* studies and mucosal irritation test of haloperidol-loaded chitosan-P2HEEI films as followed from Samanta et al. [19]

Therefore, L-PEI and its derivatives have potential as materials for pharmaceutical applications, allowing for the development of novel formulations such as cryogels, drug-loaded films for poorly water-soluble drug administration, and mucoadhesive drug delivery systems.

5.2. Future work

5.2.1. Evaluation of antimicrobial activity of physically crosslinked cryogels based L-PEI

Physically crosslinked cryogels with antimicrobial properties and surface charge control would be beneficial for biomedical, wound healing, and pharmaceutical applications. Therefore, physical cryogels based on cationic polymers are of interest for antimicrobial applications[3]. PEIs are cationic polymers, which widely used as antimicrobial agents due to the positive charge, causing an electrostatic binding to the surfaces of bacterial cells [7, 20]. To the best of our knowledge, there are no reports in the literature on antimicrobial activity of physically crosslinked cryogels based L-PEI. Thus, the antibacterial activity of L-PEI-based physical cryogels used in antimicrobial wound dressings will be investigated.

5.2.2. Tissue irritation and *in vivo* studies of haloperidol-loaded novel films for buccal drug delivery

Haloperidol (HP), an antipsychotic drug, is associated with side effects of drug-induced extrapyramidal syndrome (EPS) in conventional monotherapy [19]. It is poorly water-soluble and is commonly formulated as solutions for oral administration or injections, and as tablets [21]. The average oral dose of haloperidol ranges from 0.5 to 30 mg per day [22]. Further, HP is a BCS class 2 drug, characterized by low solubility but high permeability[23] and has poor oral bioavailability (59%)[22]. From chapter III and IV in this thesis, we prepared HP loaded films and then characterised their physicochemical properties, mucoadhesive properties *ex vivo* and *in vitro* drug release from these materials. However, these chapters did not include mucosal irritation test and *in vivo* studies of haloperidol-loaded novel films for application in transmucosal drug delivery.

The evaluation of mucosal irritation of HP-loaded novel films is an essential criterion proving that these novel products are nontoxic, non-allergic, and non-irritating[24]. The slug mucosal irritation (SMI) *in vivo* study, developed by Adriaens and co-workers [25] will be applied to quantify the toxicological properties of HP-loaded films. This test has been validated as a reliable method and is effective as a prescreening assay for determining the irritation potential of chemicals, formulations, and active ingredients to various mucosal membranes[26, 27]. The mucosal layer of the slug is located on the body's surface and is hence easily observable by the investigator. In this test, colorless mucus, secreted by slugs after contact with a test substance, is a good initial indicator of biocompatibility. The total amount of mucus produced serves as

the main criterion to test the biocompatibility of formulations since these increases on exposure to stronger irritants[28]. These assessments provide quantifiable data for test materials to be classified as nonirritating, mild, moderate, or severely irritating[27].

In vivo pharmacokinetics is also an important method to confirm the efficacy of HP loaded in novel film formulations compared with original formulation, referring to the movement of drugs through the body (adsorption, distribution, excretion and metabolism), followed from study of Samanta and co-workers [19]. Therefore, this research will be conducted on *in vivo* pharmacological studies and mucosal irritation test of haloperidol-loaded novel films for application in buccal drug delivery.

5.2.3. Synthesis of novel antimicrobial polymers for wound dressings

The increase in the number of patients suffering from healing wounds provided a substantial issue for health care professionals. Infection of the wound is a major factor in impaired wound healing [29]. Bacteria affect the equilibrium between degradative and reconstructive processes during wound healing by increasing and/or sustaining a pro-inflammatory environment that inhibits re-epithelization. The majority of chronic wounds have mixed populations of aerobic and anaerobic bacteria [29]. Due to the great prevalence in traumatic, surgical, burn, and other types of wounds, *Staphylococcus aureus* is regarded to be the most dangerous bacterium. In chronic wound infection, other bacteria such as *Pseudomonas aeruginosa*, *Escherichia coli*, and *Klebsiella pneumoniae* may also play a role [29]. Over the past two decades, there have been ongoing efforts to produce polymers with antibacterial properties. Important characteristics of cationic disinfectants are their positive charge [20]. Antimicrobial polymers are materials that can kill or limit the growth of microorganisms on a surface or in their surrounding environment. They either have an intrinsic capacity to exhibit antibacterial activity. There are four classifications of antimicrobial polymers, including those that exhibit antimicrobial activity on their own, those whose biocidal activity is conferred by their chemical modification, those that incorporate antimicrobial organic compounds with either low or high molecular weight (Mw), and those that involve the incorporation of active inorganic systems [30]. Among the researched antibacterial materials, cationic polymers have the most potential to serve as antibacterial agents due to their beneficial properties of compromising cell membrane integrity, prolonged inhibitory action, and broad-spectrum antibacterial activity [31, 32]. The vast majority of bactericidal cationic polymers published in the

scientific literature are polycations generated from quaternary ammonium compounds [33], polyethyleneimine (PEI)[7], polyethyleneimine (PEI) derivatives [32, 34] and chitosan derivatives[35].

From our previous study [36], the nucleophilic substitution reaction between L-PEI and excess of alkyl halide can be used to prepare quaternary ammonium compounds (QACs). The use of suitable base and chemical reagent ratio may prevent the over alkylation reaction [36]. QACs are nitrogen (N)-containing compounds in which N is covalently linked to four distinct groups. They are represented by the generic formula $N^{+} R_1 R_2 R_3 R_4 .X^{-}$, where R can be a hydrogen atom, a plain alkyl group or an alkyl group substituted with different functional groups, and X represents an anion [37]. Consequently, in the future work, we will be synthesized and evaluated quaternary ammonium derivatives of poly (2-hydroxyethyl ethyleneimine) or QP2HEEI and quaternary ammonium derivatives of poly (3-hydroxypropyl ethyleneimine) or QP3HPEI for antimicrobial and wound healing applications. The structures of QP2HEEI and QP3HPEI are shown in **Fig. 1**. Our preliminary experiments demonstrated a possibility to synthesize QP2HEEI and QP3HPEI and their structure was confirmed using ^{1}HNMR, ^{13}C-NMR and FTIR spectroscopy. Thermal, cytotoxicity and antimicrobial activity of these novel polymers will also be evaluated. The novel antimicrobial polymers can be formulated as a film forming spray for anti-infection and wound healing.

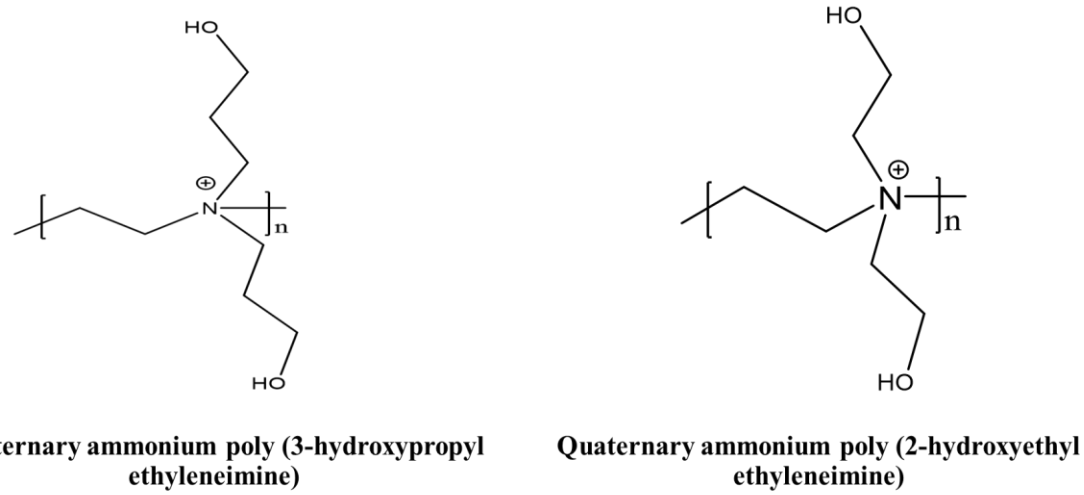

Quaternary ammonium poly (3-hydroxypropyl ethyleneimine)

Quaternary ammonium poly (2-hydroxyethyl ethyleneimine)

Fig. 1. Structures of quaternary ammonium derivatives of poly(2-hydroxyethy ethyleneimine) and poly(3-hydroxypropyl ethyleneimine).

5.3. Significance of the key findings

To the best of our knowledge, there are no reports in the literature on L-PEI cryogels formed by freezing and subsequent thawing of its aqueous solutions. Thus, the fabrication of novel physical cryogels based on L-PEI via cryotropic gelation has advantages, since this method does not require the use of cross-linkers or initiators. In addition, by controlling the freezing temperature or modifying the solvent, L-PEI cryogels can be designed with desired mechanical properties for applications ranging from cell immobilisation and tissue culture scaffolds to drug delivery systems or antimicrobial wound dressings.

This thesis also generated novel water-soluble polymers with low toxicity based on the modification of linear polyethyleneimine, including poly (2-hydroxyethyl ethyleneimine), P2HEEI, and poly(3-hydroxypropyl ethyleneimine), P3HPEI. Both polymers were effectively used as biomaterials and excipients for drug delivery, such as film-forming agents and plasticizers. Therefore, both polymers were blended with other polymers such as chitosan to optimize a glass transition temperature for applications in skin and transmucosal drug delivery as well as improved mechanical properties of polymers.

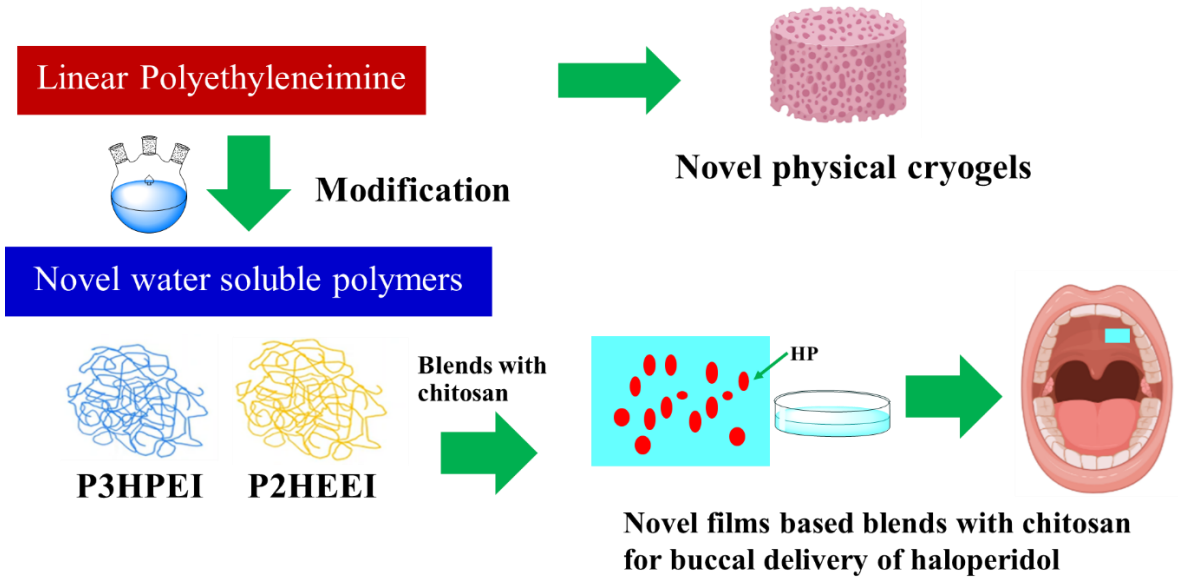

Fig. 2. Key findings of this thesis.

Novel elastic and mucoadhesive films based on blends of chitosan and linear PEI derivatives, i.e., P2HEEI and P3HPEI, were developed in this study for rapid buccal delivery of haloperidol. Consequently, L-PEI and its derivatives have potential as biomaterials and excipients for drug delivery, enabling the development of novel formulations such as cryogels,

drug-loaded films for poorly water-soluble drug administration, and mucoadhesive drug delivery system, as shown in **Fig. 2**.

References

(1) Shen, C.; Li, J.; Zhang, Y.; Li, Y.; Shen, G.; Zhu, J.; Tao, J. Polyethylenimine-Based Micro/Nanoparticles as Vaccine Adjuvants. *Int. J. Nanomedicine* **2017**, *12*, 5443–5460. https://doi.org/10.2147/IJN.S137980.

(2) Sedlacek, O.; Janouskova, O.; Verbraeken, B.; Richard, H. Straightforward Route to Superhydrophilic Poly(2-Oxazoline)s via Acylation of Well-Defined Polyethylenimine. *Biomacromolecules* **2018**, *20*. https://doi.org/10.1021/acs.biomac.8b01366.

(3) Soradech, S.; Williams, A. C.; Khutoryanskiy, V. V. Physically Cross-Linked Cryogels of Linear Polyethyleneimine: Influence of Cooling Temperature and Solvent Composition. *Macromolecules* **2022**, *55*, 9537–9546. https://doi.org/10.1021/acs.macromol.2c01308.

(4) Lungu, C. N.; Diudea, M. V.; Putz, M. V.; Grudziński, I. P. Linear and Branched PEIs (Polyethylenimines) and Their Property Space. *Int. J. Mol. Sci.* **2016**, *17* (4). https://doi.org/10.3390/ijms17040555.

(5) Choosakoonkriang, S.; Lobo, B.; Koe, G.; Koe, J.; Middaugh, C. Biophysical Characterization of PEI/DNA Complexes. *J. Pharm. Sci.* **2003**, *92*, 1710–1722. https://doi.org/10.1002/jps.10437.

(6) Xu, D.; Wang, Q.; Yang, T.; Cao, J.; Lin, Q.; Yuan, Z.; Li, L. Polyethyleneimine Capped Silver Nanoclusters as Efficient Antibacterial Agents. *Int. J. Environ. Res. Public Health* **2016**, *13* (3). https://doi.org/10.3390/ijerph13030334.

(7) Gibney, K. A.; Sovadinova, I.; Lopez, A. I.; Urban, M.; Ridgway, Z.; Caputo, G. A.; Kuroda, K. Poly(Ethylene Imine)s as Antimicrobial Agents with Selective Activity. *Macromol. Biosci.* **2012**, *12* (9), 1279–1289. https://doi.org/10.1002/mabi.201200052.

(8) Demirci, S.; Sahiner, N. PEI-Based Ionic Liquid Colloids for Versatile Use: Biomedical and Environmental Applications. *J. Mol. Liq.* **2014**, *194*, 85–92. https://doi.org/10.1016/j.molliq.2014.01.015.

(9) Lozinsky, V. I.; Galaev, I. Y.; Plieva, F. M.; Savina, I. N.; Jungvid, H.; Mattiasson, B. Polymeric Cryogels as Promising Materials of Biotechnological Interest. *Trends Biotechnol.* **2003**, *21* (10), 445–451. https://doi.org/10.1016/j.tibtech.2003.08.002.

(10) Okay, O. *Polymeric Cryogels Macroporous Gels with Remarkable Properties*; 2014; Vol. 263. https://doi.org/10.1007/978-3-319-05846-7.

(11) Păduraru, O. M.; Ciolacu, D.; Darie, R. N.; Vasile, C. Synthesis and Characterization of Polyvinyl Alcohol/Cellulose Cryogels and Their Testing as Carriers for a Bioactive Component. *Mater. Sci. Eng. C* **2012**, *32* (8), 2508–2515. https://doi.org/10.1016/j.msec.2012.07.033.

(12) Caló, E.; Khutoryanskiy, V. V. Biomedical Applications of Hydrogels: A Review of Patents and Commercial Products. *Eur. Polym. J.* **2015**, *65*, 252–267. https://doi.org/10.1016/j.eurpolymj.2014.11.024.

(13) Yuan, J. J.; Jin, R. H. Fibrous Crystalline Hydrogels Formed from Polymers Possessing a Linear Poly(Ethyleneimine) Backbone. *Langmuir* **2005**, *21* (7), 3136–3145. https://doi.org/10.1021/la047182l.

(14) Taranejoo, S.; Liu, J.; Verma, P.; Hourigan, K. A Review of the Developments of Characteristics of PEI Derivatives for Gene Delivery Applications. *J. Appl. Polym. Sci.* **2015**, *132* (25). https://doi.org/10.1002/app.42096.

(15) Patil, S.; Lalani, R.; Bhatt, P.; Vhora, I.; Patel, V.; Patel, H.; Misra, A. Hydroxyethyl Substituted Linear Polyethylenimine for Safe and Efficient Delivery of SiRNA Therapeutics. *RSC Adv.* **2018**, *8* (62), 35461–35473. https://doi.org/10.1039/C8RA06298F.

(16) Hao, J.; Heng, P. W. S. Buccal Delivery Systems. *Drug Dev. Ind. Pharm.* **2003**, *29* (8), 821–832. https://doi.org/10.1081/DDC-120024178.

(17) Sudhakar, Y.; Kuotsu, K.; Bandyopadhyay, A. K. Buccal Bioadhesive Drug Delivery - A Promising Option for Orally Less Efficient Drugs. *J. Control. Release* **2006**, *114* (1), 15–40. https://doi.org/10.1016/j.jconrel.2006.04.012.

(18) Park, D. M.; Song, Y. K.; Jee, J. P.; Kim, H. T.; Kim, C. K. Development of Chitosan-Based Ondansetron Buccal Delivery System for the Treatment of Emesis. *Drug Dev. Ind. Pharm.* **2012**, *38* (9), 1077–1083. https://doi.org/10.3109/03639045.2011.639076.

(19) Samanta, M. K.; Dube, R.; Suresh, B. Transdermal Drug Delivery System of Haloperidol to Overcome Self-Induced Extrapyramidal Syndrome. *Drug Dev. Ind. Pharm.* **2003**, *29* (4), 405–415. https://doi.org/10.1081/DDC-120018376.

(20) Domb, A. J.; Yudovin-Farber, I.; Golenser, J.; Beyth, N.; Weiss, E. I. Quaternary Ammonium Polyethyleneimine: Antibacterial Activity. *J. Nanomater.* **2010**, *2010*. https://doi.org/10.1155/2010/826343.

(21) Shan, X.; Williams, A. C.; Khutoryanskiy, V. V. Polymer Structure and Property Effects on Solid Dispersions with Haloperidol: Poly(N-Vinyl Pyrrolidone) and Poly(2-Oxazolines) Studies. *Int. J. Pharm.* **2020**, *590* (September), 119884. https://doi.org/10.1016/j.ijpharm.2020.119884.

(22) Abruzzo, A.; Cerchiara, T.; Luppi, B.; Bigucci, F. Transdermal Delivery of Antipsychotics: Rationale and Current Status. *CNS Drugs* **2019**, *33* (9), 849–865. https://doi.org/10.1007/s40263-019-00659-7.

(23) Gidla, Sushmita, Lakshmi, J Maha KSS, Prathyusha, Rao, Y. S. Formulation and Evaluation of Haloperdiol-Carrier Loaded Buccal Film. *Int. J. Curr. Adv. Res.* **2018**, *7* (9), 5–10.

(24) Chevala, N. T.; Dsouza, J. A.; Saini, H.; Kumar, L. Design and Development of Tranexamic Acid Loaded Film-Forming Gel to Alleviate Melasma. *J. Cosmet. Dermatol.* **2022**, No. September, 6863–6874. https://doi.org/10.1111/jocd.15426.

(25) Adriaens, E.; Remon, J. P. Gastropods as an Evaluation Tool for Screening the Irritating Potency of Absorption Enhancers and Drugs. *Pharm. Res.* **1999**, *16* (8), 1240–1244. https://doi.org/10.1023/A:1014801714590.

(26) Callens, C.; Adriaens, E.; Dierckens, K.; Remon, J. P. Toxicological Evaluation of a Bioadhesive Nasal Powder Containing a Starch and Carbopol 974 P on Rabbit Nasal Mucosa and Slug Mucosa. *J. Control. release Off. J. Control. Release Soc.* **2001**, *76* (1–2), 81–91. https://doi.org/10.1016/s0168-3659(01)00419-9.

(27) Shan, X.; Aspinall, S.; Kaldybekov, D. B.; Buang, F.; Williams, A. C.; Khutoryanskiy, V. V. Synthesis and Evaluation of Methacrylated Poly(2-Ethyl-2-Oxazoline) as a Mucoadhesive Polymer for Nasal Drug Delivery. *ACS Appl. Polym. Mater.* **2021**. https://doi.org/10.1021/acsapm.1c01097.

(28) Adriaens, E.; Remon, J. P. Evaluation of an Alternative Mucosal Irritation Test Using Slugs. *Toxicol. Appl. Pharmacol.* **2002**, *182* (2), 169–175. https://doi.org/https://doi.org/10.1006/taap.2002.9444.

(29) Wiegand, C.; Bauer, M.; Hipler, U. C.; Fischer, D. Poly(Ethyleneimines) in Dermal Applications: Biocompatibility and Antimicrobial Effects. *Int. J. Pharm.* **2013**, *456* (1), 165–174. https://doi.org/10.1016/j.ijpharm.2013.08.001.

(30) Muñoz-Bonilla, A.; Fernández-García, M. Polymeric Materials with Antimicrobial Activity. *Prog. Polym. Sci.* **2012**, *37* (2), 281–339. https://doi.org/10.1016/j.progpolymsci.2011.08.005.

(31) Phillips, D. J.; Harrison, J.; Richards, S. J.; Mitchell, D. E.; Tichauer, E.; Hubbard, A. T. M.; Guy, C.; Hands-Portman, I.; Fullam, E.; Gibson, M. I. Evaluation of the Antimicrobial Activity of Cationic Polymers against Mycobacteria: Toward Antitubercular Macromolecules. *Biomacromolecules* **2017**, *18* (5), 1592–1599. https://doi.org/10.1021/acs.biomac.7b00210.

(32) Lan, T.; Guo, Q.; Shen, X. Polyethyleneimine and Quaternized Ammonium Polyethyleneimine: The Versatile Materials for Combating Bacteria and Biofilms. *J. Biomater. Sci. Polym. Ed.* **2019**, *30* (14), 1243–1259. https://doi.org/10.1080/09205063.2019.1627650.

(33) Mei, L.; Lu, Z.; Zhang, X.; Li, C.; Jia, Y. Polymer-Ag Nanocomposites with Enhanced Antimicrobial Activity against Bacterial Infection. *Appl. Mater. Interfaces* **2014**, *6*, 15813–15821.

(34) Lin, J.; Qiu, S.; Lewis, K.; Klibanov, A. M. Mechanism of Bactericidal and Fungicidal Activities of Textiles Covalently Modified with Alkylated Polyethylenimine. *Biotechnol. Bioeng.* **2003**, *83* (2), 168–172. https://doi.org/10.1002/bit.10651.

(35) Sahariah, P.; Másson, M. Antimicrobial Chitosan and Chitosan Derivatives: A Review of the Structure-Activity Relationship. *Biomacromolecules* **2017**, *18* (11), 3846–3868. https://doi.org/10.1021/acs.biomac.7b01058.

(36) Soradech, S.; Kengkwasingh, P.; Williams, A. C.; Khutoryanskiy, V. V. Synthesis and Evaluation of Poly (3-Hydroxypropyl Ethylene-Imine) and Its Blends with Chitosan Forming Novel Elastic Films for Delivery of Haloperidol. *Pharmaceutics* **2022**, *14*

(2671), 1–22. https://doi.org/https://doi.org/10.3390/pharmaceutics14122671.

(37) Jain, A.; Duvvuri, L. S.; Farah, S.; Beyth, N.; Domb, A. J.; Khan, W. Antimicrobial Polymers. *Adv. Healthc. Mater.* **2014**, *3* (12), 1969–1985. https://doi.org/10.1002/adhm.201400418.